

**“HYPERBRANCHED POLYGLYCEROLS AS
BUILDING BLOCKS FOR COMPLEX
AMPHIPHILIC STRUCTURES:
SYNTHESIS, CHARACTERIZATION AND
APPLICATIONS”**

Dissertation

zur

Erlangung des Grades

“Doktor der Naturwissenschaften”

am Fachbereich Chemie, Pharmazie und Geowissenschaften
der Johannes Gutenberg-Universität in Mainz

Jörg Nieberle

geboren in Ludwigshafen am Rhein

Mainz, 2008

Dekan:

1. Berichterstatter:

2. Berichterstatter:

Tag der mündlichen Prüfung: 17. September 2008

Die vorliegende Arbeit wurde in der Zeit von November 2004 bis Januar 2008 am Institut für Organische und Makromolekulare Chemie der Johannes Gutenberg-Universität in Mainz angefertigt.

Table of Contents

1. Introduction	1
1.1 Hyperbranched Polymers	1
1.2 Ring-Opening Multibranching Polymerization (ROMBP)	1
1.2.1 Classification of Ring-Opening Multibranching Polymerizations	3
1.2.1.1 Cationic Ring-Opening Multibranching Polymerizations	4
1.2.1.2 Anionic Ring-Opening Multibranching Polymerizations	9
1.2.1.3 Catalytic Ring-Opening Multibranching Polymerizations	16
1.2.2 Core-containing Hyperbranched Polymers by Ring-Opening Multibranching Polymerization	24
1.3 Conclusions	27
1.4 References	28
2. Objectives	33
2.1 Introduction	33
2.2 Progress in Polyglycerol Synthesis	34
2.3 Amphiphilic Linear-Hyperbranched Block Copolymers	34
2.4 Novel Monomer for Non Nitrogen Containing Linear-Hyperbranched Block Copolymers	35
2.5 Amphiphilic Hyperbranched-Hyperbranched Block Copolymers	35
2.6 Negatively Charged Linear-Hyperbranched Block Copolymer Polyelectrolytes	36
2.7 Amino Acid Based Core Initiators for Polymerization of Glycidol and L-Lactide	36
2.8 Influences of Amphiphilic Polyglycerol Block Copolymers on Insulin Fibril Formation	36
2.9 References	37
3. Progress in Polyglycerol Synthesis	40
3.1 Introduction	40
3.2 Influence of the Degree of Deprotonation	42
3.2.1 Variation of the Reaction Solvent	44
3.2.2 Gradual Increase of the Degree of Deprotonation	47
3.2.3 Use of Polyglycerols as Macroinitiators	49
3.3 Continuous Spin Fractionation	55
3.4 Conclusion	59
3.5 Experimental Part	60
3.5.1 Materials	60
3.5.2 Polymerization Apparatus	60
3.5.3 Synthesis of the Hyperbranched Polyglycerols	61
3.5.4 Continuous Spin Fractionation	62
3.5.5 Hyperbranched Polyglycerols	62
3.6 References	63
4. Amphiphilic Linear-Hyperbranched Block Copolymers	66
4.1 Introduction	66
4.2 Jeffamines [®] as Macroinitiators	67
4.2.1 Bisglycidolization of the Jeffamines [®]	67
4.2.2 Synthesis of the Block Copolymers Based on Bisglycidolized Jeffamines [®]	70
4.2.2.1 Linear-Hyperbranched AB-Diblock Copolymers	70
4.2.2.2 Linear-Hyperbranched ABA-Triblock Copolymers	76

4.3 Bisglycidolized Linear Alkyl Amines as Initiators	78
4.4 Conclusion	82
4.5 Experimental Part	83
4.5.1 Materials	83
4.5.2 Characterization of the Provided Jeffamines [®]	83
4.5.2.1 Methoxy-poly(oxyethylene/oxypropylene)-2-propylamine (Jeffamine [®] XTJ-505 (M-600))	83
4.5.2.2 Methoxy-poly(oxyethylene/oxypropylene)-2-propylamine (Jeffamine [®] XTJ-507 (M-2005))	84
4.5.2.3 Poly(oxypropylene)diamine (Jeffamine [®] D-2000)	84
4.5.3 Synthesis of the Macroinitiators	84
4.5.3.1 Macroinitiator from Jeffamine [®] XTJ-505 (M-600)	85
4.5.3.2 Macroinitiator from Jeffamine [®] XTJ-507 (M-2005)	85
4.5.3.3 Macroinitiator from Jeffamine [®] XTJ-505 (D-2000)	85
4.5.4 Synthesis of the Linear-Hyperbranched Block Copolymers Starting from Jeffamine [®] Based Macroinitiators	86
4.5.4.1 Linear-Hyperbranched Block Copolymers Starting from Jeffamine [®] Based Macroinitiators	87
4.5.5 Silylation of the Block Copolymers	87
4.5.5.1 Silylated Block Copolymers Starting from Jeffamine [®] Based Macroinitiators	87
4.5.6 <i>N,N</i> -Bis(-2,3-dihydroxy-propyl)-octadecyl amine	87
4.5.7 Synthesis of <i>N,N</i> -Bis(-2,3-dihydroxy-propyl)-undec-10-enyl amine	88
4.5.7.1 Undecenyl bromide (11-Bromo-1-undecene)	88
4.5.7.2 Undec-10-enyl-phthalimide	88
4.5.7.3 Undec-10-enyl-amine	89
4.5.7.4 <i>N,N</i> -Bis(-2,3-dihydroxy-propyl)-undec-10-enyl amine	89
4.5.8 Synthesis of the Hyperbranched Polymers Using Bisglycidolized Amines as Initiators	89
4.5.8.1 Hyperbranched Polyglycerols Using <i>N,N</i> -Bis(-2,3-dihydroxy-propyl)-octadecyl amine as Initiator	90
4.5.8.2 Hyperbranched Polyglycerols Using <i>N,N</i> -Bis(-2,3-dihydroxy-propyl)-undec-10-enyl amine as Initiator	90
4.6 References	91
5 Novel Monomer for Non Nitrogen Containing Linear-Hyperbranched Block Copolymers	93
5.1 Introduction	93
5.2 Poly(glyceryl glycerol) Block Copolymers	94
5.2.1 Synthesis of (DL-1,2-Isopropylidene glyceryl) Glycidyl Ether (IGG)	94
5.2.2 Synthesis of Poly(glyceryl glycerol) Block Copolymers	96
5.3 Conclusion	98
5.4 Experimental Part	99
5.4.1 Materials	99
5.4.2 (DL-1,2-Isopropylidene glyceryl) Glycidyl Ether (IGG)	99
5.4.3 PEO- <i>b</i> -PIGG	99
5.4.4 PEO- <i>b</i> -PGG by Deprotection of PEO- <i>b</i> -PIGG	100
5.5 References	100

6 Amphiphilic Hyperbranched-Hyperbranched Block Copolymers	103
6.1 Introduction	103
6.2 Synthesis of the Hyperbranched Macroinitiators	104
6.3 Synthesis of the Hyperbranched-Hyperbranched Block Copolymers	111
6.4 Amphiphilic Character of the Hyperbranched-Hyperbranched Block Copolymers	117
6.5 Conclusion	118
6.6 Experimental Part	119
6.6.1 Materials	119
6.6.2 Modifications at the Core	119
6.6.2.1 H-PCS _x -C ₁₁ -N ₃	119
6.6.2.2 H-PCS _x -C ₁₁ -NH ₂	119
6.6.2.3 H-PCS _x -C ₁₁ -N-PG ₂	120
6.6.3 Hyperbranched-Hyperbranched Block Copolymers	120
6.6.3.1 <i>Hb</i> -H-PCS-C ₁₁ - <i>hb</i> -PG	120
6.6.3.2 <i>Hb</i> -H-PCS-C ₁₁ - <i>hb</i> -PGSi	121
6.6.3.3 <i>Hb</i> -H-PCS-C ₁₁ - <i>hb</i> -PGBz	121
6.7 References	121
7 Amino Acid Based Core Initiators for the Polymerization of Glycidol and L-Lactide	123
7.1 Introduction	123
7.2 Amino Acid Based Core Initiators	124
7.3 Hyperbranched Polyglycerols with Functional Initiator Cores	125
7.4 Poly(L-lactides) with Functional Initiator Cores	128
7.5 Conclusion	131
7.6 Experimental Part	131
7.6.1 Materials	131
7.6.2 Synthesis of the Morpholinone Derivatives	131
7.6.2.1 Phenylalanine methyl ester	131
7.6.2.2 Tryptophane methylester	132
7.6.2.3 3-Benzyl-4(2,3-dihydroxy-propyl)-6-hydroxymethyl-morpholin-2-one	132
7.6.2.4 4-(2,3-Dihydroxy-propyl)-6-hydroxymethyl-3-indolylmethyl-morpholin-2-one	132
7.6.3 Hyperbranched Polyglycerols with Amino Acids as Initiator Cores	132
7.6.4 Poly(L-Lactides) with Amino Acids as Initiator Cores	133
7.7 References	133
8 Amphiphilic Hyperbranched Block Copolymer Polyelectrolytes	135
8.1 Introduction	135
8.2 Synthesis of the Amphiphilic Hyperbranched Block Copolymer Polyelectrolytes	136
8.3 Conclusion	139
8.4 Experimental Part	139
8.4.1 Materials	139
8.4.2 Synthesis of the Nitrile Functionalized Block Copolymers	139
8.4.3 Synthesis of the Carboxylate Functionalized Block Copolymers	140
8.4.4 CMC Determination	140
8.5 References	141

9 Effect of Polyglycerol Block Copolymers on Insulin Fibril Formation	142
9.1 Introduction	142
9.2 Insulin Fibril Formation	143
9.3 Conclusion	145
9.4 Experimental Part	146
9.4.1 Materials	146
9.4.2 CMC Measurements by DPH-Fluorescence Assay	146
9.4.3 Insulin Fibril Formation Measurements by Thioflavin T Assay	147
9.5 References	147
10 Summary / Abstract	149
11 Experimental Methods and Instrumentation	150
11.1 Nuclear Magnetic Resonance Spectroscopy (NMR)	150
11.2 Gel Permeation Chromatographie (GPC)	150
11.3 Infra Red-Spectroscopy (IR)	150
11.4 Differential Scanning Calorimetry (DSC)	151
11.5 Matrix Assisted Laser Desorption Ionization – Time of Flight (MALDI-ToF)	151
11.6 Field Desorption Mass Spectrometry (FD)	151
11.7 Transmission Electron Microscopy (TEM)	151
12 Appendix	152
12.1 Synthesis of Hyperbranched Polyglycerol in a Continuous Flow Microreactor	153
12.2 Double-Hydrophilic Linear-Hyperbranched Block Copolymers Based on Poly(ethylene oxide) and Poly(glycerol)	159
12.3 Synthesis and Characterization of Poly(glyceryl glycerol) Block Copolymers	164
12.4 Gold Nanoparticles Coated with a Thermosensitive Hyperbranched Polyelectrolyte: Towards Smart Temperature and pH Nanosensors	167
12.5 Liquid Crystalline Hyperbranched Polyglycerols Forming Liquid Crystalline Mesophases	171
12.6 Polyglycerol-Based Copolymers: A New Family of Amphiphiles Circumventing Multidrug Resistance of Tumor Cells	178
Curriculum Vitae	184

Symbols and Abbreviations

5-HDON	5-hydroxymethyl-1,4-dioxan-2-one
ACE	active chain end
Ala	alanine
AM	activated monomer
ATRP	atom transfer radical polymerization
b	branched
BHO	3,3-bis(hydroxymethyl)oxetane
BP(OH) ₄	2,2',4,4'-tetrahydroxy benzophenone
CMC	critical micelle concentration
COSY	correlated spectroscopy
CSF	continuous spin fractionation
D	dublet
D-2000	Jeffamine H ₂ N-PPO ₃₃ -NH ₂
DB	degree of branching
Diglyme	diethylene glycol dimethyl ether
DLS	dynamic light scattering
DMF	dimethyl formamide
DMSO	dimethyl sulfoxide
DPH	1,6-diphenyl-1,3,5-hexatriene
DP _n	degree of polymerization
EEGE	ethoxy ethyl glycidyl ether
EHO	3-ethyl-3-(hydroxymethyl)oxetane
Et	ethyl
FD	field desorption
GPC	gel permeation chromatographie
hb	hyperbranched
HMDS	hexamethyl disilazane
IG	inverse gated
IGG	(DL-1,2-isopropylidene glyceryl) glycidyl ether
KOMe	potassium methanolate
KOtBu	potassium <i>tert</i> -butanolate
L	linear
L ₁₃	linear L ₁₃ unit of polyglycerol /abundance of linear L ₁₄ unit
L ₁₄	linear L ₁₄ unit of polyglycerol /abundance of linear L ₁₃ unit
m	multiplet
MALDI-ToF	matrix assisted laser desorption ionization time of flight
MDR	multi-drug resistant
Me	methyl
MHz	mega hertz
M _n	number average molecular weight
MS	mass spectrometry
M _w	weight average molecular weight
NMP	nitroxide mediated polymerization
NMR	nuclear magnetic resonance
PAA	poly(acrylic acid)
PB	poly(butadiene)
PCS	poly(carbosilane)
PDI	polydispersity index
PEG	poly(ethylene glycol)

Symbols and Abbreviations

PEI	poly(ethylene imine)
PEO	poly(ethylene oxide)
PG	poly(glycerol)
PGBz	benzylated poly(glycerol)
PGG	poly(glyceryl glycerol)
PGSi	persilylated poly(glycerol)
Phe	phenylalanine
PheM	3-Benzyl-4(2,3-dihydroxy-propyl)-6-hydroxymethyl-morpholin-2-one
PIGG	poly((DL-1,2-isopropylidene glyceryl) glycidyl ether)
PL	poly(lactide)
PMMA	poly(methyl methacrylate)
PPI	poly(propylene imine)
PPO	poly(propylene oxide)
PS	poly(styrene)
RES	reticuloendothelial system
RI	refractive index
ROMBP	ring-opening multi branching polymerization
ROMP	ring-opening metathesis polymerization
s	singlet
SAXS	small angle x-ray scattering
SCVP	self condensing vinyl polymerization
SMA	slow monomer addition
T	terminal
t	time
TEM	transmission electron microscopy
TfOH	trifluoromethanesulfonic acid
theo	theoretical
THF	tetrahydrofurane
ThT	Thioflavin T
TMP	1,1,1-tris(hydroxymethyl)propane
Trp	tryptophane
TrpM	4-(2,3-Dihydroxy-propyl)-6-hydroxymethyl-3-indolylmethyl-morpholin-2-one
UV	ultra violett
Val	valine
XTJ-505	Jeffamine M-600
XTJ-507	Jeffamine M-2005

1 Introduction

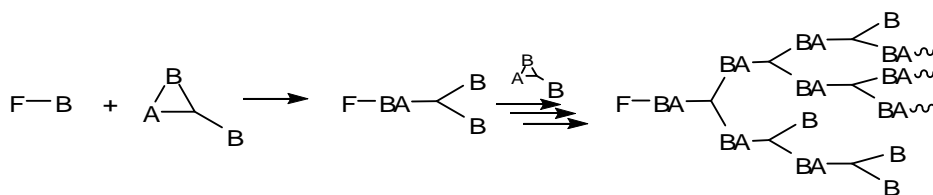
1.1 Hyperbranched Polymers

General concepts for synthesizing less perfectly branched polymeric structures than dendrimers have been treated as early as in 1952 by Flory.¹ He described a synthetic pathway leading to branched polymers based on step-growth AB_m type polycondensation of multifunctional monomers containing one A group and m ($m \geq 2$) complementary B groups. However, the term „hyperbranched polymers“ was not introduced before the late 1980ies when Kim and Webster defined dendritic macromolecules with random branch-on-branch topology and compact molecular structures obtained by polycondensation.^{2,3} The last decade has seen a renaissance of synthetic hyperbranched macromolecules, profiting from the fascination created by the perfectly branched dendrimers.⁴⁻⁹

The subsequent paragraphs will summarize hyperbranching polymerizations based on ring-opening strategies in a comprehensive manner. This chapter is based on a review-article in this area.¹⁰

1.2 Ring-Opening Multibranching Polymerization (ROMBP)

In recent years, ring-opening multibranching strategies have been established as a versatile method for the synthesis of a variety of hyperbranched homopolymers as well as complex macromolecular architectures, such as branched block copolymers or various multi-arm star polymers. Classically, hyperbranched polymers have been prepared by polycondensation of AB_m -type monomers.^{2,4,11} In the mid-1990ies, the *self-condensing vinyl polymerization* (SCVP) was introduced by Fréchet et al.,^{12,13} utilizing monomers containing a polymerizable vinyl group along with an initiating moiety. Such monomers combining an initiating with a polymerizable moiety have been termed “inimers”. The two aforementioned pathways permit the preparation of a wide variety of hyperbranched polymers but involve the major drawback of leading to broad molecular weight distributions with polydispersities in the range of $DP_n/2$. In contrast, monomers eligible for ring-opening multibranching polymerization (ROMBP) contain a strained, cyclic moiety that generates a branching point only upon ring-opening in the course of the polymerization. Such monomers are often called “latent AB_m monomers” (Scheme 1.1).



Scheme 1.1. General principle of ring-opening multibranching polymerizations. F is the single focal unit, while B depicts the reactive groups of the AB_2 monomer.

It is obvious that cyclic inimers possess structural analogy with the vinyl-inimers employed for SCVP. However, in the case of the cyclic inimers, the driving force for this type of polymerization is the ring-opening isomerization of the cyclic monomer unit.

Well in advance before hyperbranched polymers became a matter of broad scientific interest, Sandler and Berg,¹⁴ as well as Vandenberg et al.,¹⁵ studied the polymerization of glycidol, a typical cyclic latent AB_2 monomer, aiming at predominantly linear polymer architectures. However, they also observed the formation of undesired branched structures, which were characterized by Vandenberg et al. in a seminal paper published in 1985.¹⁵ This interesting work describes the generation of different chain units in the base-catalyzed polymerization of glycidol (Table 1.1).

Table 1.1. Characterization data from Vandenberg's original paper.¹⁵ The assignments I and II refer to the different linear units, while IB and IIB represent the dendritic chain units. IA and IIA belong to the terminal groups and III indicates epoxide end groups.

No.	Diluent		Catalyst		Time (h)	Temp. (°C)	Conversion (%)	η_{inh} (dL/g)	Polymer					
	Name	Vol. (mL)	Name	g					Chain Units (%) ^b					
								I	IB	IA or IIA	II	IIB	III ^a	
<i>With R-TMSGE</i>														
1	None		KOH	2.00	336	22	68 ^c	0.013	3	6	33	45	13	ND
<i>With RS-TMSGE</i>														
2	None		KOH	2.00	336	22	58 ^c	—	4	4	44	44	4	ND
3	None		KO <i>tert</i> -Bu	0.20	168	75	98 ^d	0.036	29	5	56	0	10	ND
4	DMSO	8.8 ^e	KO <i>tert</i> -Bu	0.20	47	22	89 ^f	0.034	16	5	73	5	0	ND
5	DMSO	8.8 ^e	KO <i>tert</i> -Bu	0.20	1	22	29	0.029	0	0	63	12	0	Trace?
<i>With Glycidol</i>														
6	Ether	10.0	KOH	4.00	22	22	75 ^b	0.050	1	7	35	46	10	ND
7	Ether	10.0	KOH	2.00	18	22	19 ^g	0.050	4	6	41	38	11	ND
8	CH ₂ Cl ₂	20.0	KOH	4.00	4	0								
					22	22	100 ^o	0.054	6 (6)	6 (9)	28 (24)	54 (55)	6 (6)	ND
9	CH ₂ Cl ₂	20.0	Al Porphyrin ^j	0.66	4	0								
					192	22	88 ^k	0.096	4	1	27	48	0	19
10	Ether	10.0	KO <i>tert</i> -Bu	0.33 ^l	4	0								
					168	22	100	0.011	5	11	43	38	4	ND
11	DMSO	6.0 ^e	KO <i>tert</i> -Bu	0.33 ^l	4	0								
	CH ₂ Cl ₂	20.0	KO <i>tert</i> -Bu	0.33 ^l	4	0								
	DMSO	6.0			168	22	90 ^p	0.011	5	5	49	38	2	3
12	Ether	10.0	K hexymethyl disilazane ^m	0.48 ^l	4	0	100	0.064						
	DMSO	6.0 ^e			168	22			10	10	40	37	3	Trace
<i>With TBGE</i>														
13	None	—	KOH	2.00	46	22	58 ^q	0.24						

Subsequently, cationic^{16,17} ring-opening polymerization techniques were applied to the polymerization of glycidol in the early 1990ies by Penzcek, Kubisa and Dworak in early works in this field. Further progress in this area was made by Frey et al., who established the slow monomer addition (SMA) technique for anionic polymerization of glycidol in 1999, leading to polyglycerols with moderate, in some cases narrow molecular weight distributions.¹⁸⁻²⁰ Details of the respective approaches will be discussed in the ensuing text.

As early as 1992, Suzuki and Saegusa reported the palladium-catalyzed multibranching polymerization of a cyclic carbamate, another example for a latent AB₂ monomer, leading to hyperbranched polyamines.²¹ It is important to note that Suzuki and Saegusa in this paper reported the first *initiated* type of multibranching polymerization, i.e., a chain growth mechanism. The low polydispersity ($M_w/M_n = 1.35$) demonstrates the possibility to control the growth of the polymer chains in this system. In all these reactions, the polymerization is typically initiated by a suitable initiating molecule, containing a focal unit *F* as well as reactive *B* groups that can react with the cyclic structure under ring-opening. For each AB₂ monomer being incorporated into the growing polymer molecule, two new potential polymerization sites are created, while only one is consumed.

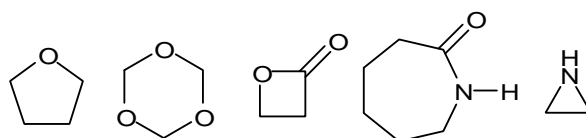
1.2.1 Classification of Ring-Opening Multibranching Polymerizations

As indicated in the previous paragraph, ring-opening multibranching polymerizations have been carried out under different conditions, utilizing a variety of monomers, initiators and catalysts. However, all reported approaches are based upon the general principle illustrated in Scheme 1.1.

In the following, a detailed classification of the respective polymerization and branching mechanisms is important, i.e., cationic, anionic and catalytic ring-opening multibranching polymerizations as well as the respective seminal works leading to their development will be treated in this paragraph. Within this context, specific prerequisites, synthetic principles and peculiarities for each particular variant will be examined and discussed.

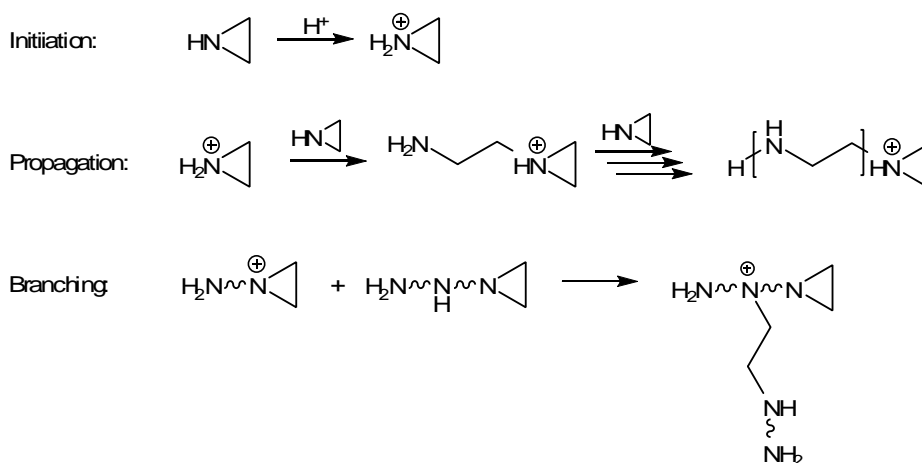
1.2.1.1 Cationic Ring-Opening Multibranching Polymerizations

In cationic polymerizations, electron-deficient initiators (mostly Brønsted- or Lewis acids) react with electron-rich monomers. The active chain end bears a positive charge with the active sites being either carbenium or oxonium ions. Molecular weights are often limited by the inherent sensitivity to impurities, chain transfer and rearrangement reactions. Suitable monomers for cationic polymerizations are vinyl monomers with electron-donating moieties or cyclic structures containing heteroatoms. The latter case is referred to as cationic ring-opening polymerization. Eligible monomers include cyclic ethers, cyclic acetals, lactones, lactams and cyclic amines (Scheme 1.2).



Scheme 1.2. Examples of common monomers for cationic ring-opening polymerizations.

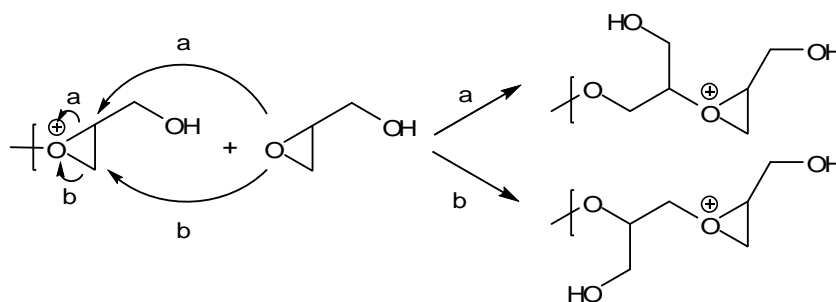
Hauser first described the ring-opening polymerization of alkyleneimines in 1969.²² It was observed that the polymerization of three membered imines (aziridines), specifically ethylene imine, leads to a product with extensive branching. Dick and Ham subsequently reported a random distribution of primary, secondary and tertiary amine groups.²³ Branching results from the formation of tertiary amine groups upon intermolecular nucleophilic attack of secondary amine nitrogens in polymer repeat units on propagating iminium centers (Scheme 1.3).



Scheme 1.3. Hyperbranching polymerization of ethylene imine.

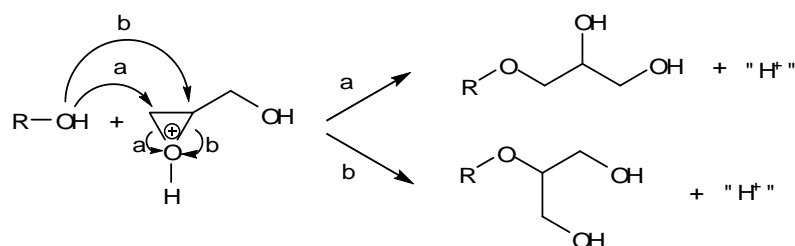
Thus, the long-known polymerization of aziridines in fact represents the oldest known ring-opening polymerization, leading to hyperbranched poly(ethyleneimine)s. The resulting materials have been available for more than 3 decades and are sold under the trade-name Lupasol[®] on a scale of several 100,000 t per year. Substitution at the aziridine ring impedes polymerization.^{24,25} The 1,2- and 2,3-disubstituted species do not polymerize; 1- and 2-substituted aziridines undergo polymerization, but polymer yields and molecular weights are limited.

Oxiranes or oxetanes with attached hydroxyl groups can be potentially polymerized by typical cationic initiators, e.g. protic or Lewis acids like trifluoromethanesulfonic acid (TfOH) or boron trifluoride etherate (BF₃·OEt₂). In the course of these reactions, branching points are generated. This justifies the term “cationic ring-opening multibranching polymerization”. Dworak and Penczek¹⁶ studied the coexistence of *active chain end* (ACE) and *activated monomer* (AM) mechanisms in the cationic polymerization of glycidol (Schemes 1.4 and 1.5). In order to investigate the comparative relevance of both concurrent reaction pathways, hyperbranched polyglycerols with molecular weights of up to 10,000 g/mol were synthesized and characterized. It is obvious that only primary hydroxyl groups would be present as substituents of the polyether chain, if the reaction proceeded exclusively by the ACE mechanism.



Scheme 1.4. Active chain end mechanism in the cationic polymerization of glycidol. α - and β -ring opening preserves the CH₂OH substituent.

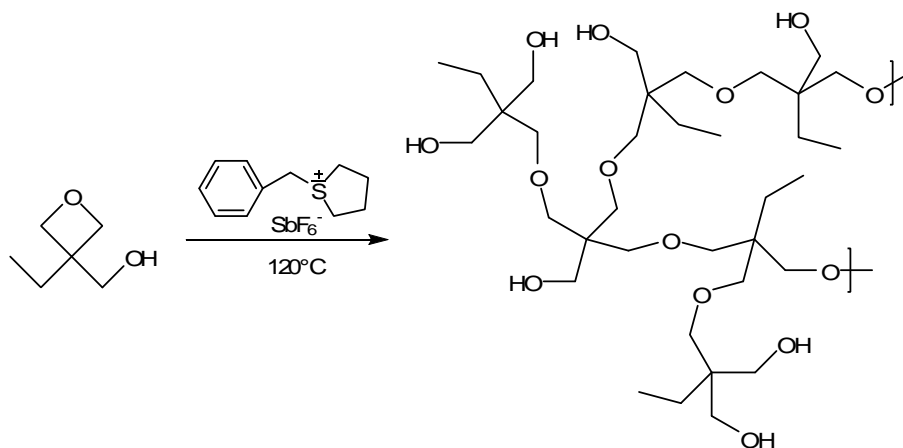
In contrast, propagation by the AM mechanism generates two different types of repeating units. R-OH in Scheme 1.5 depicts either the chain end or the side group. In the latter case, branching occurs.



Scheme 1.5. Activated monomer mechanism in the cationic polymerization of glycidol.

Dworak and Penczek explicitly analyzed the structure of the polymers, which is evidently a consequence of the polymerization mechanism. They found significant contribution of the AM mechanism to the chain growth. Also within the scope of this elegant work, a direct correlation between the specific initiator and the percentage of secondary hydroxyl groups attached to the polymer backbone was verified.¹⁷ Use of SnCl_4 or $\text{BF}_3 \cdot \text{OEt}_2$ as Lewis acidic initiators in particular proved to promote the AM mechanism.

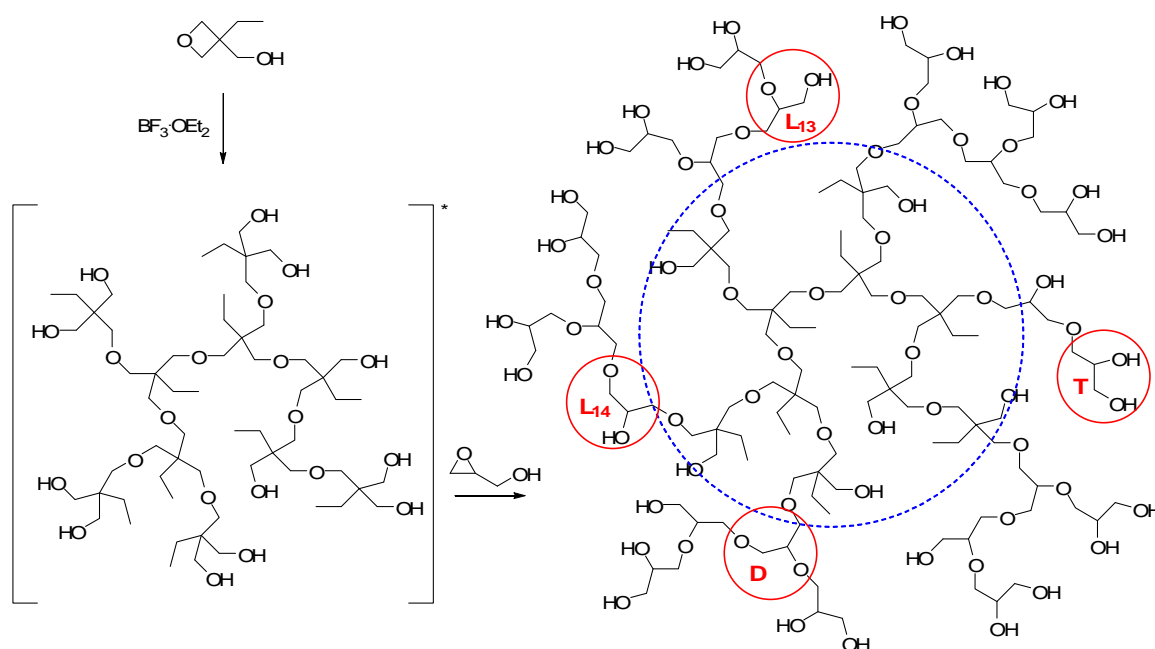
In addition to hydroxyl functional oxiranes, the congruous oxetanes have been studied as monomers in ring-opening polymerizations by Vandenberg et al., who obtained a linear and highly crystalline polymer.^{26,27} Additionally, other authors also detailed the synthesis of hyperbranched polyethers from hydroxyfunctional oxetanes.^{28,29} Mostly cationic initiators have been used in the ring-opening polymerization of oxetanes, primarily because of the higher basicity compared to three-membered oxiranes. The latter are prevalently polymerized anionically. In 1999, Magnusson et al.³⁰ published a study on the cationic ring-opening polymerization of 3-ethyl-3-(hydroxymethyl)oxetane (EHO). A convenient method for the preparation of the respective hyperbranched polyether by thermally induced bulk polymerization was introduced. The sulfonium salt initiator benzyltetramethylenesulfonium hexafluoroantimonate was used in this approach (Scheme 1.6).



Scheme 1.6. Synthesis of hyperbranched polyethers via cationic ring-opening multi-branching polymerization of EHO.

Surprisingly narrow molecular weight distributions ($M_w/M_n = 1.26 - 1.43$) at molecular weights up to 5000 g/mol were found. Detailed characterization of the hyperbranched polymers by proton-decoupled ^{13}C -NMR experiments showed a correlation between monomer conversion and degree of branching (DB). While at low conversions (<30%), predominantly linear units were formed, increased conversion lead to more dendritic units in the polymer structure. Accordingly, the possibility of tailoring the DB of these polymers by controlling the monomer conversion was later reported by Magnusson et al.³¹ Determination of the number of secondary and tertiary oxonium ions during the reaction provides the ratio of ACE- and AM mechanisms upon the polymerization of hydroxy oxetanes. A significant prevalence (90:10) of the AM mechanism was found, leading to highly branched polyethers. However, in no a case a degree of branching higher than 0.4 was obtained, which is significantly lower than the theoretical value of 0.5 for polymerizations under entirely statistical conditions. This observation leads to the assumption that upon ring-opening of oxetanes, the coexistence of ACE- and AM mechanisms adversely affects the generation of branching points.

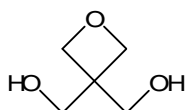
Gao et al. combined the cationic ring-opening polymerization of EHO, initiated by $\text{BF}_3 \cdot \text{OEt}_2$, with the subsequent addition of glycidol monomer to obtain amphiphilic core-shell polymers with complex hyperbranched-hyperbranched core-shell structures.³²



Scheme 1.7. Synthesis of amphiphilic core-shell copolymer by cationic polymerization of EHO and subsequent addition of glycidol. The red circles depict the terminal, linear and dendritic units of the hydrophilic polyglycerol shell.

Expectedly a higher feed ratio of glycidol monomer led to a higher solubility of the polymer in water.

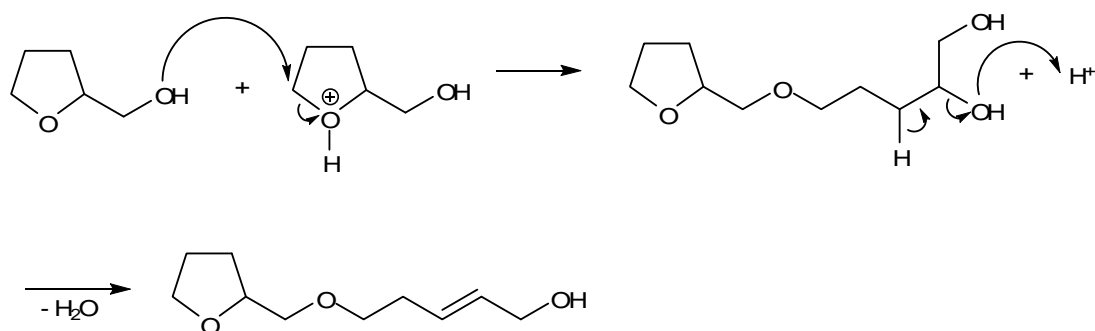
In addition to AB₂ monomers like glycidol or EHO, conveniently accessible AB₃ compounds like 3,3-bis(hydroxymethyl)oxetane (BHO, Scheme 1.8) can be used for cationic ring-opening polymerizations.



Scheme 1.8. 3,3-bis(hydroxymethyl)oxetane (BHO).

Farthing,³³ and later Vandenberg et al.,²⁷ polymerized BHO by initiation with a trifluoromethanesulfonic acid catalyst, obtaining a weakly branched polymer of low molecular weight. Interestingly, a more crystalline product of higher molecular weight was obtained when using the trimethylsilyl ether of BHO and *i*-Bu₃Al-0.7H₂O cationic catalyst as initiator. Characterization of these polymers with regard to the degree of branching is substantially constricted by the complexity and ambiguity of the respective ¹H- and ¹³C-NMR spectra. In addition, the strong aggregation of the highly hydroxyl-substituted polymers represents a severe limitation for the further characterization.

Monosubstituted derivatives of tetrahydrofuran classically have been known to be difficult to polymerize due to thermodynamic reasons.³⁴ Bednarek and Kubisa recently extended cationic hyperbranching polymerizations to the class of five-membered cyclic ethers containing hydroxyl groups as substituents.³⁵ They polymerized 2-hydroxymethyltetrahydrofuran, using a trifluoromethanesulfonic acid initiator. MALDI-ToF mass spectrometry of the obtained oligomers indicated that elimination of water took place in the course of the polymerization, which is an undesired side reaction. A possible pathway leading to a certain amount of unsaturated units in the polymer structure is given in Scheme 1.9.



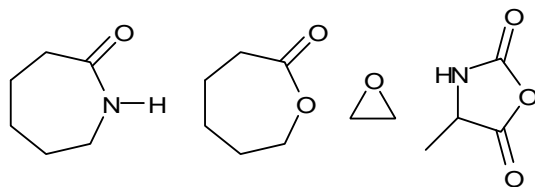
Scheme 1.9. Formation of unsaturated units in the acid-catalyzed polymerization of 2-hydroxymethyltetrahydrofuran.

In order to understand if this behaviour can be ascribed to a more complex mechanism than formerly assumed, the authors studied the polymerization of further THF derivatives and observed elimination of water in all cases. The mechanistic details necessary to explain these results still have to be evaluated. Bednarek and Kubisa suggested a reinvestigation of the polymerizability problems of five-membered cyclic ethers containing hydroxyl groups. Hyperbranched polymers obtained by cationic polymerizations are generally limited in terms of their potential for further academic investigation and potentially also for industrial application, since the number of eligible monomers is limited and other methods have proven to be superior in terms of molecular weights achievable and control over the reaction.

1.2.1.1 Anionic Ring-Opening Multibranching Polymerizations

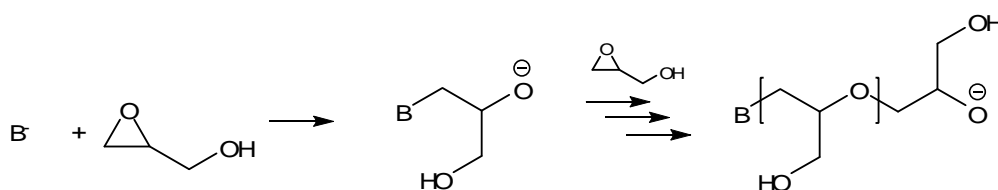
Anionic chain polymerizations exhibit many analogous characteristics as cationic polymerizations; however some distinct differences must be emphasized. Generally the propagating species are anionic ion pairs or free ions. If termination reactions are absent, further monomer addition will result in continuous chain growth. Hence, these polymerizations are often termed “living polymerizations”. Although anionic polymerizations often proceed rapidly at low temperatures, they are usually not as temperature-sensitive as cationic polymerizations. A variety of basic (nucleophilic) initiators have been used to initiate anionic polymerizations, including covalent or ionic metal amides such as NaNH_2 and $\text{LiN}(\text{C}_2\text{H}_5)_2$, alkoxides, hydroxides, cyanides, phosphines, amines and organometallic compounds like *n*-butyl lithium or phenyl magnesium bromide. The polymerization is initiated by addition of the base to the monomer, typically vinyl compounds with electron-withdrawing moieties like acrylonitrile or methyl vinyl ketone. Another group of

monomers used in anionic ring-opening polymerizations comprises ring-shaped molecules with electron-deficient carbon atoms like cyclic amides and esters (lactams or lactones), cyclic ethers (oxiranes) or Leuchs' anhydrides (Scheme 1.10).



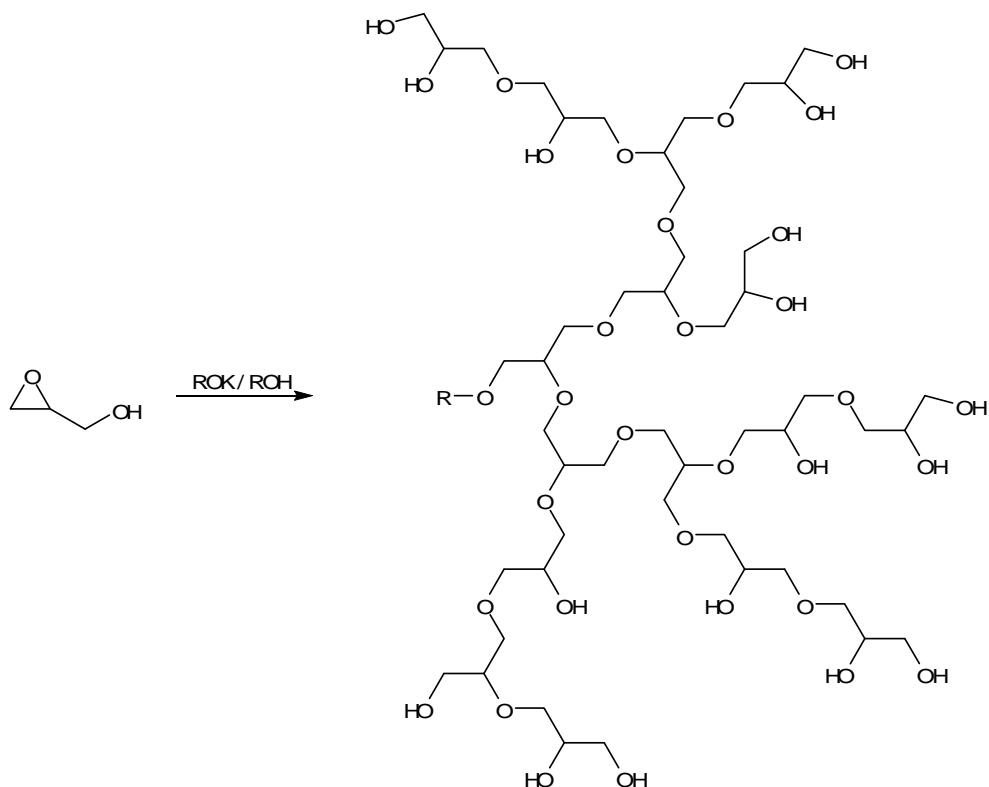
Scheme 1.10. Examples of monomers in anionic ring-opening polymerizations.

Glycidol, being a latent cyclic AB₂-type monomer containing a highly strained three membered oxirane ring, represents a monomer that can be polymerized by addition of a nucleophilic initiator. In an early work by Rider and Hill, it was casually mentioned that pyridine polymerized glycidol to a water-soluble black tar.³⁶ Sandler and Berg later observed by chance that glycidol polymerized vigorously in the presence of triethylamine, leading them to a further investigation of the effect of basic catalysts on the rate of polymerization.¹⁴ The belief that the obtained product exhibited an exclusively linear structure (Scheme 1.11) was not challenged until Vandenberg et al. characterized a variety of protected and unprotected polyglycerols in the mid-1980s.¹⁵ These polymers were prepared by initiation of glycidol with KOH base catalyst, aiming at a linear chain structure.



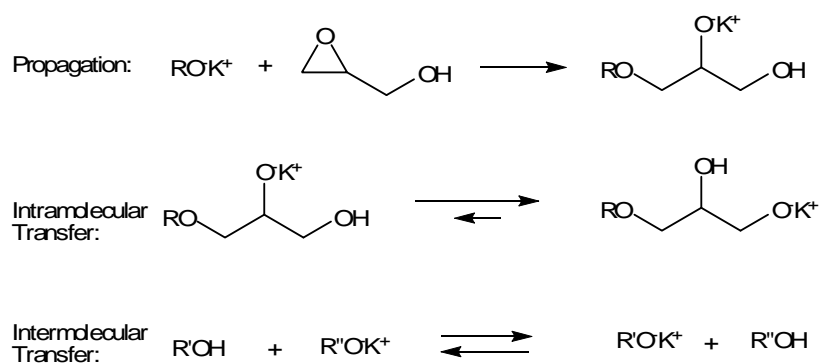
Scheme 1.11. Hypothetical formation of linear polyglycerol, as assumed by Sandler and Berg.

As part of a detailed investigation, analysis of the obtained ¹³C-NMR spectra provided the authors with initial information about the actual branched structure of polyglycerol (Scheme 1.12).



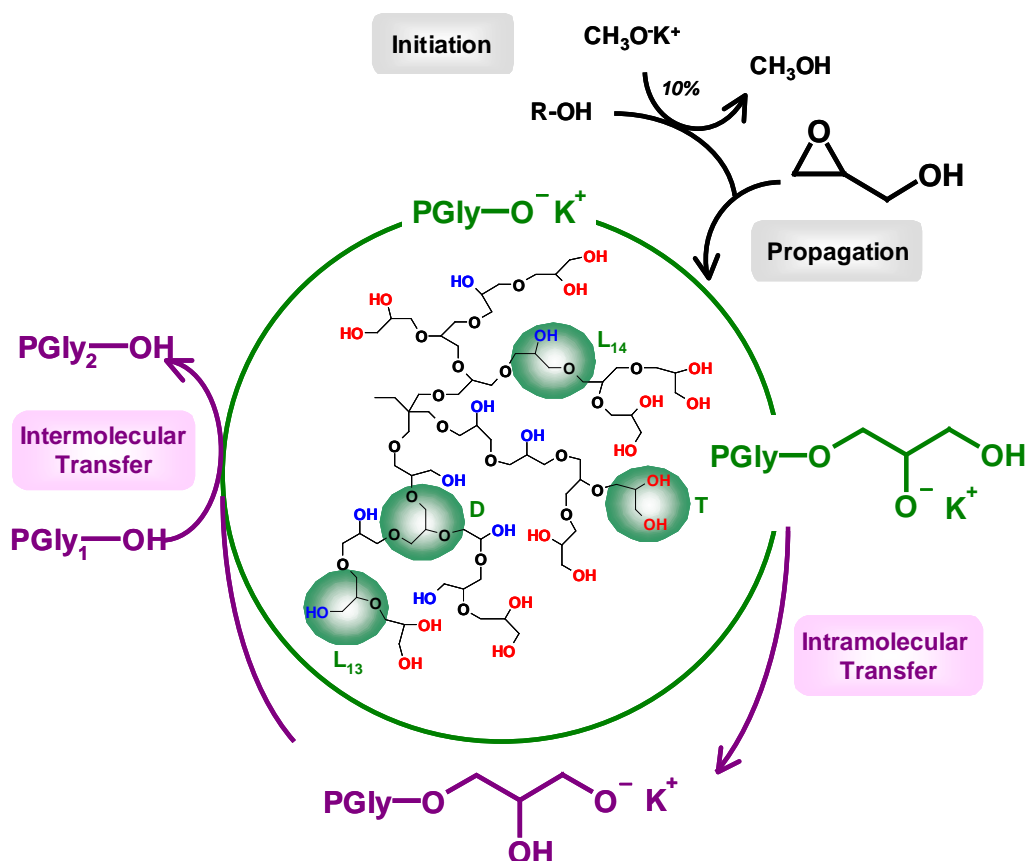
Scheme 1.12. Synthesis of hyperbranched polyglycerol via base-catalyzed polymerization of glycidol.

A 1,4-polymerization pathway involving a proton migration was concluded to be predominant in the base-catalyzed polymerization of glycidol, giving largely poly(3-hydroxyoxetane). Hydroxyl groups (or trimethylsilyloxy groups in case of the protected polyglycerols) are present on both the monomer and the polymer. Facile exchange with the propagating oxyanion was determined to result in chain branching and chain transfer. The integrant processes taking place upon growth of the polyether chain are illustrated in Scheme 1.13. Primary alkoxides are formed after the ring-opening due to intra- and intermolecular transfer. Further propagation of these species directly results in branching.



Scheme 1.13. Mechanism of the anionic polymerization of glycidol.

Extensive research involving the synthesis, characterization and structure of hyperbranched aliphatic polyethers has been carried out by Frey et al. since the late 1990s.¹⁸⁻²⁰ In analogy to concepts developed for polymerizations by ATRP^{37,38} and the synthesis of poly(propylene oxide),³⁹ conventional base initiators were replaced by a partially deprotonated polyfunctional alcohol. Controlled polymerization of glycidol was achieved by applying the slow monomer addition approach. 1,1,1-Tris(hydroxymethyl)propane (TMP), bearing three OH-groups, has been widely used as a typical multifunctional initiator core. Simultaneous chain growth is essential for obtaining well-defined hyperbranched polyglycerols with narrow molecular weight distributions. Thus, the concentration of active sites in the polymerization (alkoxides) has to be controlled by only partially deprotonating the initiator OH-groups, usually by 10% upon addition of a strong base like potassium methylate as a deprotonating agent, followed by removal of excess methanol. Slow addition of the monomer (SMA) circumvents homopolymerization initiated by deprotonated glycidol as well as any undesired cyclization reactions. Hence this technique further promotes low polydispersities and complete control of the number-average molecular weight by adjustment of the monomer/initiator ratio, when – in the ideal case - every newly formed glycerol unit is attached to the polyfunctional cores or the branched polyols already present in the reaction. The polymerization reaction involves a reversible termination mechanism; nucleophilic attack of the alkoxide takes place at the unsubstituted end of the oxirane ring, leading to a secondary alkoxide. Due to fast proton transfer equilibria, also present in linear epoxide polymerizations,³⁹ the more stable and more reactive linear alkoxide is formed to a certain extent. Both types of alkoxides are active chain ends and therefore lead to the formation of hyperbranched polyglycerols. The fundamental relevance of polyfunctional initiators and the SMA methodology for the formation of well-defined hyperbranched polymers was also shown in elegant theoretical work for SCVP⁴⁰ and by computer simulation.⁴¹ An illustration of the described mechanism is given below. Scheme 1.14 also depicts the different chain units present in the polymer structure.

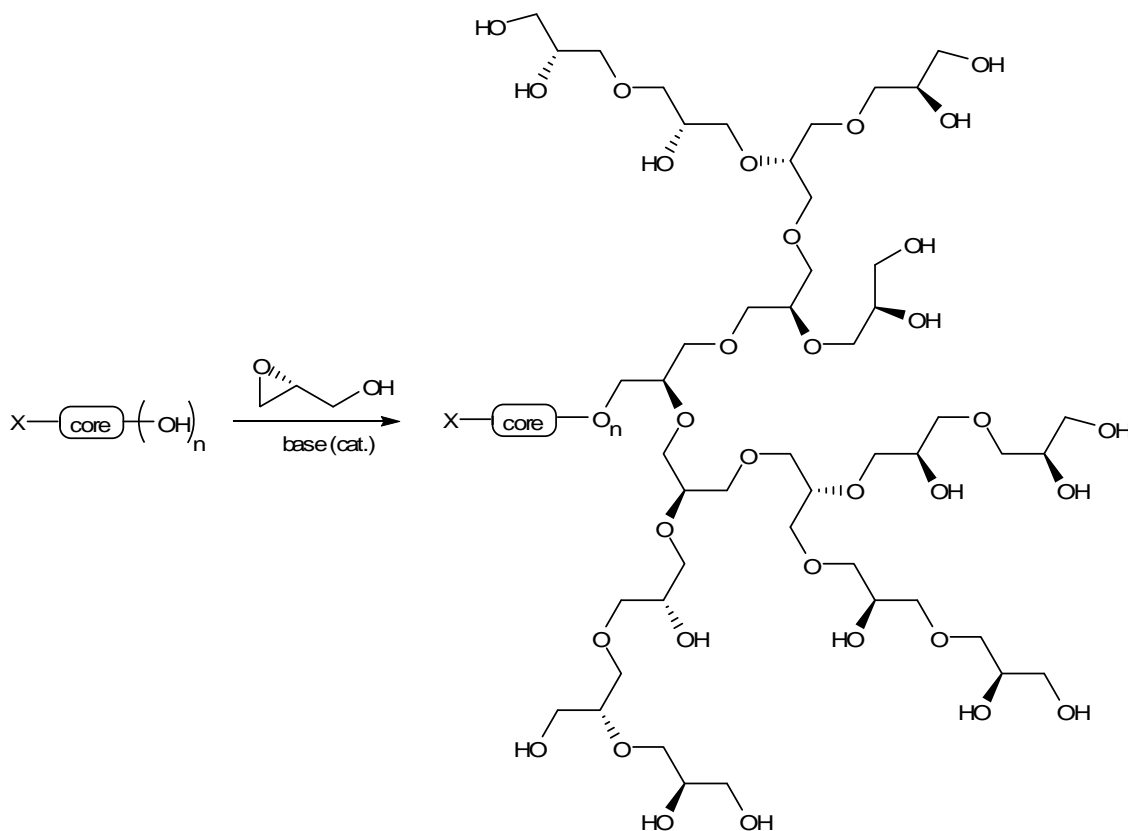


Scheme 1.14. Mechanistic pathway of the base-catalyzed ring-opening multibranching polymerization of glycidol and schematic architecture of the resulting hyperbranched polyglycerol. Examples for terminal (T), dendritic (D), linear 1,3- (L_{13}) and linear 1,4-units (L_{14}) are shaded.

If the secondary hydroxyl group propagates, the polymer chain is attached to a glycerol unit and a linear 1,3-unit (L_{13}) is generated. A linear 1,4-unit (L_{14}) is formed, when the primary hydroxyl group undergoes propagation. Reaction of both hydroxyl groups with monomer leads to the incorporation of a branched, i.e. dendritic unit (D). If a monomer unit has been deactivated by proton exchange, a terminal unit (T) with two hydroxyl end groups is formed. A detailed structural investigation of these hyperbranched polyglycerols was carried out by Frey et al. who analyzed inverse gated ^{13}C -NMR spectra in order to calculate degrees of branching (DB) and degrees of polymerization (DP_n).¹⁸ Incorporation of the TMP core into the polymer and the amount of cyclization occurring during the reaction were studied by MALDI-ToF mass spectrometry. Polymers with molecular weights of up to 10,000 g/mol (significantly higher M_n than for those obtained from the previously discussed cationic polymerizations) were prepared. They exhibited narrow molecular weight distributions ($M_w/M_n < 1.5$, mostly < 1.3) due to the pseudo chain growth

kinetics. A very interesting recent work in this area was published by Brooks et al., who modified the procedure by adding dioxane as emulsifier. In this case, very high molecular weight polyglycerols with M_n up to 700,000 g/mol have been obtained.⁴² These materials exhibit the highest molecular weights obtained for synthetic hyperbranched polymers reported to date. The reason for the formation of high molecular weight polyglycerols possessing nevertheless narrow polydispersity is not yet clear. Brooks et al. tentatively explain the effect on molecular weight by the fast proton exchange in their system. In a further study, Brooks et al. have demonstrated excellent biocompatibility and low toxicity for hyperbranched polyglycerols, similar as it has been known for a long time for poly(ethylene oxide) (PEO). This renders the material interesting for biomedical application, potentially as a substitute for PEO.⁴³

If only one of the enantiomers of glycidol is used in the polymerization, chiral hyperbranched polyglycerols can be obtained (Scheme 1.15).

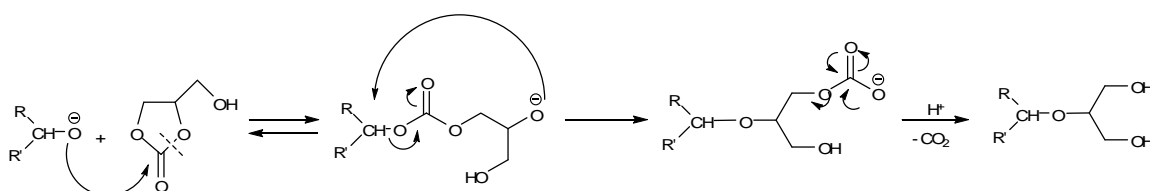


Scheme 1.15. Synthesis of chiral hyperbranched polyglycerol.

In analogy to the previously discussed racemic polyglycerols, the respective polymerization of both commercially available glycidol enantiomers has been investigated.⁴⁴ The obtained polymers exhibited similar specific optical rotation $[\alpha]$ per monomer unit as the

monomer used for polymerization. This is an important observation, since it confirms the expectation that in anionic epoxide polymerization the nucleophilic attack occurs at the least substituted end of the epoxide ring.^{37,38} In this case the chiral center is not affected. $[\alpha]$ was found to be independent of the degree of polymerization, since each monomer unit adds one chiral center to the polymer.

Rokicki et al.⁴⁵ recently reported a promising alternative synthesis of hyperbranched polyglycerol by ring-opening multibranching polymerization of glycerol carbonate, a benign monomer that can be obtained from the renewable materials glycerol and dimethyl carbonate under mild conditions. The reaction was carried out in accordance to the method established by Frey, e.g., TMP was used as a trifunctional initiator core under SMA conditions, leading to the formation of branched polyethers upon CO₂ liberation. Attack of the alkoxide can either occur at the carbonyl or alkyl carbon atoms of the cyclic carbonate group. The authors observed an additional ¹³C-NMR signal that did not appear in the spectra of the polymers obtained from glycidol polymerization. This signal can be attributed to the generation of terminal 1,3-dihydroxy units which are the result of an intramolecular rearrangement that can take place in the course of the polymerization after formation of an intermediate linear carbonate (Scheme 1.16).

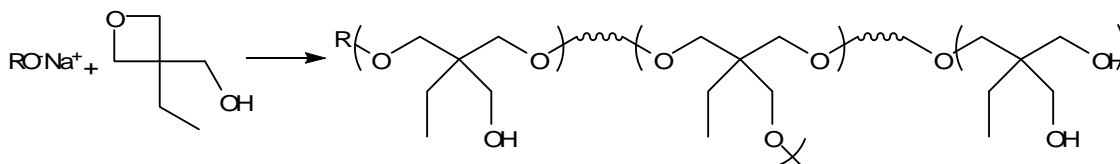


Scheme 1.16. Formation of terminal 1,3-dihydroxy units in the polymerization of glycerol carbonate.⁴⁵

The obtained polymers were of low molecular weight and polydispersities ranged between 1.2 and 1.3.

It was highlighted in the previous paragraph that multifunctional oxetanes undergo cationic ring-opening polymerizations resulting in hyperbranched polyol structures analogous to hyperbranched polyglycerols. Oxetanes have been classically considered as monomers that can only be polymerized cationically. However, some anionic polymerizations of unsubstituted oxetane using bulky aluminium-based catalysts with added Lewis acids have been reported.^{46,47} It was shown that treatment of substituted oxetanes with extremely strong nucleophiles, such as the azide anion,⁴⁸ or redox conditions with

lithium 4,4'-di-*tert*-butylbiphenylide⁴⁹ result in ring-opening, but do not promote polymerization. Smith and Mathias⁵⁰ first described the anionic ring-opening polymerization of EHO to a hyperbranched polyol using a strong base catalyst (sodium hydride) and TMP as a multifunctional initiator core. The polymerization was carried out under SMA conditions at high temperatures (>100°C) because of the high activation energy of the ring-opening.



Scheme 1.17. Ring-opening multibranching polymerization of EHO.

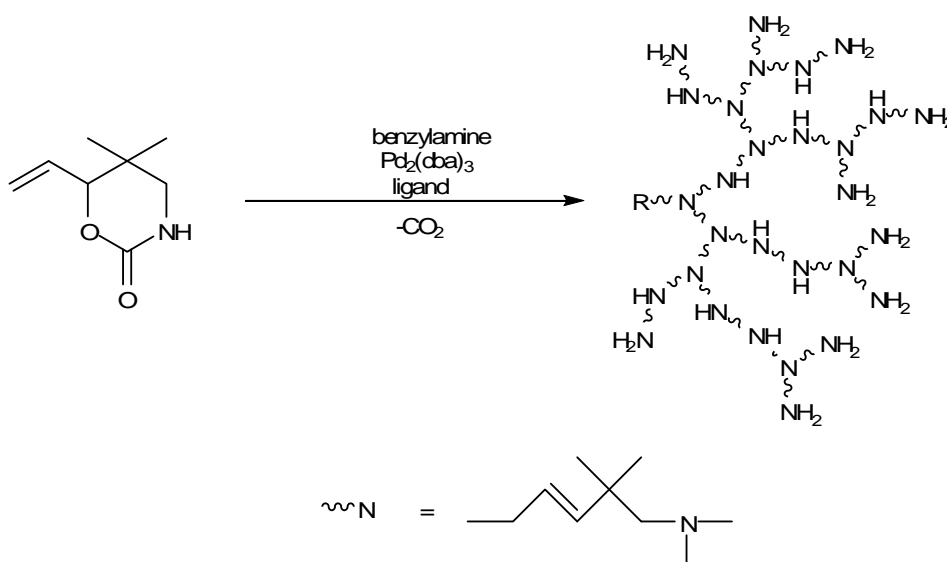
The resulting hyperbranched polyols (Scheme 1.17) were of low molecular weight and, in contrast to hyperbranched polyglycerols, dissolved in chloroform and benzene but were insoluble in water. A fraction of the polymers showed solubility in acetone and was found to have a higher degree of branching (DB=0.48) than the acetone insoluble fraction (DB=0.2). Upon usage of benzyl alcohol as a monofunctional initiator, the resulting polymer was completely soluble in acetone and NMR spectra indicated a high degree of branching.

In summary, anionic polymerization techniques represent by far the most common approach in the synthesis of well-defined hyperbranched polymers by ring-opening polymerization at present, particularly in the field of hyperbranched polyols. Numerous research groups are currently engaged in the preparation, modification and characterization of the respective polymers for a broad variety of applications, ranging from biomedicine to advanced coatings.

1.2.1.3 Catalytic Ring-Opening Multibranching Polymerizations

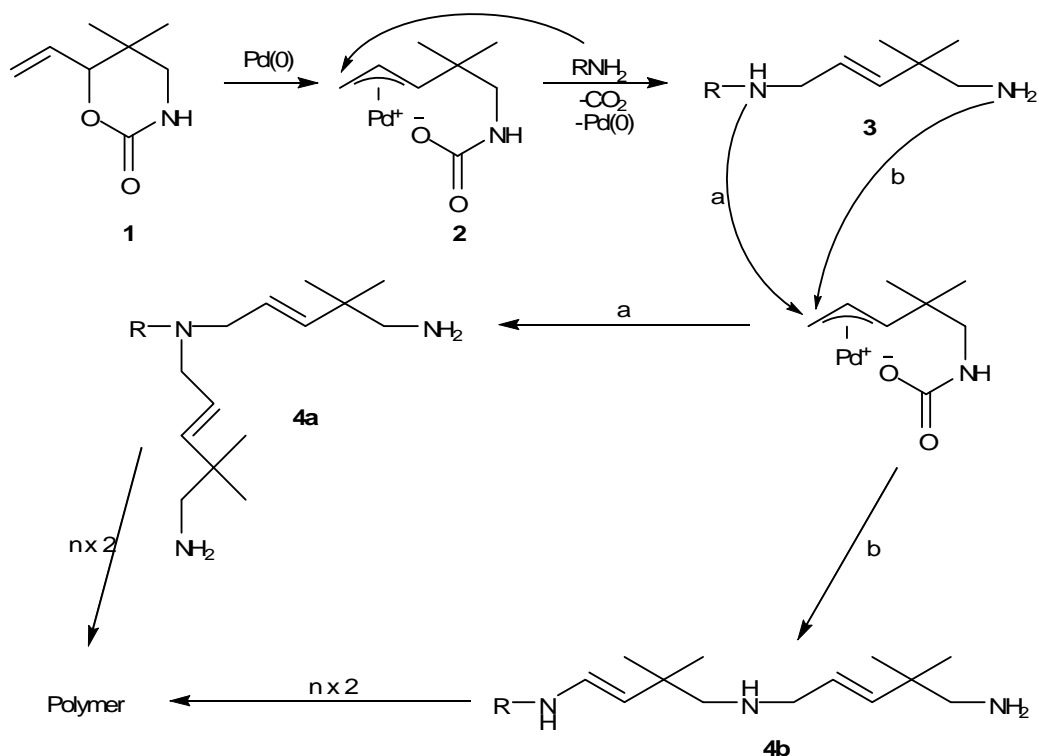
A remarkable and well-reputed example of the significance of metal catalysts in polymer science (awarded with the joint Nobel Prize in chemistry for Ziegler and Natta in 1963)⁵¹ can be found in the stereoselective polymerization of α -olefins.⁵²⁻⁵⁴ Further progress in this area, merging the exceptional work of organic, inorganic and polymer chemists afforded Chauvin, Grubbs and Schrock with the joint Nobel Prize in Chemistry 2005 for

their achievements in the domain of Ring-Opening Metathesis Polymerization (ROMP).⁵⁵ Ring-opening polymerizations of cyclic lactides and lactones initiated by nucleophiles (i.e. alcohols, amines) in the presence of suitable organometallic promoters have been outlined in numerous publications.⁵⁶⁻⁵⁹ The first ring-opening multibranching polymerization involving a transition metal catalyst was reported by Suzuki et al. in 1992.²¹ Pertinent previous studies⁶⁰ provided the authors with a concept of combining the catalytic effect of a Pd(0) complex with a suitable monomer structure for ring-opening polymerization. The monomer of choice was the cyclic carbamate 5,5-dimethyl-6-ethenylperhydro-1,3-oxazin-2-one. Benzylamine-initiated polymerization with the aid of $\text{Pd}_2(\text{dba})_3 \cdot \text{CHCl}_3 \cdot 2\text{dppe}$ catalyst at room temperature produced a hyperbranched poly-amine consisting of primary, secondary and tertiary amino-moieties upon CO_2 evolution. A simplified illustration of the reaction is given in Scheme 1.18.



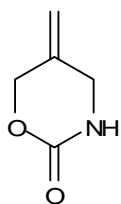
Scheme 1.18. Catalytic polymerization of 5,5-dimethyl-6-ethenylperhydro-1,3-oxazin-2-one.

The mechanism proposed by Suzuki and co-workers is depicted in Scheme 1.19. It involves the π -allylpalladium complex **2** as the key intermediate. The amine initiator is assumed to attack the electrophilic site of **2** to produce the diamine **3**, releasing carbon dioxide and regenerating a Pd(0) complex. Depending on which of the amino groups of **3** reacts, two different triamines, **4a** and **4b**, are possible.



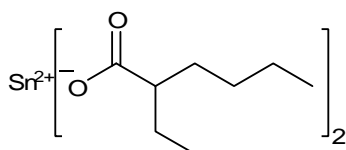
Scheme 1.19. Mechanism of the catalytic polymerization of 5,5-dimethyl-6-ethenylperhydro-1,3-oxazin-2-one.

A peculiarity of this work becomes obvious when the molecular weight distribution of the obtained polymer is considered. After the transformation of secondary amino groups into carbamate groups (to prevent interaction with the polystyrene beads in the GPC column) a very low polydispersity of 1.35 was found at a molecular weight of about 3,000 g/mol. Since the amount of initiator employed determines the molecular weights obtained, Suzuki et al. in fact developed the first case of a controlled ring-opening multi-branching polymerization, avoiding broad molecular weight distributions and undesired side reactions. Paralleling this pioneering work, further studies were carried out utilizing a slightly varied cyclic carbamate structure (Scheme 1.20).⁶¹ 5-Methyleneperhydro-1,3-oxazin-2-one was polymerized by a Pd(0) catalyst of very similar structure. Triphenylphosphine was found to be a better ligand than bis(diphenylphosphino)ethane (dppe) in this case. Narrowly dispersed ($M_w/M_n = 1.3-1.5$) and highly branched polymers with molecular weights between 2000 and 3000 g/mol were obtained also in this work.



Scheme 1.20. 5-Methylenepiperidin-2-one.

Stannous octoate (SnOct_2) is a widely used initiator in polylactide synthesis^{62,63} as well as in the polymerization of lactones with alcohols.^{56-59,64,65}

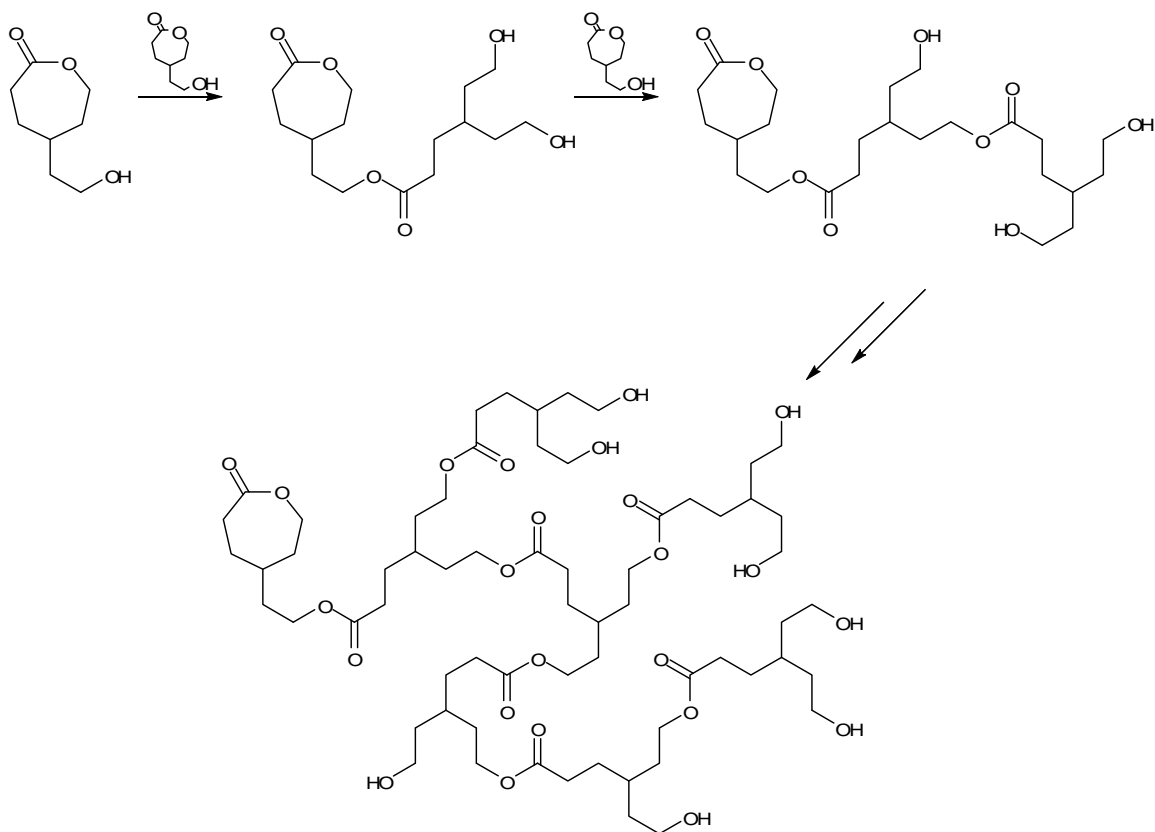


Scheme 1.21. Stannous octoate (SnOct_2).

The explicit initiation mechanism presumably depends on the temperature and has not been entirely elucidated to date. Two basic types of mechanisms have been proposed in the literature: a direct catalytic type,^{66,67} where the catalyst serves to activate the monomer through coordination with its carbonyl oxygen, and monomer insertion type mechanisms,⁶⁸⁻⁷⁴ involving the catalyst as co-initiator along with either purposely added or adventitious hydroxyl impurities. In the latter case, polymerization proceeds through an activated stannous alkoxide bond.

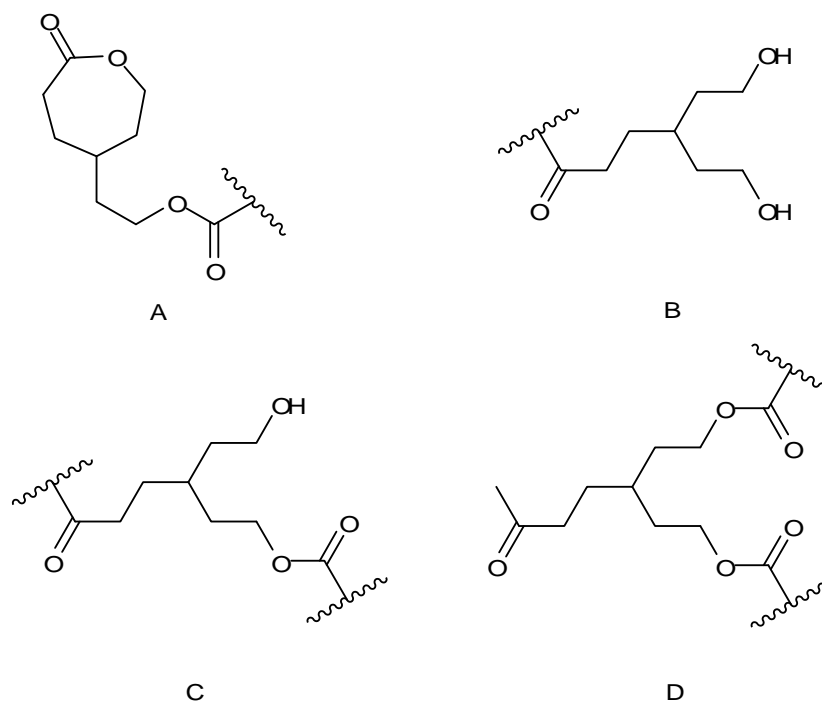
In 1999, Fréchet et al. reported an elegant approach to hyperbranched polyesters of high molecular weight, based on the ring-opening polymerization of a monomer containing an ϵ -caprolactone ring as well as a primary alcohol group (4-(2-hydroxyethyl)- ϵ -caprolactone), i.e., a lactone-based inimer structure.⁷⁵

Bulk polymerization was carried out at elevated temperature in the presence of a catalytic amount of SnOct_2 .^{76,77} Scheme 1.22 depicts the pathway of this ring-opening multi-branching polymerization leading to high molecular weight hyperbranched polymers ($M_w = 65,000\text{-}85,000$ g/mol) with a polydispersity of ca. 3.2. Like in SCVP, broad polydispersities are in line with expectation for a one-pot synthesis of this type.



Scheme 1.22. Catalytic polymerization of 4-(2-hydroxyethyl)- ϵ -caprolactone.

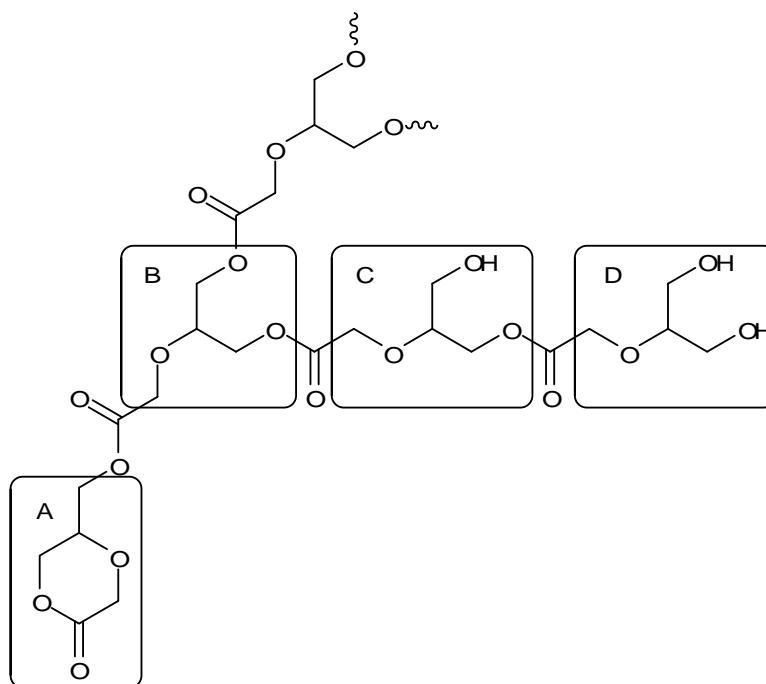
The reaction was found to proceed faster when the amount of catalyst was increased. However, smaller amounts of catalyst tended to give polymers with elevated molecular weights. In agreement with other hyperbranched polymers possessing a large number of hydroxyl end groups, like the previously discussed polyglycerol, the obtained polyester was soluble in polar solvents such as DMSO, DMF and methanol, but insoluble in THF, CH_2Cl_2 and CHCl_3 . In order to determine the relative amount of linear, terminal and dendritic subunits (Scheme 1.23), ^{13}C -NMR-spectra of the polymer were recorded and compared to spectra obtained from suitable model compounds. The degree of branching was then calculated to be 0.50 according to the definition established by Hawker, Lee and Fréchet, which confirms the hyperbranched structure.¹³



Scheme 1.23. Structure of the possible subunits in the polyester **1**: The focal unit A, terminal units B, linear units C and dendritic units D are depicted.

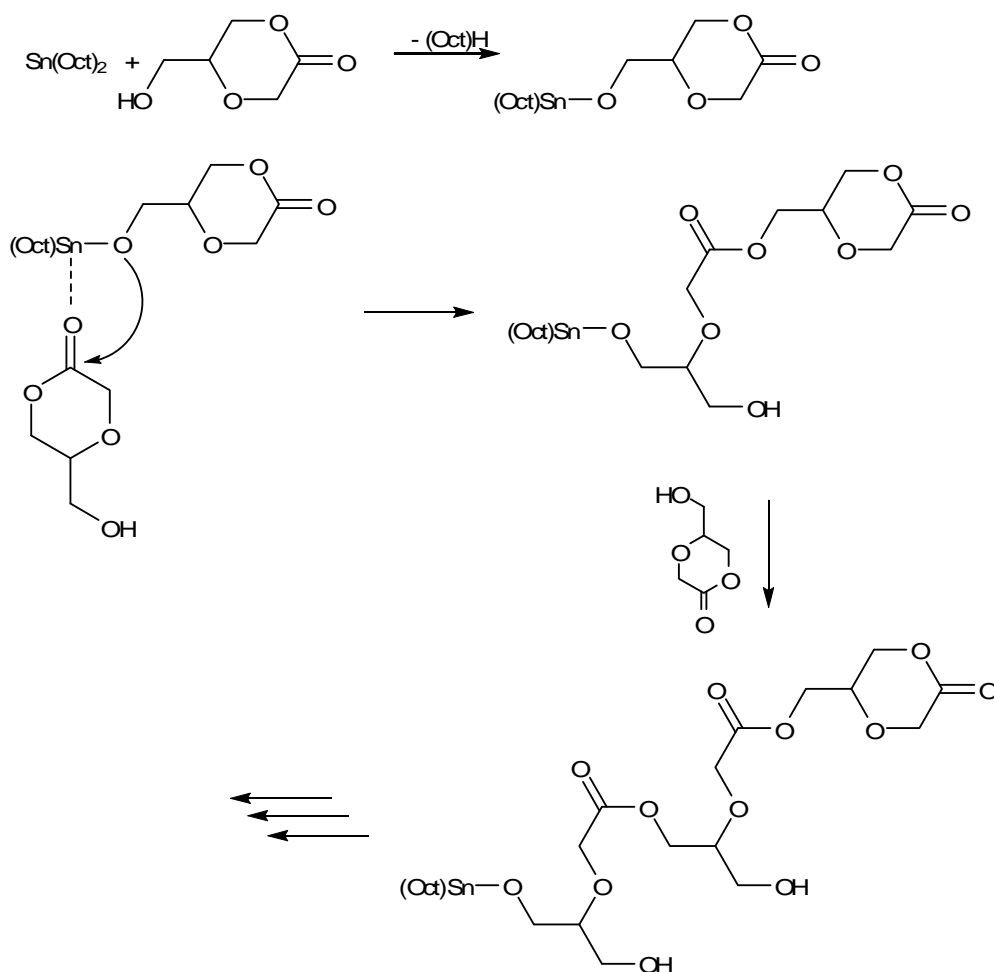
Another hyperbranched polyester was recently prepared and characterized in elegant work by Rokicki et al.⁷⁸ They described the synthesis of 5-hydroxymethyl-1,4-dioxan-2-one (5-HDON) and its application for the preparation of hyperbranched polymers by ring-opening multibranching polymerization initiated by the $\text{Sn}(\text{Oct})_2$ catalyst.

The theoretical structure of the obtained polymers and oligomers is shown in Scheme 1.24. Similar to the hyperbranched polyester prepared by Fréchet et al., four main subunits are possible. The polymerization starts at the core unit A. Dendritic subunit B is completely substituted and therefore represents the branching point, while C depicts a linear fragment of the molecule. The terminal units D contain two unsubstituted hydroxymethyl groups.



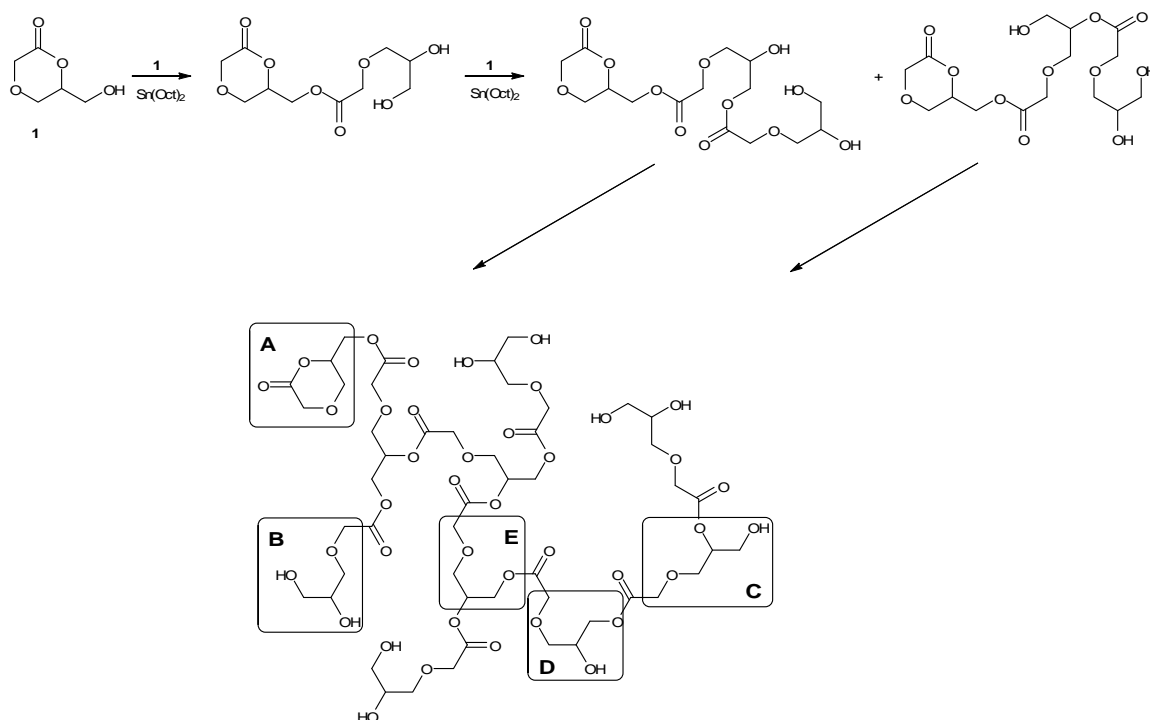
Scheme 1.24. Theoretical structure of poly(5-HDON).

Characterization by MALDI-ToF mass spectrometry showed a relatively small fraction of polymer containing either hydrolyzed 5-HDON or glycerol as the core unit. Comparably high molecular weights ($M_n = 25,000 - 44,000$ g/mol) and low polydispersities ($M_w/M_n = 1.7 - 2.0$) were found by GPC analysis. Detailed investigation by NMR-spectroscopy revealed that use of an anionic initiator (DBU) lead to the incorporation of more dendritic units into the polymer structure. However, extending the reaction time to 72h instead of 24h at increased temperature (110°C instead of 75°C) gave highly branched polymers with the $\text{Sn}(\text{Oct})_2$ catalyst. These observations appear to confirm earlier assumptions about a temperature dependence of the mechanism in question. The authors therefore suggest the predominance of a coordination-insertion mechanism (Scheme 1.25) at lower temperatures. The respective reaction pathway favours the incorporation of linear subunits (C). Higher temperatures and longer reaction times, however, promote $\text{Sn}(\text{Oct})_2$ to act as a transesterification catalyst and hence result in a larger amount of branched structures.



Scheme 1.25. Mechanism of the coordination-insertion polymerization of 5-HDON in the presence of $\text{Sn}(\text{Oct})_2$.

A hyperbranched polyester of closely related structure was prepared by Yu et al. who polymerized 6-hydroxymethyl-1,4-dioxan-2-one (6-HDON) with $\text{Sn}(\text{Oct})_2$ catalyst at elevated temperatures over periods of 1 – 8 days.⁷⁹ Molecular weights were found in the range of 7,800 to 25,600 g/mol with polydispersities between 2.0 and 3.0. The polymers with high molecular weights were only obtained when the catalyst concentration was fixed at 1/400 (molar ratio to feed). Increasing or decreasing the amount of catalyst resulted in lower molecular weights. Degrees of branching were determined by quantitative ^{13}C inverse gated NMR spectrum analysis and found to be 0.4. The polymerization reaction and the different units of the obtained polyesters are illustrated in Scheme 1.26. Terminal units A and B, linear units C and D as well as dendritic units E are present in the polymer structure and can be assigned to the respective signals in the NMR spectra. Like the polyester prepared by Parzuchowski et al. (Scheme 1.24), this polymer consists of glycerol and glycolic acid units, which renders it biodegradable and biocompatible.



Scheme 1.26. Synthesis and structure of poly(6-HDON).

Catalytic ring-opening multibranching polymerizations have become a fitting method for the preparation of hyperbranched polyesters with considerable degrees of polymerization. The accordant high molecular weights are often conveniently accessible because the sensitivity to traces of impurities is less distinct than in cationic or anionic polymerization techniques. Furthermore Pd(0) complexes have been shown to be useful catalysts in the controlled synthesis of hyperbranched polyamines.

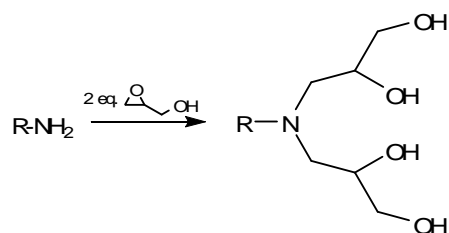
1.2.2 Core-containing Hyperbranched Polymers by Ring-Opening Multibranching Polymerization

Macromolecular encapsulation in dendritic polymers has received broad attention in recent years.⁸⁰⁻⁸⁷ Detailed studies on dendrimers have revealed that at some critical dendrimer generation, the core is encapsulated by the sterically crowded and densely packed branched architecture.^{88,89} It has been demonstrated for perfectly branched dendrimers that the site isolation of a core moiety in a dendritic scaffold is of great interest with respect to optical properties and for catalysis. Within this context, Fréchet et al. introduced a solvatochromic chromophore (4-(*N,N*-dimethylamino)-1-nitrobenzene) at the focal point of a polybenzylether dendrimer.⁹⁰ It has also been shown that manganese and zinc-

porphyrins encapsulated by a dendritic structure exhibit better stability and improved regioselectivity in catalytic processes.^{91,92} Additionally, dendritic encapsulation of active core moieties has been proposed to serve as a model for the shielding of active centers in naturally occurring enzymes.⁹³

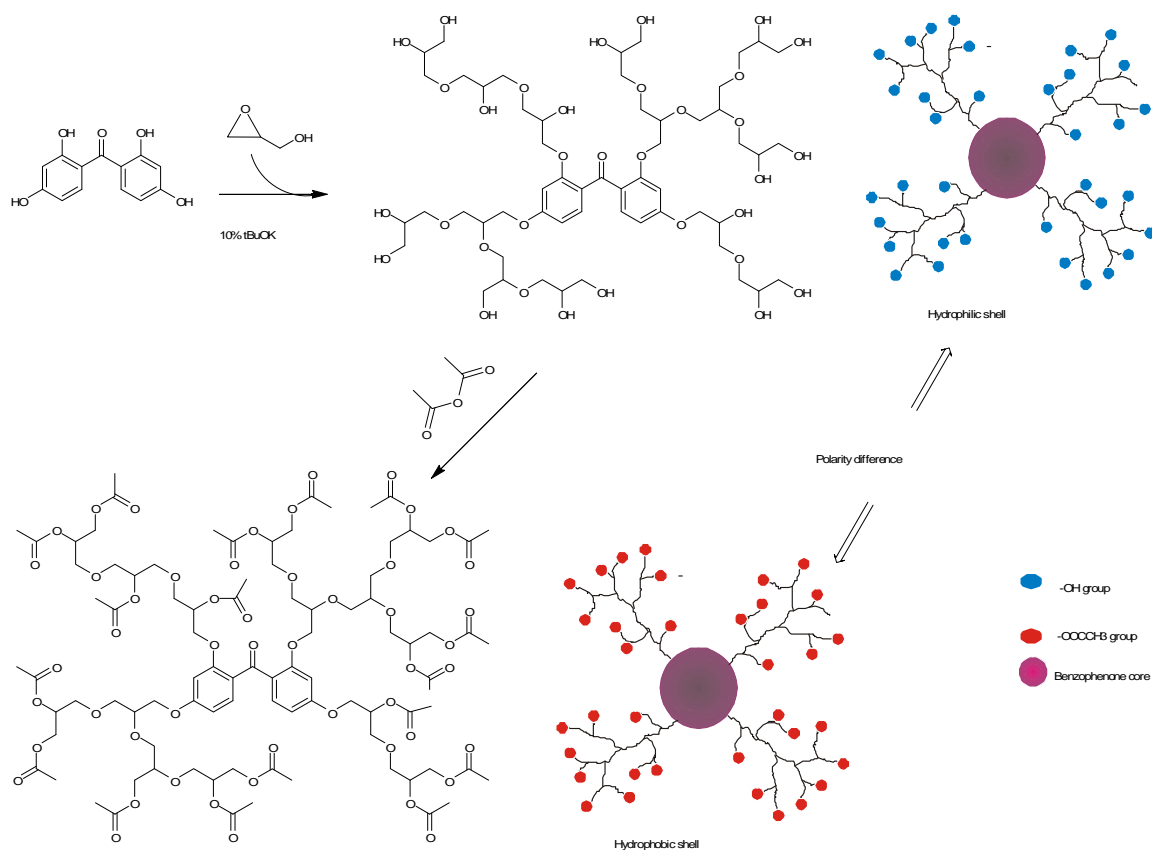
Resembling dendrimers in a majority of their characteristics and being accessible much less tediously, well-defined hyperbranched polymers containing an encapsulated single core moiety have qualified for analogous studies. Tian et al. used a modified triphenylamine as core for the synthesis of a conjugated hyperbranched polymer.⁹⁴ A direct influence of the hyperbranched architecture on both UV-absorption and fluorescence properties of the core was observed. Furthermore, post-polymerization modification of a nitrophenyl ester core, subsequent to the formation of the dendritic structure has been reported.^{95,96}

Competing homopolymerization of the branched monomer is an often disregarded reaction in the synthesis of core-containing hyperbranched polymers. For simple statistical reasons, the majority of the hyperbranched macromolecules are unlikely to possess a core unit in a conventional B_n/AB_m -type copolycondensation. In a very elegant study, Žagar and Žigon demonstrated this in 2002 for commercially available hyperbranched polyesters (Boltorn) obtained from an AB_2 monomer and B_3 functional core molecule.⁹⁷ Unequivocal evidence of the incorporation of a specific core into all species present in the distribution of a hyperbranched structure can only be given by mass spectrometry, usually MALDI-ToF MS. We recently studied the incorporation of different initiator cores into hyperbranched polyglycerols under the previously described SMA conditions.⁹⁸ The employed cores were structurally different, including mono- and bifunctional n -alkyl amines as well as photoactive cores, such as benzylamine and 1-naphthylmethylamine and a typical triplet photosensitizer, 2,2',4,4'-tetrahydroxy benzophenone $BP(OH)_4$. Bisglycidolization of the amines prior to polymerization (Scheme 1.27) was found to result in improved molecular weight control ($M_n = 1600$ to 8400 g/mol) and polydispersity ($1.5 < M_w/M_n < 2.5$).



Scheme 1.27. Bisglycidolization of the amine initiator-cores.

The macromolecules obtained from polymerization of glycidol initiated by the tetrahydroxyfunctional benzophenone BP(OH)₄ were of narrow polydispersity ($1.5 < M_w/M_n < 2$) and exhibited molecular weights between 1,500 and 5,800 g/mol. The phenolic nature of the initiator hydroxyl groups and the facile deprotonation of this core led to fast and complete incorporation into the growing hyperbranched polymers. The applied synthetic strategy is depicted in Scheme 1.28.



Scheme 1.28. Synthetic approach for the incorporation of a benzophenone core into hyperbranched polyglycerols and peracetylation of the obtained polymer.

Complete incorporation of the photoactive core moiety into the well-defined hyperbranched structure was conclusively evidenced by MALDI-ToF mass spectrometry. Figure 1.1 shows the central part of the MALDI-ToF mass spectrum (between 500 and 3,000 g/mol) of a benzophenone core containing polymer with 80 glycidol units.

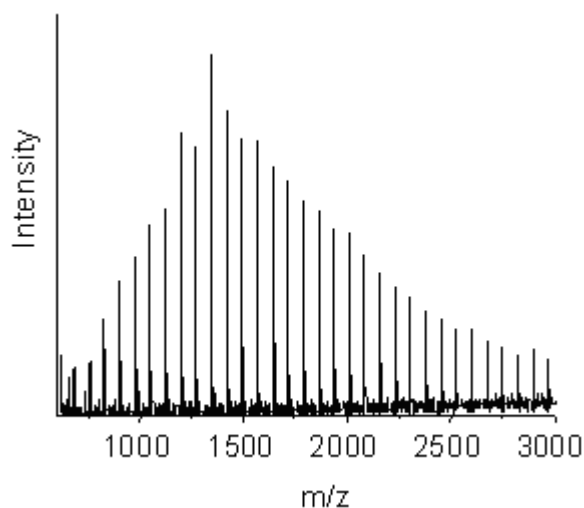


Figure 1.1. MALDI-ToF mass spectrum of benzophenone-cored hyperbranched polyglycerol.

The molar mass of the glycidol units ($M = 74.1$) is represented by the mass differences between the peaks. The mass of each signal in the molecular weight distribution corresponds to the sum of the mass of the benzophenone core and the mass of the respective number of glycidol repeating units plus one lithium ion (attached to the polymer upon the ionization process in the instrument). Only a single distribution mode can be observed, verifying the absence of masses corresponding to non-core containing polyglycerol-homopolymers and therefore proving the quantitative incorporation of the initiator core. The benzophenones substituted with a hyperbranched PG-corona showed high photostability even after prolonged irradiation in methanol. Such polymer encapsulated benzophenones can be conveniently separated from the reaction media by dialysis or membrane filtration and hence represent very promising materials with respect to application as easily-recoverable and reusable photocatalysts.

1.3 Conclusions

In this chapter it has been demonstrated that ring-opening multibranching polymerizations are well-established as a versatile and often preferential method for the controlled synthesis of well-defined hyperbranched polymers with moderate polydispersity. The heterocyclic monomers discussed in the precedent text generally represent latent AB_m monomers eligible for pseudo chain growth (polymerization by ring-opening = chain growth, condensation of the pending B group with the heterocycle = step growth). A major advantage of ring-opening polymerizations compared to conventional polycondensa-

tions is the generic absence of condensation products. This inherent characteristic allows for the application of cationic, anionic and catalytic polymerization techniques in the initiated polymerization of suitable cyclic monomers, using functional initiators to achieve remarkable control over molecular weights and polydispersity. Employing slow monomer addition conditions, pseudo chain growth was realized for glycidol, permitting a certain extent of control over molecular weights.

Understanding and controlling the branching pattern as well as molar mass represents an important issue for the elucidation of structure property correlations as well as the assembly of more complex polymer architectures using ring-opening multibranching polymerizations.

However, presently there exist only few examples of hyperbranched materials with elevated molecular weights exceeding 10,000 g/mol. Additionally, the number of publications on amphiphilic hyperbranched block copolymer structures and on their biomedical applications is very limited. Consequently the thesis at hand embraces these topics and explores challenges as well as the intriguing potential and possible applications.

1.4 References

1. Flory, P. J. *J. Am. Chem. Soc.* **1952**, 74, 2718.
2. Kim, Y. H., Webster, O. W. *Polym. Prepr. (Am. Chem. Soc. Div. Polym. Chem.)* **1988**, 29, 310.
3. Kim, Y. H.; Webster, O. W. *J. Am. Chem. Soc.* **1990**, 112, 4592.
4. Kim, Y. H. *J. Polym. Sci., Part a: Polym. Chem.* **1998**, 36, 1685-1698.
5. Sunder, A.; Heinemann, J.; Frey, H. *Chem. Eur. J.* **2000**, 6, 2499-2506.
6. Voit, B. *J. Polym. Sci., Part A: Polym. Chem.* **2000**, 38, 2505-2525.
7. Jikei, M.; Kakimoto, M. *Prog. Polym. Sci.* **2001**, 26, 1233-1285.
8. Yates, C. R.; Hayes, W. *Eur. Polym. J.* **2004**, 40, 1257-1281.
9. Gao, C.; Yan, D. *Prog. Polym. Sci.* **2004**, 29, 183-275.
10. Wilms, D.; Nieberle, J.; Frey, H., Ring-Opening Multibranching Polymerization. In *Hyperbranched Polymers*, Frey, H.; Yan, D.; Gao, C., Eds. Wiley VCH: Weinheim and New York, 2007.
11. Voit, B. I. *Acta Polym.* **1995**, 46, 87-99.
12. Fréchet, J. M. J.; Henmi, M.; Gitsov, I.; Aoshima, S.; Leduc, M. R.; Grubbs, R. B. *Science* **1995**, 269, 1080-1083.

13. Hawker, C. J.; Fréchet, J. M. J.; Grubbs, R. B.; Dao, J. *J. Am. Chem. Soc.* **1995**, 117, 10763-10764.
14. Sandler, S. R.; Berg, F. R. *J. Polym. Sci., Part a: Polym. Chem.* **1966**, 4, 1253.
15. Vandenberg, E. J. *J. Polym. Sci., Part A: Polym. Chem.* **1985**, 23, 915.
16. Tokar, R.; Kubisa, P.; Penczek, S.; Dworak, A. *Macromolecules* **1994**, 27, 320-322.
17. Dworak, A.; Walach, W.; Trzebicka, B. *Macromol. Chem. Phys.* **1995**, 196, 1963-1970.
18. Sunder, A.; Hanselmann, R.; Frey, H.; Mülhaupt, R. *Macromolecules* **1999**, 32, 4240-4246.
19. Sunder, A.; Frey, H.; Mülhaupt, R. *Macromol. Symp.* **2000**, 153, 187-196.
20. Sunder, A.; Mülhaupt, R.; Haag, R.; Frey, H. *Advanced Materials* **2000**, 12, 235-+.
21. Suzuki, M.; Ii, A.; Saegusa, T. *Macromolecules* **1992**, 25, 7071.
22. Hauser, M., Alkylene Imines. In *Ring-Opening Polymerization*, Frisch, K. C.; Reegen, S. L., Eds. Marcel Dekker: New York, 1969.
23. Dick, R. C.; Ham, G. E. *Macromol. Sci.* **1970**, A4, 1301.
24. van de Velde, M.; Goethals, E. J. *Macromol. Chem. Macromol. Symp.* **1986**, 6, 271.
25. Baklouti, M.; Chaabouni, R.; Sledz, J.; Schue, F. *Polym. Bull.* **1989**, 21, 243.
26. Vandenberg, E. J.; Mullis, J. C.; Juvet, R. S., Jr. *J. Polym. Sci., Part a: Polym. Chem.* **1989**, 27, 3083.
27. Vandenberg, E. J.; Mullis, J. C.; Juvet, R. S., Jr.; Miller, T.; Nieman, R. A. *J. Polym. Sci., Part a: Polym. Chem.* **1989**, 27, 3113.
28. Bednarek, M.; Biedron, T.; Helinski, J.; Kaluzynski, K.; Kubisa, P.; Penczek, S. *Macromol. Rapid Commun.* **1999**, 20, 369-372.
29. Yan, D. Y.; Hou, J.; Zhu, X. U.; Kosman, J. J.; Wu, H. S. *Macromol. Rapid Commun.* **2000**, 21, 557-561.
30. Magnusson, H.; Malmström, E.; Hult, A. *Macromol. Rapid Commun.* **1999**, 20, 453-457.
31. Magnusson, H.; Malmström, E.; Hult, A. *Macromolecules* **2001**, 34, 5786-5791.
32. Xu, Y. Y.; Gao, C.; Kong, H.; Yan, D. Y.; Luo, P.; Li, W. W.; Mai, Y. Y. *Macromolecules* **2004**, 37, 6264-6267.
33. Farthing, A. C. *J. Chem. Soc.* **1955**, 3648.
34. Dreyfuss, M. D.; Westphal, J.; Dreyfuss, P. *Macromolecules* **1968**, 1.
35. Bednarek, M.; Kubisa, P. *J. Polym. Sci. Part A: Polym. Chem.* **2006**, 44, 6484-6493.
36. Rider, T. H.; Hill, A. J. *J. Am. Chem. Soc.* **1930**, 52, 1521.

37. Patten, T. E.; Matyjaszewski, K. *Adv. Mater.* **1998**, 10, 901-+.
38. Endo, M.; Aida, T.; Inoue, S. *Macromolecules* **1987**, 26, 2983.
39. Bailey, F. E.; Koleske, V., Alkylene Oxides and their Polymers. In *Surface Science Series*, Schick, M. J.; Fowkes, F. M., Eds. Marcel Dekker: New York, 1990; Vol. 35, p 35.
40. Radke, W.; Litvinenko, G.; Müller, A. H. E. *Macromolecules* **1998**, 31, 239-248.
41. Hanselmann, R.; Hölter, D.; Frey, H. *Macromolecules* **1998**, 31, 3790-3801.
42. Kainthan, R. K.; Muliawan, E. B.; Hatzikiriakos, S. G.; Brooks, D. E. *Macromolecules* **2006**, 39, 7708-7717.
43. Kainthan, R. K.; Janzen, J.; Levin, E.; Devine, D. V.; Brooks, D. E. *Biomacromolecules* **2006**, 7, 703-709.
44. Sunder, A.; Mülhaupt, R.; Haag, R.; Frey, H. *Macromolecules* **2000**, 33, 253-254.
45. Rokicki, G.; Rakoczy, P.; Parzuchowski, P.; Sobiecki, M. *Green Chemistry* **2005**, 7, 529-539.
46. Amass, A. J.; Perry, M. C.; Riat, D. S.; Tighe, B. J.; Colclough, E.; Stewart, M. J. *Eur. Polym. J.* **1994**, 30, 641-646.
47. Takeuchi, D.; Aida, T. *Macromolecules* **1996**, 29, 8096-8100.
48. Nayak, U. G.; Whistler, R. L. *J. Org. Chem.* **1968**, 33.
49. Mudryk, B.; Cohen, T. *J. Org. Chem.* **1989**, 54, 5657.
50. Smith, T. J.; Mathias, L. J. *Polymer* **2002**, 43, 7275-7278.
51. Mülhaupt, R. *Macromol. Chem. Phys.* **2003**, 204, 289-327.
52. Ziegler, K.; Holzkamp, E.; Breil, H.; Martin, H. *Angew. Chem.* **1955**, 67, 426.
53. Ziegler, K. *Angew. Chem.* **1964**, 76, 545.
54. Natta, G. *Science* **1965**, 147, 261.
55. Grubbs, R. H., *Handbook of Metathesis*. Wiley-VCH: New York, 2003.
56. Lundberg, R. D.; Cox, E. F., In *Ring-Opening Polymerization*, Risch, K. C.; Reegen, S. L., Eds. Marcel Dekker: New York, London, 1969; Vol. 6, p 266.
57. Löfgren, A.; Albertsson, A.-C.; Dubois, P.; Jérôme, R., Recent Advances in Ring-Opening Polymerization of Lactones and Related Compounds. *J. Macromol. Sci. Rev. Macromol. Chem. Phys.* 1995, p 379.
58. Kricheldorf, H. R.; Sumbel, M. *Eur. Polym. J.* **1991**, 25, 585.
59. Kricheldorf, H. R.; Boettcher, C. *Makromol. Chem.* **1993**, 194, 1653.
60. Suzuki, M.; Sawada, S.; Saegusa, T. *Macromolecules* **1989**, 22, 1507.

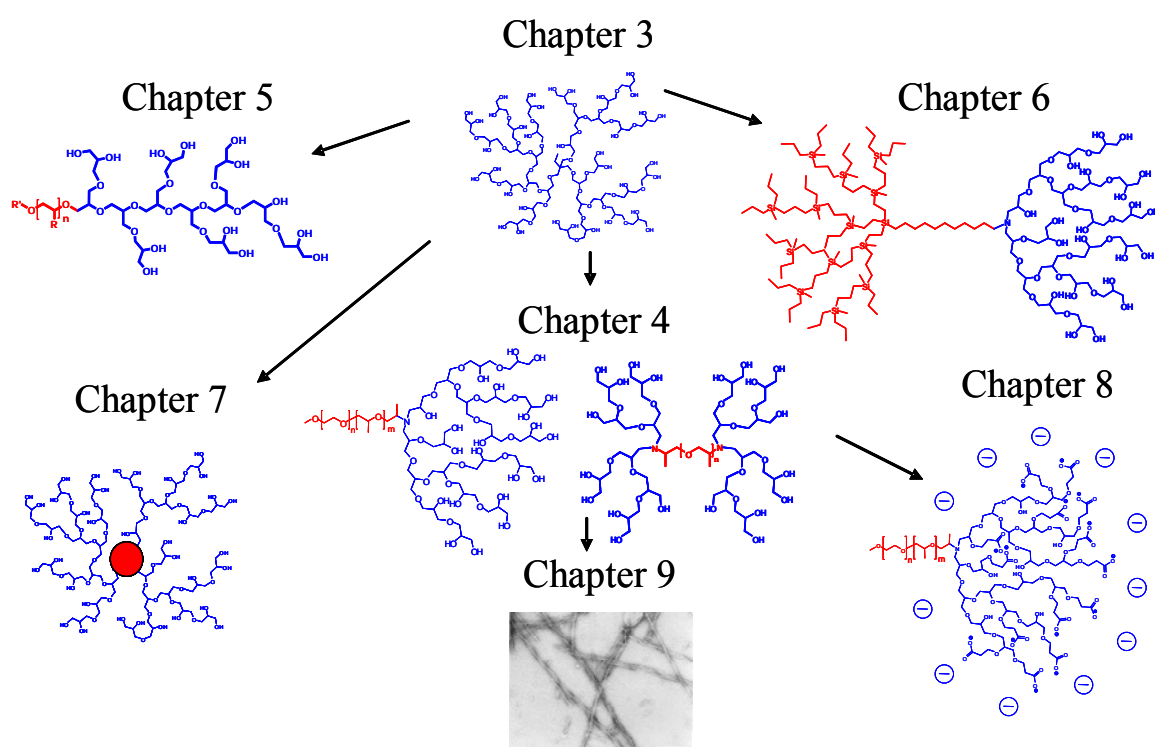
61. Suzuki, M.; Yoshida, S.; Shiraga, K.; Saegusa, T. *Macromolecules* **1998**, 31, 1716-1719.
62. Leenslag, J. W.; Pennings, A. J. *Makromol. Chem.* **1987**, 188, 1809.
63. Schwach, G.; Coudane, J.; Engel, R.; Vert, M. *J. Polym. Sci., Part A: Polym. Chem.* **1997**, 35, 3431-3440.
64. Schindler, A.; Hibionada, Y. M.; Pitt, C. G. *J. Polym. Sci., Part a: Polym. Chem.* **1982**, 20, 319.
65. Kim, S. H.; Han, Y.; Kim, Y. H.; Hong, S. I. *Makromol. Chem.* **1992**, 193, 1623.
66. Du, Y. J.; Lemstra, P. J.; Nijenhuis, A. J.; Vanaert, H. A. M.; Bastiaansen, C. *Macromolecules* **1995**, 28, 2124-2132.
67. Kricheldorf, H. R.; Kreisersaunders, I.; Boettcher, C. *Polymer* **1995**, 36, 1253-1259.
68. Storey, R. F.; Taylor, A. E. *J. Macromol. Sci., Pure Appl. Chem.* **1998**, A35, 723-750.
69. Kowalski, A.; Libiszowski, J.; Duda, A.; Penczek, S. *Polym. Prepr. (Am. Chem. Soc., Div. Polym. Chem.)* **1998**, 39, 74.
70. Kowalski, A.; Duda, A.; Penczek, S. *Macromol. Rapid Commun.* **1998**, 19, 567-572.
71. Kowalski, A.; Duda, A.; Penczek, S. *Macromolecules* **2000**, 33, 689-695.
72. Duda, A.; Penczek, S.; Kowalski, A.; Libiszowski, J. *Macromol. Symp.* **2000**, 153, 41-53.
73. Kowalski, A.; Libiszowski, J.; Duda, A.; Penczek, S. *Macromolecules* **2000**, 33, 1964-1971.
74. Kricheldorf, H. R.; Kreiser-Saunders, I.; Stricker, A. *Macromolecules* **2000**, 33, 702-709.
75. Liu, M. J.; Vladimirov, N.; Fréchet, J. M. J. *Macromolecules* **1999**, 32, 6881-6884.
76. Trollsas, M.; Hedrick, J. L.; Mecerreyes, D.; Dubois, P.; Jerome, R.; Ihre, H.; Hult, A. *Macromolecules* **1998**, 31, 2756-2763.
77. Veld, P. J. A. I.; Velner, E. M.; VanDeWitte, P.; Hamhuis, J.; Dijkstra, P. J.; Feijen, J. *J. Polym. Sci., Part a: Polym. Chem.* **1997**, 35, 219-226.
78. Parzuchowski, P. G.; Grabowska, M.; Tryznowski, M.; Rokicki, G. *Macromolecules* **2006**, 39, 7181-7186.
79. Yu, X. H.; Feng, J.; Zhuo, R. X. *Macromolecules* **2005**, 38, 6244-6247.
80. Newkome, G. R.; Moorefield, C. N.; Vögtle, F., In *Dendritic Molecules: Concepts, Synthesis, Perspectives*, VCH: Weinheim, 1996.
81. Newkome, G. R.; He, E. F.; Moorefield, C. N. *Chem. Rev.* **1999**, 99, 1689-1746.

82. Fischer, M.; Vögtle, F. *Angew. Chem. Int. Ed.* **1999**, 38, 885-905.
83. Bosman, A. W.; Jansen, H. M.; Meijer, E. W. *Chem. Rev.* **1999**, 99, 1665.
84. Hecht, S.; Fréchet, J. M. J. *Angew. Chem. Int. Ed.* **2001**, 40, 74-91.
85. Gorman, C. B.; Smith, J. C. *Acc. Chem. Res.* **2001**, 34, 60-71.
86. Grayson, S. M.; Fréchet, J. M. J. *Chem. Rev.* **2001**, 101, 3819.
87. Cameron, C. S.; Gorman, C. B. *Adv. Funct. Mater.* **2002**, 12, 17-20.
88. Tomalia, D. A.; Naylor, A. M.; Goddard, I., W. A. *Angew. Chem. Int. Ed.* **1990**, 29, 138.
89. Devadoss, C.; Bharathi, P.; Moore, J. S. *Angew. Chem. Int. Ed.* **1997**, 36, 1633-1635.
90. Hawker, C. J.; Wooley, K. L.; Fréchet, J. M. J. *J. Am. Chem. Soc.* **1993**, 115, 4375.
91. Bhyrappa, P.; Young, J. K.; Moore, J. S.; Suslick, K. S. *J. Am. Chem. Soc.* **1996**, 118, 5708-5711.
92. Vestberg, R.; Nystrom, A.; Lindgren, M.; Malmström, E.; Hult, A. *Chem. Mater.* **2004**, 16, 2794-2804.
93. Smith, D. K.; Diederich, F. *Chem. Eur. J.* **1998**, 4, 1353-1361.
94. Hua, J. L.; Li, B.; Meng, F. S.; Ding, F.; Qian, S. X.; Tian, H. *Polymer* **2004**, 45, 7143.
95. Gittins, P. J.; Alston, J.; Ge, Y.; Twyman, L. J. *Macromolecules* **2004**, 37, 7428-7431.
96. Gittins, P. J.; Twyman, L. J. *J. Am. Chem. Soc.* **2005**, 127, 1646-1647.
97. Zagar, E.; Zigon, M. *Macromolecules* **2002**, 35, 9913-9925.
98. Pastor-Perez, L.; Barriau, E.; Berger-Nicoletti, E.; Kilbinger, A. F. M.; Perez-Prieto, J.; Frey, H.; Stiriba, S. E. *Macromolecules* **2008**, 41, 1189-1195.

2 Objectives

2.1 Introduction

Among hyperbranched polymers, polyglycerol is one of the most promising and commonly used macromolecules due to its biocompatibility¹ and versatility. Intense efforts have been undertaken to thoroughly characterize these molecules and optimize the synthetic pathway.²⁻⁹ Selective modifications of the multiple end groups have revealed remarkable potential for applications such as liquid-crystalline materials,^{10,11} hydrogels,¹² polyelectrolytes¹³ and hybrid materials for biomineralization.^{14,15} However, the synthesis of high molecular weight polyglycerols still involves many intricacies. Furthermore, only few complex structures like star¹⁶⁻²³ or block copolymers^{24,25} incorporating polyglycerol have been realized so far. Particularly biocompatible block copolymers are considered promising candidates for biomedical applications.²⁶



Scheme 2.1. General scope of this thesis: “Hyperbranched polyglycerols as building blocks for complex amphiphilic structures: Synthesis, characterization and biomedical applications”.

Therefore, the scope of this thesis (Scheme 2.1) is the enhancement of the synthetic process leading to polyglycerols derivatives which implies improved molecular weight control for a broad molecular weight range as well as the assembly of more complex structures like amphiphilic block copolymers. The latter will be investigated in terms of their biomedical properties.

2.2 Progress in Polyglycerol Synthesis

Polyglycerols with molecular weights of up to 2,000 g/mol can be reproducibly synthesized with good molecular weight control and narrow polydispersities by anionic ring-opening multibranching polymerization (ROMBP), applying the slow monomer addition technique,⁵⁻⁹ as well as by cationic polymerization.^{3,4} Although polyglycerols with higher molecular weights (up to 20,000g/mol) and even very high molecular weight polyglycerols (50,000-100,000g/mol) have been realized, either molecular weight distribution or molecular weight control were uncontrollable in these cases. Consequently, chapter 3 will focus on the achievement of improved control over molar masses and narrow polydispersities for the obtained materials. In order to understand the occurring problems, different solvents will be tested. Furthermore the influence of the degree of deprotonation of the initiating core molecule will be examined in detail. Continuous addition of the afforded base as well as the development of a two step synthetic pathway using well defined low molecular weight polyglycerols as macroinitiators will be described. Additionally, continuous spin fractionation will be applied to lower the polydispersity of broadly distributed polyglycerols.

2.3 Amphiphilic Linear-Hyperbranched Block Copolymers

Amphiphilic linear-linear diblock copolymers as well as the corresponding triblock copolymers have been of broad interest for a long time.²⁷ Examples for well-established and studied systems are PEO-*b*-PPO-*b*-PEO, known as Pluronics (BASF)^{28,29} or Poloxamer, PEO-*b*-PHB-*b*-PEO,³⁰ PS-*b*-PAA,³¹ PS-*b*-PMMA-*b*-PAA,³² PS-*b*-PB-anh.³³ The fact that linear and dendritic polymers significantly differ in their physical and chemical properties motivates the combination of these two macromolecular structure units. To date, various linear-dendritic structures have been realized, showing fascinating phase behavior due to their self assembly and solvent interactions.³⁴⁻³⁹ Especially biocompatible amphiphilic block copolymers offer various applications.⁴⁰ Based on the ROMBP (highlighted in chapter 1), glycidol was polymerized onto amine end functionalized linear ali-

phatic chains as macroinitiators after a preliminary bisglycidolization step.^{24,41} Although attachment of glycidol to the linear starting molecules was evidenced, control over molecular weights and polydispersities remained a challenge to overcome. In chapter 4 the knowledge acquired within the context of the work covered in chapter 1 will be applied to achieve molecular weight control for more complex structures, namely amphiphilic AB and ABA block copolymers consisting of linear PPO and hyperbranched PG blocks. Furthermore the improved methodology will be adopted for linear amine end functionalized alkyl chains as initiator cores. An existing double bond will provide access to various block copolymers via hydrosilylation reaction.

2.4 Novel Monomer for Non Nitrogen Containing Linear-Hyperbranched Block Copolymers

A convenient 3-step strategy for the synthesis of well-defined amphiphilic, linear hyperbranched block copolymers, namely *linear-polystyrene-block-(1,2-polybutadiene-hypergrafted-polyglycerol)*²⁵ and *linear-polyisoprene-block-(hyperbranched-polyglycerol)*⁴² was developed. In chapter 5 a novel monomer for anionic polymerization, 2,2-dimethyl-4-oxiranylmethoxymethyl-[1,3]dioxolane, was synthesized. The homopolymerization as well as the polymerization onto commercially available poly(ethylene oxide)s forming a second block, will be discussed. Removal of the acetyl protecting groups leads to novel linear poly(glyceryl glycerol) (PGG) blocks. These polymers will be described in chapter 5.

2.5 Amphiphilic Hyperbranched-Hyperbranched Block Copolymers

Well-defined amphiphilic block copolymers with two hyperbranched blocks of different polarity have not been reported to date. The aim of chapter 6 is to broaden the insight into the relationship between structure and amphiphilic properties by preparing and analyzing a block copolymer with two different branched blocks: one block with hydrophilic and one block with hydrophobic properties. For the hydrophilic part, *hb*-polyglycerol will be chosen. Recently our group reported the attachment of hyperbranched polycarbosilanes to a double bond containing a PS-PB core.⁴³ On this account the hydrophobic part will be obtained by hydrosilylation reaction of an AB₂-carbosi-lane monomer in the presence of a functional core. The synthesis of a low molecular weight multifunctional

core by facile organic synthesis steps, permitting the efficient attachment of both polymer blocks will be presented in this chapter. The obtained hyperbranched-hyperbranched block copolymers will be investigated in detail.

2.6 Negatively Charged Linear-Hyperbranched Block Copolymer Polyelectrolytes

The preparation of carboxylated hyperbranched polyglycerols, carried out by post-modification of the hydroxyl groups via Michael addition of acrylonitrile followed by hydrolysis, has recently been reported by our group.¹³ Applying this method to the previously synthesized amphiphilic block copolymers will lead to extraordinary structures. This approach will be presented in chapter 7.

2.7 Amino Acid Based Core Initiators for Polymerization of Glycidol and L-Lactide

Besides glycerine, lactides as well as amino acids represent well known repeat units for biomedical polymers. Therefore connecting these biocompatible polymers is an interesting approach that is very promising in terms of novel biocompatible structures. Chapter 8 will cover the incorporation of morpholinone derivatives based on bisglycidolized amino acids as core initiators for the further anionic ROMBP of glycidol as well as the catalytic polymerization of lactone.

2.8 Influences of Amphiphilic Polyglycerol Block Copolymers on Insulin Fibril Formation

Insulin is a small protein hormone that is crucial for the control of glucose metabolism and in diabetes treatment. Upon exposure to elevated temperatures, low pH, organic solvents and agitation, insulin is susceptible to fibril formation.⁴⁴ Nonionic surfactants like polysorbates (commercially known as Tween[®]) were found useful to improve the handling of proteins, permitting a higher degree of stability and safety upon processing, storage and use of the protein drug.⁴⁵ Dendrimers were shown to have similar effects on protein fibrillation.⁴⁶ Combining these types of structures, the influence of the polyglycerol-based amphiphiles (described in chapter 4) on the fibril formation will be studied by Thioflavin T fluorescence and presented in chapter 9.

2.9 References

1. Kainthan, R. K.; Janzen, J.; Levin, E.; Devine, D. V.; Brooks, D. E. *Biomacromolecules* **2006**, 7, 703-709.
2. Vandenberg, E. J. *J. Polym. Sci., Part A: Polym. Chem.* **1985**, 23, 915.
3. Tokar, R.; Kubisa, P.; Penczek, S.; Dworak, A. *Macromolecules* **1994**, 27, 320-322.
4. Dworak, A.; Walach, W.; Trzebicka, B. *Macromol. Chem. Phys.* **1995**, 196, 1963-1970.
5. Sunder, A.; Hanselmann, R.; Frey, H.; Mülhaupt, R. *Macromolecules* **1999**, 32, 4240-4246.
6. Sunder, A.; Frey, H.; Mülhaupt, R. *Macromol. Symp.* **2000**, 153, 187-196.
7. Sunder, A.; Mülhaupt, R.; Haag, R.; Frey, H. *Adv. Mater.* **2000**, 12, 235-239.
8. Kautz, H.; Sunder, A.; Frey, H. *Macromol. Symp.* **2001**, 163, 67-73.
9. Kainthan, R. K.; Muliawan, E. B.; Hatzikiriakos, S. G.; Brooks, D. E. *Macromolecules* **2006**, 39, 7708-7717.
10. Sunder, A.; Quincy, M. F.; Mülhaupt, R.; Frey, H. *Angew. Chem. Int. Ed.* **1999**, 38, 2928-2930.
11. Erber, M. G., L.; Kirsten, J.; Nieberle, Gehringer, L., J.; Donnio, B.; Frey, H. *submitted* **2007**.
12. Oudshoorn, M. H. M.; Rissmann, R.; Bouwstra, J. A.; Hennink, W. E. *Biomaterials* **2006**, 27, 5471-5479.
13. Barriau, E.; Frey, H.; Kiry, A.; Stamm, M.; Gröhn, F. *Colloid Polym. Sci.* **2006**, 284, 1293-1301.
14. Balz, M.; Barriau, E.; Istratov, V.; Frey, H.; Tremel, W. *Langmuir* **2005**, 21, 3987-3991.
15. Frey, H.; Shen, Z.; Barriau, E.; Loges, N.; Balz, M.; Tremel, W. *Abstracts of Papers of the American Chemical Society* **2006**, 231, -.
16. Sunder, A.; Mülhaupt, R.; Frey, H. *Macromolecules* **2000**, 33, 309-314.
17. Sunder, A.; Frey, H.; Mülhaupt, R. *Abstracts of Papers of the American Chemical Society* **1999**, 217, U458-U458.
18. Sunder, A.; Turk, H.; Haag, R.; Frey, H. *Macromolecules* **2000**, 33, 7682-7692.
19. Burgath, A.; Sunder, A.; Neuner, I.; Mülhaupt, R.; Frey, H. *Macromol. Chem. Phys.* **2000**, 201, 792-797.
20. Gottschalk, C.; Wolf, F.; Frey, H. *Macromol. Chem. Phys.* **2007**, 208, 1657-1665.

21. Maier, S.; Sunder, A.; Frey, H.; Mülhaupt, R. *Macromol. Rapid Commun.* **2000**, 21, 226-230.
22. Chen, Y.; Shen, Z.; Barriau, E.; Kautz, H.; Frey, H. *Biomacromolecules* **2006**, 7, 919-926.
23. Shen, Z.; Chen, Y.; Barriau, E.; Frey, H. *Macromol. Chem. Phys.* **2006**, 207, 57-64.
24. Istratov, V.; Kautz, H.; Kim, Y. K.; Schubert, R.; Frey, H. *Tetrahedron* **2003**, 59, 4017-4024.
25. Barriau, E.; Marcos, A. G.; Kautz, H.; Frey, H. *Macromol. Rapid Commun.* **2005**, 26, 862-867.
26. Demina, T.; Grozdova, I.; Krylova, O.; Zhirnov, A.; Istratov, V.; Frey, H.; Kautz, H.; Melik-Nubarov, N. *Biochemistry* **2005**, 44, 4042-4054.
27. Lodge, T. P. *Macromol. Chem. and Phys.* **2003**, 204, 265-273.
28. Michels, B.; Waton, G.; Zana, R. *Langmuir* **1997**, 13, 3111-3118.
29. Marinov, G.; Michels, B.; Zana, R. *Langmuir* **1998**, 14, 2639-2644.
30. Li, J.; Li, X.; Ni, X. P.; Leong, K. W. *Macromolecules* **2003**, 36, 2661-2667.
31. Zhang, L. F.; Shen, H. W.; Eisenberg, A. *Macromolecules* **1997**, 30, 1001-1011.
32. Yu, G. E.; Eisenberg, A. *Macromolecules* **1998**, 31, 5546-5549.
33. Breulmann, M.; Förster, S.; Antonietti, M. *Macromol. Chem. Phys.* **2000**, 201, 204-211.
34. Gitsov, I.; Frechet, J. M. J. *Macromolecules* **1994**, 27, 7309-7315.
35. van Hest, J. C. M.; Delnoye, D. A. P.; Baars, M. W. P. L.; van Genderen, M. H. P.; Meijer, E. W. *Science* **1995**, 268, 1592-1595.
36. Roman, C.; Fischer, H. R.; Meijer, E. W. *Macromolecules* **1999**, 32, 5525-5531.
37. Cho, B. K.; Jain, A.; Nieberle, J.; Mahajan, S.; Wiesner, U.; Gruner, S. M.; Turk, S.; Rader, H. J. *Macromolecules* **2004**, 37, 4227-4234.
38. Cho, B. K.; Jain, A.; Mahajan, S.; Ow, H.; Gruner, S. M.; Wiesner, U. *J. Am. Chem. Soc.* **2004**, 126, 4070-4071.
39. Gitsov, I.; Zhu, C. *Journal of the American Chemical Society* **2003**, 125, 11228-11234.
40. Lambrych, K. R.; Gitsov, I. *Macromolecules* **2003**, 36, 1068-1074.
41. Nieberle, J. *Diploma Thesis* **2004**.
42. Barriau, E. Hyperbranched Polyether Polyols As Building Blocks For Complex Macromolecular Architectures. PhD, Johannes Gutenberg-Universität, Mainz, 2005.

43. Marcos, A. G.; Pusel, T. M.; Thomann, R.; Pakula, T.; Okrasa, L.; Geppert, S.; Gronski, W.; Frey, H. *Macromolecules* **2006**, *39*, 971-977.
44. Brange, J.; Andersen, L.; Laursen, E. D.; Meyn, G.; Rasmussen, E. *J. Pharm. Sci.* **1997**, *86*, 517-525.
45. Bam, N. B.; Cleland, J. L.; Yang, J.; Manning, M. C.; Carpenter, J. F.; Kelley, R. F.; Randolph, J. W. *J. Pharm. Sci.* **1998**, *87*, 1554-1559.
46. Heegaard, P. M. H.; Boas, U.; Otzen, D. E. *Macromolecular Bioscience* **2007**, *7*, 1047-1059.

3. Progress in Polyglycerol Synthesis

3.1 Introduction

During the last decade intense efforts have been undertaken targeting the preparation of hyperbranched polymers with control over molecular weight and degree of branching. It has been known for a long time that polycondensation of AB_m monomers leads to hyperbranched polymers with broad molecular weight distributions.¹ An alternative strategy avoiding an uncontrolled polymerization reaction is based on the slow addition of suitable latent AB_m (mostly AB_2) monomers. In the family of oxiranes, glycidol can be considered as a highly reactive monomer with latent AB_2 -monomer structure. This compound has been studied with respect to the preparation of linear polyethers over the past 40 years by different groups.^{2,3} Vandenberg et al. published the first work on the characterization of these polymeric materials, briefly discussing the branched polymer topology and gave a first assignment of NMR-signals typical of branching points.⁴ In the mid-1990ies, Penczek and Dworak presented the preparation of hyperbranched polyether polyols by cationic ring-opening polymerization of glycidol.^{5,6} Based on the slow monomer addition (SMA) approach, glycidol was successfully polymerized via anionic ring-opening polymerization of the monomer onto a partially deprotonated multifunctional alcohol (1,1,1-tris(hydroxymethyl)propane, TMP) as initiator core in 1999.⁷⁻⁹ The resulting hyperbranched structure is shown in Figure 3.1.

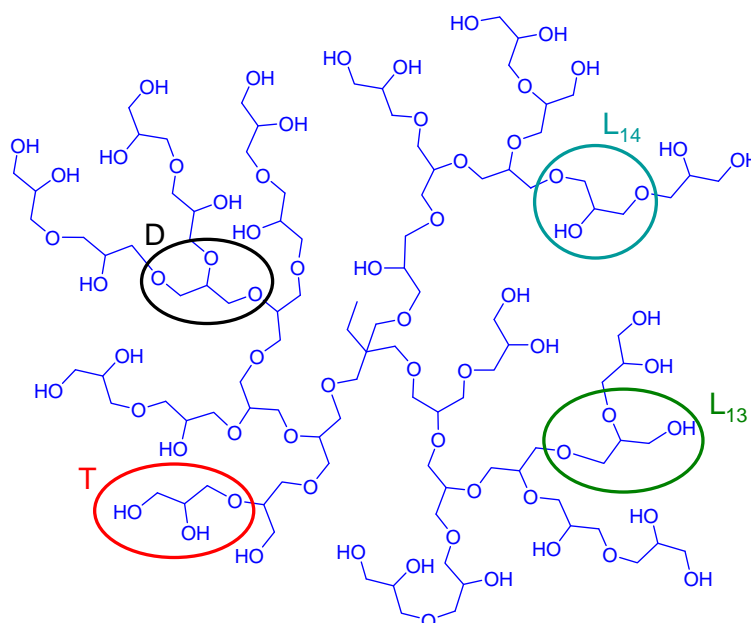
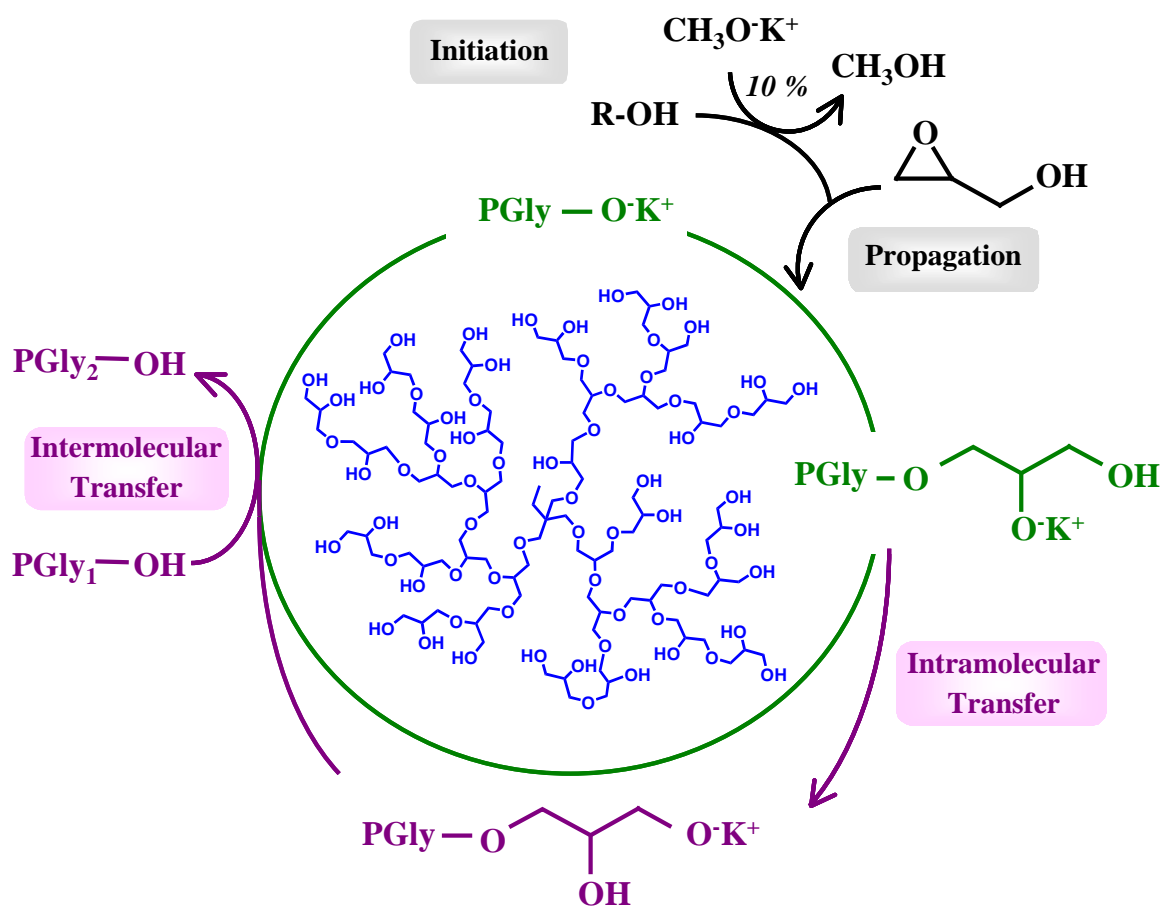


Figure 3.1. Structure of hyperbranched polyglycerol ($DP_n = 32$, $M_n = 2,500$ g/mol).

Activity of all potential propagation sites of the growing polyfunctional macromolecules, as shown in Scheme 3.1, is ensured by a fast protonation / deprotonation equilibrium.



Scheme 3.1. Mechanism of the anionic ring-opening multibranching polymerization of glycidol.

Further improvement of the reaction conditions was realized by adjustment of the process parameters: a) increased stirring intensity and refinement of the stirrer geometry afforded improved mixing efficiency; b) the use of a high-boiling, aprotic aliphatic ether, diethylene glycol dimethyl ether (diglyme), as an inert and emulsifying solvent resulted in higher molecular weights (up to 20,000 g/mol) under readily controllable conditions (however, an increase in polydispersities as well as the loss of reproducibility for these high molecular weight polymers could not be avoided); c) scale-up was successfully achieved by individual construction of a 2 l reactor that is capable of producing up to 1 kg of hyperbranched polyglycerol within two days.¹⁰ ^{13}C NMR spectroscopy allows to distinguish between dendritic (D), linear (L_{13} , L_{14}) and terminal (T) units and therefore to calculate the degree of branching (DB). Due to small fractions of homopolymer formed

in the course of the reaction, the obtained DBs range between 0.53 and 0.59, slightly below the calculated ideal value of 0.67 under SMA conditions.^{11,12}

Recently, Brooks et al. modified the established procedure by replacing diglyme with dioxane as emulsifier. In this case, very high molecular weight polyglycerols with M_n up to 700,000 g/mol have been obtained.¹³ These materials exhibit the highest molecular weights reported to date for synthetic hyperbranched polymers. The reason for the formation of these high molecular weight polyglycerols that possess remarkably narrow polydispersities ($M_w/M_n=1.1-1.4$) however remains unclear. Brooks et al. tentatively explain the impact of the solvent on molecular weight by the fast proton exchange in their system. In a further study, the same authors demonstrated excellent biocompatibility and low toxicity for hyperbranched polyglycerols, similar as it has been shown for poly(ethylene oxide) (PEO).¹⁴ These characteristics render the material highly promising for biomedical application, potentially as a substitute for linear PEO, possessing the advantages of branched structures.

This chapter highlights the relation between the initiator core degree of deprotonation on the properties of the obtained polymers. In this context, the systematic employment of strategies circumventing the previously occurring problems in terms of molar mass control and broadening of molecular weight distributions is described. A gradual increase of the degree of deprotonation of the initiating species was studied in different solvents. Furthermore, the delayed introduction of additional base to the reaction system has been carried out. In addition, the first successful development of an efficient synthesis protocol for the controlled preparation of well-defined, higher molecular weight hyperbranched polyglycerols (M_n up to 20,000 g/mol) via a two step, macroinitiator-based approach is presented.

3.2 Influence of the Degree of Deprotonation

The basic principle of “living” polymerizations like atom transfer radical polymerization (ATRP) is to keep the concentration of active chain ends low compared to the number of so-called dormant species, i.e. potentially active sites. In combination with a rapid exchange equilibrium that leads to deactivation of active sites after a few propagation steps,¹⁵ highly controlled chain growth with linear dependence of the degree of polymerization on the monomer conversion can be achieved. In analogy to this concept and paralleling the synthetic strategy used for the polymerization of propylene oxide,¹⁶ the trifunc-

tional TMP is only partially deprotonated upon use as initiator. This approach permits the control of the concentration of active sites (alkoxides) in the polymerization, leading to simultaneous growth of all chain ends and thus control of molecular weight while considerably narrowing the polydispersity. In a typical experiment, TMP is reacted with a suitable deprotonating agent (e.g. potassium *tert*-butanolate followed by removal of excess *tert*-butanol) to convert 10% of the hydroxyl groups into alkoxide units. As the polymerization proceeds, the initial concentration of active species (10%) with respect to all hydroxyl end groups decreases rapidly because the incorporation of each glycidol monomer generates a new hydroxyl group representing a dormant chain end. This decrease is demonstrated in Figure 3.2 for polyglycerol with a trifunctional initiator core like TMP.

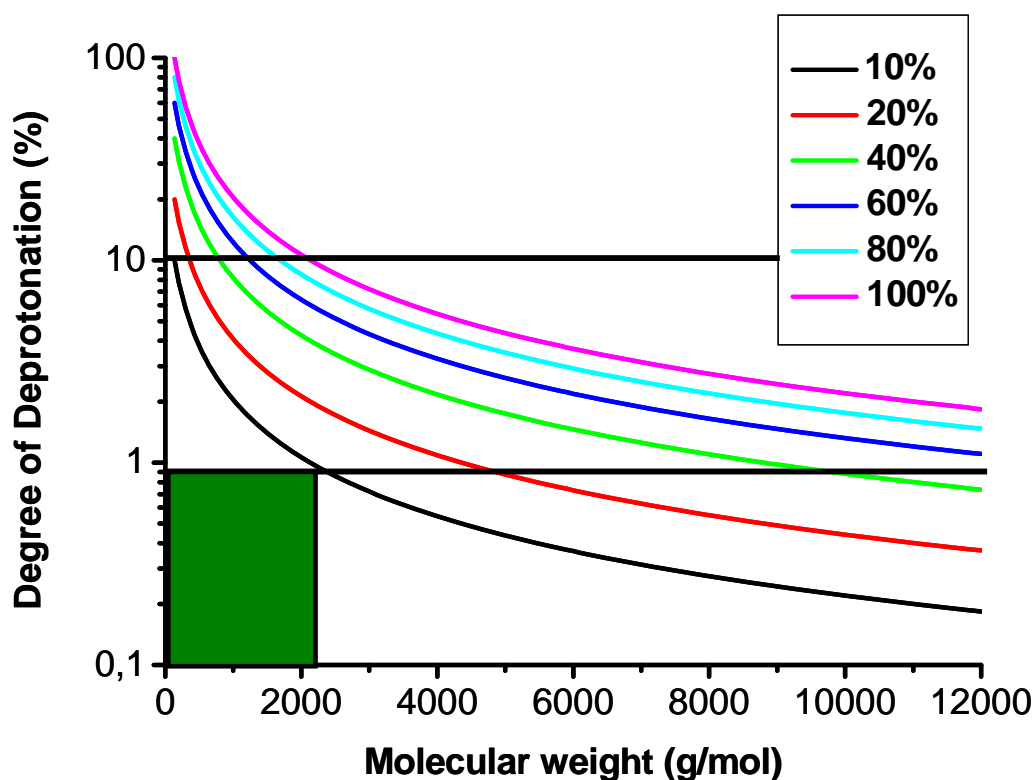


Figure 3.2. Decrease of the degree of deprotonation calculated for PG with trifunctional initiator core, starting with 10, 20, 40, 60, 80 and 100% of initial deprotonation.

It is obvious from Figure 3.2 that the initial degree of deprotonation drastically decreases in the first stage of the reaction. When the initiator is deprotonated by 10%, the corresponding polyglycerol with a molecular weight of 2,000 g/mol bears only around 1% of alkoxide groups. Up to this threshold (marked with a black line in Figure 3.2), the reproducibility of the product properties is excellent. Although higher molecular masses can

be realized by the previously described method, broad polydispersities and a lack of control occurs from time to time. This undesired behavior may be attributed to the fact that polyglycerol becomes more and more viscous with increasing molecular weight while the solubility in diglyme simultaneously decreases. These changes in physical properties possibly influence the inter- and intramolecular transfer of the alkoxides, leading to a rapid growth of particular polymer chains, while others remain small, resulting in broad molecular weight distributions. Decreased degrees of deprotonation may also influence the kinetics of the reaction because the fundamental basics of the slow monomer addition technique are not sufficiently fulfilled anymore. As the rate of monomer addition to the growing polymer chain is reduced due to a smaller relative number of alkoxide groups, the formation of homopolymer from unreacted monomer may become more significant. Thus an increase of the degree of deprotonation may appear to be a promising approach. The respective initiator species (50% and 100% deprotonated TMP) were studied by Holger Kautz, who observed polydispersities exceeding 3.¹⁷ The loss of molecular weight and polydispersity control was mainly attributed to the initial and persistent poor solubility of the highly deprotonated initiator core. For a further investigation of the impact of solubility problems and the absence of a sufficiently large number of dormant species in the beginning of the reaction, variation of the reaction solvent and a gradual increase of the degree of deprotonation have been considered as promising approaches to obtain more insight into the reaction mechanism.

3.2.1 Variation of the Reaction Solvent

The standard procedure for glycidol polymerization employs diglyme as an inert, high-boiling and aprotic aliphatic ether solvent. It has to be mentioned that the solubility of low molecular weight polyols in their crude and deprotonated state is strongly limited. Therefore, the more polar compounds tetraglyme and NMP were investigated as solvents in previous studies.¹⁷ Reactions in tetraglyme resulted in significantly broadened molecular weight distributions (> 6.0). NMP removal from the product by precipitation into acetone was not quantitative and the polydispersity indices were not improved either. The range of reaction solvents to be considered for glycidol polymerization is strongly limited by the low solubility of the propagating polyglycerols (particularly excluding apolar solvents) and the high temperature of 120°C (requiring a high-boiling point). Furthermore, protic solvents cannot be used due to their capability of initiating the polymerization. Following these considerations, dimethylformamide (DMF) as a highly polar aprotic sol-

vent with a boiling point of 153°C appeared to be an appropriate candidate. Polyglycerols with target molecular weights of 1,000, 2,000, and 5,000 g/mol were synthesized in DMF. The respective characterization data is listed in Table 3.1.

Table 3.1. ^1H NMR and GPC data taken from PGs prepared in DMF.

Sample	$M_{n,\text{theo}}$ (g/mol)	$M_{n,\text{NMR}}$ (g/mol)	$M_{n,\text{GPC}}$ (g/mol) ^{a)}	PDI_{GPC} ^{a)}
PG-01-DMF	1,000	1,080	920	1.80
PG-02-DMF	2,000	1,820	1,040	1.82
PG-05-DMF	5,000	4,950	600	2.25

^{a)} measured in DMF with PS-standards

In all stages of the reaction the growing polymers remained soluble in DMF, even in the partially deprotonated state. However, from the characterization data, it is obvious that solubility is not the only factor influencing molecular weight control. In the case of the sample PG-01, adequate molecular weight control was achieved. However, the obtained polydispersity is higher than the respective value obtained when the reaction is carried out in diglyme. Furthermore, at low initiator-to-monomer ratios, the reaction in DMF leads to much lower molecular weights than targeted. It should be noted that molecular masses calculated by ^1H -NMR spectroscopy are misleading in these cases, as it is not possible to distinguish between polymers incorporating the initiator core and PG homopolymers without TMP core. Surprisingly, in the case of PG-5 the obtained molecular weight by GPC was the lowest, indicating poor reproducibility of the molecular weights in this solvent. The high polarity of DMF (dielectric coefficient: $\epsilon = 32 \text{ C/Vm}$) accelerates the inter- and intramolecular cation exchange equilibria. Due to the high nucleophilicity of the alkoxides, reactivity is significantly increased. Consequently, homopolymerization of glycidol can easily occur even at low monomer concentrations, resulting in the observed discrepancy between targeted and experimentally achieved molecular weights. This assumption is further verified by the results obtained by Brooks et al. who used dioxane as reaction solvent. As the polarity of dioxane is relatively low, stabilizing effects by the growing polyglycerols comparable to crown ethers may favor intramolecular proton transfer. Accordingly the polymer molecules incorporating potassium counter ions grow rapidly, while other cores are not incorporated at all. Hence, narrowly distributed high molecular weight polymers are obtained without noticeable control over mo-

molecular weight. It would be interesting to investigate whether increased degrees of deprotonation lead to a higher incorporation rate of the TMP initiator despite the negative effect on polydispersity. Therefore a sequence of experiments with 10%, 20% and 40% deprotonation of the OH-groups was carried out in dioxane. Table 3.2 summarizes the characterization data obtained from these samples after dialysis in methanol.

Table 3.2. ^1H NMR- and GPC characterization data for PG prepared in dioxane after purification by dialysis.

Sample	Degree of deprotonation	$M_{n,theo}$ (g/mol)	$M_{n,GPC}$ (g/mol) ^{a)}	PDI_{GPC} ^{a)}
PG-06-10-dioxane	10%	6,000	87,000	1.2
PG-06-20-dioxane	20%	6,000	44,900	4.6
PG-06-40-dioxane	40%	6,000	8,900	2.5

^{a)} measured in DMF with PS-standards

In all cases mixtures of low and high molecular weight fractions were observed. Low molecular weight fractions can be removed by techniques like dialysis. The polymer that was obtained after deprotonating 10% of the initiator OH-groups exhibited narrow molecular weight distribution after dialysis in methanol. Brooks et al. reported similar molecular masses and polydispersities, but disclaimed the necessity of dialysis workup.¹³ Figure 3.3, depicting the GPC curve of the products before dialysis, clearly shows a sizeable low molecular weight fraction besides the narrowly distributed high molecular weight polymer. Like suspected, at higher degrees of deprotonation theoretical and experimental molecular weights converge, but broad multimodal distributions are obtained that remain even after dialysis. Thus it can be concluded that increased initial degrees of deprotonation lead to a higher incorporation of the initiator core and hence lower molecular weights, but also result in a loss of control over the polymerization reaction.

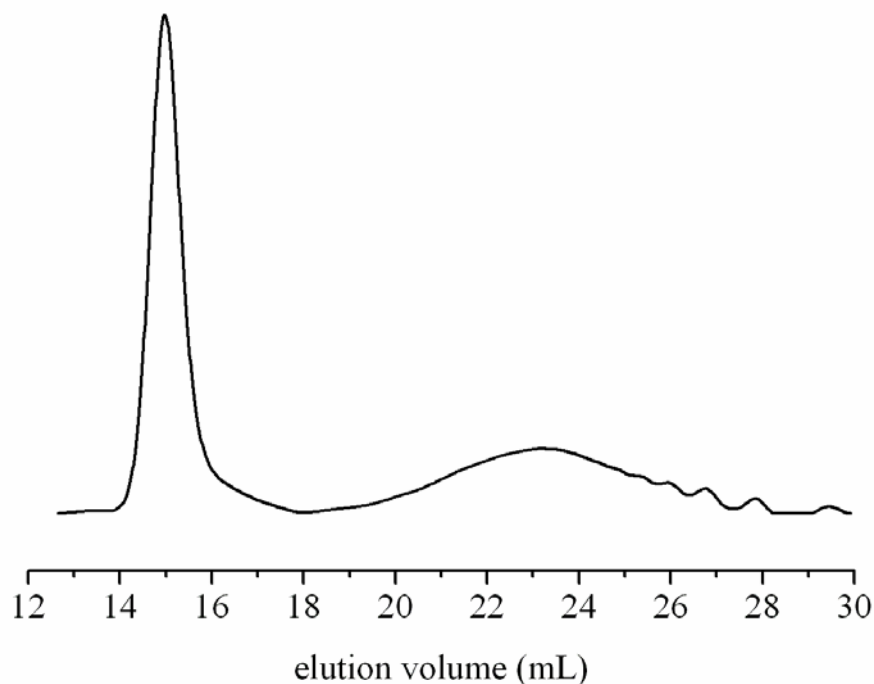


Figure 3.3. GPC curve obtained from PG-06-10-dioxane (10% of initial deprotonation) measured in DMF.

In summary, the method of Brooks using dioxane as a solvent provides access to polyglycerols with M_n higher than 60,000 g/mol while the SMA of glycidol to a polyfunctional initiator core permits excellent reproducibility and narrow molecular weight distributions up to 2,000 g/mol. However, there exists an obvious gap between these regions. Well-defined polyglycerols with molecular weights around 10,000 g/mol have not been realized to date. As described above, maintaining the degree of deprotonation between 1 and 10 % (black lines in Figure 3.2) appears to be a strict requirement for adequate molecular weight control.

3.2.2 Gradual Increase of the Degree of Deprotonation

Keeping the degree of deprotonation constant during the whole reaction process involves more difficulties than obvious at first sight. Permanent base addition via a second pump would facilitate homopolymerization of the monomer without incorporation of the TMP core. Thus, it has to be ensured that the monomer has fully reacted before new base is added to the system. Using alkoxides as deprotonation agent requires complete removal of the formed alcohol before further monomer addition. Otherwise, the corresponding alc-oxides can potentially initiate the growth of new polymer chains. Taking these considerations into account, the addition of monomer was stopped after a fourth of the glyci-

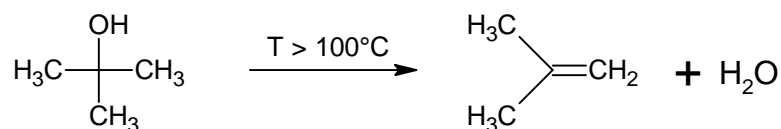
dol had been added and the reaction solution was stirred for 30 minutes before new base was injected. Subsequently, the formed alcohol was distilled off for an additional hour before the SMA of glycidol was continued. This procedure was repeated three times. Table 3.3 summarizes the characterization data obtained from the respective polyglycerols with targeted molecular weights of 5,000 g/mol.

Table 3.3. ^1H NMR- and GPC characterization data obtained from PG prepared via supplementary addition of alkoxides.

Sample	Base (1 mol% in THF)	T (°C)	$M_{n,\text{theo}}$ (g/mol)	$M_{n,\text{GPC}}$ (g/mol) ^{a)}	PDI_{GPC} ^{a)}
PG-05-A	KOMe	120	5,000	1,000	2.6
PG-05-B	KOtBu	120	5,000	20,900	2.5
PG-05-C	KOtBu	80	5,000	17,300	2.8

^{a)} measured in DMF with PS-standards

The obtained data shows that comparably broad molecular weight distributions result from this approach in all cases and no molecular weight control was achieved. In the case of KOMe as deprotonating agent, significantly lower molecular weights than calculated were obtained. Insufficient removal of the resulting methanol during the reaction accounts for the formation of methanolate initiator cores that accordingly start new polymer chains and decrease the resulting molecular weight average. Due to its bulky structure KOtBu is known to be a poor direct initiator for the polymerization of glycidol. On the other hand it tends to decompose above 100°C as shown in Scheme 3.2. Therefore the reaction was carried out at 120°C and 80°C successively. The results however were quite similar. In contrast to the approach involving KOMe, the resulting molecular weights were higher than theoretical values. As high molecular polyglycerols possess more OH-groups and therefore are more likely to be deprotonated than the respective low molecular weight PGs, higher degrees of polymerization were obtained than expected.



Scheme 3.2. Decomposition of *t*-butanol at high temperatures.

No improvement in molecular weight control was achieved by this time-consuming method. Using bases like hydrides would eliminate the problem of the resulting alcoholates, but a preference for homopolymerization of glycidol may still exist.

3.2.3 Use of Polyglycerols as Macroinitiators

It has already been pointed out in the preceding paragraphs that well-defined low molecular weight polyglycerols are accessible in large quantities. As these compounds possess multifunctionality due to the high number of hydroxyl groups, they should offer high potential for the use as macroinitiators in further efforts to obtain higher molecular weight polyglycerols under controlled conditions. TMP-core containing polyglycerols with an average molecular weight of 1,200 g/mol correspond to an average degree of polymerization of 14.4 and thus 17.4 OH-groups. Deprotonating 10% of these alcohol groups resembles a degree of deprotonation of 60% related to TMP as initiator core, corresponding to the blue line in Figure 3.2. This curve enters the marked region between 1% and 10% of deprotonation at a molecular weight of around 1,200 g/mol. Assuming that the aforementioned considerations are correct, molecular weights exceeding 10,000 g/mol should be accessible. The resulting molecular masses are summarized in Table 3.4. Targeted and obtained molecular weights are in excellent agreement with regard to polystyrene standards. Furthermore, the resulting polydispersities remain nearly constant and show only a slight increase compared to the respective value of the macroinitiator. Figure 3.4 depicts the corresponding GPC curves, showing complete disappearance of the initial macroinitiators. All GPC measurements were carried out in DMF, applying linear polystyrol (PS) and linear poly(ethylene glycol) (PEG) standards. As GPC is a relative characterization method, a systematical error does occur. Two complementary effects have to be considered. Hyperbranched structures are very compact, resulting in comparably low hydrodynamic radii. Thus, molecular weights calculated from linear standards are generally underestimated. This effect amplifies with increasing molecular weights. On the other hand, the use of PS standards may lead to an overestimation of polyglycerol molecular masses due to the different chemical structures. PEG, which resembles polyglycerols in its repeat unit structure, does not show the latter effect. Consequently, for low molecular weight polyglycerols (up to 3,000 g/mol), PEG standards are better suited, while for molecular masses between 5,000 and 20,000 g/mol, PS standards seems to be more reliable. Molecular weight determination of the resulting polymers using $^1\text{H-NMR}$

spectra is also imprecise. It is impossible to distinguish between core-containing polymer and glycerol homopolymer. Incomplete removal of methanol traces or diglyme leads to miscalculations. Furthermore, with increasing molecular weights, the signals of the TMP core become more and more difficult to differentiate from the noise-induced signal. Scaling of the integrated peaks hence becomes less reliable.

Table 3.4. ^1H NMR- and GPC characterization data obtained from PGs prepared by using low molecular weight polyglycerols as macroinitiator.

Sample	Initiator	$M_{n,\text{theo}}$ (g/mol)	$M_{n,\text{GPC}}$ (g/mol) ^{a)}	PD_{GPC} ^{a)}	$M_{n,\text{NMR}}$ (g/mol)
PG-01	TMP	1,000	1,200 ^{a)}	1.54 ^{a)}	1,200
PG-05-01	PG-01	5,000	5,200 ^{b)}	1.65 ^{b)}	5,400
PG-06-01	PG-01	6,000	6,100 ^{b)}	1.61 ^{b)}	6,300
PG-08-01	PG-01	8,000	8,200 ^{b)}	1.48 ^{b)}	7,400
PG-10-01	PG-01	10,000	10,500 ^{b)}	1.73 ^{b)}	12,700
PG-10-05	PG-05-01	10,000	10,300 ^{b)}	1.86 ^{b)}	10,000
PG-20-01	PG-01	20,000	20,700 ^{b)}	1.69 ^{b)}	27,300
PG-20-05	PG-05-01	20,000	19,900 ^{b)}	1.81 ^{b)}	23,800

^{a)} measured in DMF with PEG-standards

^{b)} measured in DMF with PS-standards

It has to be noted that extensive drying of the macroinitiator is essential for improved molecular weight control. Even very small residual traces of remaining alcohol or other impurities lead to multimodal molar mass distributions. Table 3.4 also proves that polyglycerols with molecular weights of 5,000 g/mol can be applied as macroinitiators for higher molecular weights as well. In this case, deprotonation of 10% of the OH groups affords a highly viscous material that is insoluble in diglyme. Hence, deprotonation should be carried out inside the reactor, as the transfer of the deprotonated PG from an external flask is nearly impossible. The resulting molecular weights are slightly higher than those obtained from using a PG-01 macroinitiator.

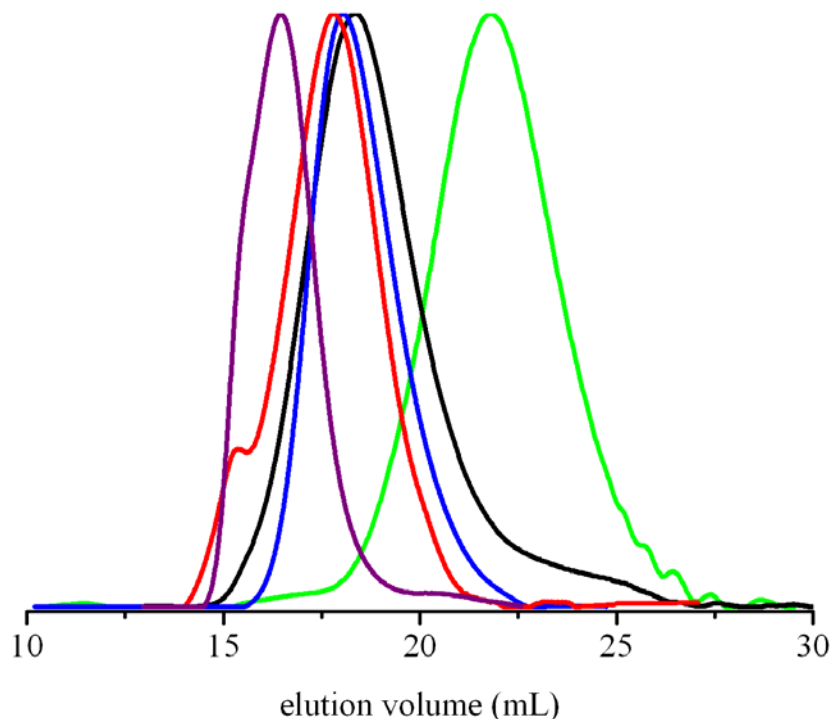


Figure 3.4. GPC curves of PG-01 macroinitiator (green), PG-05-01 (black), PG-08-01 (blue), PG-10-01 (red), PG-20-01 (purple) measured in DMF.

Besides molar mass and molecular weight distribution, the degree of branching (DB) is a crucial property of hyperbranched polymers. The DB was first introduced by Kim¹⁸ and Fréchet et al.¹⁹ as a topological measure for cascade-branched macromolecules with high degrees of polymerization. In these cases, the functionality of the initiator core (f) is negligible and the number of terminal groups is nearly identical with the number of dendritic groups ($T = D + f$). The calculated DBs are thus overestimated, especially for low molecular weight polymers (Equation 3.1).

$$DB_{\text{Fréchet}} = \frac{D + T}{D + T + L} \quad (\text{eq. 3.1})$$

Frey et al. refined this concept and developed a general definition for AB_n -polymerizations (Equation 3.2).²⁰

$$DB_{\text{Frey}} = \frac{2D}{2D + L} \quad (\text{eq. 3.2})$$

In an ideal bulk polymerization of an AB₂ monomer, the DB equals 0.5, independent of the used monomer, because a ratio of D : L : T = 1 : 2 : 1 is obtained.²⁰ Applying the SMA technique ([M] << [I], Chapter 1.2.1.1), which corresponds to the progress of a “pseudo chain growth” from a kinetic point of view, the ratio can be altered to D : L : T = 1 : 1 : 1 and a theoretical maximum of DB = 66,7% can be achieved.^{11,12} The obtained DBs for the ROMBP of glycidol under SMA conditions were found to range between 0.53 and 0.59. They can be calculated from inverse gated (IG) ¹³C NMR spectra, which permit the integration of carbon core signal intensities. Figure 3.5 lists the assignments of the different structural units present in hyperbranched polyglycerols.

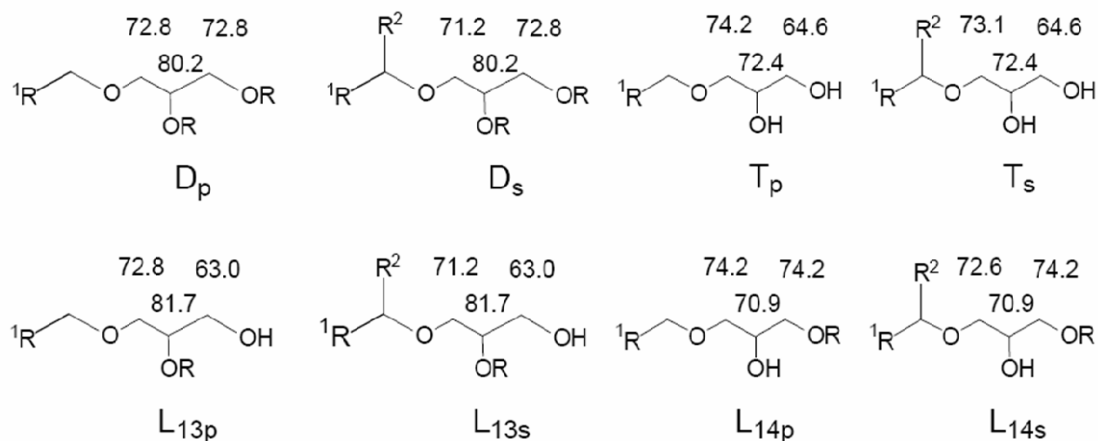


Figure 3.5. Assignment of ¹³C NMR signals (in ppm) for each structural unit. Indices p and s indicate that the respective group is attached to a primary or a secondary alkoxide.

Since the L₁₃ (63.0 & 81.7 ppm), the D (80.2 ppm) and the T (64.6 ppm) signals generate isolated peaks, the integral of one L₁₄ unit can be calculated according to Equation 3.3.

$$L_{1,4} = [\Sigma(\text{all integrals}) - 3(L_{13} + D + T)] / 3 \quad (\text{eq. 3.3})$$

A typical IG ¹³C-NMR spectrum (PG-06-01) is shown in Figure 3.6. All structural units depicted in Figure 3.5 can be assigned to the respective signals and no side products are observed.

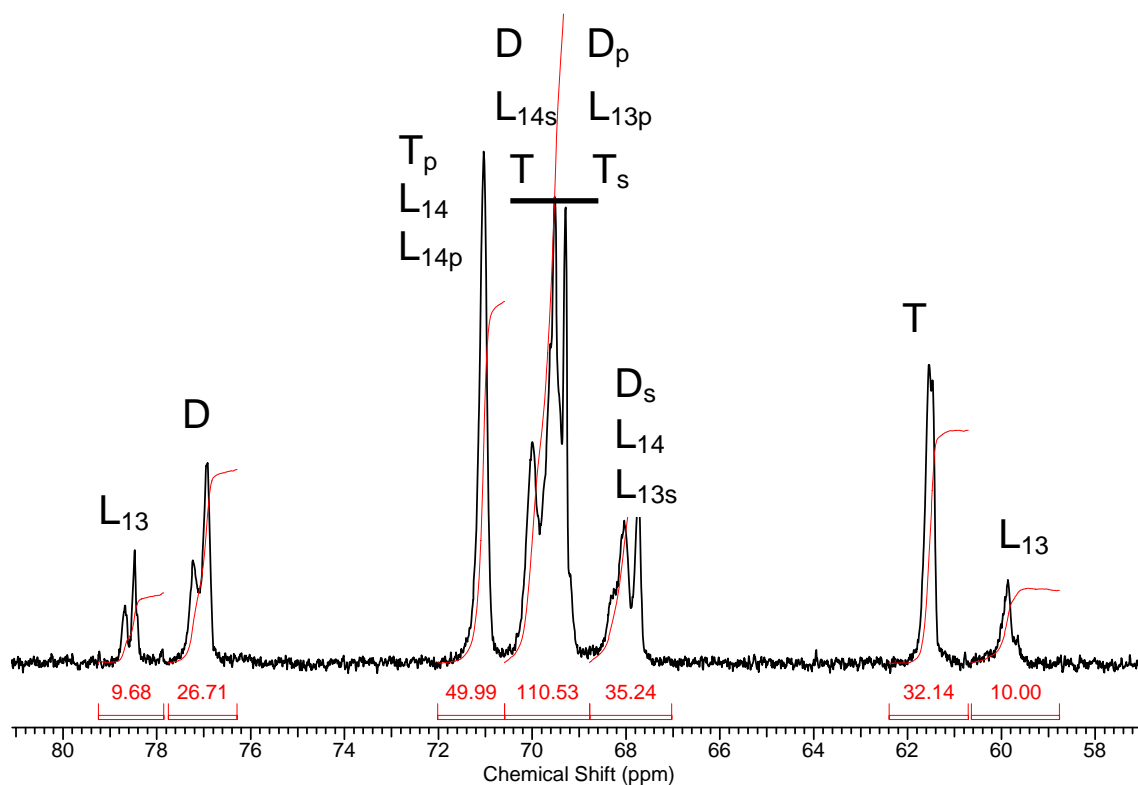


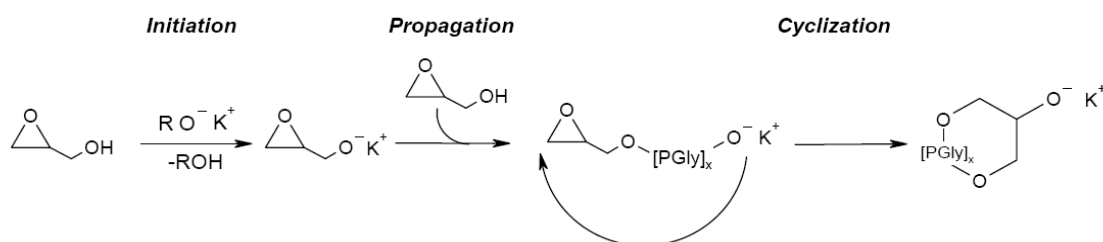
Figure 3.6. IG ^{13}C NMR spectrum for PG-06-01 in MeOD.

Table 3.5 comprises the relative amounts of each structural unit and the resulting DBs calculated by using equations 3.1 and 3.2.

The data listed in Table 3.5 clearly confirms the remarkable degree of reaction control achieved via the SMA technique. All polymers prepared by using polyglycerols as macroinitiators possess DBs from 0.60 to 0.65. These values range above the previously publicized data with reported values found between 0.52 and 0.59. The maximum DB that can be theoretically obtained under SMA equals 0.67. As both equations neglect formation of cycles occurring to a certain extent in early stages of the reaction (Scheme 3.3), the determined degrees of branching are found below this theoretical value. The observed higher values obtained by using the DB_{Frey} equation leads to the conclusion that cycle formation does not occur when macroinitiators are used for the ROMBP of glycidol. Since the degree of branching of the macroinitiator PG-05-01 ($\text{DB} = 0.61$) is significantly higher than the one of PG-01 ($\text{DB} = 0.55$), the resulting degrees of branching are consequently above the ones obtained in the latter case.

Table 3.5. IG ^{13}C NMR spectroscopy characterization data obtained from PG prepared by using low molecular weight polyglycerols as macroinitiators.

Sample	L ₁₃	L ₁₄	D	T	DB _{Frey}	DB _{Fréchet}
PG-01	11.8%	23.4%	21.2%	43.6%	54.7%	64.8%
PG-05-01	11.7%	25.0%	29.2%	34.1%	61.4%	63.3%
PG-06-01	11.1%	25.5%	29.2%	34.2%	61.5%	63.4%
PG-08-01	10.3%	25.8%	29.1%	34.8%	61.7%	63.9%
PG-10-01	10.5%	25.3%	30.4%	33.7%	62.9%	64.1%
PG-10-05	10.4%	22.7%	30.5%	36.4%	64.8%	66.9%
PG-20-01	10.0%	27.4%	28.7%	33.9%	60.5%	62.6%
PG-20-05	10.0%	24.9%	31.4%	33.7%	63.6%	65.1%



Scheme 3.3. Homopolymerization of glycidol by intramolecular ring-opening, resulting in the formation of cyclic compounds.

It is noticeable that the DBs calculated by equation 3.1 are overestimated, particularly for lower molecular weight polymers. This directly results from the fact that the respective approximation equates dendritic and terminal units, which is clearly deficient at low degrees of polymerization. Nevertheless, degrees of branching found in the literature have frequently been calculated by this method. Hence, it is interesting to compare the respective values. It is further remarkable that the ratio of L₁₃ to L₁₄ units is found to be around 1 : 2.25 in all cases, which confirms the significance of intramolecular transfer to the more stable primary alkoxides.

In summary, using low molecular weight polyglycerols as macroinitiators has shown to be a successful approach for PGs with molar masses in the range from 5,000 to 20,000 g/mol. All measurements confirm the excellent molecular weight control in these cases.

3.3 Continuous Spin Fractionation

Removal of low molecular weight compounds is one of the major challenges in the synthesis of narrowly distributed polyglycerols. Inconsistent polymer composition has shown to be particularly unfavorable for pharmaceutical applications and some specific technical purposes. The usual work-up by precipitation of the polymer into acetone only removes very low molecular weight species (mostly residual monomer and oligomers), tends to be incomplete and often results in a significantly lower yield. Dialysis has proven to be an efficient method for the isolation of compounds with a molar mass higher than a certain threshold value determined by the respective tubing. However this method cannot be applied when the undesired polymer fraction and the targeted species exhibit a similar molecular weight. In these cases, purification by dialysis is either impossible or involves substantial loss of material. Efficient separation techniques like gel permeation chromatography (GPC)²¹⁻²³ or high performance liquid chromatography (HPLC)^{24,25} are available for analytical purposes on the milligram scale. To some extent these procedures can also be used for preparative purposes, but the amount of fractionated polymers typically does not exceed 1 g of polymer.²³ Thus scale-up for the production of several kilograms or even tons per day is unfeasible or at least highly uneconomic. In 2002, the group of Prof. B. A. Wolf developed the so-called continuous spin fractionation, a method providing more flexible and economic access to large quantities of polymer fractions with sufficient uniformity.^{26,27} It is based on the establishment of liquid/liquid phase equilibria and can be applied for practically any soluble polymer. The basic principle is sketched in Figure 3.7. Those macromolecular species with superior solubility are transferred from the source phase (feed, green) into a receiving phase (extracting agent, colorless), whereas the less soluble components remain in the source phase. Problems resulting from viscosities of concentrated polymer solutions, resulting in kinetic retardation of equilibrium formation are efficiently suppressed by squeezing the feed through spinning nozzles (grey). The consequent extension of the interface between the phases liberates short polymer chains from interactions with their neighboring macromolecules and favors their entropic preference. The droplets, separated from the low molecular weight

material, contain the gel fraction (blue) and the saturated continuous phase, the sol fraction (yellow). The insets show the respective differential molecular weight distributions.

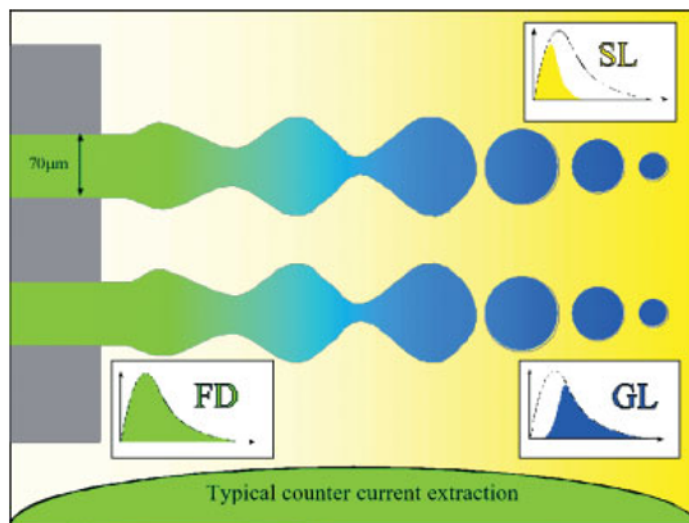


Figure 3.7. General principle of the continuous spin fractionation technique.

Like already indicated, solvent and precipitants must be selected carefully for each individual system in order to optimize the separation efficiency of the fractionation. For hyperbranched polyglycerols, the combination of water as solvent and isopropanol as precipitant have proven to be the most effective combination. Spin fractionation was carried out at 25°C. The applied apparatus is depicted in Figure 3.8.

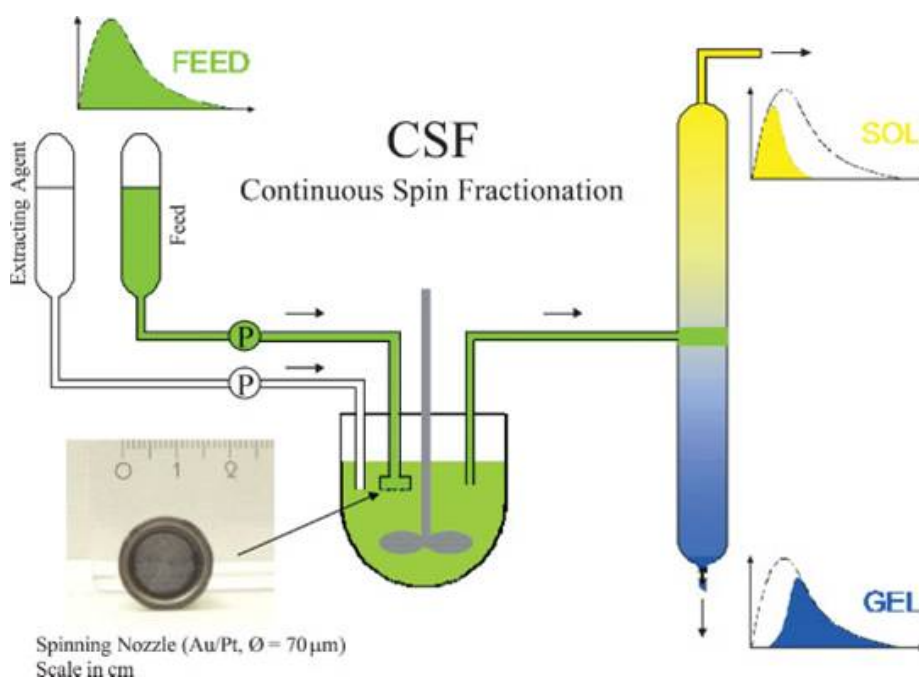


Figure 3.8. Apparatus used for continuous spin fractionation.

The set-up consists of two reservoirs for the feed and extracting agents, which are transported by means of pumps allowing for precise flow control. In addition to the spinning nozzles, a mixing vessel allowing vigorous stirring is required. Subsequently, the two phase mixture flows freely from the mixing vessel into a column of 2 cm inner diameter and 2 m length, where macroscopic phase separation takes place, so that gel and sol phases can be collected continuously. In cooperation with the group of Prof. B. Wolf continuous spin fractionation experiments have been carried out by Fatemeh Samadi. Table 3.6 summarizes the results obtained via GPC (measured in DMF with PS and PEG standards) before and after CSF treatment of three representative polyglycerol samples.

Table 3.6. GPC data obtained before and after CSF.

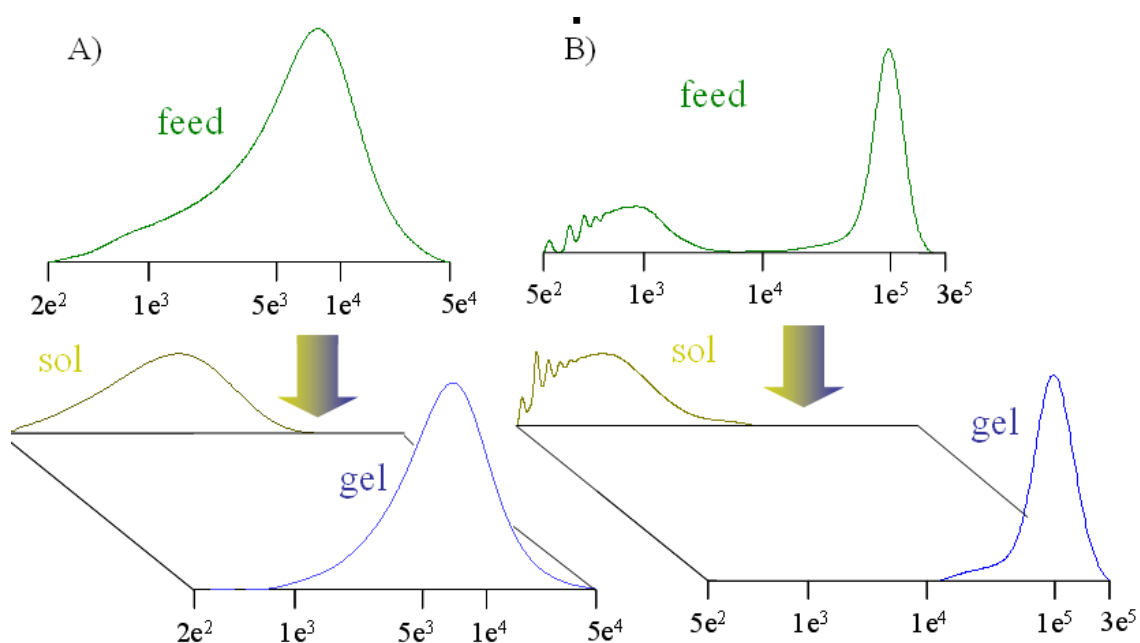
Sample	M _n (g/mol) ^{a)}	PDI ^{a)}	M _n (g/mol) ^{b)}	PDI ^{b)}	Weight %
PG-05-10-diglyme-feed	5,050	1.8	6,240	2.2	100%
PG-05-10-diglyme-sol	1,440	1.5	1,860	1.7	13%
PG-06-10-diglyme-gel	6,160	1.4	9,260	1.5	87%
PG-06-10-dioxane-feed	1,120	23.6	1,280	44.7	100%
PG-06-10-dioxane-sol	550	2.2	650	2.6	18%
PG-06-10-dioxane-gel	36,690	1.1	69,190	1.3	82%
PG-15-10-diglyme-feed	31,330	1.7	53,220	2.3	100%
PG-15-10-diglyme-sol	1,030	2.6	1,160	2.9	13%
PG-15-10-diglyme-gel	3,680	1.5	68,160	2.0	87%

^{a)} measured in DMF with PEG-standards

^{b)} measured in DMF with PS-standards

Like indicated in the preceding paragraphs, PEG standards are more reliable below molar masses of 2,000 g/mol, while above 5,000 g/mol PS standards have to be used for reference. Table 3.6 contains both values for each sample. The corresponding GPC curves of PG-06-10-diglyme and PG-06-10-dioxane are shown in Scheme 3.4. The data given in the first line of table 3.6 corresponds to a PG prepared by the conventional method using TMP as core, deprotonated to an extent of 10% by potassium *t*-butylate in diglyme as a

solvent. The molar mass is slightly higher than the value of 5,000 g/mol with a PDI of 2.2. The respective GPC curve (Scheme 3.4 A) shows a shoulder towards the small molecular weight region, which almost completely disappears after CSF. Consequently, the obtained average molecular weight increases to 9,260 g/mol and polydispersity can be narrowed to 1.5. Remarkable enhancement can be achieved in the case of the polymers synthesized in dioxane. It has been reported in chapter 3.2.1 that mixtures of low molecular weight compounds and very narrowly distributed high molecular weight fractions are present in these cases, resulting in extremely broad distributions with regard to the whole spectrum. The wide gap between these regions of the molecular weight distribution permits a smooth separation of the two corresponding peaks by CSF (Scheme 3.4 B).



Scheme 3.4. GPC diagrams (molecular weights given on the abscissa in [g/mol]) of PG-06-10-diglyme (A) and PG-06-10-dioxane (B) before and after CSF.

The results obtained from high molecular weight polyglycerols prepared in diglyme are less conspicuous. Polymer PG-15-10-diglyme which shows a monomodal distribution with a slight shoulder (PDI = 2.3) can hardly be separated into gel and sol fraction as the present high molecular weight polymers exhibit similar behavior in solvent and precipitant. However, residual low molecular weight fractions can be efficiently removed, resulting in a lower polydispersity (PDI = 2.0). In conclusion, the technique of continuous spin fractionation is a highly versatile method for the removal of low molecular weight

polyglycerol traces and consequently for the achievement of lower polydispersities in the case of polyglycerols with initially broad molecular weight distributions.

3.4 Conclusion

Hyperbranched polyglycerol represents a remarkably versatile branched polymer structure. The multifunctionality generated by a large number of OH-groups results in a characteristic highly polar structure. In addition, facile synthetic accessibility and well-studied biocompatibility render hyperbranched polyglycerols very interesting materials for technical applications and biomedical purposes where it is essential that narrowly distributed polymers are available over a broad range of molecular weights.

Further insight into the relation between reaction solvent, degree of deprotonation during the ring-opening multibranching polymerization of glycidol and the characteristics of the obtained polymers has been achieved within the scope of this work. Based on these results, a novel concept for the preparation of hyperbranched polyglycerols with molecular weights up to 20,000 g/mol has been developed, applying a two step synthesis pathway. Starting from a partially deprotonated TMP core, low molecular weight *hb*-PGs were prepared using the known synthetic protocol that has been established since the late 1990ies. In a subsequent reaction sequence, these well defined polymers were used as hyperbranched macroinitiator cores in order to obtain high molecular weight *hb*-PGs with remarkably low polydispersity ($M_w/M_n < 1.8$). Molecular weight control was shown to be excellent and undesired low molecular weight side products were absent.

The technique of continuous spin fractionation has been discovered as an efficient method for polyglycerol work-up. Residual monomer- and oligomer traces can be quantitatively removed from *hb*-PG compositions to result in samples with significantly reduced polydispersities. The respective post-synthesis treatment of polyglycerols prepared in dioxane has proven to be particularly effective for a facile, clear separation and isolation of the characteristic low- and high molecular weight fractions. Thus CSF represents a qualified purification method that is also applicable for the kilogram scale.

In addition, the first example of a hyperbranching polymerization carried out in a microstructured reactor, employing the known anionic ring-opening multibranching polymerization of glycidol has been carried out in the group of Prof. Frey and can be found in the appendix (chapter 11). Combining these innovations, low molecular weight polymers can

be produced in high quantities applying a microstructured reaction system. These well defined polymers can be partially deprotonated to provide efficient macroinitiators for the further ROMBP of glycidol. Molecular masses up to 20,000 g/mol can be realized by this two step approach, under retention of the macroinitiator. Replacing diglyme with dioxane as reaction solvent, narrowly distributed, very high molecular weight PGs can be obtained after work-up by continuous spin fractionation which removes residual monomeric and oligomeric impurities. Consequently, an elegant two-step synthesis protocol providing convenient access to hyperbranched polyglycerols over a wide molecular weight range in large quantities has been successfully consolidated.

3.5 Experimental Part

3.5.1 Materials

All chemicals were purchased from *Acros Organics*. Acetone p.a., methanol p.a., Dowex[®] 50WX8, 200-400 mesh, ion exchange resin, 1,1,1-trishydroxymethyl-propane (TMP) and 1M potassium *tert*-butylate solution in THF were used as received. THF was distilled over sodium prior to use. Diglyme and glycidol were purified by distillation over calcium hydride. Methanol-d₄ was purchased from *Deutero GmbH*.

3.5.2 Polymerization Apparatus

Polymerizations were carried out in the polymerization set-up displayed in Figure 3.15. The reaction vessel (A) is a glass reactor with a 5-necked flat-lid. In order to maintain the appropriate reaction temperature, the reaction vessel is immersed into an oil bath (B). Temperature control is achieved by a heating plate (C) in connection with a contact thermometer (D). The central neck of the lid of the reaction vessel (NS 29) bears a water-cooled metal case for the stirring shaft (E) which is agitated by an electrical stirrer (F). Furthermore, the lid of the stirrer is equipped with a vacuum/argon inlet (G), allowing to carry out the reactions under argon atmosphere. The monomer solution is stored under argon in a reservoir funnel (H) and slowly added to the initiator solution using a dosing pump (I). In order to avoid thermal oligomerization and to maintain ideal monomer incorporation, a free-hanging tube (J) is used for the addition of the monomer into the reaction vessel. Since the pump is not pressure resistant, an additional pressure control valve (K) is installed between pump and monomer inlet. The diluting solvent for the monomer is continuously distilled off using a Dean-Stark trap (L) with reflux condenser (M) and

receiving flask (N). The reactor is working at ambient pressure, thus, an oil bubbler (O) is attached to the reflux condenser (M). In the case of the 2000 mL reactor, additional safety devices are installed: the loss of cooling liquid (used for the condenser and the case of the stirring shaft as well as the loss of lubricant from the case of the stirring shaft leads to a turn-off of all electrical equipment. After each reaction the polymerization apparatus has to be cleaned thoroughly. The pump is rinsed with THF and dried under vacuum. All reactor parts and the reservoir funnel are washed with methanol and subsequently cleaned and dried.

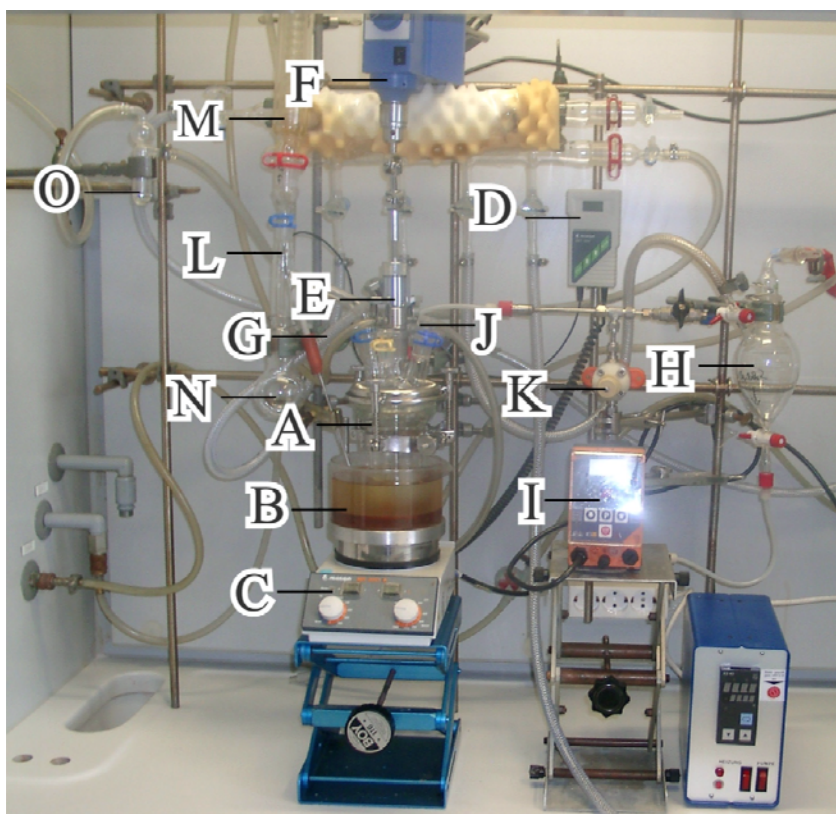


Figure 3.15. Polymerization set-up for ROMBP of glycidol.

3.5.3 Synthesis of the Hyperbranched Polyglycerols

All syntheses described in chapters 3.2 and 3.3 were carried out under argon atmosphere in the polymerization apparatus described in chapter 3.6.2. Freshly distilled THF (ca. 50 mL) were injected to the reservoir funnel under and the pump was run until THF no bubbles were observed upon THF addition to the reactor. The desired amount of glycidol was filled into the reservoir funnel to the remaining THF in Ar-counter flow. TMP or the polyglycidol macroinitiator were deprotonated to a certain amount (usually 10%) with a potassium tert-butyrate solution in THF in a one-neck flask. The mixture was heated to

70°C bath temperature on a rotary evaporator. The resulting alcohol was removed under vacuum. Subsequently, the initiator was dissolved/emulsified in 20ml freshly distilled solvent (diglyme, dioxane or DMF respectively) and transferred into the reactor in Ar-counter flow. The oil bath was heated to 120°C and the stirrer was run at 600 revolutions per minute and the pump was started. A pumping rate of 5 drops per minute was adjusted and the size of the drops was adjusted to 50%. When the addition of glycidol was completed, additional 25 mL distilled THF were filled into the reservoir and the pump was restarted in order not to lose any glycidol remaining in the tube connected to the pump. After the reaction was finished, products were dissolved in methanol and stirred with a cation exchange resin. Subsequently, the solution was filtered over a sintered filter (pore size 1) and washed with methanol. The resulting polymer was precipitated twice into cold acetone as methanol solution and dried for 12 h under vacuum at 100°C. Hyperbranched polyglycerols are transparent, viscous materials. Yields are between 80 and 95% depending on the polymer size.

3.5.4 Continuous Spin Fractionation

The continuous spin fractionation set-up is displayed schematically in Figure 3.8. The system involves an analogous plunger pump (Ismatec, Wertheim-Mondfeld, Germany) for the feed (typical fluxes 0.3 to 12 mL/min) and a diaphragm pump Gamma 5 (Prominent, Heidelberg, Germany) for the extracting agent (typical fluxes 1 to 30 mL/min). The used devices for the spinning nozzle are made of an Au/Pt alloy with 1035 holes and 60 or 70 μm diameter. The capacity of the mixing vessel is 1 L. The two phase mixture was flows freely from the mixing vessel into a column of 2 cm diameter and 2 m length where macroscopic phase separation takes place such that the gel phase and the sol phase can be collected continuously. This set-up allows throughputs up to 100 g/h.

3.5.5 Hyperbranched Polyglycerols

400 MHz- ^1H -NMR (d_4 -methanol, 25°C): δ [ppm] = 0.87 (t, 3H, CH_3 -, TMP), 1.37 (q, 2H, CH_3 - CH_2 -, TMP), 3.31 – 3.89 (m, CH_2 -O-, TMP, CH , PG, CH_2 , PG).

100 MHz- ^{13}C -NMR (d_4 -methanol, 25°C): δ [ppm] = 8.54, 23.76, 44.74, 59.18, (TMP), 62.61, 62.80 (L_{13}), 64.44, 64.52 (T), 70.68 -71.37 (L_{14} , $\text{L}_{13\text{s}}$, D_s), 72.26 – 72.97 (T, $\text{L}_{14\text{s}}$, $\text{L}_{13\text{p}}$, D), 74.00 (T_p , L_{14}), 79.83, 80.09 (D), 81.42, 81.58 (L_{13}).

IR (ATR): $\nu(\text{cm}^{-1})$ = 3353 (O-H), 2871 (C-H), 1065 (C-O-C), further characteristic peaks: 1457, 1326, 929, 871, 532.

3.6 References

1. Flory, P. J. *J. Am. Chem. Soc.* **1952**, 74, 2718.
2. Sandler, S. R.; Berg, F. R. *J. Polym. Sci., Part a: Polym. Chem.* **1966**, 4, 1253.
3. Tsuruta, T. I., S.; Koenuma, H. *Makromol. Chem.* **1968**, 112, 58-65.
4. Vandenberg, E. J. *J. Polym. Sci., Part A: Polym. Chem.* **1985**, 23, 915.
5. Tokar, R.; Kubisa, P.; Penczek, S.; Dworak, A. *Macromolecules* **1994**, 27, 320-322.
6. Dworak, A.; Walach, W.; Trzebicka, B. *Macromol. Chem. Phys.* **1995**, 196, 1963-1970.
7. Sunder, A.; Hanselmann, R.; Frey, H.; Mülhaupt, R. *Macromolecules* **1999**, 32, 4240-4246.
8. Sunder, A.; Frey, H.; Mülhaupt, R. *Macromol. Symp.* **2000**, 153, 187-196.
9. Sunder, A.; Mülhaupt, R.; Haag, R.; Frey, H. *Adv. Mater.* **2000**, 12, 235-239.
10. Kautz, H.; Sunder, A.; Frey, H. *Macromol. Symp.* **2001**, 163, 67-73.
11. Radke, W.; Litvinenko, G.; Müller, A. H. E. *Macromolecules* **1998**, 31, 239-248.
12. Hanselmann, R.; Hölter, D.; Frey, H. *Macromolecules* **1998**, 31, 3790-3801.
13. Kainthan, R. K.; Muliawan, E. B.; Hatzikiriakos, S. G.; Brooks, D. E. *Macromolecules* **2006**, 39, 7708-7717.
14. Kainthan, R. K.; Janzen, J.; Levin, E.; Devine, D. V.; Brooks, D. E. *Biomacromolecules* **2006**, 7, 703-709.
15. Patten, T. E.; Matyjaszewski, K. *Adv. Mater.* **1998**, 10, 901-+.
16. Bailey, F. E.; Koleske, V., Alkylene Oxides and their Polymers. In *Surface Science Series*, Schick, M. J.; Fowkes, F. M., Eds. Marcel Dekker: New York, **1990**; Vol. 35, p 35.
17. Kautz, H. *Ph. D. Thesis, University of Freiburg* 2003.
18. Kim, Y. H. *Macromol. Symp.* **1994**, 77, 21.
19. Hawker, C. J.; Lee, R.; Fréchet, J. M. J. *J. Am. Chem. Soc.* **1997**, 113, 4583.
20. Hölter, D.; Burgath, A.; Frey, H. *Acta Polym.* **1997**, 48, 30-35.

21. Glöckner, G., *Polymercharakterisierung durch Flüssigkeitschromatographie*. Hüthig: Heidelberg, **1982**.
22. Potschka, M. D., P. L., *Strategies in Size Exclusion Chromatographie*. American Chemical Society: Washington, D.C., **1996**.
23. Tung, L. H., *Fractionation of synthetic polymers*. Dekker: New York, **1977**.
24. Meyer, V. R., *Practical High-performance Liquid Chromatography*. Wiley: New York, **1994**.
25. Snyder, L. R. K., J. J., *Introduction to Modern Liquid Chromatography*. Wiley: New York, **1979**.
26. Eckelt, J. H., T.; Loske, S.; Wolf, B. A. Ger. 10202591, **2002**.
27. Eckelt, J.; Haase, T.; Loske, S.; Wolf, B. A. *Macromolecular Materials and Engineering* **2004**, 289, 393-399.
28. Hessel, V.; Löwe, H.; Müller, A.; Kolb, G., *Chemical Micro Process Engineering 1+2. Fundamentals, Modelling and Reactions/Processes and Plants*. Wiley-VCH: Weinheim, **2005**.
29. Ehrfeld, W.; Hessel, V.; Löwe, H., *Microreactors: New Technology for Modern Chemistry*. Wiley-VCH: Weinheim, **2000**.
30. Thayer, A. M. *Chem. Eng. News* **2005**, 83, 43.
31. DeWitt, S. H. *Curr. Opin. Chem. Biol.* **1999**, 3, 350-356.
32. Jähnisch, K.; Hessel, V.; Löwe, H.; Baerns, M. *Angew. Chem. Int. Ed.* **2004**, 43, 406-446.
33. Watts, P.; Haswell, S. J. *Chem. Soc. Rev.* **2005**, 34, 235-246.
34. Pennemann, H.; Watts, P.; Haswell, S. J.; Hessel, V.; Löwe, H. *Org. Process Res. Dev.* **2004**, 8, 422-439.
35. Jensen, K. F. *Chem. Eng. Sci.* **2001**, 56, 293-303.
36. Kiwi-Minsker, L.; Renken, A. *Catal. Today* **2005**, 110, 2-14.
37. Hessel, V.; Kolb, G.; de Bellefon, C. *Catal. Today* **2005**, 110, 1-1.
38. Kockmann, N.; Brand, O.; Fedder, G. K., *Micro Process Engineering*. Wiley-VCH: Weinheim, **2006**.

39. Hessel, V.; Serra, C.; Löwe, H.; Hadziioannou, G. *Chem. Ing. Tech.* **2005**, 77, 1693-+.
40. Iwasaki, T.; Yoshida, J. *Macromolecules* **2005**, 38, 1159-1163.
41. Honda, T.; Miyazaki, M.; Nakamura, H.; Maeda, H. *Lab Chip* **2005**, 5, 812-818.
42. Wu, T.; Mei, Y.; Xu, C.; Byrd, H. C. M.; Beers, K. L. *Macromol. Rapid Commun.* **2005**, 26, 1037-1042.
43. Liu, S. H.; Chang, C. H. *Chem. Eng. Technol.* **2007**, 30, 334-340.

4 Amphiphilic Linear-Hyperbranched Block Copolymers

4.1 Introduction

In the previous chapter, the successful development of a highly efficient two-step synthesis protocol for the preparation of hyperbranched polyglycerol structures with narrow polydispersities and controlled molecular weights was presented. Controlled synthesis of this polymer has been a challenging task for years and opens a broad range of possible approaches for the preparation of complex architectures like star or block copolymers containing hyperbranched building units. Although amphiphilic linear-linear diblock copolymers and the corresponding triblock copolymers have been of broad interest for a long time,¹⁻⁶ there exist only few examples of linear-hyperbranched structures in the literature.⁷⁻¹² An example for a well-established and studied biocompatible, amphiphilic linear-linear block copolymer system is represented by the industrially relevant PEO-*b*-PPO-*b*-PEO block copolymers, known as Pluronics[®] (BASF)^{13,14} or Poloxamer[®]. As mentioned previously, the fact that linear and dendritic polymers significantly differ in their physical and chemical properties motivates the combination of these two macromolecular structure units. Thus, substitution of the linear PEO blocks of the Pluronics[®] with hyperbranched polyglycerols would result in extremely versatile structures, opening a broad field of potential scientific and industrial applications. Based on the ROMBP principle (highlighted in chapter 1), glycidol was polymerized onto amine end-functionalized linear aliphatic chain macroinitiators after a preceding bisglycidolization step.^{15,16} Although attachment of glycidol to the linear starting molecules was evidenced, control over molecular weights and polydispersities remained a challenge to be overcome. In this chapter the knowledge acquired within the context of the work covered in chapter 3 will be applied to achieve molecular weight control for more complex structures, namely amphiphilic AB and ABA block copolymers consisting of linear PPO and hyperbranched PG blocks. Furthermore the improved methodology will be adopted for linear amine end functionalized alkyl chains as initiator cores. An existing double bond will provide access to various block copolymers via hydrosilylation reaction. Biomedical applications of these systems will be discussed in chapters 9 as well as in the appendix.

4.2 Jeffamines[®] as Macroinitiators

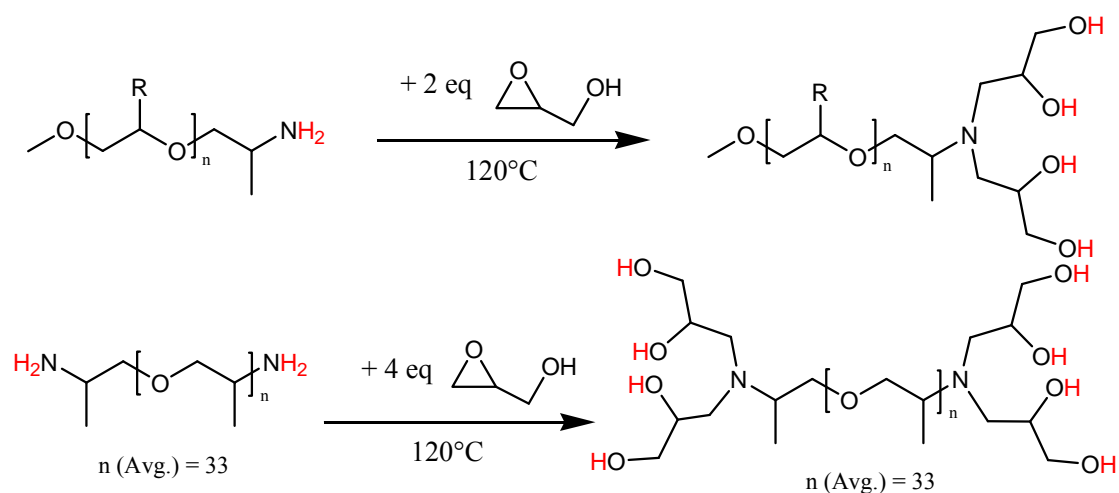
For the synthesis of the linear-hyperbranched block copolymers, three different kinds of Jeffamines[®] were chosen. As the linear chain should represent the hydrophobic part of the amphiphiles, Jeffamines[®] with predominantly polypropylene oxide units were used. For biomedical applications (chapters 9 & 10) the hydrophobic linear chain should possess a molecular weight of around 2,000 g/mol. Thus a mono- and a diamine with the respective chain length were selected (M-2005, D-2000). In order to facilitate characterization of the resulting polymers, a shorter chain length was chosen in additional experiments (M-600). Table 4.1 lists the corresponding data of the applied Jeffamines[®].

Table 4.1. Average molecular weights and composition of the Jeffamines[®] employed.

Jeffamine [®]	Molecular weight (g/mol)	PPO-units	PEO-units
XTJ-505 (M-600)	600	9	1
XTJ-507 (M-2005)	2,000	29	6
D-2000	2,000	33	0

4.2.1 Bisglycidolization of the Jeffamines[®]

In a first step the Jeffamines[®] were bisglycidolized to form efficient initiators, bearing four hydroxyl groups per amine end group as initiating sites for the subsequent anionic ring-opening multibranching polymerization (ROMBP) of glycidol (Scheme 4.1). It was proven that the additional bisglycidolization step is an important factor for the control of the following polymerization, since initiator functionality is a crucial parameter in the hyperbranching polymerization of glycidol, determining the eventual polydispersity of the system.¹⁷ At neutral conditions (pH = 7), amine groups are more nucleophilic than alcohol groups. Hence they can easily be bisglycidolized. The polymerization is carried out under basic conditions, thus the deprotonated alcohol groups become more reactive than the amine groups.



Scheme 4.1. Syntheses of the macroinitiators (functional H-atoms are highlighted in red).

Incorporation of incompletely bisglycidolized amines would lead to a significant loss of molecular weight control due to the polydispersity of the initiator. Since the chemical homogeneity of the macroinitiators determines the homogeneity of the synthesized block copolymers, all macroinitiators were investigated in detail by NMR spectroscopy, GPC, IR-spectroscopy, FD-, ESI- and MALDI-ToF mass spectrometry. Amine conversion upon the macroinitiator preparation was shown to be quantitative. The polydispersities of the macroinitiators ranged between 1.1 and 1.3 and thus correspond to the polydispersities of the Jeffamines[®], as depicted in Table 4.2.

Table 4.2. Theoretical and experimental molecular masses of the Jeffamines[®] and the resulting macroinitiators calculated from ^1H -NMR-spectra and GPC elugrams.

Sample	$M_{n,\text{th}}$ (g/mol)	$M_{n,\text{NMR}}$ (g/mol)	$M_{n,\text{GPC}}$ (g/mol)	PDI_{GPC}
XTJ-505 ($\text{PPO}_{10}\text{NH}_2$)	600	600	630	1.2
$\text{PPO}_{10}\text{N-PG}_2$	750	750	770	1.2
XTJ-507 ($\text{PPO}_{35}\text{NH}_2$)	2,000	1,980	2,650	1.3
$\text{PPO}_{35}\text{N-PG}_2$	2,150	2,130	2,750	1.3
D-2000 ($\text{H}_2\text{N-PPO}_{33}\text{-NH}_2$)	2,000	1,990	2,410	1.1
$\text{PG}_2\text{-N-PPO}_{33}\text{-N-PG}_2$	2,300	2,290	2,680	1.1

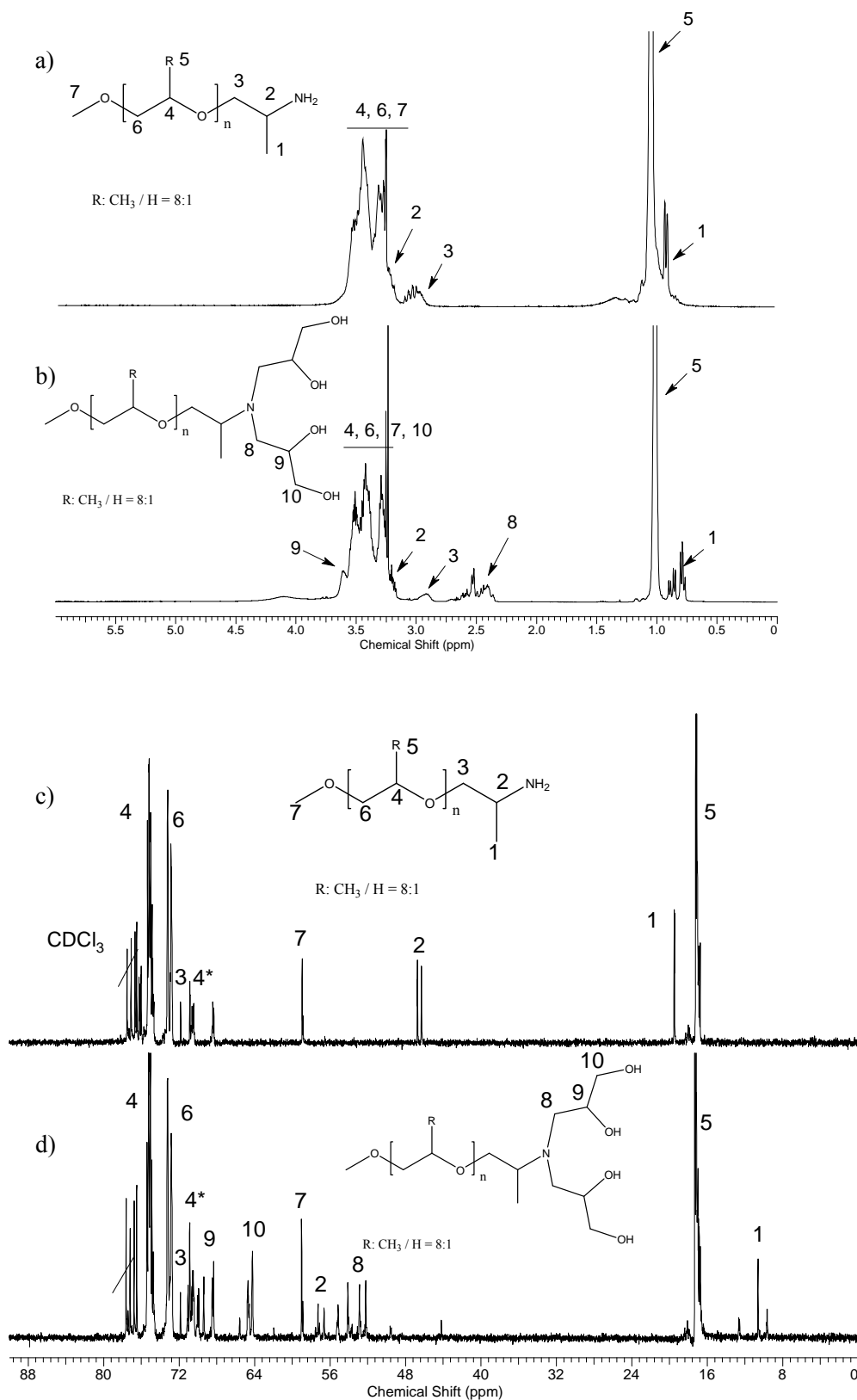


Figure 4.1. 1H -NMR spectra of the Jeffamine[®] XTJ-505 (a) and the resulting macroinitiator (b) in CDCl₃. ^{13}C -NMR spectra of the Jeffamine[®] XTJ-505 (c) and the resulting macroinitiator (d) in CDCl₃.

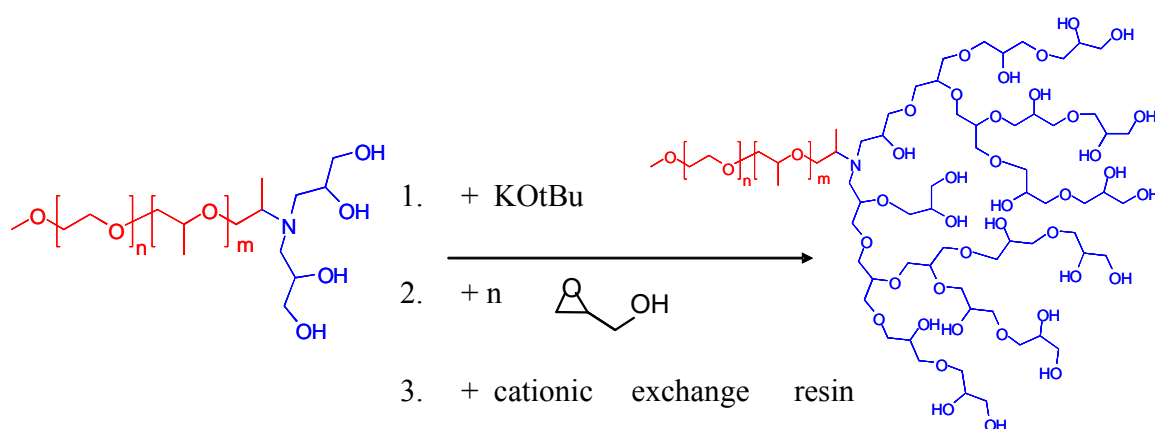
Figure 4.1 shows the ^1H - as well as the ^{13}C -NMR spectra of the Jeffamine[®] XTJ-505. As it is clearly visible, the methyl protons of the PPO chain are isolated from the other signals and hence can be normalized to 27 (average of 9 PPO units per polymer molecule). The numbers marked with a star belong to the PEO units incorporated into the polymer.

4.2.2 Synthesis of the Block Copolymers Based on Bisglycidolized Jeffamines[®]

Starting from the macroinitiators described in chapter 4.2.1, linear-hyperbranched AB- and ABA-block copolymers were synthesized via ROMBP of glycidol. The size of the targeted hyperbranched polyglycerol blocks was varied in a molar mass range between 800 and 6,000 g/mol. Furthermore, the influence of the degree of deprotonation was identified to play a key role for precision of molecular weight control as well as for narrow molecular weight distributions. In order to support the characterization data obtained, selected samples were persilylated and analyzed in analogy to the non-modified polymers.

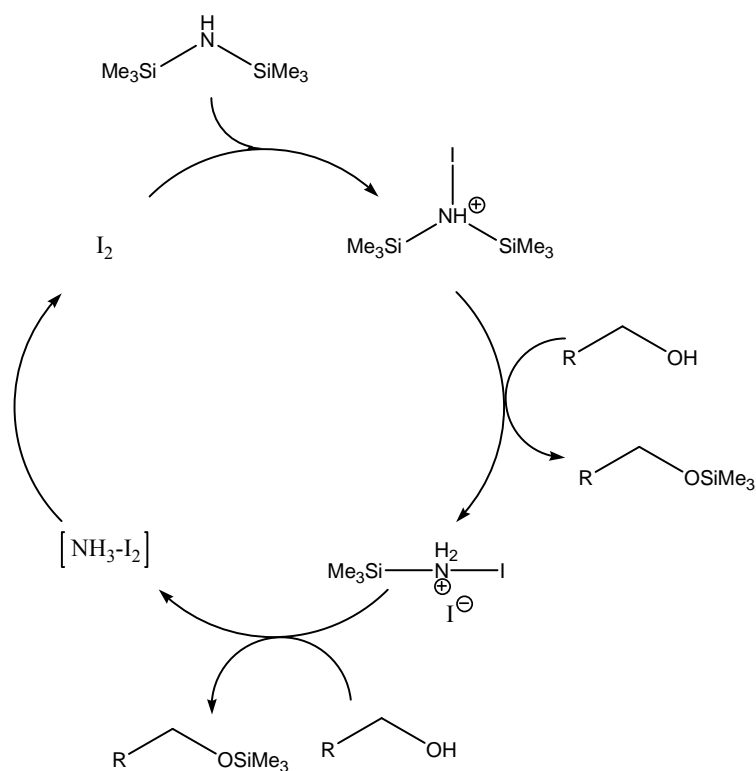
4.2.2.1 Linear-Hyperbranched AB-Diblock Copolymers

The first investigations involved the use of AB systems based on the macroinitiators XTJ-505-PG₂ and XTJ-507-PG₂ for the ROMBP of glycidol (Scheme 4.2).



Scheme 4.2. Synthesis of the AB block copolymers starting from bisglycidolized Jeffamines[®].

Preceding studies¹⁶ were carried out under standard reaction conditions, e.g., 10% deprotonation of the respective alcohol groups and led to attachment of glycidol to the linear starting molecules. However, control over molecular weights and polydispersities remained a challenge to be mastered. ¹H-NMR spectroscopy as well as GPC analysis gave molecular weights significantly higher than expected, indicating incomplete incorporation of the macroinitiators. Molecular weight control decreased rapidly with increasing target molecular weight of the polyglycerol block. This observation confirms the results discussed in chapter 3: As the polypropylene oxide chain of the macroinitiator leads to an enhanced solubility of the deprotonated initiators in diglyme (compared to TMP), higher degrees of deprotonation may be promising for an improved control over the reaction. Deprotonation degrees of 20% and 40% were explored to ensure the required equilibration between protonation and deprotonation in early stages of the polymerization. In order to support the characterization data and to exclude aggregation effects due to the presence of hydrogen bonds, selected samples of the AB-block copolymers were silylated by reaction with 1,1,1,3,3,3-hexamethyldisilazane (HMDS). Iodine was used as a catalyst.¹⁸ The proposed reaction mechanism is depicted in Scheme 4.3.



Scheme 4.3. Proposed mechanism of the silylation of alcohols by reaction with HMDS and iodine catalyst.¹⁸

Compared to TMP-containing polyglycerols, $^1\text{H-NMR}$ results of the PPO-based polymers are more reliable because the signal intensity of the methyl groups of the PPO chain provides reasonable integrals. Figure 4.2 exemplifies how molecular mass determination can be achieved in these cases. Like mentioned before, the Jeffamine[®] XTJ-505 contains an average of 9 PPO units. As the glycidol block only slightly influences the signal of the PPO methyl groups, the corresponding isolated signal can still be standardized to 27. The 32 hydrogen atoms of the Jeffamine[®], which can be found in the region between 3.3 and 3.8 ppm, have to be subtracted from this integral. The resulting value divided by 5 (5 protons per repeat unit) corresponds to the degree of polymerization of the glycidol block. It has to be mentioned that thorough drying of the samples is important, since traces of methanol or diglyme falsify the calculated values. Furthermore, PG homopolymers are indistinguishable from the PG blocks of the block copolymers. Therefore it is necessary to confirm the NMR results with further characterization methods.

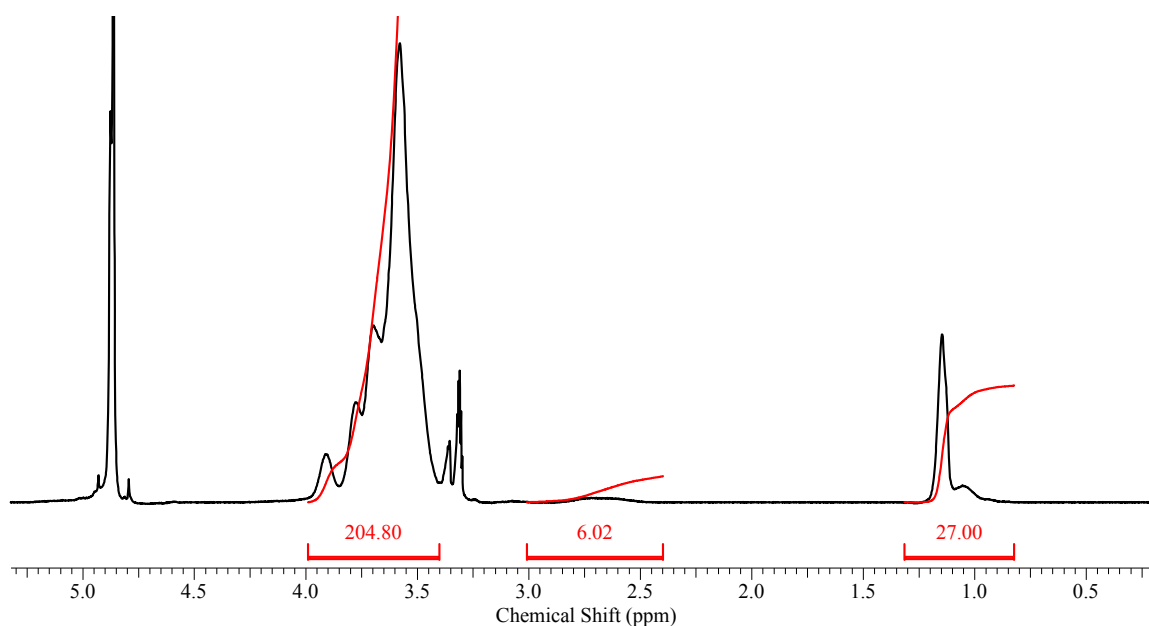


Figure 4.2. $^1\text{H-NMR}$ spectra of the block copolymer $\text{PPO}_{10}\text{-N-PG}_x$ with 20% of deprotonation and a targeted M_w of 1,600g/mol (respective sample in grey color in Table 4.3 and Figure 4.3).

Determination of the molar mass distribution can be achieved by GPC analysis. In addition to the aforementioned problematic issues with respect to an accurate characterization of hyperbranched polymers (Chapter 3), it has to be taken into account that the samples

covered in this chapter are amphiphilic block copolymers. As the molecular weight of the branched PG block of the polymers is varied, while the PPO chain remains unchanged, the sample compositions and hence the corresponding hydrodynamic radii differ on a non-negligible scale. The amphiphilic character may also lead to undesired aggregation phenomena. The latter problem can be eliminated by silylation of the OH end groups in order to prevent hydrogen bonding and to reduce the amphiphilic nature of the polymers.

Table 4.3. $^1\text{H-NMR}$ and GPC characterization data obtained for the silylated and non silylated AB block copolymers based on Jeffamine[®] XTJ-505 ($\text{PPO}_{10}\text{-N-PG}_2$) under variation of the degree of deprotonation and the size of the PG block.

Sample	Deprot. / Silylation	x_{th}	$M_{n,\text{th}}$ (g/mol)	$M_{n,\text{NMR}}$ (g/mol)	$M_{n,\text{GPC}}$ (g/mol)	PDI_{GPC}
$\text{PPO}_{10}\text{-N-PG}_x$	-	0	600	600	630	1.2
$\text{PPO}_{10}\text{-N-PG}_x$	-	2	750	750	770	1.2
$\text{PPO}_{10}\text{-N-PG}_x(\text{SiMe}_3)_{x+2}$	silyl.	2	1,050	1,030	820	1.2
$\text{PPO}_{10}\text{-N-PG}_x$	10%	13.5	1,600	2,940	2,550	2.0
$\text{PPO}_{10}\text{-N-PG}_x$	20%	13.5	1,600	3,160	3,040	1.4
$\text{PPO}_{10}\text{-N-PG}_x(\text{SiMe}_3)_{x+2}$	silyl.	13.5	2,780	6,500	4,950	1.6
$\text{PPO}_{10}\text{-N-PG}_x$	40%	13.5	1,600	1,340	1,780	1.4
$\text{PPO}_{10}\text{-N-PG}_x(\text{SiMe}_3)_{x+2}$	silyl.	13.5	2,780	2,930	2,750	1.5
$\text{PPO}_{10}\text{-N-PG}_x$	10%	54	4,600	27,850	8,060	3.5
$\text{PPO}_{10}\text{-N-PG}_x(\text{SiMe}_3)_{x+2}$	silyl.	54	8,860	70,750	15,590	3.0
$\text{PPO}_{10}\text{-N-PG}_x$	20%	54	4,600	6,410	6,060	1.8
$\text{PPO}_{10}\text{-N-PG}_x$	40%	54	4,600	3,930	4,720	1.5

As the linear PPO chain structurally rather resembles PEG than PS (and because the molecular weights of the polyglycerol blocks are moderate), PEG standards are more reli-

able for GPC characterization of these polymers. Hence all GPC data in this chapter are based on PEG standards. Table 4.3 summarizes the NMR and GPC data obtained from the materials based on bisglycidolized Jeffamine[®] XTJ-505 (PPO₁₀NPG₂). It is obvious that that higher degrees of deprotonation resulted in a narrowing of the polydispersities. Molecular weights obtained with deprotonation rates of 10% were also higher than theoretically expected. This is particularly valid for the 4,000 g/mol PG block target molecular weight specimen (black rows in Table 4.3). A considerable difference in molar mass values calculated from NMR and GPC has to be noted, which results from the dominance of the hyperbranched PG block in the respective polymeric structure and consequent molecular weight underestimation by GPC due to the pronounced compactness of the branched structure (cp. Chapter 3.2.3). Increasing the degree of deprotonation to 20% provides well defined diblock copolymers ($PDI \leq 1.8$). Nevertheless, molecular weights are still higher than targeted due to incomplete initiator core incorporation. Unfortunately, 40% deprotonation of the initiator alcohol groups resulted in highly viscous materials with poor solubility in diglyme. However, homogeneous solutions can still be obtained after ultrasonic treatment. Characterization data after formation of the polyglycerol block proves complete incorporation of the initiator molecules as well as narrow molecular weight distributions and excellent molecular weight control. Figure 4.3 depicts a selection of the corresponding GPC curves obtained from the non silylated samples (assigned by color).

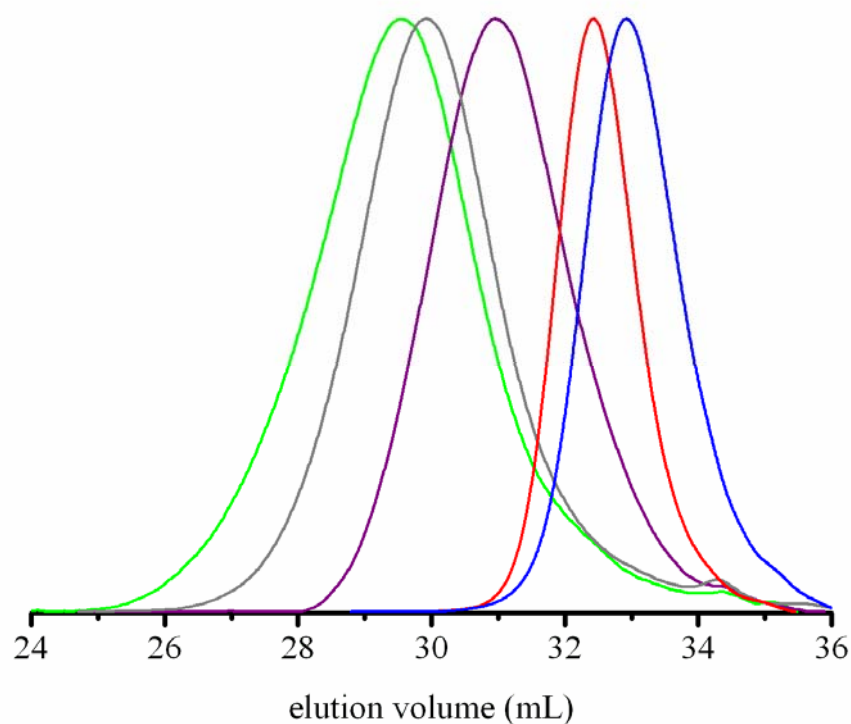


Figure 4.3. GPC curves of linear-hyperbranched PPO₁₀PG_x block copolymers listed in Table 4.3 (assigned by color).

Encouraged by the promising results achieved by using Jeffamine[®] of XTJ-505 as macroinitiator for the glycidol polymerization, analogous experiments were performed using Jeffamine[®] XTJ-507. As the longer PPO-chain of the polymer leads to lower charge density and higher flexibility of the deprotonated macroinitiators, solubility problems were significantly reduced, e.g., no ultrasonic treatment was required for complete dissolution of the macroinitiators in diglyme. Nevertheless, homogenous solutions were only realized upon heating to 120°C. Table 4.4 contains the experimental data obtained from the respective block copolymers. In all cases, deprotonation degrees of 40% were used.

Table 4.4. $^1\text{H-NMR}$ and GPC characterization data obtained from AB block copolymers based on the Jeffamine[®] XTJ-507 ($\text{PPO}_{35}\text{-N-PG}_2$) at varying size of the PG block.

Sample	x_{th}	$M_{n,\text{th}}$ (g/mol)	$M_{n,\text{NMR}}$ (g/mol)	$M_{n,\text{GPC}}$ (g/mol)	PDI_{GPC}
$\text{PPO}_{35}\text{N-PG}_x$	2	2,150	2,130	2,250	1.3
$\text{PPO}_{35}\text{N-PG}_x$	13	3,000	3,210	3,230	1.4
$\text{PPO}_{35}\text{N-PG}_x$	27	4,000	3,840	3,940	1.4
$\text{PPO}_{35}\text{N-PG}_x$	40	5,000	5,210	4,810	1.7
$\text{PPO}_{35}\text{N-PG}_x$	74	7,500	8,730	8,400	2.4

The data summarized in Table 4.4 shows good agreement between theoretical and experimental molecular weights. Attachment of up to 30 glycerol units is possible keeping molecular weight distributions narrow, whereas larger polyglycerol blocks lead to a moderate increase in polydispersity. Since the amphiphilic character of the polymers requires a certain ratio between the two different blocks, suitable compositions can be conveniently achieved by this synthesis protocol. Using such well-defined amphiphilic block copolymers with up to 30 glycerol units as macroinitiators for further addition of glycidol (Chapter 3) may also lead to higher molecular weight species incorporating the corresponding Jeffamines[®].

4.2.2.2 Linear-Hyperbranched ABA-Triblock Copolymers

As the previously mentioned Pluronics[®] represent linear ABA triblock copolymers, a special interest in the corresponding *hb-l-hb*-ABA triblock copolymers (Figure 4.4) is apparent, in order to obtain the structural analogs of the linear Pluronics.

Previously conducted work in this field revealed that application of standard polymerization conditions leads to significant problems such as broad multimodal molar mass distributions of the resulting polymers.¹⁶ However, as the examined initiators possess 8 instead of 4 initial OH-groups, superior molecular weight control is expected according to theoretical considerations.¹⁷ Deprotonation of 40% of the OH-groups resulted in poorly soluble macroinitiators (visual inspection of the mixture), while lower degrees of deprotonation (20% and 30% respectively) resulted in significantly improved solubility. Table

4.5 lists the corresponding data of the respective polymers. Selected GPC curves (30% of deprotonation) are shown in Figure 4.4.

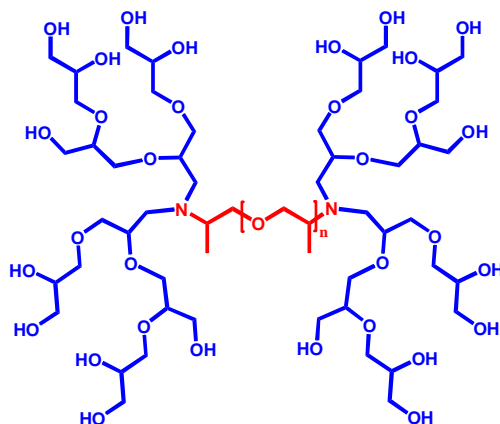


Figure 4.4. Structure of the resulting ABA triblock copolymers.

Table 4.5. $^1\text{H-NMR}$ and GPC characterization data obtained from ABA block copolymers based on Jeffamine[®] D2000 ($\text{PG}_2\text{-N-PPO}_{33}\text{-N-PG}_2$) at varying degree of deprotonation and molecular weight of the PG block.

Sample	Deprot.	x_{th}	$M_{n,\text{th}}$ (g/mol)	$M_{n,\text{NMR}}$ (g/mol)	$M_{n,\text{GPC}}$ (g/mol)	PDI_{GPC}
$\text{PG}_x\text{-N-PPO}_{33}\text{-N-PG}_x$	-	2	2,300	2,290	2,680	1.1
$\text{PG}_x\text{-N-PPO}_{33}\text{-N-PG}_x$	20%	13	4,000	5,980	6,310	1.4
$\text{PG}_x\text{-N-PPO}_{33}\text{-N-PG}_x$	30%	13	4,000	4,430	4,770	1.2
$\text{PG}_x\text{-N-PPO}_{33}\text{-N-PG}_x$	40%	13	4,000	3,350	3,870	1.5
$\text{PG}_x\text{-N-PPO}_{33}\text{-N-PG}_x$	20%	27	6,000	7,230	7,420	1.6
$\text{PG}_x\text{-N-PPO}_{33}\text{-N-PG}_x$	30%	27	6,000	6,030	6,120	1.3
$\text{PG}_x\text{-N-PPO}_{33}\text{-N-PG}_x$	40%	27	6,000	5,880	5,720	1.5
$\text{PG}_x\text{-N-PPO}_{33}\text{-N-PG}_x$	20%	40	8,000	8,300	8,740	2.2
$\text{PG}_x\text{-N-PPO}_{33}\text{-N-PG}_x$	30%	40	8,000	8,210	8,390	1.7
$\text{PG}_x\text{-N-PPO}_{33}\text{-N-PG}_x$	40%	40	8,000	6,070	6,300	2.0

It is obvious that the described approach allowed for a remarkable enhancement of the previously reported results,¹⁶ with the ideal degree of deprotonation of initial OH groups amounting to 30% with respect to polydispersities over the whole molecular weight range. However, proceeding to higher molecular weights is associated with a moderate broadening in the molecular weight distribution, comparable to the results obtained from the AB block copolymers. Figure 4.5 visualizes this effect and shows the corresponding monomodal GPC curves of the polymers obtained at 30% deprotonation. The colors correspond to those in Table 4.5.

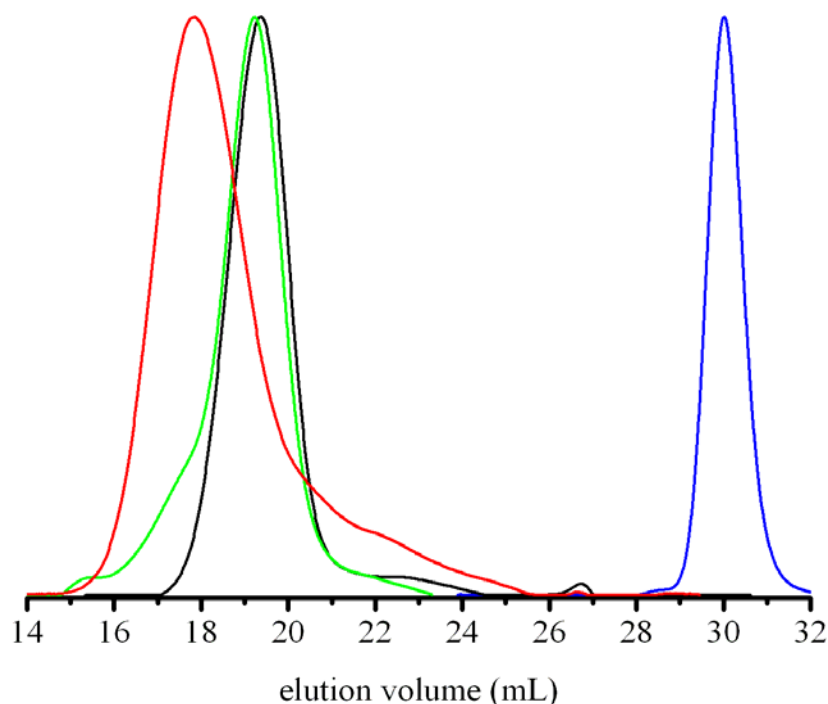
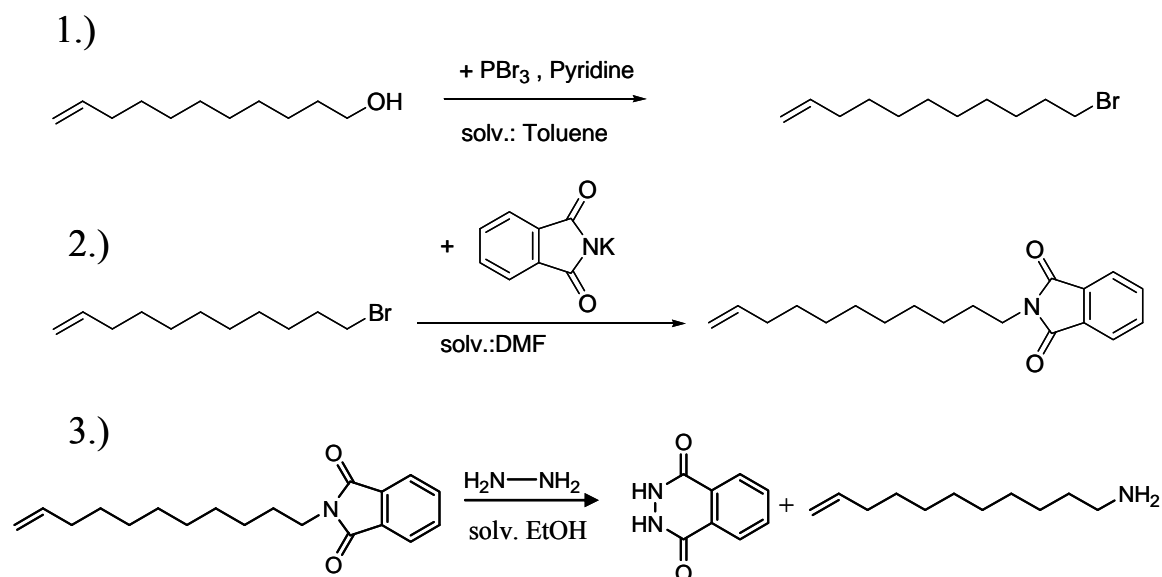


Figure 4.5. GPC curves of linear-hyperbranched $\text{PG}_x\text{-N-PPO}_{33}\text{-N-PG}_x$ block copolymers listed in Table 4.5, using a 30% deprotonation degree of the initial OH-groups.

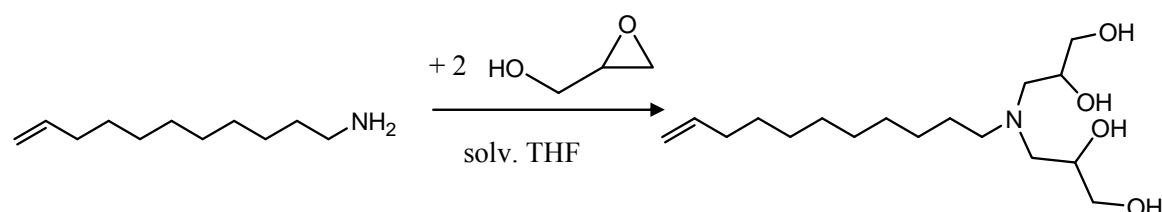
4.3 Bisglycidolized Linear Alkyl Amines as Initiators

The application of amine functionalized linear alkyl chains as hydrophobic part for block copolymer structures has been reported in previous studies.^{15,19-21} In order to investigate whether the aforementioned improvement in polymerization control can be transferred to these systems as well, two different types of linear alkyl amines were applied in corresponding reactions (octadecyl amine and undecenyl amine). While octadecyl amine is commercially available at a reasonable price, undecenyl amine was synthesized in a three step synthetic pathway, depicted in Scheme 4.4.



Scheme 4.4. Synthetic pathway to undecenyl amine starting from commercially available undecenyl alcohol.

The ω -unsaturated alcohol was transformed into the respective bromide via nucleophilic substitution using phosphorus tribromide (78% yield).²² In order to obtain the corresponding amine, a Gabriel synthesis protocol was applied using potassium phthalimide (76% yield)²³ and hydrazine (45% yield),^{23,24} resulting in an overall yield of 27% after 3 steps. It should be mentioned that an excess of hydrazine has to be avoided as well as elevated temperatures during the work-up with hydrochloric acid after step 3 in order to protect the double bond. The amine was subsequently bisglycidolized (Scheme 4.5) to yield the tetrafunctional alcohol in quantitative yield.



Scheme 4.5. Bisglycidolization of undecenyl amine.

The commercially available octadecyl amine was analogously converted into the bisglycidolized initiator for subsequent ROMBP of glycidol. Initial results obtained from using octadecyl amine as initiator indicated slightly improved results at 20% deprotonation in-

stead of 40%. Particularly in the case of larger polyglycerol blocks, enhanced reaction control was achieved. Due to the facilitated handling of the less deprotonated species, 20% deprotonation was applied for analogous studies involving the bisglycidolized undecenyl amine, leading to similarly promising results. The respective results are shown in Table 4.6.

Table 4.6. $^1\text{H-NMR}$ and GPC characterization data obtained from ABA block copolymers based on bisglycidolized alkyl amines at varying degree of deprotonation and size of the PG block.

Sample	Deprot.	x_{th}	$M_{n,\text{th}}$ (g/mol)	$M_{n,\text{NMR}}$ (g/mol)	$M_{n,\text{GPC}}$ (g/mol)	PDI_{GPC}
$\text{C}_{18}\text{H}_{37}\text{-N-PG}_x$	-	2	417	417	480	1.0
$\text{C}_{18}\text{H}_{37}\text{-N-PG}_x$	20%	14	1,300	1,380	1,520	1.5
$\text{C}_{18}\text{H}_{37}\text{-N-PG}_x$	40%	14	1,300	1,370	1,380	1.4
$\text{C}_{18}\text{H}_{37}\text{-N-PG}_x$	20%	30	2,500	2,570	2,690	1.3
$\text{C}_{18}\text{H}_{37}\text{-N-PG}_x$	40%	30	2,500	3,420	4,480	1.8
$\text{CH}_2=\text{CH-C}_9\text{H}_{18}\text{-N-PG}_x$	-	2	317	317	390	1.0
$\text{CH}_2=\text{CH-C}_9\text{H}_{18}\text{-N-PG}_x$	20%	11	1,000	1,280	1,240	1.2
$\text{CH}_2=\text{CH-C}_9\text{H}_{18}\text{-N-PG}_x$	20%	18	1,500	1,620	1,780	1.4
$\text{CH}_2=\text{CH-C}_9\text{H}_{18}\text{-N-PG}_x$	20%	25	2,000	2,160	2,740	1.6

The GPC curves of the undecenyl alcohol based samples (colored in Table 4.6) are visualized in Figure 4.6.

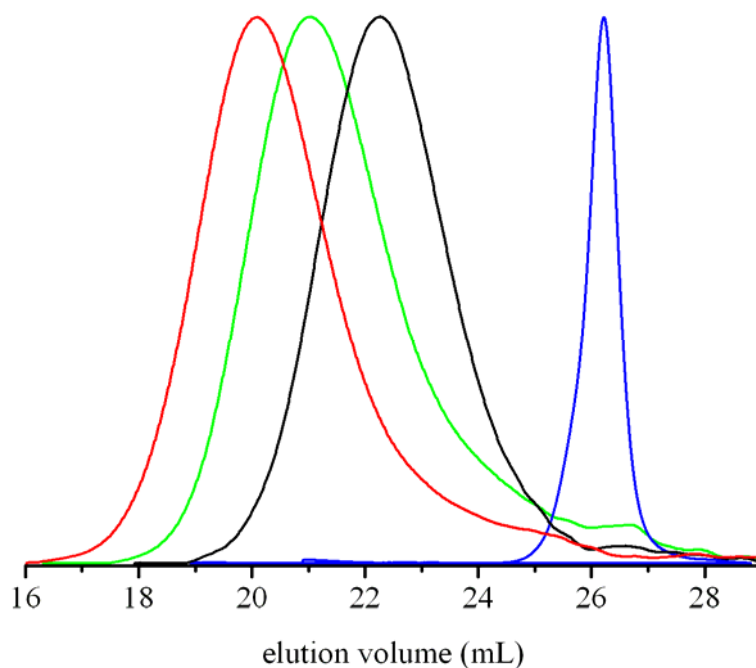


Figure 4.6. GPC curves of the hyperbranched polymers using undecenyl amine as initiator listed in Table 4.6 achieved by 20% deprotonation of the initial OH-groups.

For a further transformation of these polymers by subsequent reaction sequences, the presence of the single, “focal” double bond is essential. It can be unequivocally evidenced by $^1\text{H-NMR}$ spectroscopy (Figure 4.7).

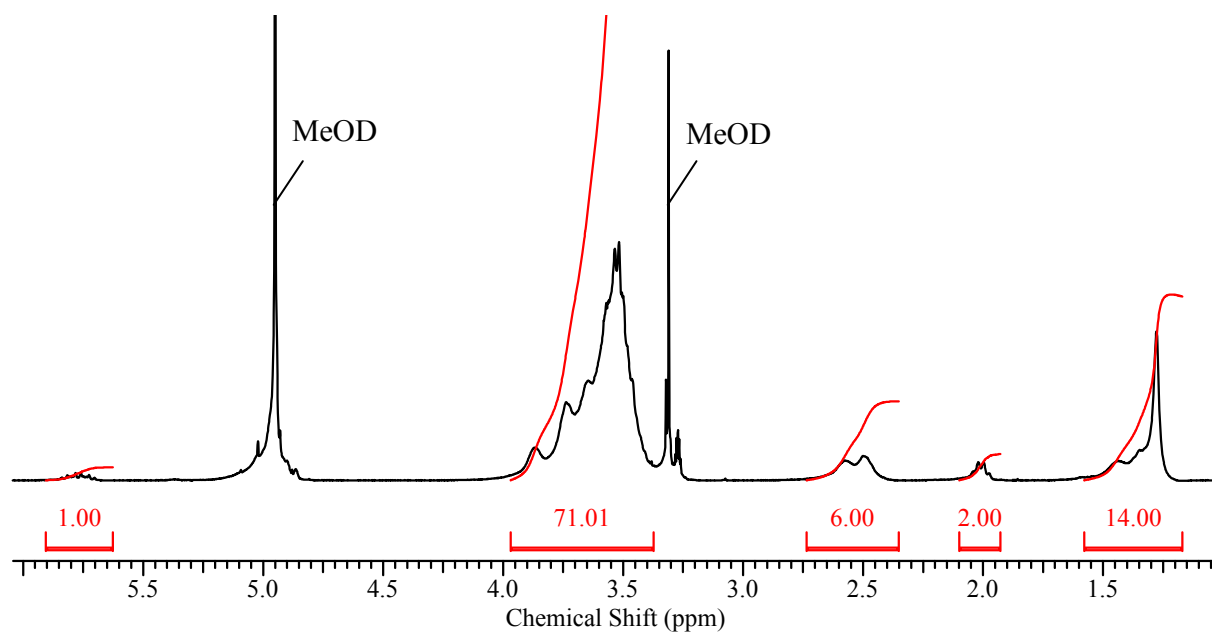


Figure 4.7. $^1\text{H-NMR}$ (methanol- d_4) spectra of the *hb* polymer based on a bisglycidolized undecenylamine initiator (black color in Table 4.6 and Figure 4.6).

Methanol has been found to be an excellent solvent for NMR studies of this kind of polymers. Although the presence of the double bond can be confirmed, a drawback of using methanol as a solvent for this system lies in the overlap of the solvent peak with one of the double bond signals. Nonetheless, excellent integral agreement with theoretical values is found, especially for smaller polyglycerol blocks. Presence of the unsaturated site within these structures opens a wide range for subsequent modification steps and further tailoring of the polymers. For instance, double bonds are known to react with thiols under free radical conditions. Earlier results showed that exposition of polyglycerols with incorporated linear alkyl chain and terminal double bond to an excess of thiol in the presence of free radicals generated by dibenzoylperoxide (BPO) leads to quantitative addition of the thiol to the double bond.²⁰ Additional potential lies in hydrosilylation reactions with silanes. As most of these reactions are carried out in non-polar solvents, the introduction of cleavable protecting groups (acetal²⁵ or silyl¹⁸ groups) might be necessary as an additional step. However, these polymers offer high potential with respect to an application as reactants in the assembly of complex macromolecular structures and in the tailoring of block copolymers.

4.4 Conclusion

In a preliminary account glycidol was polymerized onto amine end functionalized linear aliphatic chains as macroinitiators after a bisglycidolization step.¹⁵ Although attachment of glycidol to the linear starting molecules was evidenced, control over molecular weights and polydispersities remained a challenge to overcome. In this chapter the knowledge acquired within the context of the work covered in chapter 3 was applied to achieve molecular weight control. Well defined amphiphilic copolymers containing hydrophilic hyperbranched polyglycerol blocks and linear, apolar poly(propylene oxide) blocks have been realized. Furthermore bisglycidolized linear alkyl amines with long alkyl chain have been examined as initiators. The hyperbranched blocks were synthesized by the previously described ROMBP of glycidol onto these initiators. Determination of the molecular weights of the synthesized polymers by NMR-spectroscopy and GPC showed a significant effect of the degree of deprotonation during the monomer addition. Starting from bisglycidolized Jeffamines[®] as macroinitiators, a degree of deprotonation of 10% as applied earlier¹⁵ resulted in unexpectedly high molar masses of the resulting polymers and leads to a pronounced tendency of the materials to form aggregates. Broad

polydispersities in the range of 3 to 6 were obtained. Deprotonation degrees of 20% lead to lower polydispersities. Proceeding to 40% of deprotonation, target molecular weights can be efficiently met under excellent control of the reaction. Solubility problems as well as the requirement of an adequate equilibrium between active and dormant end groups impede the use of higher degrees of deprotonation. The characterization data for persilylated samples confirm the results obtained from the non-silylated polymers. As part of additional studies, *Hb-PG-b-l-PPO-b-hb-PG* ABA block copolymers have been synthesized. An optimum degree of deprotonation of 30% has been found in these cases. Initiators based on linear alkyl amines led to eligible results at degrees of deprotonation of 20%. The presence of a terminal double bond offers intriguing potential with respect to the assembly of complex macromolecular structures.

4.5 Experimental Part

4.5.1 Materials

The Jeffamines[®] were provided by the *Huntsman Corporation*. All other chemicals were purchased from *Aldrich* or *Acros Organics*. Acetone p.a., methanol p.a., Dowex[®] 50WX8, 200-400 mesh, ion exchange resin, 1,1,1-trishydroxymethyl-propane (TMP) and 1M potassium *tert*-butylate solution in THF were used as received. THF and toluene were distilled over sodium prior to use. Diglyme and glycidol were purified by distillation over calcium hydride. Methanol-d₄ was purchased from *Deutero GmbH*.

4.5.2 Characterization of the Provided Jeffamines[®]

4.5.2.1 Methoxy-poly(oxyethylene/oxypropylene)-2-propylamine (Jeffamine[®] XTJ-505 (M-600))

Ø: PPO = 8, PEO = 1 ⇒ C₃₀H₆₃NO₁₀: (M_w = 597.4 g/mol)

300 MHz-¹H-NMR (CDCl₃): δ [ppm] = 0.91 (d, 3H, CH₂-CHCH₃-NH₂), 1.03 (d, 24H, CH₃, PPO), 2.97 – 3.54 (m, 34H, CH₂-CHCH₃-NH₂, CH₂-CHCH₃-NH₂, CH₂, PPO, CH₂, PEO, CH, PPO, CH₃-O-).

75 MHz-¹³C-NMR (CDCl₃): δ [ppm] = 17.24 (CH₃ PPO), 19.61 (CH₂-CHCH₃-NH₂), 46.37 - 46.79 (CH-NH₂), 59.01 (CH₃-O-), 70.58 - 70.88 (CH₂, PEO), 71.86 (CH₂-CHCH₃-NH₂), 72.85 – 73.24 (CH₂, PPO), 74.89 - 75.22 (CH, PPO).

GPC (DMF): M_n = 630, M_w/M_n = 1.2

IR (ATR): $\nu(\text{cm}^{-1}) = 2970, 2866$ (C-H), 1097 (C-O-C), further characteristic peaks: 1453, 1343, 1297, 1013, 925, 862.

4.5.2.2 Methoxy-poly(oxyethylene/oxypropylene)-2-propylamine (Jeffamine[®] XTJ-507 (M-2005))

\emptyset : PPO = 28, PEO = 6 \Rightarrow $\text{C}_{100}\text{H}_{203}\text{NO}_{35}$: ($M_w = 1978.4$ g/mol)

300 MHz-¹H-NMR (CDCl_3): δ [ppm] = 0.94 (d, 3H, $\text{CH}_2\text{-CHCH}_3\text{-NH}_2$), 1.07 (d, 84H, CH_3 , PPO), 2.97 – 3.54 (m, 114H, $\text{CH}_2\text{-CHCH}_3\text{-NH}_2$, $\text{CH}_2\text{-CHCH}_3\text{-NH}_2$, CH_2 , PPO, CH_2 , PEO, CH , PPO, $\text{CH}_3\text{-O-PPO}$).

75 MHz-¹³C-NMR (CDCl_3): δ [ppm] = 17.30 (CH_3 PPO), 19.50 ($\text{CH}_2\text{-CHCH}_3\text{-NH}_2$), 46.31 - 46.74 (CH-NH_2), 58.85 ($\text{CH}_3\text{-O}$), 70.42 - 70.60 (CH_2 , PEO), 72.76 - 73.21 (CH_2 , PPO), 71.77 ($\text{CH}_2\text{-CHCH}_3\text{-NH}_2$), 74.95 - 75.34 (CH , PPO).

GPC (DMF): $M_n = 2650$, $M_w/M_n = 1.3$

IR (ATR): $\nu(\text{cm}^{-1}) = 2970, 2866$ (C-H), 1095 (C-O-C), further characteristic peaks: 1451, 1372, 1346, 1296, 1013, 924, 864.

4.5.2.3 Poly(oxypropylene)diamine (Jeffamine[®] D-2000)

\emptyset : PPO = 33 \Rightarrow $\text{C}_{102}\text{H}_{208}\text{N}_2\text{O}_{33}$: ($M_w = 1989.4$ g/mol)

300 MHz-¹H-NMR (CDCl_3): δ [ppm] = 0.93 (d, 6H, $\text{CH}_2\text{-CHCH}_3\text{-NH}_2$), 1.06 (d, 96H, CH_3 , PPO), 3.01 – 3.66 (m, 102H, $\text{CH}_2\text{-CHCH}_3\text{-NH}_2$, $\text{CH}_2\text{-CHCH}_3\text{-NH}_2$, CH_2 , PPO, CH , PPO).

75 MHz-¹³C-NMR (CDCl_3): δ [ppm] = 17.24 (CH_3 PPO), 19.61 ($\text{CH}_2\text{-CHCH}_3\text{-NH}_2$), 46.36 - 46.79 (CH-NH_2), 72.84 - 73.26 (CH_2 , PPO), 75.02 - 75.37 (CH , PPO), 76.24 ($\text{CH}_2\text{-CHCH}_3\text{-NH}_2$).

GPC (DMF): $M_n = 2410$, $M_w/M_n = 1.1$

IR (ATR): $\nu(\text{cm}^{-1}) = 2969, 2929, 2865$ (C-H), 1095 (C-O-C), further characteristic peaks: 1452, 1372, 1344, 1296, 1013, 927, 867.

4.5.3 Synthesis of the Macroinitiators

The macromolecular initiators were obtained by dropwise addition of a stoichiometric amount of glycidol to the Jeffamine[®] at 120°C under argon atmosphere over 30 minutes. The mixture was stirred for an additional two hours. The material was purified by precipitation into ethyl acetate. Yield: quantitative.

4.5.3.1 Macroinitiator from Jeffamine[®] XTJ-505 (M-600)

Ø: PPO = 8, PEO = 1 ⇒ C₃₆H₇₅NO₁₄: (M_w = 745.5 g/mol)

400 MHz-¹H-NMR (CDCl₃): δ [ppm] = 0.84 (d, 3H, CH₂-CHCH₃-N), 1.05 (d, 24H, CH₃, PPO), 2.45 – 3.55 (m, 44H, CH₂-CHCH₃-N, CH₂-CHCH₃-N, CH₂, PPO, CH₂, PEO, CH, PPO, CH₃-O-, N-CH₂-CHOH-CH₂OH, N-CH₂-CHOH-CH₂OH, N-CH₂-CHOH-CH₂OH).
 100 MHz-¹³C-NMR (CDCl₃): δ [ppm] = 10.57 (CH₂-CHCH₃-N), 17.27 (CH₃ PPO), 52.15 - 52.81 (N-CH₂-CHOH-CH₂OH), 54.06 (CH₂-CHCH₃-N), 58.95 (CH₃-O-), 64.18 - 64.64 (N-CH₂-CHOH-CH₂OH), 68.28 - 68.40 (N-CH₂-CHOH-CH₂OH), 70.43 - 70.82 (CH₂, PEO), 72.76 - 73.15 (CH₂, PPO), 74.68 – 75.34 (CH, PPO), 76.43 (CH₂-CHCH₃-N).

GPC (DMF): M_n = 770, M_w/M_n = 1.2

IR (ATR): ν(cm⁻¹) = 3421 (O-H), 2969, 2871 (C-H), 1095 (C-O-C), further characteristic peaks: 2361, 1455, 1372, 1342, 1296, 927, 859.

4.5.3.2 Macroinitiator from Jeffamine[®] XTJ-507 (M-2005)

Ø: PPO = 28, PEO = 6 ⇒ C₁₀₆H₂₁₅NO₃₉: (M_w = 2126.5 g/mol)

300 MHz-¹H-NMR (CDCl₃): δ [ppm] = 0.84 – 1.06 (m, 87H, CH₂-CHCH₃-N), 1.05 (d, 24H, CH₃, PPO), 2.45 – 3.55 (m, 44H, CH₂-CHCH₃-N, CH₂-CHCH₃-N, CH₂, PPO, CH₂, PEO, CH, PPO, CH₃-O-, N-CH₂-CHOH-CH₂OH, N-CH₂-CHOH-CH₂OH, N-CH₂-CHOH-CH₂OH).

75 MHz-¹³C-NMR (CDCl₃): δ [ppm] = 17.19 – 18.17 (CH₂-CHCH₃-N, CH₃, PPO), 52.04 (N-CH₂-CHOH-CH₂OH), 54.06 (CH₂-CHCH₃-N), 58.96 (CH₃-O-), 64.26 - 64.63 (N-CH₂-CHOH-CH₂OH), 68.28 - 68.40 (N-CH₂-CHOH-CH₂OH), 70.45 - 70.52 (CH₂, PEO), 71.78 - 73.31 (CH₂, PPO), 75.06 – 75.45 (CH, PPO), 76.43 (CH₂-CHCH₃-N).

GPC (DMF): M_n = 2750, M_w/M_n = 1.3

IR (ATR): ν(cm⁻¹) = 3472 (O-H), 2969, 2867 (C-H), 1095 (C-O-C), further characteristic peaks: 1452, 1372, 1345, 1296, 1013, 925, 864.

4.5.3.3 Macroinitiator from Jeffamine[®] D-2000

Ø: PPO = 33 ⇒ C₁₁₄H₂₃₂N₂O₄₁: (M_w = 2285.6 g/mol)

300 MHz-¹H-NMR (CDCl₃): δ [ppm] = 0.84 - 1.08 (m 102, CH₂-CHCH₃-N, CH₃, PPO), 2.39 – 2.72 (m, 8H, N-CH₂-CHOH-CH₂OH), 2.8 – 3.15 (m, 4H, CH₂-CHCH₃-N), 3.23 – 3.67 (m, 110H, CH₂-CHCH₃-N, CH₂, PPO, CH, PPO, N-CH₂-CHOH-CH₂OH, N-CH₂-CHOH-CH₂OH).

75 MHz- ^{13}C -NMR (CDCl_3): δ [ppm] = 10.41 ($\text{CH}_2\text{-CHCH}_3\text{-N}$), 17.21 (CH_3 PPO), 51.93 - 55.48 ($\text{N-CH}_2\text{-CHOH-CH}_2\text{OH}$), 57.45 ($\text{CH}_2\text{-CHCH}_3\text{-N}$), 64.19 - 64.58 ($\text{N-CH}_2\text{-CHOH-CH}_2\text{OH}$), 68.04 - 69.21 ($\text{N-CH}_2\text{-CHOH-CH}_2\text{OH}$), 70.31 - 70.85 ($\text{CH}_2\text{-CHCH}_3\text{-N}$), 72.79 - 73.24 (CH_2 , PPO), 75.02 - 75.23 (CH , PPO).

GPC (DMF): $M_n = 2680$, $M_w/M_n = 1.1$

IR (ATR): $\nu(\text{cm}^{-1}) = 3418$ (O-H), 2969, 2928, 2865 (C-H), 1094 (C-O-C), further characteristic peaks: 2361, 1452, 1372, 1343, 1296, 925, 861.

4.5.4 Synthesis of the Linear-Hyperbranched Block Copolymers Starting from Jeffamine[®] Based Macroinitiators

All syntheses described in chapter 4.2 were carried out under argon atmosphere in the polymerization apparatus described in chapter 3.6.2. Freshly distilled THF (ca. 50 mL) was injected to the reservoir funnel under argon atmosphere and the pump was run until no bubbles were observed upon THF addition to the reactor. The desired amount of glycidol was filled into the reservoir funnel to the remaining THF in Ar-counter flow. The corresponding macroinitiator was deprotonated to a certain amount (10-40%) with a potassium *tert*-butylate solution in THF in a one-neck flask. The mixture was heated to 70°C bath temperature on a rotary evaporator. The resulting alcohol was removed under vacuum. Subsequently, the initiator was dissolved/emulsified in 20ml freshly distilled diglyme (sometimes treatment in an ultrasonic bath was required) and transferred into the reactor in Ar-counter flow. The oil bath was heated to 120°C and the stirrer was run at 600 revolutions per minute and the pump was started. A pumping rate of 5 drops per minute was employed and the size of the drops was adjusted to 50%. When the addition of glycidol was completed, an additional 25 mL of freshly distilled THF were filled into the reservoir and the pump was restarted in order not to lose any glycidol remaining in the tube connected to the pump. After the reaction was finished, products were dissolved in methanol and stirred with a cation exchange resin. Subsequently, the solution was filtered over a sintered filter (pore size 1) and washed with methanol. The resulting polymer was precipitated twice into cold acetone as a methanol solution and dried for 12 h in vacuo at 100°C. The block copolymers are yellowish, transparent, viscous materials. Yields are between 70 and 95% depending on the polymer size.

4.5.4.1 Linear-Hyperbranched Block Copolymers Starting from Jeffamine[®] based Macroinitiators

300 MHz-¹H-NMR (D₂O / MeOD): δ [ppm] = 0.87 – 1.03 (m, CH₂-CHCH₃-N, CH₃, PPO), 2.45 – 3.55 (m, CH₂-CHCH₃-N, CH₂-CHCH₃-N, CH₂, PPO, CH₂, PEO, CH, PPO, CH₃-O-, CH, PG, CH₂, PG), 4.54 (m, -OH).

75 MHz-¹³C-NMR (CDCl₃): δ [ppm] = 17.66 (CH₃ PPO), 50.54 (CH₂-CHCH₃-N), 58.47 (CH₃-O-), 62.86 (L₁₃), 64.99 (T), 70.47 (L₁₄), 71.28 (L_{13s}, D_s), 72.37 (T), 72.76 (L_{14s}, L_{13p}, D, CH₂, PEO), 73.50 (T_s, CH₂, PPO), 74.28 – 74.74 (T_p, L₁₄, L_{13s}), 76.49 (CH₂-CHCH₃-N), 77.74 (CH, PPO), 79.77 (L₁₃), 81.72 (D).

IR (ATR): ν (cm⁻¹) = 3375 (O-H), 2873 (C-H), 1067 (C-O-C), further characteristic peaks: 1642, 1452, 1326, 929, 864, 577.

4.5.5 Silylation of the Block Copolymers

A solution of 80mmol HMDS in 100 ml CH₂Cl₂ was added over a period of 30 minutes to a vigorously stirred suspension of the alcohol (100 mmol) and I₂ (1.0 mmol) in CH₂Cl₂ (40 ml). The solution was stirred for 48h. A clear solution was obtained. After the reaction was completed 30g of powdered Na₂S₂O₃ were added portion wise. The mixture was stirred for an additional 30 min, filtered and washed twice with CH₂Cl₂. The solvent was removed in vacuo and the product was purified by dialysis in CHCl₃ p.a.

4.5.5.1 Silylated Block Copolymers Starting from Jeffamine[®] Based Macroinitiators

300 MHz-¹H-NMR (CDCl₃): δ [ppm] = -0.15 - 0.26 (m, SiCH₃, CH₂-CHCH₃-N), 1.09 (d, 24H, CH₃, PPO), 3.31 – 3.86 (m, CH₂-CHCH₃-N, CH₂-CHCH₃-N, CH₂, PPO, CH₂, PEO, CH, PPO, CH₃-O, N-CH₂-CHOSiMe₃-CH₂OSiMe₃, CH₂, PG, CH, PG).

IR (ATR): ν (cm⁻¹) = 2955, 2901, 2868 (C-H), 1097 (C-O-C), further characteristic peaks: 1457, 1249, 1010, 835, 749, 685, 628, 527.

4.5.6 *N,N*-Bis(-2,3-dihydroxy-propyl)-octadecyl amine

A solution of 34.9g octadecyl amine (0.13 mol) was dissolved in 50ml THF and cooled to 0°C. 2eq of glycidol were dissolved in 50ml THF and added over a period of 2h. The reaction was allowed to warm to room temperature and the THF was removed in vacuo. The solid product is obtained quantitatively.

300 MHz-¹H-NMR (CDCl₃): δ [ppm] = 0.88 (t, 3H, -CH₃), 1.19-1.32 (m, 30H, -CH₂-), 1.44 (m, 2H, -CH₂-CH₂-N-), 2.44-2.66 (m, 6H, -CH₂-N-), 3.45-3.78 (m, 6H, -CHOH-CH₂-OH), 4.14 (s, 4H, -OH).

IR (ATR): ν(cm⁻¹) = 3420 (O-H), 2910, 2840 (C-H) further characteristic peaks: 730, 1450.

4.5.7 Synthesis of *N,N*-Bis(-2,3-dihydroxy-propyl)-undec-10-enyl amine

4.5.7.1 Undecenyl bromide (11-Bromo-1-undecene)

Undecenyl alcohol (100 g, 0.59 mol) was dissolved in a mixture of 175ml dry toluene and 16ml pyridine. The solution was cooled to -10°C and kept at -5 to -10°C while a solution of 64g (0.23 mol) of phosphorus tribromide in 175ml dry toluene was added over a period of two hours. Then the reaction mixture was allowed to warm to room temperature and heated till reflux for 14 h. The liquid was filtered from the solid residue and the residue was washed with toluene. The washings were added to the liquid layer and the toluene was removed under reduced pressure. The remaining residue was distilled at reduced pressure. A yield of 108g (78%) was obtained. Bp. 64°C (2.3*10⁻³mbar).

300 MHz-¹H-NMR (CDCl₃): δ [ppm] = 1.30-1.43 (m, 12H, CH₂), 1.86 (qui., 2H, -CH₂-CH₂-Br), 2.05 (qua., -CH₂-CH=CH₂), 3.41 (t, 2H, -CH₂-CH₂-Br), 4.97 (dd, 2H, -CH₂-CH=CH₂), 5.89-5.75 (m, 1H, -CH₂-CH=CH₂).

IR (ATR): ν(cm⁻¹) = 2930, 2850 (C-H), 3080 (CH=CH₂), further characteristic peaks: 910, 1460.

4.5.7.2 *N*-undec-10-enyl-phthalimide

A mixture of 100.9g (0.44mol) 11-bromo-1-undecene and 88.6g (0.48mol) potassium phthalimide in 800ml DMF was heated to 60h under reflux. After cooling to room temperature the mixture was filtered. The solution was added to 800ml of a half saturated NaCl-solution and extracted three times with ether (800ml total). The ether extracts were washed with a saturated NaCl solution (80ml) and dried over Na₂SO₄. The ether solution was then filtered and the solvent removed from the filtrate in vacuo to give 99g (76%) *N*-undec-10-enyl-phthalimide. This material was used without further purification.

300 MHz-¹H-NMR (CDCl₃): δ [ppm] = 1.09-1.32 (m, 12H, CH₂), 1.66 (m., 2H, -CH₂-CH₂-Phth.), 2.00 (qua., -CH₂-CH=CH₂), 3.67 (t, 2H, -CH₂-CH₂-Phth), 4.93 (dd, 2H, -CH₂-CH=CH₂), 5.73-5.86 (m, 1H, -CH₂-CH=CH₂), 7.65-7.88 (m, 4H, Phth.).

4.5.7.3 Undec-10-enyl amine

A mixture of 96.2g *N*-undec-10-enyl-phthalimide (0.32 mol) and hydrazine monohydrate (0.30 mol) in 600ml ethanol were refluxed for 2h. The solution was cooled to room temperature and treated with 450ml concentrated HCl. The resulting salt was removed by filtration and the residue washed with water. The combined filtrates were evaporated to give a yellow solid. The solid was dissolved in 700ml of a 1N solution of sodium hydroxide, extracted with ether (2x 600ml) and dried over Na₂SO₄. The ether was evaporated to give a yellow oil. The oil was purified by vacuum distillation (64°C, 2.3* 10⁻³ mbar) to give a clear colorless oil. A yield of 22.7g (41%) was obtained.

300 MHz-¹H-NMR (CDCl₃): δ [ppm] = 1.07-1.44 (m, 14H, CH₂), 2.03 (qua., -CH₂-CH=CH₂), 2.67 (t, 2H, -CH₂-NH₂), 4.94 (dd, 2H, -CH₂-CH=CH₂), 5.74-5.87 (m, 1H, -CH₂-CH=CH₂).

IR (ATR): ν(cm⁻¹) = 3332 (N-H), 2920, 2850 (C-H), 3080 (CH=CH₂), further characteristic peaks: 910,1460.

4.5.7.4 *N,N*-Bis(-2,3-dihydroxy-propyl)-undec-10-enyl amine

A solution of 22.7g undec-10-enyl amine (0.13 mol) was dissolved in 50ml THF and cooled to 0°C. 2 eq of glycidol were dissolved in 50ml THF and added over a period of 2h. The reaction mixture was allowed to warm to room temperature and THF was removed in vacuo. The product is obtained quantitatively and crystallizes below 25°C.

300 MHz-¹H-NMR (CDCl₃): δ [ppm] = 1.09-1.39 (m, 14H, CH₂), 2.03 (qua., -CH₂-CH=CH₂), 2.44-2.65 (m, 6H, -CH₂-N-), 3.45-3.76 (m, 6H, -CHOH-CH₂-OH), 4.35 (s, 4H, -OH), 4.95 (dd, 2H, -CH₂-CH=CH₂), 5.77-5.86 (m, 1H, -CH₂-CH=CH₂).

IR (ATR): ν(cm⁻¹) = 3420 (O-H), 2910, 2840 (C-H), 3070 (CH=CH₂), further characteristic peaks: 910,1450.

4.5.8 Synthesis of the Hyperbranched Polymers Using Bisglycidolized Alkyl Amines as Initiators

All syntheses described in chapter 4.3 were carried out under argon atmosphere in the polymerization apparatus described in chapter 3.6.2. Freshly distilled THF (ca. 50 mL)

was injected to the reservoir funnel under and the pump was run until no bubbles were observed upon THF addition to the reactor. The desired amount of glycidol was filled into the reservoir funnel to the remaining THF in Ar-counter flow. The corresponding initiator was deprotonated to a certain amount (20-40%) with a potassium *tert*-butylate solution in THF in a one-neck flask. The mixture was heated to 70°C bath temperature on a rotary evaporator. The resulting alcohol was removed under vacuum. Subsequently, the initiator was dissolved/emulsified in 20ml freshly distilled diglyme and transferred into the reactor in Ar-counter flow. The oil bath was heated to 120°C and the stirrer was run at 600 revolutions per minute and the pump was started. A pumping rate of 5 drops per minute was employed and the size of the drops was adjusted to 50%. When the addition of glycidol was completed, an additional 25 mL of freshly distilled THF were filled into the reservoir and the pump was restarted in order not to lose any glycidol remaining in the tube connected to the pump. After the reaction was finished, products were dissolved in methanol and stirred with a cation exchange resin. Subsequently, the solution was filtered over a sintered filter (pore size 1) and washed with methanol. The resulting polymer was precipitated twice into cold acetone as a methanol solution and dried for 12 h in vacuo at 100°C. The polymers are yellowish, transparent, viscous materials. Yields are between 80 and 95% depending on the polymer size.

4.5.8.1 Hyperbranched Polyglycerols Using *N,N*-Bis(-2,3-dihydroxy-propyl)-octadecyl amine as Initiator

300 MHz-¹H-NMR (MeOD): δ [ppm] = 0.88 (t, 3H, -CH₃), 1.19-1.45 (m, 32H, -CH₂-), 2.44-2.66 (m, 6H, -CH₂-N-), 3.35-3.85 (m, -CHOH-CH₂-OH).

IR (ATR): $\nu(\text{cm}^{-1})$ = 3380 (O-H), 2880 (C-H) 1070 (C-O-C) further characteristic peaks: 730, 1450. 1640.

4.5.8.2 Hyperbranched Polyglycerols Using *N,N*-Bis(-2,3-dihydroxy-propyl)-undec-10-enyl amine as Initiator

300 MHz-¹H-NMR (MeOD): δ [ppm] = 1.09-1.39 (m, 14H, CH₂), 2.03 (qua., -CH₂-CH=CH₂), 2.44-2.65 (m, 6H, -CH₂-N-), 3.45-3.76 (m, -CHOH-CH₂-OH), 4.95 (dd, 2H, -CH₂-CH=CH₂), 5.77-5.86 (m, 1H, -CH₂-CH=CH₂).

IR (ATR): $\nu(\text{cm}^{-1})$ = 3380 (O-H), 2870 (C-H), 1067 (C-O-C), further characteristic peaks: 720, 1450, 1640.

4.6 References

1. Förster, S.; Antonietti, M. *Adv. Mater.* **1998**, 10, 195-+.
2. Förster, S.; Plantenberg, T. *Angew. Chem. Inter. Edit.* **2002**, 41, 689-714.
3. Taton, D.; Leborgne, A.; Sepulchre, M.; Spassky, N. *Macromol. Chem. Phys.* **1994**, 195, 139-148.
4. Dimitrov, P.; Rangelov, S.; Dworak, A.; Haraguchi, N.; Hirao, A.; Tsvetanov, C. *B. Macromol. Symp.* **2004**, 215, 127-139.
5. Halacheva, S.; Rangelov, S.; Tsvetanov, C. *Macromolecules* **2006**, 39, 6845-6852.
6. Erberich, M.; Keul, H.; Möller, M. *Macromolecules* **2007**, 40, 3070-3079.
7. Kricheldorf, H. R.; Stukenbrock, T. *J. Polym. Sci. Part a: Polym. Chem.* **1998**, 36, 31-38.
8. Kwak, S. Y.; Ahn, D. U.; Choi, J.; Song, H. J.; Lee, S. H. *Polymer* **2004**, 45, 6889-6896.
9. Al-Muallem, H. A.; Knauss, D. M. *J. Polym. Sci. Part a: Polym. Chem.* **2001**, 39, 152-161.
10. An, S. G.; Cho, C. G. *Polym. Bul.* **2004**, 51, 255-262.
11. Marcos, A. G.; Pusel, T. M.; Thomann, R.; Pakula, T.; Okrasa, L.; Geppert, S.; Gronski, W.; Frey, H. *Macromolecules* **2006**, 39, 971-977.
12. Barriau, E.; Marcos, A. G.; Kautz, H.; Frey, H. *Macromol. Rapid Commun.* **2005**, 26, 862-867.
13. Michels, B.; Waton, G.; Zana, R. *Langmuir* **1997**, 13, 3111-3118.
14. Marinov, G.; Michels, B.; Zana, R. *Langmuir* **1998**, 14, 2639-2644.
15. Istratov, V.; Kautz, H.; Kim, Y. K.; Schubert, R.; Frey, H. *Tetrahedron* **2003**, 59, 4017-4024.
16. Nieberle, J. *Diploma Thesis* **2004**.
17. Hanselmann, R.; Hölter, D.; Frey, H. *Macromolecules* **1998**, 31, 3790-3801.
18. Karimi, B.; Golshani, B. *J. Org. Chem.* **2000**, 65, 7228-7230.

19. Barriau, E. Hyperbranched Polyether Polyols As Building Blocks For Complex Macromolecular Architectures. PhD, Johannes Gutenberg-University, Mainz, **2005**.
20. Sunder, A. Controlled Polymerization Of Glycidol For The Synthesis Of Hyperbranched Polyglycerols and Polyether Polyols With Variable Molecular Architectures. Ph.D., Albert-Ludwigs-University, Freiburg im Breisgau, **2000**.
21. Kautz, H. *Ph. D. Thesis, University of Freiburg*, **2003**.
22. Marvel, C. S.; Garrison, W. E. *J. Am. Chem. Soc.* **1959**, 81, 4737-4744.
23. Gagne, M. R.; Stern, C. L.; Marks, T. J. *J. Am. Chem. Soc.* **1992**, 114, 275-294.
24. Leone-Bay, A.; Paton, D. R.; Freeman, J.; Lercara, C.; O'Toole, D.; Gschneidner, D.; Wang, E.; Harris, E.; Rosado, C.; Rivera, T.; DeVincent, A.; Tai, M.; Mercogliano, F.; Agarwal, R.; Leipold, H.; Baughman, R. A. *J. Med. Chem.* **1998**, 41, 1163-1171.
25. Haag, R.; Stumbe, J. F.; Sunder, A.; Frey, H.; Hebel, A. *Macromolecules* **2000**, 33, 8158-8166.

5 Novel Monomer for Non Nitrogen Containing Linear-Hyperbranched Block Copolymers

5.1 Introduction

Poly(ethylene oxide) (PEO) is probably the most important biocompatible polymer because of its very low toxicity, excellent solubility in aqueous solutions, extremely low immunogenicity and antigenicity.¹⁻³ PEO also exhibits good pharmacokinetic and biodistribution behavior.¹⁻³ Animal studies have shown that it exhibits high persistence in the blood stream and low accumulation in reticuloendothelial system (RES) organs, liver, and spleen. PEO shows the propensity to exclude proteins, other macromolecules, and particulates from its surroundings *in vivo*. These properties of PEO are exploited for a plethora of applications and have been attributed to its high chain mobility associated with conformational flexibility and water-binding capability via hydrogen bonds.^{4,5} As already highlighted in the previous chapters hyperbranched polyglycerol (PG) obtained by cationic^{6,7} or anionic⁸⁻¹² ring-opening multibranching polymerization (ROMBP) of glycidol has recently been demonstrated to exhibit similarly excellent biocompatibility properties as PEO,^{13,14} but in addition offers possibilities for versatile further functionalization due to its polyfunctionality. Consequently combining these kinds of structures offers great potential for various biomedical applications. Linear diblock copolymers of PEO and linear PG blocks have been reported by Spassky et al.,¹⁵ who demonstrated that ethoxyethyl glycidyl ether (EEGE) can be polymerized via an anionic mechanism. The ethoxy ethyl protecting group can be conveniently removed, yielding a linear poly(glycerol) with free hydroxyl groups in every repeat unit.¹⁶⁻¹⁹ The synthesis of linear poly(glycerol)s and the respective linear block copolymers has been described by Tsvetanov et al.,^{20,21} and an elegant, more recent work by Möller et al.²² presented linear poly(glycerol)s with orthogonal protecting groups. In numerous papers, the synthesis of linear polymers with dendrimer block²³⁻²⁷ has been described, based on multi-step approaches. Only few papers, however, have detailed the preparation of novel linear-hyperbranched block copolymers.^{28,29} Frederick Wurm developed a convenient 4-step (2-pot) approach for the synthesis of double hydrophilic linear-hyperbranched block copolymers consisting exclusively of an aliphatic polyether structure based on poly(ethylene oxide) (PEO) and poly(glycerol) (PG) which can be found in the appendix.

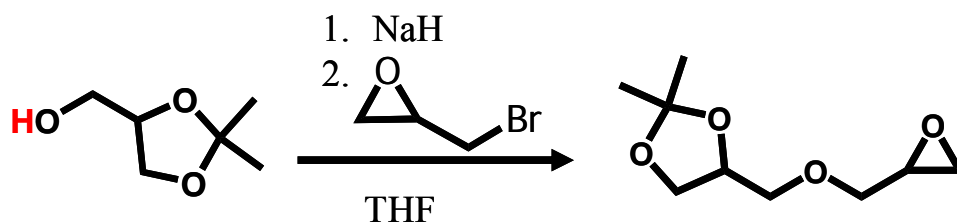
This chapter presents a novel monomer for the anionic polymerization in order to increase the degree of branching in these types of structures.

5.2 Poly(glyceryl glycerol) Block Copolymers

First work on the synthesis of a novel monomer for the synthesis of block copolymers based on PEO and poly(glyceryl glycerol)s (PGG) that can be viewed as a perfect first generation dendronized polymer based on (poly)glycerol will be presented in this chapter.

5.2.1 Synthesis of (DL-1,2-Isopropylidene glyceryl) Glycidyl Ether (IGG)

A new bifunctional oxirane monomer for anionic polymerization has been designed that can be readily synthesized, using epibromohydrine and commercially available DL-1,2-isopropylidene glycerol (solketal). After purification by column chromatography 92% of pure product were obtained. The preparation of the new epoxide monomer is shown in Scheme 5.4.



Scheme 5.1. Synthesis of (DL-1,2-isopropylidene glyceryl) glycidyl ether (IGG).

The signals in the $^1\text{H-NMR}$ as well as in the $^{13}\text{C-NMR}$ spectrum of the monomer can be perfectly assigned by regarding the corresponding 2D-NMR spectra. Both COSY-NMR and HSQC-NMR in CDCl_3 are depicted in Figure 5.1.

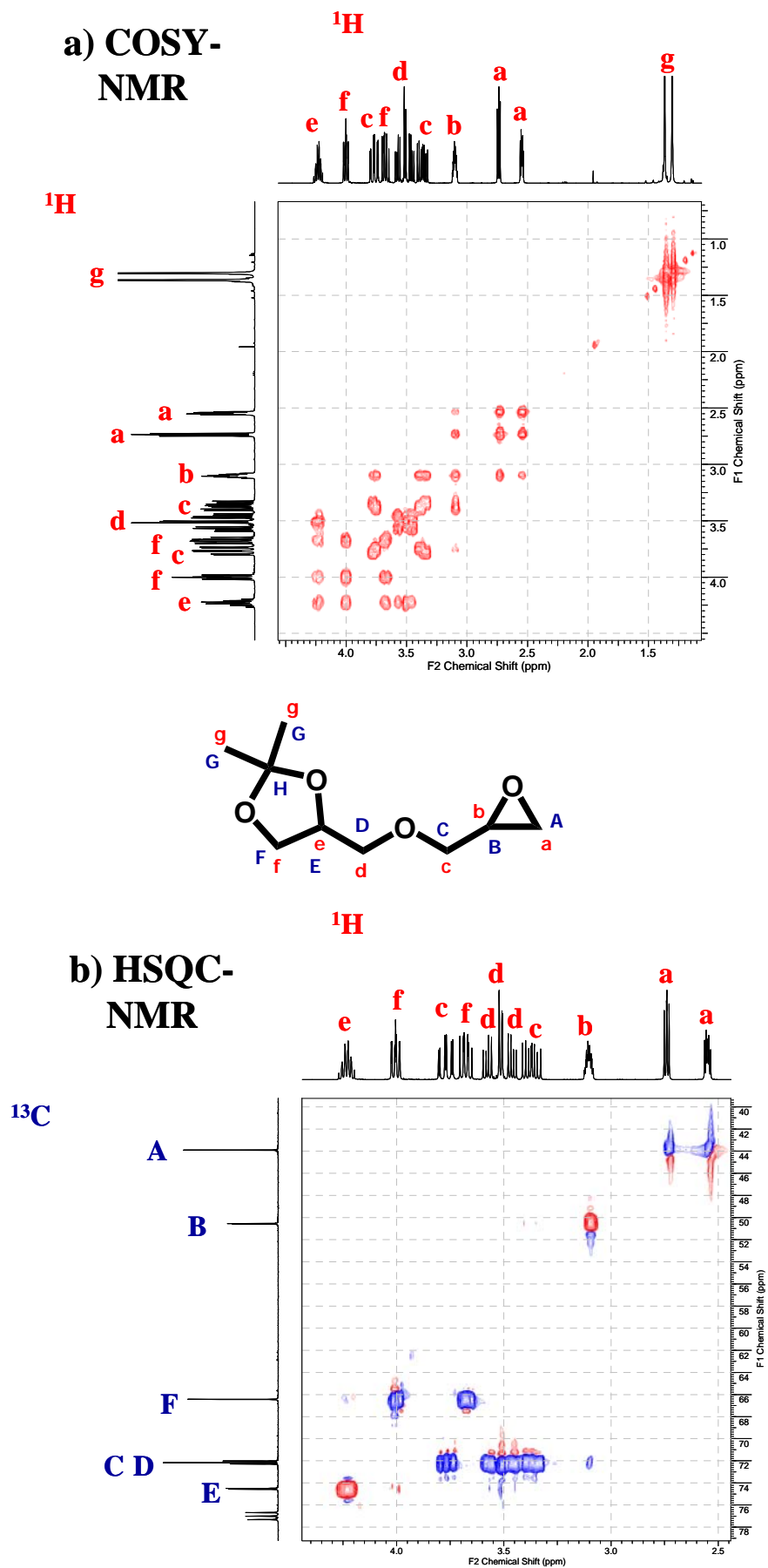
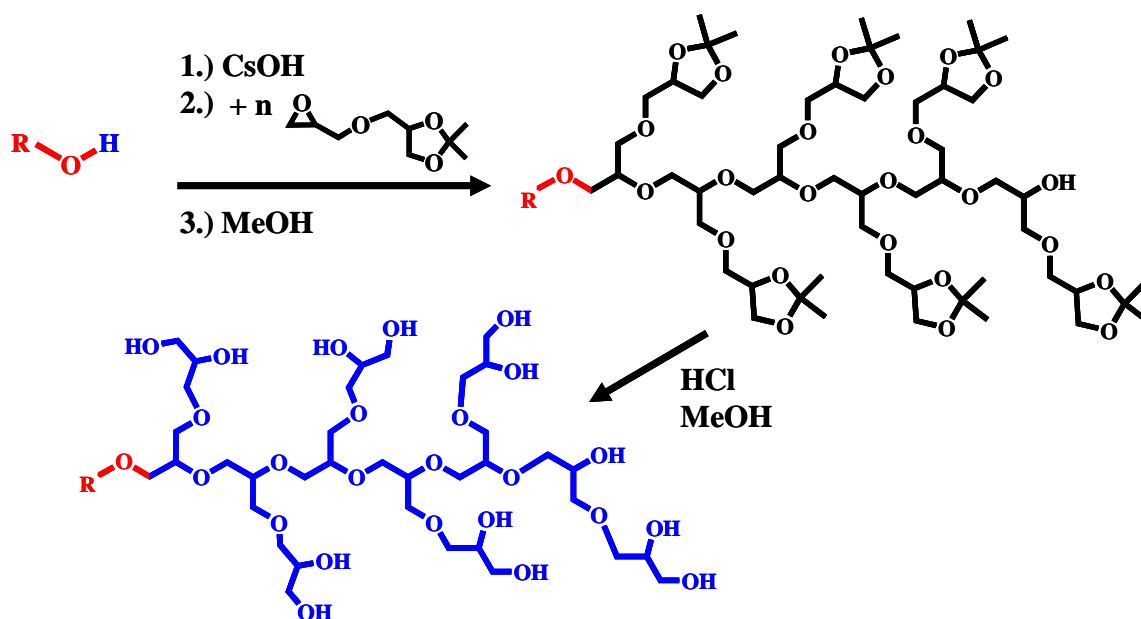


Figure 5.1. a) 2D-COSY-NMR of IGG in CDCl_3 ; b) 2D-HSQC-NMR of IGG in CDCl_3 .

5.2.2 Synthesis of Poly(glyceryl glycerol) Block Copolymers

The newly designed monomer for anionic polymerization, DL-1,2-isopropylidene glyceryl glycidyl ether (IGG) was tested towards homopolymerization as well as polymerized onto commercially available poly(ethylene oxide) blocks and converted to well-defined block copolymers yielding poly(glyceryl glycerol)s after simple deprotection with diluted hydrochloric acid (Scheme 5.2). IGG actually represents an orthogonally protected dimer of glycerol. The synthesis avoids contact with hazardous material that could cause problems in quantitative removal and is therefore suitable for biomedical application.



Scheme 5.2. Synthetic pathway for the preparation of poly(glyceryl glycerols).

The resulting monomer (DL-1,2-isopropylidene glyceryl) glycidyl ether (IGG) was polymerized onto deprotonated commercially available PEO chains using Cs counter ions. IGG exhibits orthogonal behavior in terms of a dimer of glycerol. The epoxide group acts as the polymerizable, latent glycerol moiety, while the acetal protecting group is very stable during anionic polymerization and can be conveniently cleaved subsequent to polymerization to generate the side chain glycerol moiety. Hydrolytic cleavage of the acetal protecting group after polymerization using diluted HCl can be performed directly in the polymerization vessel without additional workup steps. Gel permeation chromatography (GPC) revealed a narrow molecular weight distribution. It was found that in the case of the PIGG-polymers PS-standards were more reliable, while the NMR results of the PGG polymers were confirmed by PEG standards (Table 5.1).

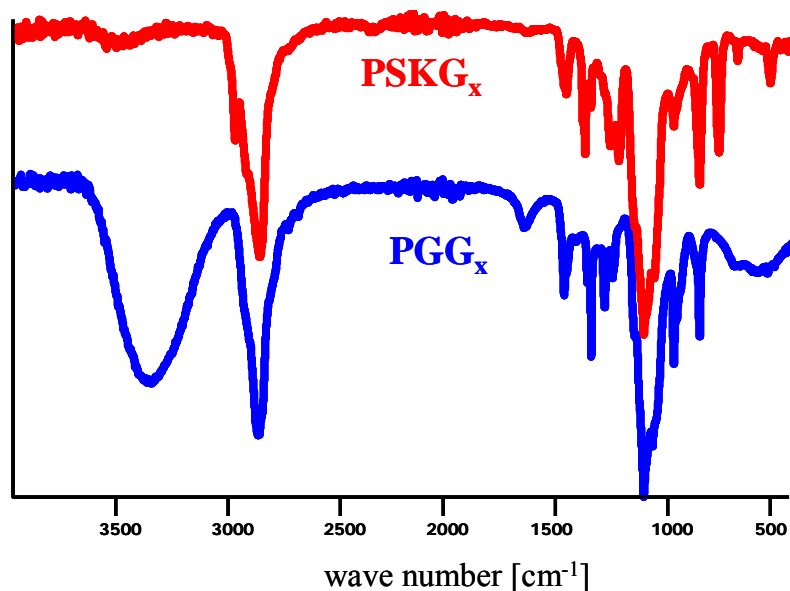
Table 5.1. Characterization data of poly(glycerol glycerol) polymers (PGG) prepared via both strategies: Polymerization of (DL-1,2-isopropylidene glycerol) glycidyl ether (IGG).

sample	DP _{n,th}	DP _{n,NMR}	DP _{n,GPC} ¹	M _{n,GPC} ¹ (g/mol)	DP _{n,GPC} ²	M _{n,GPC} ² (g/mol)	PDI ²
PEO ₄₅ -PIGG _x	10	11	11	4,000	6	3,100	1.15
PEO ₄₅ -PGG _x	10	10	13	4,400	9	3,300	1.18
PEO ₁₁₄ -PIGG _x	25	26	25	9,800	9	6,800	1.05
PEO ₁₁₄ -PGG _x	25	22	42	11,300	19	7,800	1.09

¹ determined via GPC (refractive index detection) using *N,N*-dimethylformamide (DMF) as an eluent (*polystyrene*- standards)

² determined via size exclusion chromatography (refractive index detection) using *N,N*-dimethylformamide (DMF) as an eluent (*poly(ethylene oxide)*- standards)

Deprotection of the pending glycerol units via acetal cleavage was complete within several minutes. NMR-spectroscopy as well as IR spectroscopy confirmed full deprotection of the acetal protecting group (Figure 5.2 & 5.3).

**Figure 5.2.** IR-spectra of PEO₄₅-PIGG₁₀ and PEO₄₅-PGG₁₀.

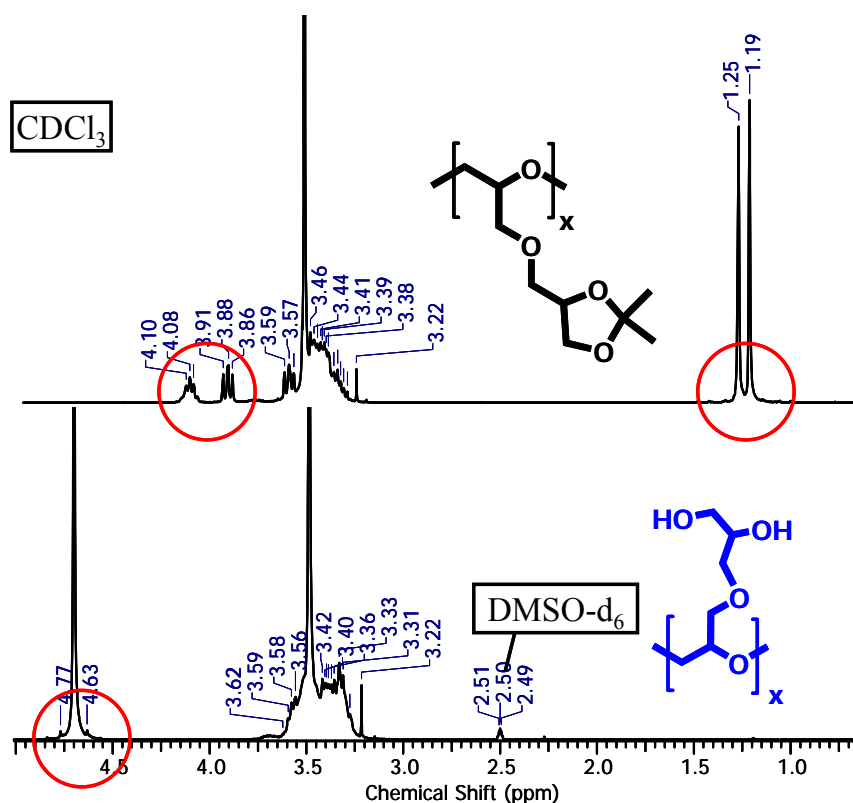


Figure 5.3. $^1\text{H-NMR}$ spectra of $\text{PEO}_{45}\text{-PIGG}_{10}$ and $\text{PEO}_{45}\text{-PGG}_{10}$.

The resulting polymer bears two additional hydroxyl groups in every PGG repeat unit. Regarding the degree of branching for these materials, in fact a polyglycerol pseudo-dendrimer structure is obtained, since only one linear group is included, while the number of dendritic and terminal groups is equal to the degree of polymerization.

5.3 Conclusion

The first synthesis of poly(glyceryl glycerols) (PGG), introducing a new solketyl glycidyl ether monomer (IGG) was shown. The resulting polymers are suitable for biomedical applications. Further progress based on this approach has been achieved by Frederik Wurm and can be found in the appendix of this thesis. Due to their multifunctionality these PEO-analogous functional polymers can be used for a variety of further applications, e.g., as macroinitiators for the anionic ring-opening multibranching polymerization (ROMBP) of glycidol leading to well-defined linear-hyperbranched *l*-poly(ethylene oxide)–*hb*-poly(glycerol) block copolymers.

5.4 Experimental Part

5.4.1 Materials

Diglyme (99% Acros), glycidol and methoxy ethanol (99.5% Acros) for polymerizations were purified by distillation from CaH_2 directly prior to use. Ethylene oxide 99.5% (Aldrich) was used without further purification. Polyethylene oxide monomethyl ether was purchased from Fluka and used as received. Cesium hydroxide monohydrate was purchased from Acros and used as received. Deuterated chloroform- d_1 and DMSO- d_6 were purchased from Deutero GmbH and dried and stored over molecular sieves. Methanol, chloroform, and other solvents and reagents were purchased from Acros and used as received as not otherwise mentioned.

5.4.2 (DL-1,2-Isopropylidene glyceryl) Glycidyl Ether (IGG)

To a vigorously stirred suspension of 2.65g NaH (0,1106mol) in dry THF (200mL) under argon atmosphere a solution of 14.6g solketal in dry THF (50mL) were added. After 15 hours 15.15g (0,1106mol) Epibromhydrin were added dropwise and the mixture was heated to 50°C for 48 hours. Precipitated NaBr was removed by filtration, THF was evaporated. The crude product was purified by column chromatography (silica, diethyl ether: petroleum ether 5:3, $R_f = 0.55$). Yield: 92%.

$^1\text{H-NMR}$ (400 MHz, CDCl_3 , δ in ppm): 4.3 (m, 1H, CH acetal), 4.07 (m, 1H), 3.88-3.39 (m, 6H), 3.17 (m, 1H), 2.81 (t, 1H, CH_2 epoxide), 2.63 (q, 1H, CH_2 epoxide), 1.44 (s, 3H, CH_3), 1.38 (s, 3H, CH_3).

$^{13}\text{C-NMR}$ (97 MHz, CDCl_3 , δ in ppm): 109.4 (quart. C acetal), 74.6 (tert. CH acetal), 74.4-74.1 (CH_2), 66.6 (CH_2 , acetal), 50.7 (CH, epoxide), 44.1 (CH_2 epoxide), 26.7 CH_3 , acetal), 25.3 (CH_3 , acetal).

5.4.3 PEO-*b*-PIGG

Cesium hydroxide monohydrate was suspended in benzene in a Schlenk flask and a stoichiometric amount of methoxyethanol was added under argon with a syringe. Stirring at 60°C for 30 minutes and evacuation at 90°C for two hours gave the cesium alcoxide which was cooled to 0°C. Then ethylene oxide was cryo transferred to a graduated ampoule, diluted with dioxane (ca. 50 weight %) and added to the initiator via canula. The mixture was allowed to slowly warm up to room temperature and polymerization was performed for 2 days in vacuo. Then the flask was back filled with argon, the appropriate amount of freshly dried solketyl glycidyl ether (IGG) was added with a syringe and tem-

perature was raised to 80-90°C for 48-72 h. The polymerization was terminated by addition of methanol and acidic ion exchange resin. Filtration and precipitation in cold diethyl ether resulted in the pure polymer.

For the polymerizations using commercially available MPEGs, the macroinitiator was dissolved in benzene (20 weight%) and partially deprotonated (80-90%) using cesium hydroxide, analogously to the previous procedure.

300 MHz-¹H-NMR (CDCl₃): δ [ppm] = 1.2 (-OCH₃), 1.4 (CH₃, acetal), 2.6 – 3.9 (m, CH₂, PEO, -O-CH₂CH₃, PG, -O-CH₂C₂H₃O, PG), 4.8 (-O-CH(CH₃)-O-).

IR (ATR): ν(cm⁻¹) = 2873 (C-H), 1067 (C-O-C), further characteristic peaks 1350, 1254.

5.4.4 PEO-*b*-PGG by deprotection of PEO-*b*-PIGG

The acetal protecting groups of PIGG were removed by the addition of 1 M hydrochloric acid to a 20% solution of the polymer in ethanol and stirring for 30 min. Afterwards an excess of potassium carbonate was added for neutralization. Filtration and precipitation in diethyl ether gave the pure block copolymer, which was dried in vacuo for 2 days at 80°C.

300 MHz-¹H-NMR (D₂O / MeOD): δ [ppm] = 1.2 (-OCH₃), 2.45 – 3.65 (m, CH₂, PEO, CH, PG, CH₂, PG), 4.78 (m, -OH).

75 MHz-¹³C-NMR (MeOD): δ [ppm] = 58.5 (CH₃-O-), 64.9 (T), 71.3 (D), 72.4 (T), 72.8 (D, CH₂, PEO), 74.3 – 74.7 (T), 81.7(D).

IR (ATR): ν(cm⁻¹) = 3375 (O-H), 2873 (C-H), 1067 (C-O-C).

5.6 References

1. Zalipsky, S. *Adv. Drug Del. Rev.* **1995**, 16, 157-182.
2. Roberts, M. J.; Bentley, M. D.; Harris, J. M. *Adv. Drug Del. Rev.* **2002**, 54, 459-476.
3. Merrill, E. W., *Poly(ethylene glycol) Chemistry: Biotechnical and Biomedical Applications*, Plenum Press: New York, 1992.
4. Needham, D.; McIntosh, T. J.; Lasic, D. D. *Biochim. Et Biophys. Acta* **1992**, 1108, 40-48.
5. Torchilin, V. P.; Omelyanenko, V. G.; Papisov, M. I.; Bogdanov, A. A.; Trubetskoy, V. S.; Herron, J. N.; Gentry, C. A. *Biochim. Et Biophys. Acta -Biomembranes* **1994**, 1195, 11-20.

6. Tokar, R.; Kubisa, P.; Penczek, S.; Dworak, A. *Macromolecules* **1994**, *27*, 320-322.
7. Dworak, A.; Walach, W.; Trzebicka, B. *Macromol. Chem. Phys.* **1995**, *196*, 1963-1970.
8. Sunder, A.; Hanselmann, R.; Frey, H.; Mülhaupt, R. *Macromolecules* **1999**, *32*, 4240-4246.
9. Kainthan, R. K.; Muliawan, E. B.; Hatzikiriakos, S. G.; Brooks, D. E. *Macromolecules* **2006**, *39*, 7708-7717.
10. Sunder, A.; Frey, H.; Mülhaupt, R. *Macromol. Symp.* **2000**, *153*, 187-196.
11. Sunder, A.; Mülhaupt, R.; Haag, R.; Frey, H. *Adv. Mater.* **2000**, *12*, 235-239.
12. Kautz, H.; Sunder, A.; Frey, H. *Macromol. Symp.* **2001**, *163*, 67-73.
13. Kainthan, R. K.; Janzen, J.; Levin, E.; Devine, D. V.; Brooks, D. E. *Biomacromolecules* **2006**, *7*, 703-709.
14. Kainthan, R. K.; Gnanamani, M.; Ganguli, M.; Ghosh, T.; Brooks, D. E.; Maiti, S.; Kizhakkedathu, J. N. *Biomaterials* **2006**, *27*, 5377-5390.
15. Taton, D.; Leborgne, A.; Sepulchre, M.; Spassky, N. *Macromol. Chem. Phys.* **1994**, *195*, 139-148.
16. Dworak, A.; Baran, G.; Trzebicka, B.; Walach, W. *Reactive & Functional Polymers* **1999**, *42*, 31-36.
17. Lapienis, G.; Penczek, S. *Biomacromolecules* **2005**, *6*, 752-762.
18. Jamroz-Piegza, M.; Utrata-Wesolek, A.; Trzebicka, B.; Dworak, A. *Europ. Polym. J.* **2006**, *42*, 2497-2506.
19. Dimitrov, P.; Utrata-Wesolek, A.; Rangelov, S.; Walach, W.; Trzebicka, B.; Dworak, A. *Polymer* **2006**, *47*, 4905-4915.
20. Dimitrov, P.; Rangelov, S.; Dworak, A.; Haraguchi, N.; Hirao, A.; Tsvetanov, C. B. *Macromolecular Symp.* **2004**, *215*, 127-139.
21. Halacheva, S.; Rangelov, S.; Tsvetanov, C. *Macromolecules* **2006**, *39*, 6845-6852.
22. Erberich, M.; Keul, H.; Möller, M. *Macromolecules* **2007**, *40*, 3070-3079.
23. Gitsov, I.; Frechet, J. M. J. *Macromolecules* **1993**, *26*, 6536-6546.
24. Gitsov, I.; Wooley, K. L.; Hawker, C. J.; Ivanova, P. T.; Frechet, J. M. J. *Macromolecules* **1993**, *26*, 5621-5627.
25. vanHest, J. C. M.; Delnoye, D. A. P.; Baars, M. W. P. L.; ElissenRoman, C.; vanGenderen, M. H. P.; Meijer, E. W. *Chem. Europ. J.* **1996**, *2*, 1616-1626.

26. Nguyen, P. M.; Hammond, P. T. *Langmuir* **2006**, 22, 7825-7832.
27. Santini, C. M. B.; Johnson, M. A.; Boedicker, J. Q.; Hatton, T. A.; Hammond, P. T. *J. Polym. Sci. Part A-Polym. Chem.* **2004**, 42, 2784-2814.
28. Marcos, A. G.; Pusel, T. M.; Thomann, R.; Pakula, T.; Okrasa, L.; Geppert, S.; Gronski, W.; Frey, H. *Macromolecules* **2006**, 39, 971-977.
29. Barriau, E.; Marcos, A. G.; Kautz, H.; Frey, H. *Macromol. Rapid Commun.* **2005**, 26, 862-867.
30. Hanselmann, R.; Hölter, D.; Frey, H. *Macromolecules* **1998**, 31, 3790-3801.
31. Newkome, G. M., C. N.; Vögtle, F., *Dendrimers and Dendrons: Concepts, Syntheses, Applications*. Wiley-VCH: Weinheim, Germany, 2001.
32. Fréchet, J. M. J. T., D. A., *Dendrimers and Other Dendritic Polymers*. John Wiley & Sons Ltd: New York, USA, 2001.
33. Van Rheenen, V.; Kelly, R. C.; Cha, D. Y. *Tetrahedron Let.* **1976**, 1973-1976.
34. Banks, P.; Peters, R. H. *J. Polym. Sci. Part A-Polym. Chem.* **1970**, 8, 2595-&.
35. Stolarzewicz, A. *Makromol. Chem.-Macromol. Chem. Phys.* **1986**, 187, 745-752.
36. Stolarzewicz, A.; Grobelny, Z. *Makromol. Chem.-Macromol. Chem. Phys.* **1992**, 193, 531-538.
37. Kolb, H. C.; Andersson, P. G.; Sharpless, K. B. *J. Am. Chem. Soc.* **1994**, 116, 1278-1291.
38. Haag, R.; Sunder, A.; Stumbe, J. F. *J. Am. Chem. Soc.* **2000**, 122, 2954-2955.
39. Feng, X. S.; Taton, D.; Chaikof, E. L.; Gnanou, Y. *J. Am. Chem. Soc.* **2005**, 127, 10956-10966.
40. Feng, X. S.; Taton, D.; Chaikof, E. L.; Gnanou, Y. *Biomacromolecules* **2007**, 8, 2374-2378.
41. Göltner, C. C., H.; Antonietti, M. *Chemie unserer Zeit* **1999**, 33, 200-205.
42. Förster, S.; Antonietti, M. *Adv. Mater.* **1998**, 10, 195-+.
43. Förster, S.; Plantenberg, T. *Angew. Chem. Int. Ed.* **2002**, 41, 689-714.

6 Amphiphilic Hyperbranched - Hyperbranched Block Copolymers

6.1 Introduction

In the previous chapters (Chapters 5 & 6), the successful synthesis of amphiphilic linear-hyperbranched block copolymers containing a hyperbranched polyglycerol block of narrow polydispersity and controlled molecular weights was presented. This work encourages developing even more complex structures, such as amphiphilic hyperbranched-hyperbranched block copolymers. To date there exist few examples of block *co*-dendrimers realized by coupling of two previously synthesized dendron blocks. These blocks consist either of different chemical structure or different peripheral functionalization. In 1992, Hawker et al. reported the coupling of prefabricated aromatic ester and ether wedges to a polyfunctional core resulting in segmented block copolymers.¹ An amphiphilic diblock dendrimer was synthesized by Okada et al., who divergently prepared core functional poly(amido amine) (PAMAM) dendritic wedges that were functionalized with hydrophobic sugar moieties or hydrophobic phthaloyl groups. After activation of the core the hemi-spherical blocks were linked through an urea bond.² In the groups of Nierengarten and Gallani the interfacial properties of amphiphilic diblock dendrimers were studied systematically. They varied the generation of the dendritic wedges modified with either hydrophobic or hydrophilic groups on the periphery, and thus the hydrophobic/hydrophilic balance.³⁻⁵ A deviation in the behavior from traditional amphiphiles was observed for larger generation dendrimers exhibiting more complicated isotherms, with non straightforward temperature dependence. Interestingly, the formation of stable Langmuir films could be achieved, although bulky functional groups like fullerenes were incorporated in the diblock dendrimers. The first report on the formation of self-assembled supramolecular structures was reported by Wegner et al. for block codendrimers consisting of [G3]-poly(benzyl ether) (PBE) and an aliphatic [G3]-poly(methallyl dichloride) (PMDC) (Figure 6.1 a).⁶ In selective solvents vesicles with a diameter of 100nm are formed. The special architecture of the polymer results in a membrane thickness that is less than the thickness of membranes formed by linear-linear copolymers of the same molecular weight. The formation of microdomains in the melt was observed with a slightly modified hydrogen bond-containing diblock codendrimer [G3]-PBE-*b*-[G3]-poly(2,2-bis(hydroxymethyl) propionic acid). SAXS diffraction patterns

showed the presence of a layered structure below 50°C and a transition to the disordered melt above 50°C, when the hydrogen bonds are broken.⁷ “Click chemistry” also found its way into the preparation of diblock codendrimers. Jin et al. reported the coupling of an azide-functionalized PBE and PAMAM dendrons bearing a propargyl group at the focal point (Figure 6.4 b).⁸

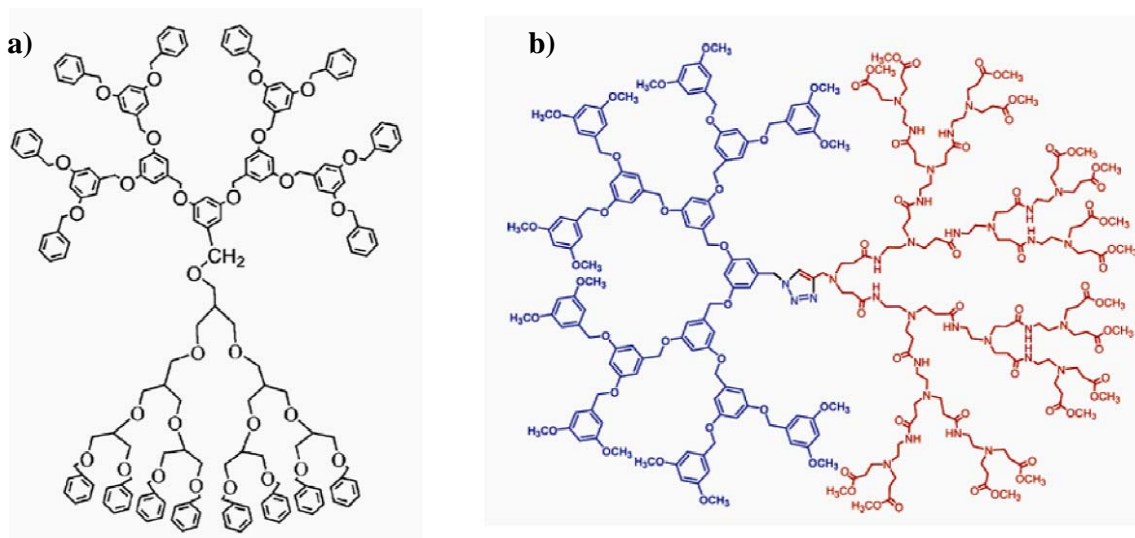


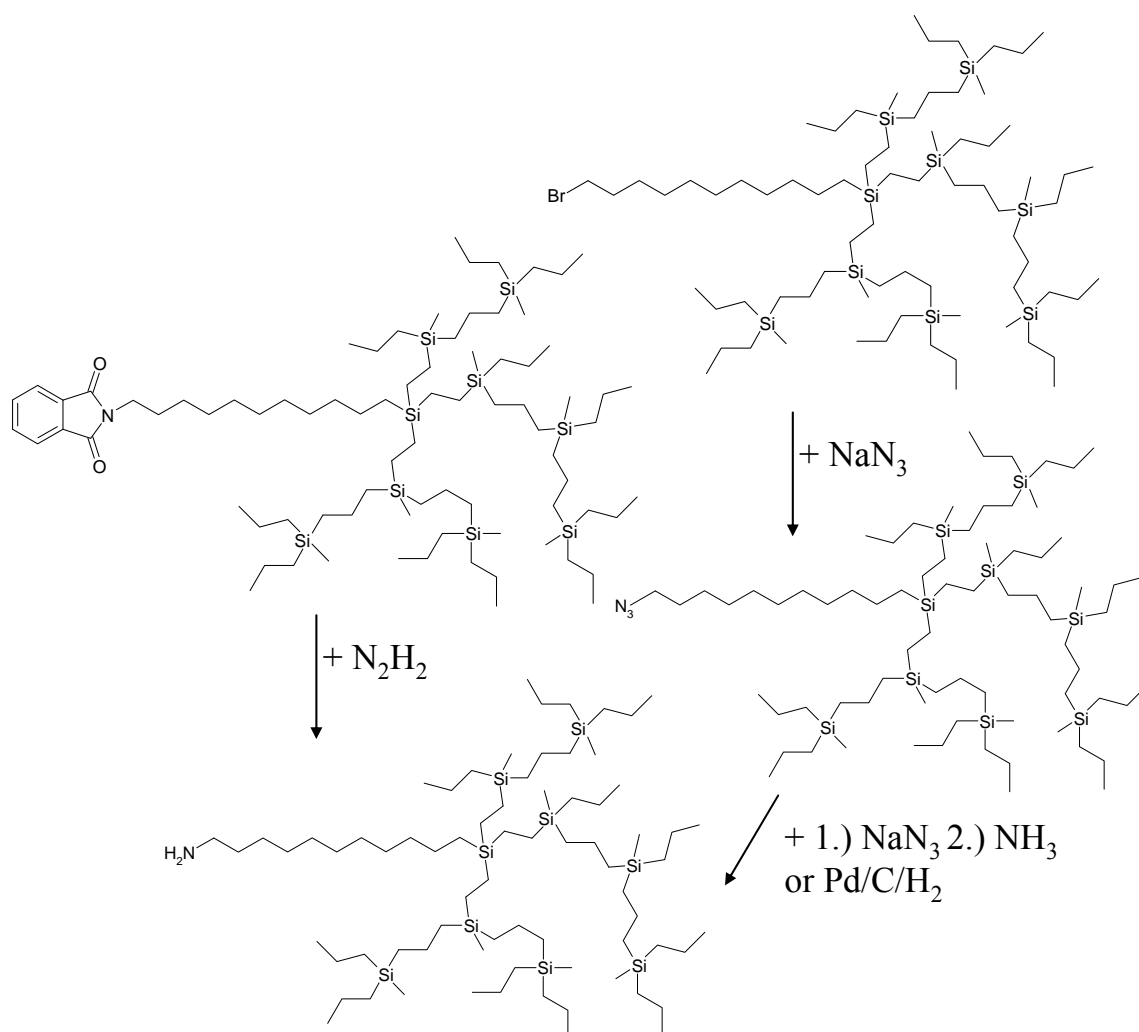
Figure 6.1. Examples for block codendrimers: a) PBE-*b*-PMDC,⁶ b) PBE-*b*-PAMAM.⁸

The application of dendrimers wedges in block codendrimers is always limited by the time consuming stepwise synthesis. Additionally, molecular weights are limited to the respective dendrimers generations. However, to date no example of block copolymers with two chemically different hyperbranched blocks has been reported. This chapter presents the results of the collaboration with Hanna Schüle who synthesized core-functional hyperbranched polycarbosilanes.⁹ These are used as macroinitiators in the ROMBP of glycidol leading to novel hyperbranched-hyperbranched amphiphiles.

6.2 Synthesis of the Hyperbranched Macroinitiators

Carbosilane dendrimers wedges with an amine group at the focal point have been reported by van Heerbeek et al. They introduced the amine by reaction of a halide with liquid ammonia or through the intermediate azide or phthalimide.¹⁰⁻¹² Similar reaction conditions have been applied in our group for hyperbranched carbosilane wedges.⁹ Trivinylsilanes possessing an end-functionalized undecene spacer group (phthalimide or bromo-end group) were synthesized and subsequently used as initiators for the one pot polym-

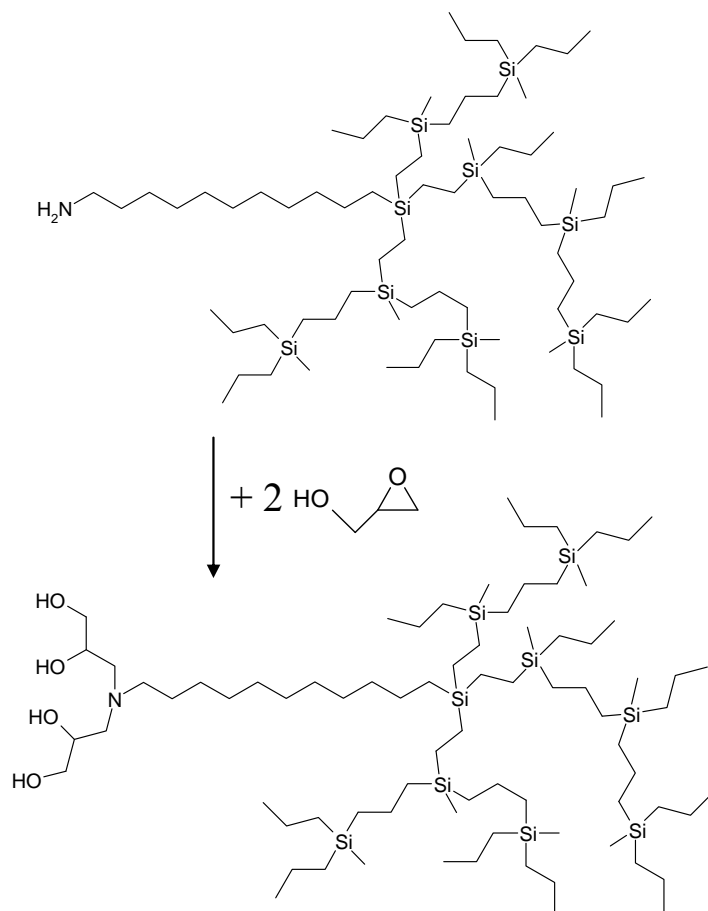
erization of diallylmethylsilane using the Karstedt catalyst and applying the slow monomer addition technique.⁹ As the reactivity of the vinylic groups of the initiator is much higher than the one of the allylic groups of the silane monomer the core molecule was completely incorporated. Furthermore, it must be mentioned, that the allylic groups at the periphery and at the linear branching points of the carbosilanes reduce the stability of these structures under harsh reaction conditions and due to their sensitivity to light. In order to enhance the inertness of the polymers before the attachment of the glycidol block (high reaction temperature, strong basic conditions) the allylic groups were hydrogenated. Subsequently the core-functional groups of these polymers were transformed into amine groups. Scheme 6.1 summarizes these reaction pathways.



Scheme 6.1. Preparation of amine-functionalized polycarbosilanes.⁹

Bisglycidolized amines are obtained by reaction of the amine-functional polycarbosilanes with two equivalents of glycidol (Scheme 6.2) in analogy to Chapter 4. The higher nu-

cleophilicity of the amine compared to the hydroxyl groups results in a preferred two-fold reaction at the primary amine.



Scheme 6.2. Synthesis of bisglycidolized macroinitiators.

In order to realize good control in the synthesis of polyglycerol, no free amines are allowed in the reaction, hence a slight excess of glycidol was used (2.2-3 equivalents) and the reaction was completed at 60°C . Remaining glycidol can be removed under high vacuum. In some cases the NMR spectra revealed a higher degree of substitution, i.e. three or four glycidols attached to the core. This is a result of ring-opening of glycidol by hydroxyl groups which can occur at increased temperatures. However, this is not detrimental for the reaction control. The reactions at the focal group of the polycarbosilane can be observed by NMR spectroscopy. An example of $^1\text{H-NMR}$ spectra for amine-functional polycarbosilane and macroinitiator obtained after bisglycidolization is shown in Figure 6.2. After hydrogenation or cleavage of the phthalimide group, the methylene protons adjacent to the primary amine give rise to a triplet at 2.67ppm, distinct from the starting material with signals at 3.24ppm for the azide or 3.66ppm for the phthalimide. Bisglycidolization results in broad signals between 3.88-3.39ppm and 2.75-2.39ppm belonging to

the methylene groups next to oxygen and amine, respectively. The integral ratio for these signals indicates that 2.5 to 3 equivalents of glycidol are added per amine group.

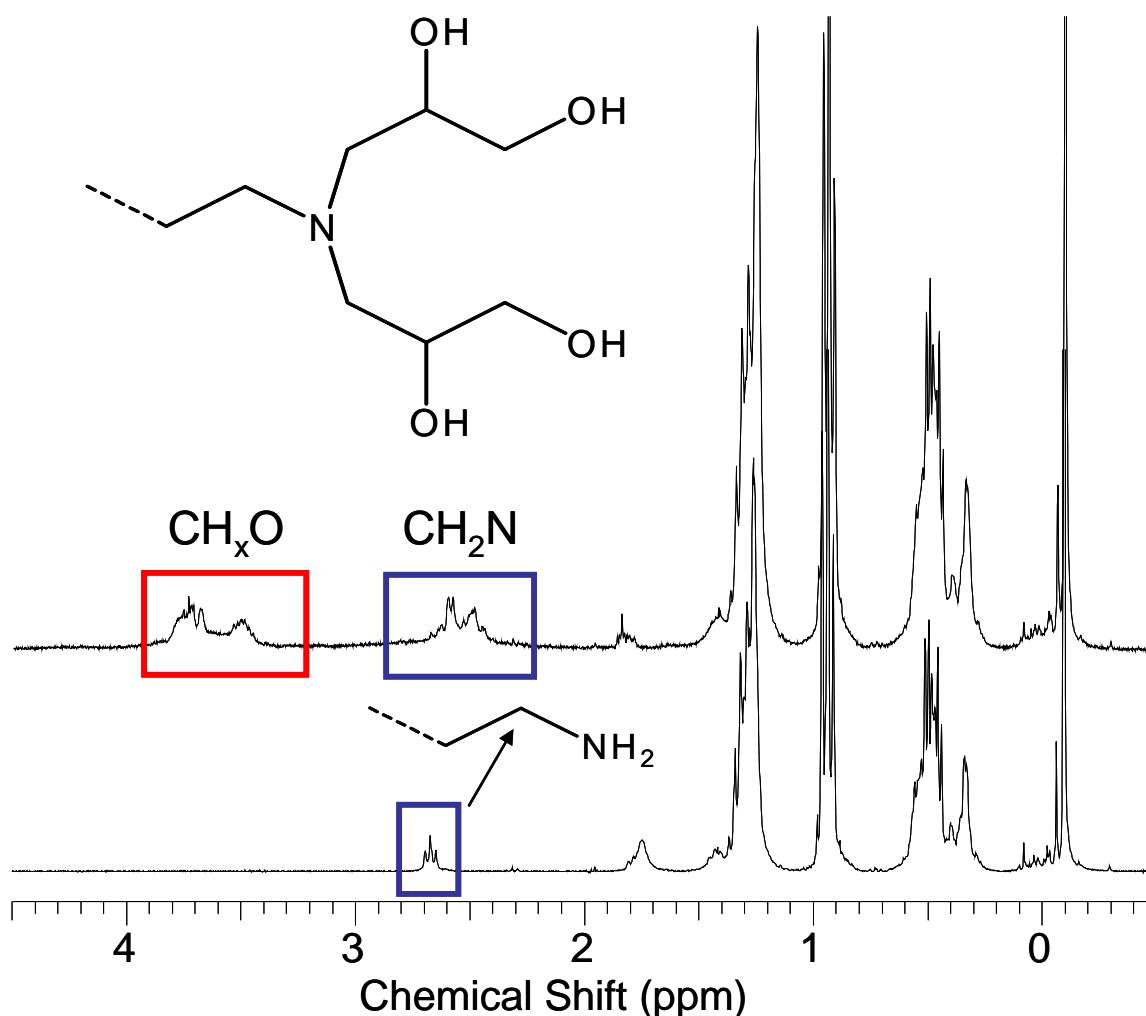


Figure 6.2. Examples of ¹H-NMR spectra in CDCl₃ for amine-functional PCS (bottom) and bisglycidolized macroinitiator (top).

The reaction sequence leading to polycarbosilane macroinitiators via azide reduction can also be conveniently followed by IR-spectroscopy as shown in Figure 6.3. The hydrogenation of double bonds is accompanied by the disappearance of the characteristic signal for the C=C valence vibration at $\tilde{\nu} = 1630\text{cm}^{-1}$. The nucleophilic substitution with sodium azide results in a strong absorption at $\tilde{\nu} = 2100\text{cm}^{-1}$, which in turn disappears after reduction. Although the primary amine is not detected in the respective spectrum, after bisglycidolization the hydroxyl groups are clearly visible with a broad signal between $\tilde{\nu} = 3100\text{-}3300\text{cm}^{-1}$.

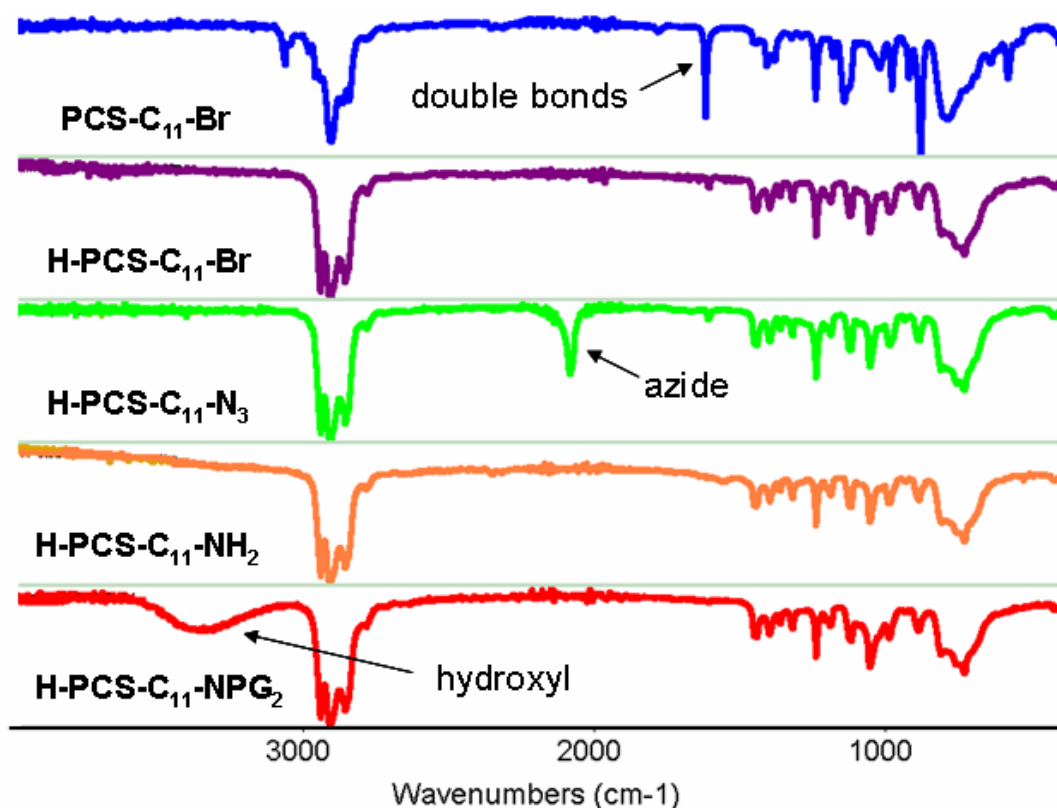


Figure 6.3. IR-spectra for the reaction sequence targeting polycarbosilane macroinitiators.

In Table 6.1 GPC results for different polycarbosilanes with amines at the focal point are summarized and compared with the respective bisglycidolized macroinitiators. For the lowest molecular weight polymer (H-PCS₅-C₁₁-X), GPC results in THF are not analyzable (dashed line, Fig 6.4 (A)) probably due to the strongly amphiphilic character of the sample. Besides a higher molecular weight shoulder, which can be explained by weak aggregation, the distribution revealed a distinct signal at lower molecular weights. Unfunctionalized polycarbosilanes are insoluble in polar solvents. However, with the bisglycidolized core attached, low molecular weight samples became slightly soluble in DMF. Thus, the GPC curve for H-PCS₅-C₁₁-NPG₂ was measured in DMF, showing a narrow molecular weight distribution with only a small low molecular weight shoulder. Further analysis by NMR and MALDI confirmed that no degradation of the sample occurred. For higher molecular weight samples monomodal curves are obtained in THF for all stages of the reaction. The GPC curve for H-PCS₂₂-NPG₂ in DMF (Figure 6.4 (B)) shows a narrow distribution (PDI~1.2) indicating the collapsed nature of the carbosilane block. For H-PCS₅₄-NPG₂ the apolar nature of the polycarbosilane is dominant, rendering the polymer insoluble in DMF.

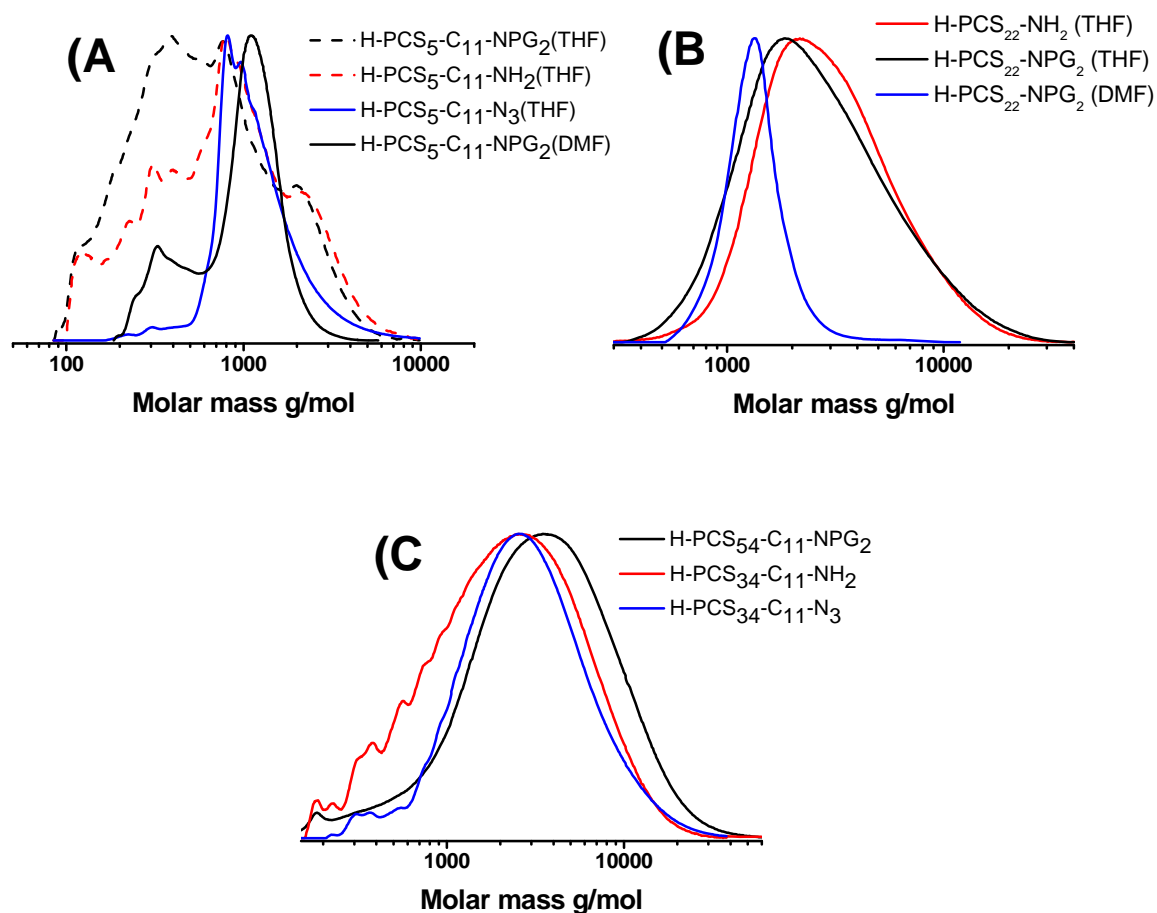


Figure 6.4. GPC curves for different examples of core-functional polycarbosilanes: (A) H-PCS₅-C₁₁-X, (B) H-PCS₂₂-C₁₁-X, (C) H-PCS₃₄-C₁₁-X .

Table 6.1. GPC results for core-functional polycarbosilanes.

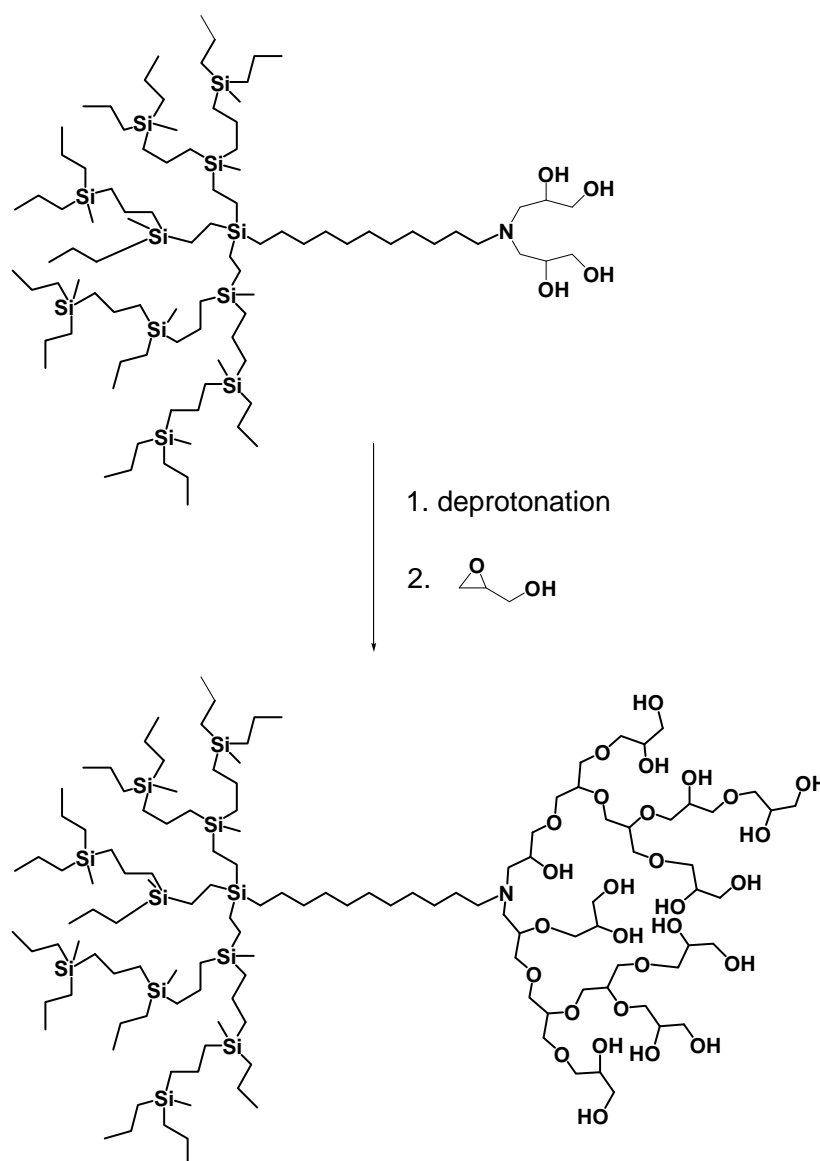
Sample	$M_{n,GPC,THF}$ (g/mol)	$PDI_{GPC,THF}$
H-PCS ₅ -C ₁₁ -N ₃	1,070	1.23
H-PCS ₅ -C ₁₁ -NH ₂	-	-
H-PCS ₅ -C ₁₁ -N-PG ₂	-	-
H-PCS ₂₂ -C ₁₁ -NH ₂	2,390	1.54
H-PCS ₂₂ -C ₁₁ -N-PG ₂	1,830	1.82
H-PCS ₃₄ -C ₁₁ -NH ₂	1,210	2.65
H-PCS ₃₄ -C ₁₁ -N-PG ₂ ^a	2,490	2.05

a) after dialysis

noted 3/2). This in turn is the lowest molecular weight peak observed for the macroinitiator. Thus, the spectra are exactly shifted by two glycidol units, which confirms the quantitative transformation. In other cases the distributions belonging to three or four glycidol units are observed as well, rendering the analysis even more intricate.

6.3 Synthesis of the Hyperbranched-Hyperbranched Block Copolymers

Bisglycidolized carbosilane macroinitiators can be applied for the synthesis of hyperbranched-hyperbranched amphiphiles containing a hydrophobic carbosilane block and a hydrophilic polyglycerol block (Scheme 6.3).



Scheme 6.3. Ring-opening polymerization of glycidol applying polycarbosilane macroinitiator.

The synthesis of these block copolymer structures was performed similar to the described protocol in chapters 3 to 5, i.e. in order to obtain nucleophilic species that are capable of ring opening multibranching polymerization (ROMBP) of glycidol, the macroinitiators were partially deprotonated using cesium hydroxide or potassium *tert*-butylate. Degrees of deprotonation of around 30% are advantageous to retain a certain solubility of the initiator and thus a homogeneous reaction mixture. The formed byproducts water or *tert*-butanol were completely removed under vacuum, since they could act as initiators in the polymerization of glycidol as well (Chapter 3). The polymerization reaction was performed by slow addition of the respective amount of glycidol dissolved in THF to a suspension/solution of the deprotonated initiator in diglyme or THF at 60°C. After completed polymerization the products were treated with ion exchange resin and purified by precipitation or dialysis.

The ring opening polymerization of glycidol was performed with macroinitiators containing 5, 22 or 54 carbosilane units. The polymerization results are summarized in Table 6.2.

Table 6.2. Polymerization results for polycarbosilane macroinitiators.

Sample	$M_{n,GPC,THF}$ (g/mol)	$PDI_{GPC,THF}$	$T_{g,DSC}$ (°C)
H-PCS ₅ -C ₁₁ -N ₃	1,070	1.23	-
H-PCS ₅ -C ₁₁ -N-PG ₅₅	5,060 ^a	1.57	-32
H-PCS ₅ -C ₁₁ -N-PG ₅₅ Bz	5,540	1.26	n.d.
H-PCS ₂₂ -C ₁₁ -N-PG ₂	1,830	1.82	-75/-58
H-PCS ₂₂ -C ₁₁ -N-PG ₁₅	2,800	2.15	-83
H-PCS ₂₂ -C ₁₁ -N-PG ₁₅ Si	2,340	1.89	-81/-58
H-PCS ₅₄ -C ₁₁ -N-PG ₂	2,490	2.05	-79
H-PCS ₅₄ -C ₁₁ -N-PG ₂	no attachment of PG		

a) GPC in DMF.

From the polymerization results it is obvious that the molecular weight of the carbosilane block is crucial for the accessibility of the initiating moiety. While the oligomeric initiator was suitable for the polymerization of glycidol, initiation was completely inhibited for

the largest macroinitiator and hence no polyglycerol block could be attached. In Figures 6.6 and 6.7 GPC results for the PCS-C₁₁-PG polymers are compared with the respective initiators.

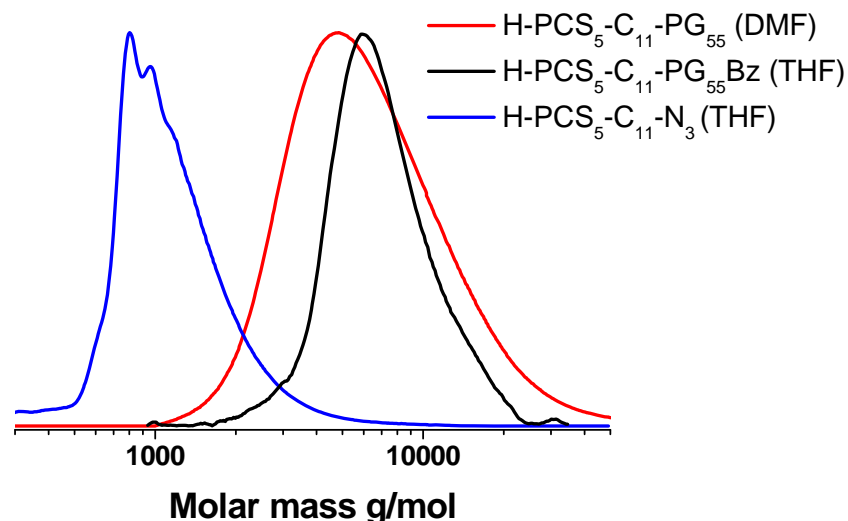


Figure 6.6. GPC curves for H-PCS₅-C₁₁-X.

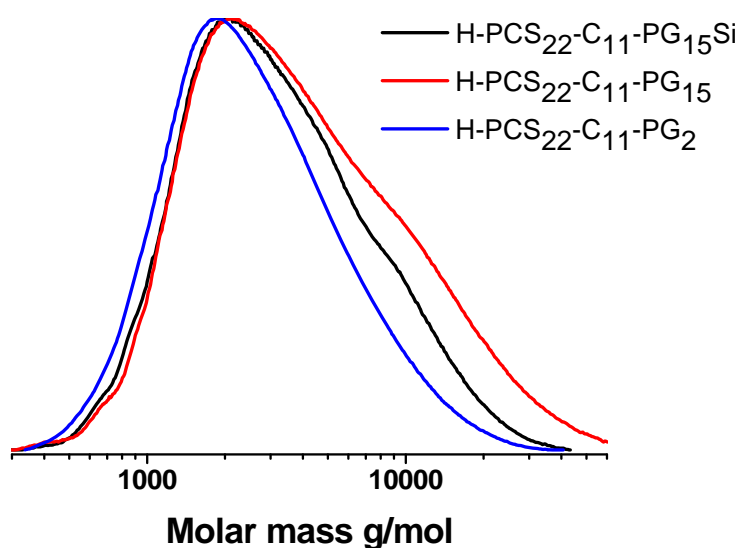
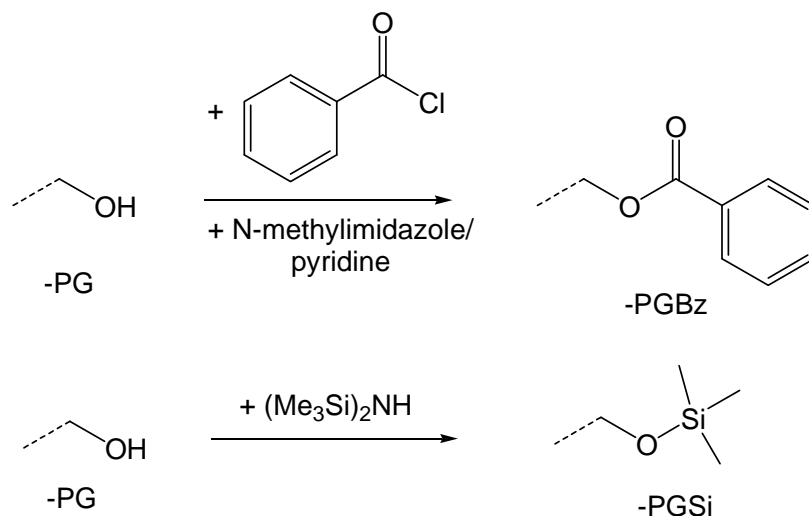


Figure 6.7. GPC curves for H-PCS₂₂-C₁₁-X in THF.

The molecular weight increase is palpable, though accompanied by an increase in polydispersity. The latter is caused by a high molecular weight tailing, likely due to weak hydrogen bond interactions and aggregation due to the hydroxyl end groups. Chemical masking of the free hydroxyl groups of the polyglycerol block with benzoyl (-PGBz) or trimethylsilyl (-PGSi) protecting groups removes the amphiphilic properties of the polymer (Scheme 6.4). Analysis for these samples shows that the actual polydispersity is

lower than observed for the amphiphile and equal to the respective macroinitiator (Table 6.2).



Scheme 6.4. Protection of hydroxyl groups using benzoyl chloride or by silylation using hexamethyldisilazane.

Growth of the polyglycerol block can be observed in the $^1\text{H-NMR}$ spectrum. In Figure 6.8 the spectra for macroinitiator and a typical block copolymer are presented. As reference for the carbosilane block the signal for Si-CH_3 is marked (blue). Compared to this signal the increased molecular weight of the polyether structure (red) is obvious.

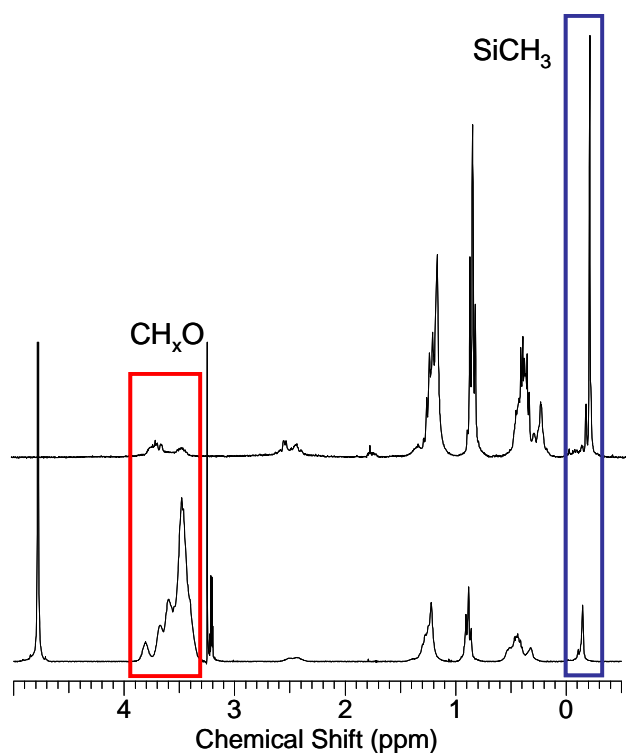


Figure 6.8. $^1\text{H-NMR}$ spectra for $\text{H-PCS}_5\text{-C}_{11}\text{-PG}_{55}$ in MeOD-d_4 (bottom) and $\text{H-PSC}_5\text{-C}_{11}\text{-PG}_2$ in CDCl_3 (top).

MALDI-ToF spectrometry is a versatile tool to analyze the structural composition of a polymer. However, for block copolymer structures analysis is often complicated and not straightforward due to the combination of the different molecular weight distributions resulting from the presence of a large variety of combinations of all monomer units present. In Figure 6.9 the spectrum for H-PCS₂₂-C₁₁-PG₁₅ is given showing a monomodal distribution with a peak maximum at ~3500 g/mol. However, single peak assignment is futile because of the large number of peaks representing manifold possible combinations of carbosilane and glycerol units in the polymer.

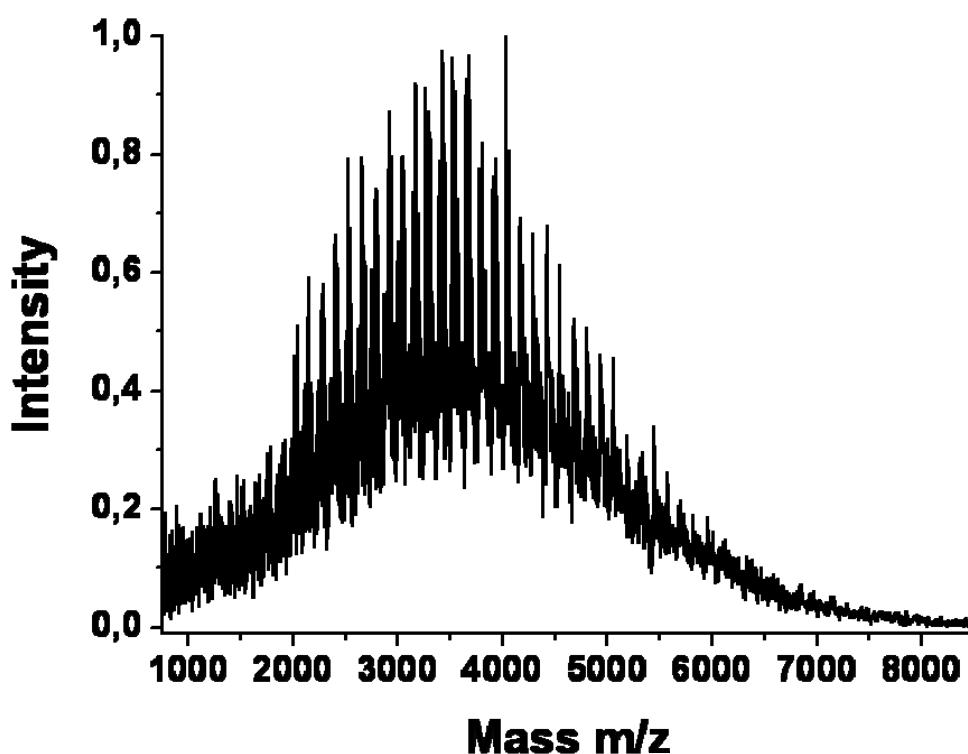


Figure 6.9. MALDI-ToF spectrum for H-PCS₂₂-C₁₁-PG₁₅.

In contrast a diminished number of possible combinations can be expected for H-PCS₅-C₁₁-PG₅₅ with an oligomeric carbosilane block. And indeed, three distributions of major intensity are visible in the spectrum (Figure 6.10). The enlarged section shown in Figure 6.11 reveals that the mass increment in each distribution equals 74.1g/mol, corresponding to a glycidol repeating unit. Thus, the main distributions can be assigned to polymers containing 3, 4 or 5 etc. carbosilane units and increasing amounts of glycidol.

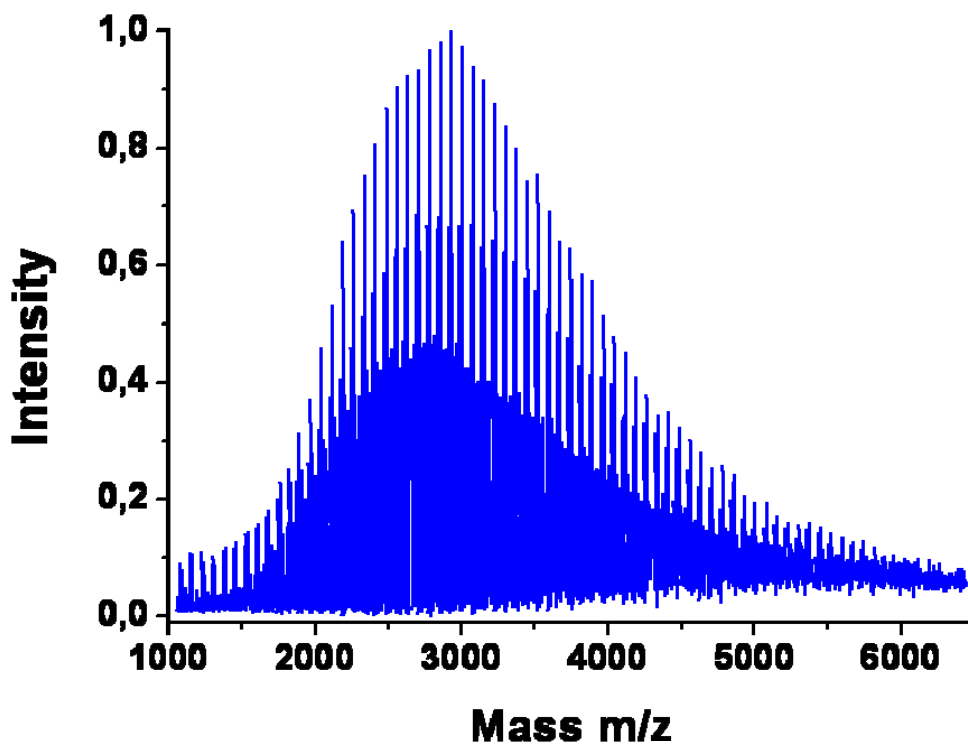


Figure 6.10. MALDI-ToF spectrum for H-PCS₅-C₁₁-PG₅₅.

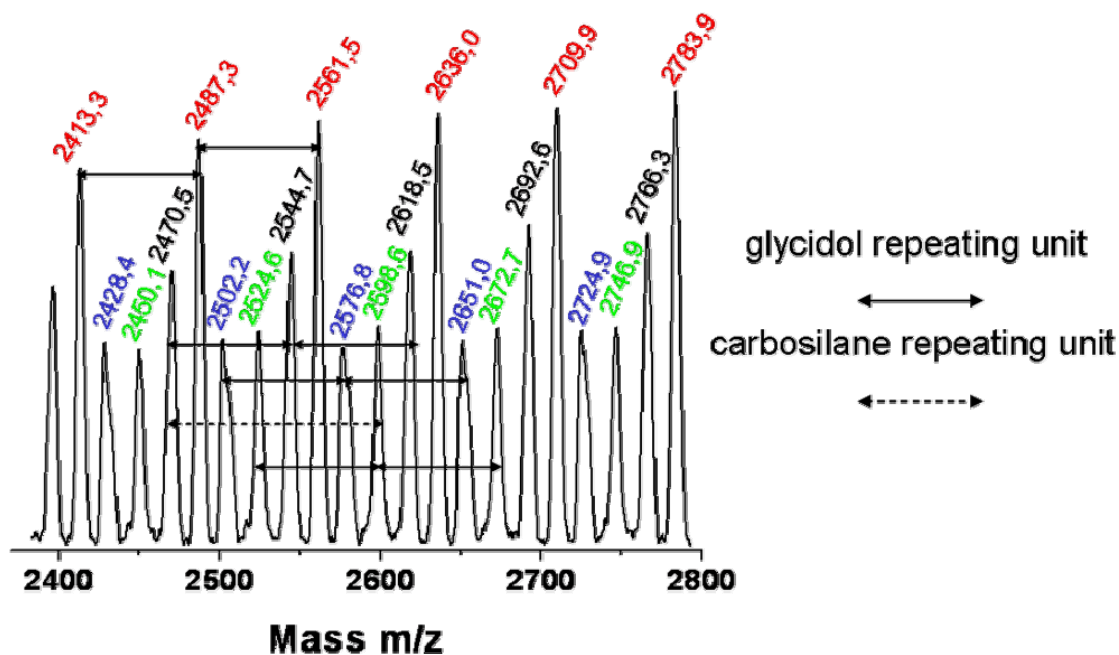


Figure 6.11. Section of MALDI-ToF spectrum for H-PCS₅-C₁₁-PG₅₅.

6.4 Amphiphilic Character of the Hyperbranched-Hyperbranched Block Copolymers

The amphiphilic character of the samples can be demonstrated using an extraction experiment. Therefore, aqueous solutions of methyl orange, rose bengal and congo red (each ~5mg/ml) were prepared. These dyes are insoluble in chloroform, thus upon addition of chloroform to the dye solution no color change of the chloroform layer (bottom) is visible after vigorous shaking. The result of this blank test can be seen in Figure 6.12 left with a colorless chloroform layer at the bottom and a colored aqueous solution on top. The amphiphilic block copolymer H-PCS₂₂-C₁₁-PG₁₅ is soluble in chloroform. However, due to the insolubility of polyglycerol in this solvent the formation of micelles with a polycarbosilane exterior is expected.

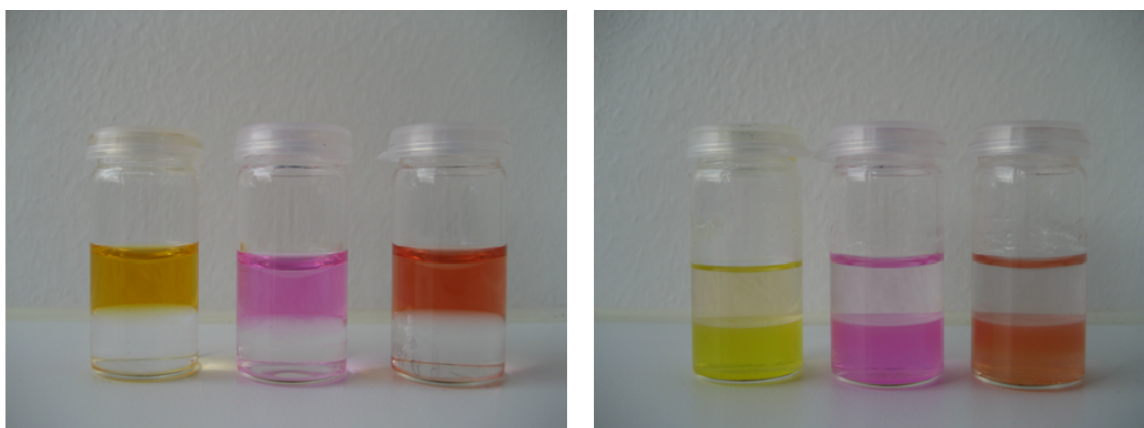


Figure 6.12. Extraction experiments: left) blank test and right) test with amphiphile (each with methyl orange, rose bengal and congo red).

Mixing of equal volumes of dye solution with a solution of the polymer in chloroform (~4mg/ml) results in complete extraction of the dye from the aqueous phase into the chloroform layer (Figure 6.12 right). Thus, the dye is efficiently encapsulated into the polar interior of the micelles, confirming the polymers' amphiphilic character.

The micelles can be visualized, when dried chloroform solutions of the polymer are examined using transmission electron microscopy (TEM). The spherical structures are uniform in size and visible without staining due to the strong electron scattering contrast of silicon (Figure 6.13).

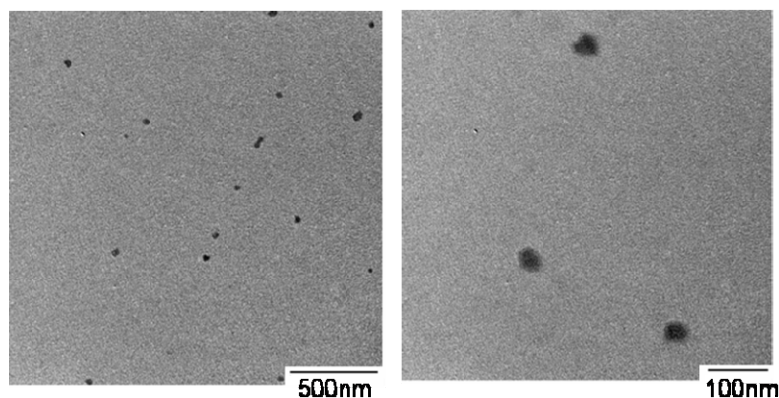


Figure 6.13 TEM images of solution cast sample of H-PCS₂₂-C₁₁-PG₁₅ (prepared from 0.5mg/ml solutions in CHCl₃).

6.5 Conclusion

In this chapter it was demonstrated that core-functional carbosilane wedges allow further application in block copolymer synthesis. Bisglycidolized amine functional polymers were successfully employed as macroinitiators for glycidol polymerization. This resulted in the first example of amphiphilic hyperbranched-hyperbranched polymer structures (Figure 6.14).

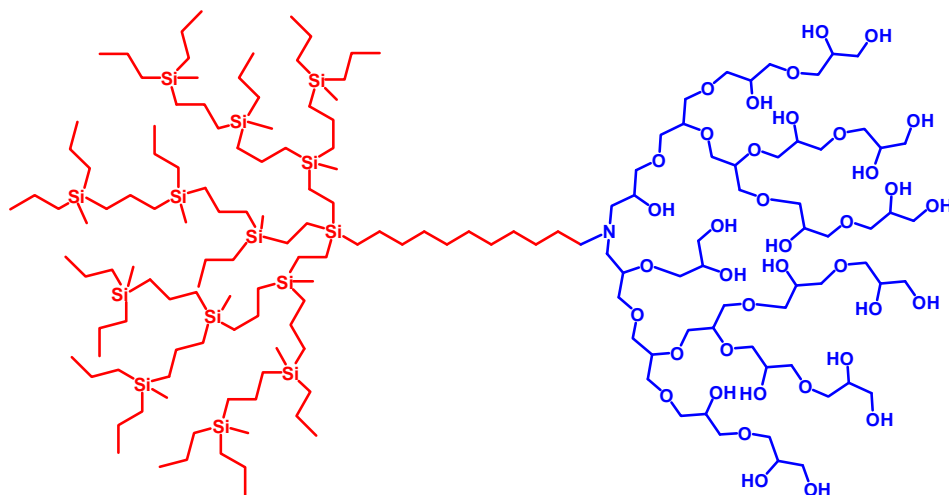


Figure 6.14. Structure of *hb*-PCS-C₁₁-*hb*-PG.

On the one hand, the size of the preliminary synthesized polycarbosilane block was shown to be limited in order to allow the attachment of the polyglycerol block. With a degree of polymerization up to 22 for the hyperbranched silane block the ROMBP of glycidol leading to the second block was feasible, while a DP_n of 55 inhibited the attachment of glycidol. On the other hand, with low molecular weight polycarbosilanes the size of the glycerol block can be varied over a broader molecular weight range. The at-

tachment of over 50 glycerol units was carried out. The resulting block copolymers possessed polydispersities from 1.5 to 2.1, mainly dominated by the molar mass distribution of the initial carbosilane block. The incorporation of both blocks was verified by MALDI-ToF mass spectrometry. Further masking of the functional OH-groups of the glycerol block with benzoyl or trimethylsilyl protecting groups confirmed the successful synthesis by neutralizing the amphiphilic character, which was furthermore demonstrated by dye encapsulating experiments and TEM images.

6.6 Experimental Part

6.6.1 Materials

All chemicals were purchased from *Aldrich* or *Acros Organics*. Acetone p.a., methanol p.a., cesium hydroxide monohydrate, Dowex[®] 50WX8, 200-400 mesh, ion exchange resin, and 1M potassium *tert*-butylate solution in THF were used as received. THF was distilled over sodium prior to use. Diglyme and glycidol were purified by distillation over calcium hydride. Chloroform-d and Methanol-d₄ were purchased from *Deutero GmbH*.

6.6.2 Modifications at the Core

6.6.2.1 H-PCS_x-C₁₁-N₃

Reactions were performed in DMF/THF at 60°C employing 2-20 equivalents sodium azide. As an example 1.81g (0.62mmol) PCS₂₀-C₁₁-Br and 0.81g (12.4mmol) sodium azide were suspended in 10ml DMF/THF and heated at 60°C for 24h. The solvents were removed under vacuum and the residue dissolved in chloroform. The solution was washed with water and dried with MgSO₄.

¹H-NMR (300 MHz, CDCl₃): δ [ppm]: 3.24 (-CH₂N₃) 1.45-1.10 (CH₂); 0.93 (CH₃); 0.73-0.24 (-CH₂Si); -0.10 (-SiCH₃).

6.6.2.2 H-PCS_x-C₁₁-NH₂

a) Via the phthalimide. A solution of 6.5g H-PCS-C₁₁-PI (M=1700; 3.8mmol) and 0.9g (18mmol) hydrazine in 40ml ethanol/THF were heated at 60°C for 18h. The white precipitate was removed by filtration and the solution evaporated to dryness. The residue was dissolved in diethyl ether and washed with a 1M NaOH-solution. Remaining phthalhydrazide was removed by dialysis (MWCO = 1000g/mol).

b) Via the azide. Staudinger reduction. A solution of 2.0g PCS-C₁₁-N₃ (M=1400; 1.4mmol) and 0.75g triphenylphosphine in 10ml THF were stirred for 18h (evolution of gas normally ceased after the first hours). After addition of aqueous ammonia solution (0.7ml, 35%) the reaction mixture was stirred for another 18h. The solvent was removed and the triphenylphosphite separated by a short column in CHCl₃/MeOH 9:5. The amine-functional polymer was eluted from the column by addition of triethylamine to the eluent. Yield: 1.2g (60%).

Reduction with hydrogen. Hydrogen was bubbled through a solution of 1.39g (0.48mmol) PCS₂₀-C₁₁-N₃ in 5ml ethyl acetate/methanol (4:1) and 50mg Pd/C. After complete reduction of the azide the solution was filtered over Celite and the pure polymer obtained after removal of the solvent. Yield: quant.

¹H-NMR (300 MHz, CDCl₃): δ [ppm]: 2.67 (-CH₂NH₂); 1.84-1.64 (-NH₂); 1.45-1.10 (CH₂); 0.93 (CH₃); 0.73-0.24 (-CH₂Si); -0.10 (-SiCH₃).

6.6.2.3 H-PCS_x-C₁₁-N-PG₂

A solution of 67mg (0.9mmol) glycidol in 1ml dry THF is added drop wise to a solution of 1.20g (0.04mmol) PCS₂₀-C₁₁-NH₂. After complete addition the reaction mixture is heated to 60°C for 18h. Unreacted glycidol is removed under vacuum at 100°C. Yield: quantitative.

¹H-NMR (300 MHz, CDCl₃): δ [ppm]: 3.84-3.42 (CH_xO); 2.72-2.38 (CH_xN); 1.45-1.10 (CH₂); 0.93 (CH₃); 0.73-0.24 (-CH₂Si); -0.10 (-SiCH₃).

6.6.3 Hyperbranched-Hyperbranched Block Copolymers

6.6.3.1 Hb-H-PCS-C₁₁-hb-PG

Bisglycidolized amine functionalized *hb*-PCS (H-PCS-C₁₁-PG₂) was dissolved in benzene and partially deprotonated (30% of the OH-groups) by adding cesium hydroxide. The solution was stirred for one hour at 90°C at atmospheric pressure and subsequently for two more hours under vacuum to remove benzene and water. The completely dried macroinitiator was dissolved in THF and heated till reflux. The polymerization reaction was performed by slow addition of the respective amount of a 10% solution of glycidol in THF via a syringe pump (Lambda VIT-FIT syringe pump). After addition was completed, a cation exchange resin (Dowex[®] 50WX8, 200-400 mesh) was added and the mixture was stirred for one more hour. Subsequently, the solution was filtered over a sintered filter (pore size 1) and washed with CHCl₃, Et₂O or MeOH, depending on the size

of the blocks. The resulting polymer was purified by dialysis in the respective solvent. Yields: 80-90%.

$^1\text{H-NMR}$ (300 MHz, CDCl_3 / MeOD-d_4): δ [ppm]: 3.86-3.30 (CH_xO); 2.59-2.29 (CH_xN); 1.48-1.07 (CH_2); 0.97-0.76 (CH_3); 0.61-0.24 ($-\text{CH}_2\text{Si}$); -0.04-(-0.24) ($-\text{SiCH}_3$).

6.6.3.2 *Hb-H-PCS-C₁₁-hb-PGSi*

A solution of 8mmol HMDS in 10ml chloroform was added dropwise to a stirred suspension of *hb-H-PCS-C₁₁-hb-PG* (10mmol OH groups) and iodine (0.1mmol) in chloroform (40ml). After stirring for 24h a clear solution was obtained. 3g of powdered $\text{Na}_2\text{S}_2\text{O}_3$ were added portion-wise. The mixture was stirred for another 30 minutes, filtered and washed twice with chloroform. The solvents were removed under vacuum and the product was purified by dialysis in CHCl_3 .

$^1\text{H-NMR}$ (300 MHz, CDCl_3): δ [ppm]: 3.84-3.33 (CH_xO); 1.48-1.07 (CH_2); 0.97-0.76 (CH_3); 0.61-0.24 ($-\text{CH}_2\text{Si}$); 0.04-0.21 ($-\text{O-SiCH}_3$); -0.04-(-0.24) ($-\text{SiCH}_3$).

6.6.3.3 *Hb-H-PCS-C₁₁-hb-PGBz*

A solution of *hb-H-PCS-C₁₁-hb-PG* (3mmol OH groups), benzoyl chloride (3.3ml) and *N*-methylimidazole (0.1ml) in pyridine (30ml) was heated to 80°C and stirred for 12h. After removal of most of the solvent, 2.6g K_2CO_3 was added to the residue, dissolved in 100ml toluene. The solution was filtered and washed with toluene. Pyridine impurities were removed by azeotropic distillation of the toluene. The product was purified by dialysis in CHCl_3 .

$^1\text{H-NMR}$ (300 MHz, CDCl_3): δ [ppm]: 8.07-7.32 (CH , Bz), 3.86-3.30 (CH_xO); 2.59-2.29 (CH_xN); 1.48-1.07 (CH_2); 0.97-0.76 (CH_3); 0.61-0.24 ($-\text{CH}_2\text{Si}$); -0.04-(-0.24) ($-\text{SiCH}_3$).

6.7 References

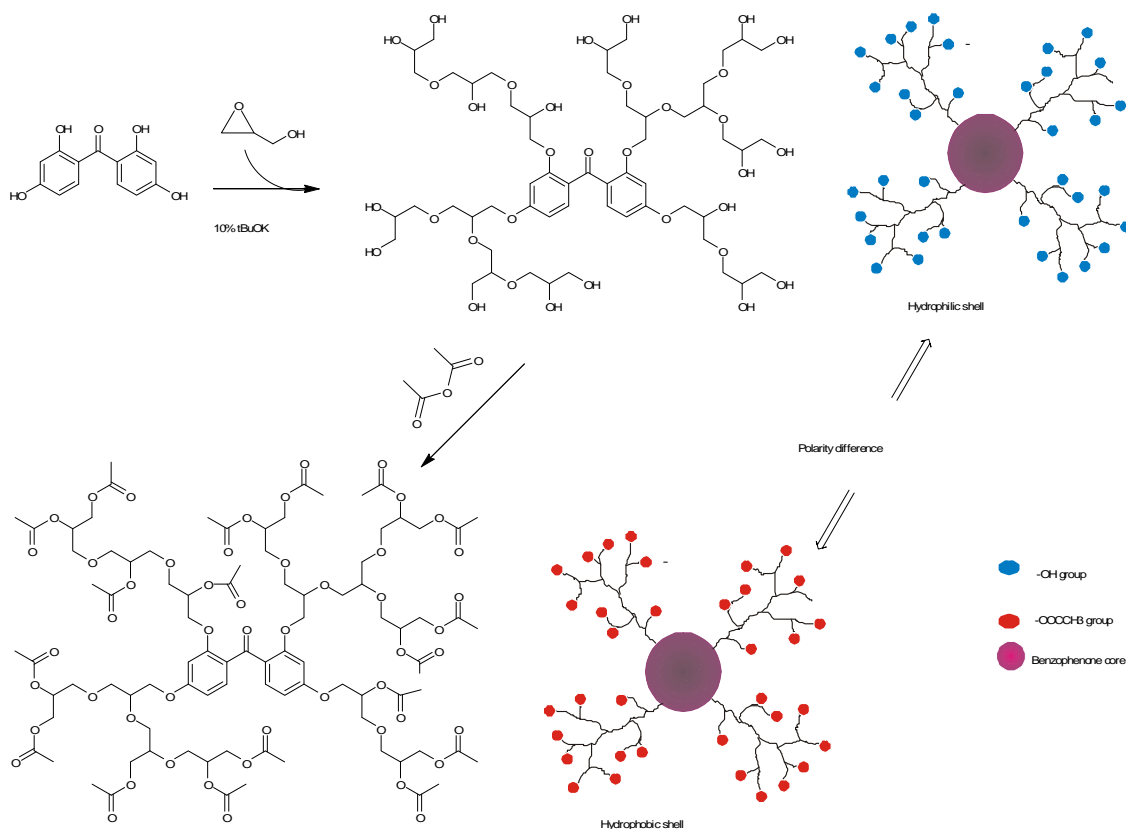
1. Hawker, C. J.; Frechet, J. M. J. *Journal of the American Chemical Society* **1992**, 114, 8405-8413.
2. Aoi, K.; Itoh, K.; Okada, M. *Macromolecules* **1997**, 30, 8072-8074.
3. Bury, I.; Donnio, B.; Gallani, J. L.; Guillon, D. *Langmuir* **2007**, 23, 619-625.
4. Nierengarten, J. F.; Eckert, J. F.; Rio, Y.; Carreon, M. D.; Gallani, J. L.; Guillon, D. *Journal of the American Chemical Society* **2001**, 123, 9743-9748.
5. Zhang, S.; Rio, Y.; Cardinali, F.; Bourgoigne, C.; Gallani, J. L.; Nierengarten, J. F. *Journal of Organic Chemistry* **2003**, 68, 9787-9797.

6. Yang, M.; Wang, W.; Yuan, F.; Zhang, X. W.; Li, J. Y.; Liang, F. X.; He, B. L.; Minch, B.; Wegner, G. *Journal of the American Chemical Society* **2005**, 127, 15107-15111.
7. Yuan, F.; Wang, W.; Yang, M.; Zhang, X. J.; Li, J. Y.; Li, H.; He, B. L. *Macromolecules* **2006**, 39, 3982-3985.
8. Lee, J. W.; Kim, B. K.; Kim, J. H.; Shin, W. S.; Jin, S. H. *Journal of Organic Chemistry* **2006**, 71, 4988-4991.
9. Schüle, H. Functionalization of hyperbranched polycarbosilanes - Block copolymers and electrochemistry. Johannes-Gutenberg University, Mainz, 2008.
10. Amore, A.; van Heerbeek, R.; Zeep, N.; van Esch, J.; Reek, J. N. H.; Hiemstra, H.; van Maarseveen, J. H. *Journal of Organic Chemistry* **2006**, 71, 1851-1860.
11. van Heerbeek, R.; Kamer, P. C. J.; van Leeuwen, P. N. M. W.; Reek, J. N. H. *Organic & Biomolecular Chemistry* **2006**, 4, 211-223.
12. van Heerbeek, R.; Reek, J. N. H.; Kamer, P. C. J.; van Leeuwen, P. W. N. M. *Tetrahedron Letters* **1999**, 40, 7127-7130.

7 Amino Acid Based Core Initiators for the Polymerization of Glycidol and L-Lactide

7.1 Introduction

Besides glycerol, lactide as well as various amino acids are well-studied repeat units for biomedical polymers. The combination of such biocompatible polymers thus represents an interesting and promising approach for novel and precisely tunable biocompatible structures. Chapter 4 highlighted the use of bisglycidolized amines as core initiators for the ROMBP of glycidol. However, the presence of an additional acidic group represents a challenge. It has been demonstrated for perfectly branched dendrimers that the site isolation of the core moiety in a dendritic scaffold is of great importance with respect to optical properties. In this context, Fréchet et al. introduced a solvatochromic chromophore (4-(*N,N*-dimethylamino)-1-nitrobenzene) at the focal point of a polybenzylether dendrimer.¹ Depending on the polarity of the solvent and the generation of the dendrimer, changes in the UV-vis absorption of the encapsulated photoactive core and a morphology transition from an extended to a more globular macromolecular structure was observed. Furthermore, it was shown that manganese and zinc-porphyrins coated by dendritic structures exhibit better stability and improved regioselectivity in catalytic processes.^{2,3} However, only few corresponding examples involving hyperbranched structures have been reported to date. Fossum et al. investigated the effect of enhanced core reactivity on molecular weight, polydispersity and the degree of branching.⁴ The incorporation of different UV-active initiator cores such as benzylamine, 1-naphthylmethylamine and a typical triplet photosensitizer, 2,2',4,4'-tetrahydroxy benzophenone BP(OH)₄, into hyperbranched polyglycerols under SMA conditions was studied by Frey et al.^{5,6} The macromolecules obtained from the polymerization of glycidol onto the tetra-hydroxyfunctional benzophenone BP(OH)₄ core exhibited narrow polydispersity ($1.5 < M_w/M_n < 2$) and molecular weights between 1,500 and 5,800 g/mol. The phenolic nature of hydroxyl groups at the core and facile deprotonation enabled a fast and quantitative incorporation into the growing hyperbranched polymers. The synthetic strategy employed is depicted in Scheme 7.1.

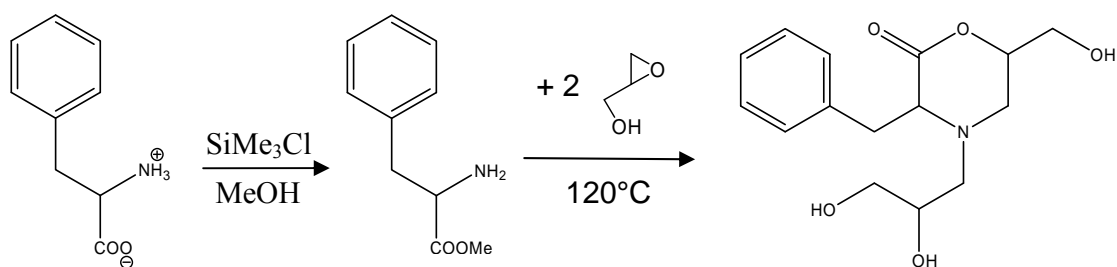


Scheme 7.1. Synthetic approach for the incorporation of a benzophenone core into hyperbranched polyglycerols and peracetylation of the obtained polymer.

Complete incorporation of the photoactive core moiety into the well-defined hyperbranched structure was conclusively evidenced by MALDI-ToF mass spectrometry. Figure 1.1 shows the central part of the MALDI-ToF mass spectrum (between 500 and 3,000 g/mol) of a benzophenone core containing polymer with 80 glycidol units.⁵ Consequently, in this chapter the UV-active amino acids L-phenylalanine and L-tryptophan were chosen as core molecules combining both biocompatible and optical properties.

7.2 Amino Acid Based Core Initiators

As the amine group of amino acids can be protonated by the carboxylic group of the same molecule, a mere bisglycidolization step (as described in chapter 4) is not applicable. Supplementary addition of triethylamine is required. Addition of a base is not an option, as it can lead to the undesired ring-opening of glycidol itself. In order to reduce side reactions, the deprotonation step was carried out in situ directly before the polymerization (chapter 7.3). In order to obtain well-defined initiators an alternative 2-step approach was applied (Scheme 7.2).



Scheme 7.2. 2-step synthetic pathway for the preparation of morpholinone derivative of phenylalanine.

The first step involves the transformation of the amino acids into the corresponding esters using trimethylsilyl chloride. The ester was then treated with 2.1 equivalents of glycidol at 0°C. As already discussed in previous chapters the addition of 3 or 4 units of glycidol occurs as an undesired side reaction even at low temperatures. All samples were heated to 120°C for the removal of solvent (THF) and residual glycidol. Methanol was also removed via intramolecular esterification reaction and the corresponding morpholinone derivatives were obtained. Purification by column chromatography gave the pure morpholinone derivatives with exactly 3 hydroxyl groups (Figure 7.1).

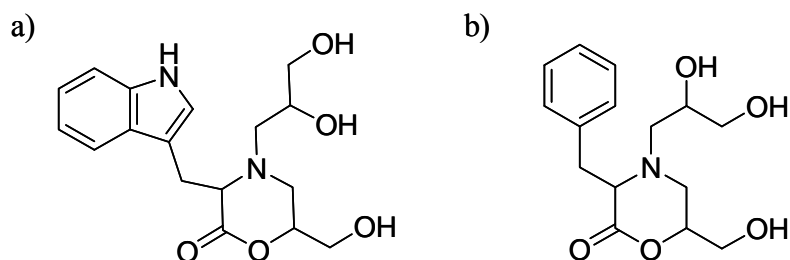
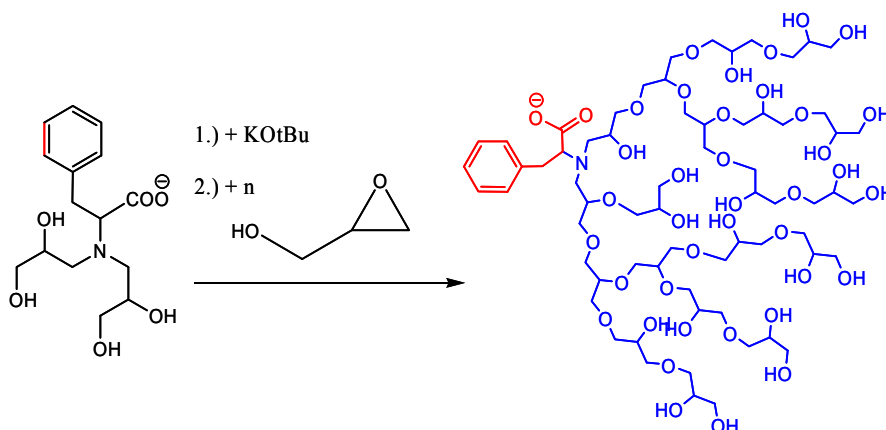


Figure 7.1. a) 4-(2,3-dihydroxypropyl)-6-hydroxymethyl-3-indolylmethylmorpholin-2-one; b) 3-benzyl-4(2,3-dihydroxy-propyl)-6-hydroxymethyl-morpholin-2-one.

7.3 Hyperbranched Polyglycerols with Functional Initiator Cores

As already mentioned two pathways were tested for the incorporation of amino acids as core molecules into hyperbranched polyglycerols. In a first approach, the amino acid was deprotonated with triethylamine in the reactor vessel and two equivalents of glycidol were added. After stirring for one hour at room temperature the mixture was heated to 120°C and the ROMBP of glycidol was carried out as described in the previous chapters (Scheme 7.3). In a second test experiment an additional equivalent of base concerning

hydrochloric triethylamine was added (1.00 eq based on COOH which corresponds to 0.25 eq based on the OH-groups of the initiator) as the reaction with the hydrochloric triethylamine might occur as side reaction.



Scheme 7.3. ROMBP of glycidol with in situ bisglycidolized phenylalanine initiator.

In the second approach the morpholinone derivatives described in the previous paragraph were used as initiators. Table 7.1 summarizes the corresponding results. The morpholinones are marked with an additional “M”.

Table 7.1. Amino acid-based core initiators for hyperbranched polyglycerols.

Sample	t-BuOK (eq/OH)	$M_{n,theo}$ (g/mol)	$M_{n,NMR}$ (g/mol)	$M_{n,GPC}$ (g/mol)	PD_{GPC}
A) PhePG ₁₆	0.2 eq	1,500	980	700	4.2
B) PhePG ₁₆	0.45 eq	1,500	1,480	1,500	4.3
C) PheMPG ₁₆	0.2 eq	1,500	620	520	1.2
D) TrpPG ₁₆	0.2 eq	1,500	870	820	4.4
E) TrpPG ₁₆	0.45 eq	1,500	1,600	1,750	6.2
F) TrpMPG ₁₆	0.2 eq	1,500	590	540	1.2

It is obvious that the hydrochloric triethylamine (0.25 equivalents) in reactions A, B, D and E are mainly transformed into triethylamine by the additional base. Hence, almost no reaction occurs when 0.2 eq of base are added (Table 7.1 A & D) because only some of the bisglycidolized amino acids are deprotonated and thus transformed into active initiating species for the ROMBP of glycidol. Increasing the amount of potassium *tert*-

butanolate to compensate for this side reaction leads to hyperbranched molecules with good agreement between theoretical and experimental molecular weights in $^1\text{H-NMR}$ spectroscopy (Figure 7.2) as well as in GPC (Figure 7.3). However, molar mass distributions are very broad. Although the incorporation of the core molecule into all species present in the molecular weight distribution can be evidenced by GPC (RI- and UV signal overlap, Figure 7.3) narrow distributions like in the case of the benzophenone cores were not achieved.

This might stem from the higher reactivity of the OH groups directly connected to the aromatic system as well as from the absence of the acidic group.

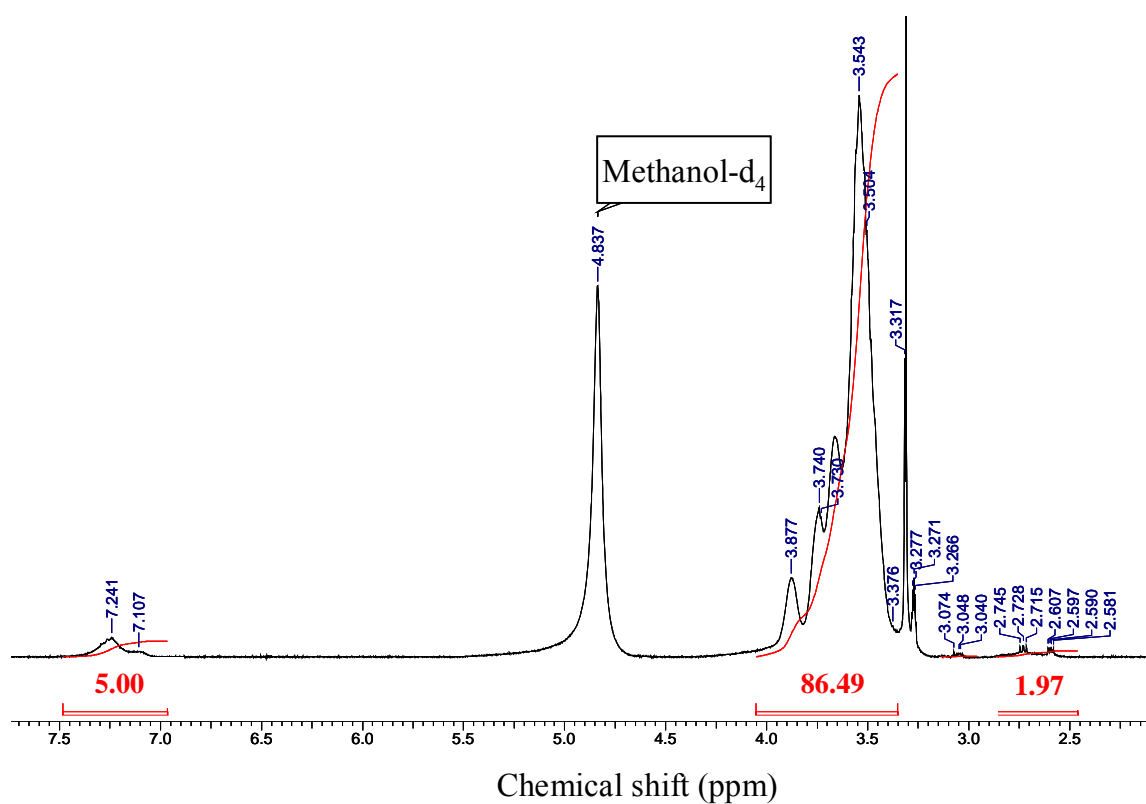


Figure 7.2. $^1\text{H-NMR}$ spectrum of PhePG₁₆ (Table 7.1 B) in methanol- d_4 .

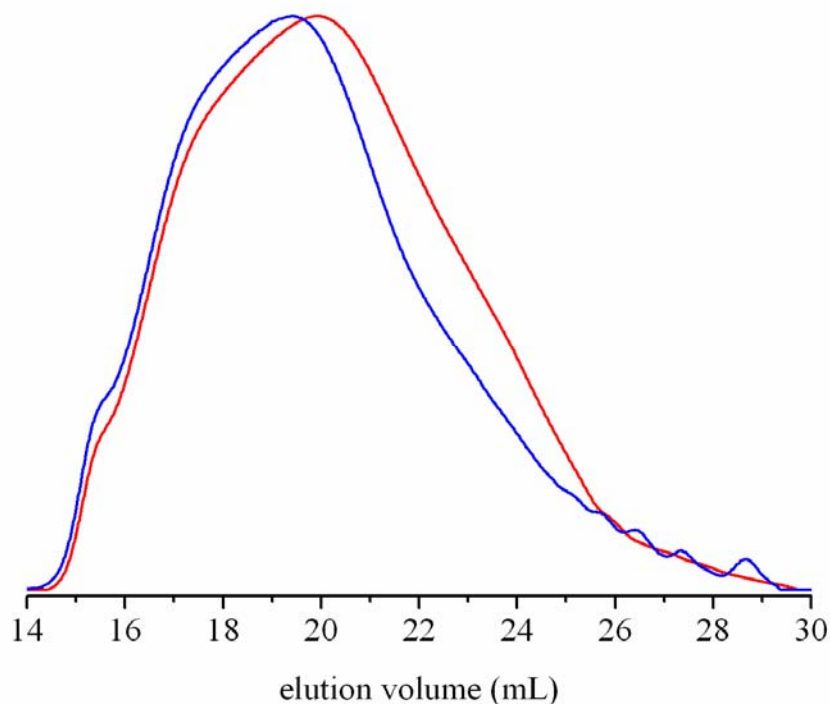


Figure 7.3. GPC curves of PhePG₁₆ (Table 7.1 B) in DMF; UV (red), RI (blue).

Surprisingly, the morpholinone derivatives did not act as suitable core initiators (Table 7.1 C & F) and the formation of oligomers that were removed during the work-up was predominant. Cleavage of the ester bond by the alcohol may have resulted in a non reactive deprotonated carboxylic group.

7.4 Poly(L-lactides) with Functional Initiator Cores

Stannous octoate (SnOct₂) is a widely used initiator in polylactide synthesis⁷⁻⁹ as well as in the polymerization of lactones with alcohols.¹⁰⁻¹⁵ The presented morpholinone derivatives are structurally comparable and thus considered promising candidates for a polymerization catalyzed by stannous octoate. Sterical hindrance of the morpholinones however prevented successful homopolymerization. Hence, lactide, the diester of lactic acid, was added as a second monomer (Figure 7.4). It was important to investigate whether the morpholinones act as initiator cores or if they are simply incorporated as comonomers.



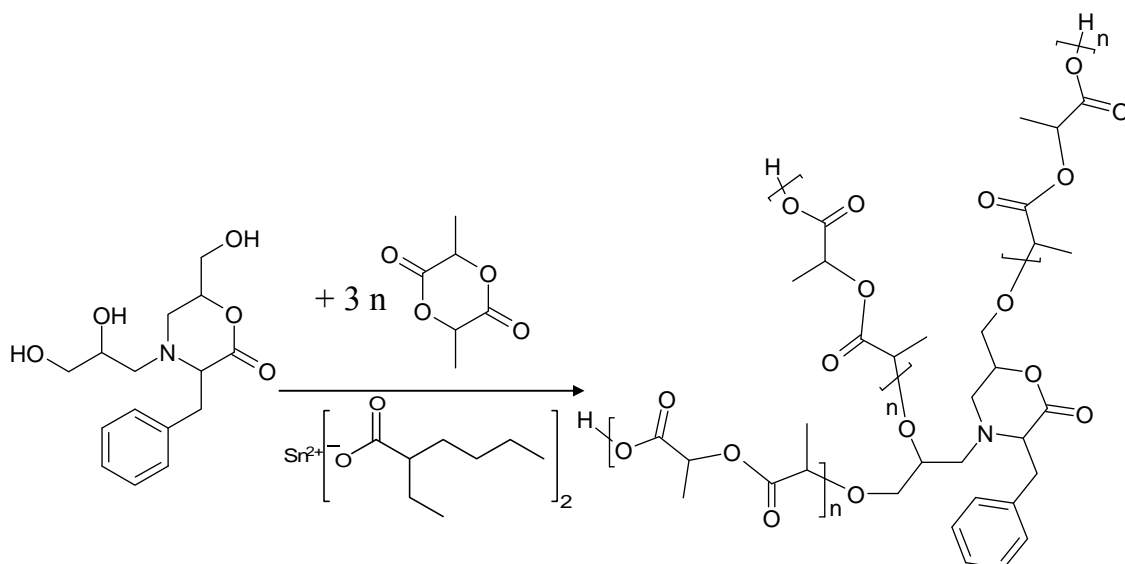
Figure 7.4. Structure of L-lactid acid (left) and L-lactide (right).

The polymerization reactions were carried out in bulk with a varying ratio of morpholinone derivative and lactide. Table 7.2 summarizes the results.

Table 7.2. Amino acid based core initiators for L-lactides.

Sample	X _{th}	M _{n,th} (g/mol)	X _{GPC,bulk}	M _{n,GPC,bulk} (g/mol)	PDI _{GPC,bulk}
PhePL _x	7	1,300	6	1,200	1.3
PhePL _x	17	2,700	15	2,400	1.3
PhePL _x	35	5,300	16	2,600	1.3
PhePL _x	80	11,700	30	4,600	1.2
PhePL _x	195	28,000	53	7,800	1.1
TrpPL _x	12	2,000	9	1,600	1.5
TrpPL _x	20	3,200	15	2,500	1.8
TrpPL _x	40	6,000	24	3,700	1.4
TrpPL _x	90	13,100	23	3,600	1.8
TrpPL _x	220	31,600	95	13,800	1.2

The number of incorporated lactide monomers is generally lower than targeted. This may be caused by partial sublimation of lactide monomer due to the stringent reaction conditions (bulk polymerization at 120°C). In the case of lactide/morpholinone ratios exceeding 20, traces of lactide were found after reaction times of 24 hours. However, the observed data is in contradiction with expectation for higher molar masses, if the morpholinones actually copolymerized. On the other hand, complete incorporation of the morpholinones as initiator cores, affording three arm star polymers (Scheme 7.2) was confirmed by GPC analysis, as the UV-signal ($\lambda = 254\text{nm}$) generated by the core molecules is identical to the RI curve (Figure 7.5).



Scheme 7.2. Synthetic pathway of the three arm star polymer.

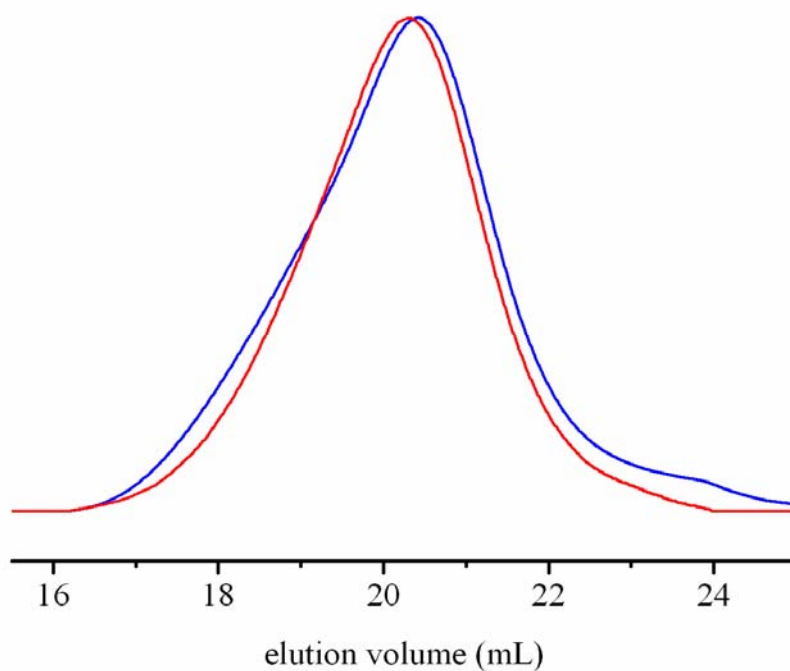


Figure 7.5. GPC curves of TrpPL_{theo,40} (Table 7.2) in DMF; UV- (red) and RI signals (blue).

In order to support this assumption, a second experiment was carried out, using diglyme as reaction solvent to avoid loss of lactide by sublimation. In all cases molecular weights did not exceed 800 g/mol, i.e. only oligomers were obtained. A major fraction of the lactide remained unreacted under these conditions. However, using equimolar amounts of morpholinone and lactide resulted in full conversion of the lactide without any ring-opening polymerization of the morpholinone.

7.5 Conclusion

This chapter describes the use of UV-active amino acids (L-phenylalanine and L-tryptophan) as core molecules for hyperbranched polyglycerols and polylactides. The presence of the carboxylic acid group within these molecules required an additional step for bisglycidolization of the amine group. Triethylamine was used to deprotonate the amino acid. It was shown that the in situ reaction of these initiators only resulted in hyperbranched polyglycerols, when a sufficient amount of base was added to deprotonate the acidified triethylene amine as well as a certain amount of the OH groups of the polymers. Although complete incorporation of the molecules was evidenced, polydispersities were around 4. The transformation into morpholinone derivatives possessing three OH and no free acidic group resulted in a non-active core molecule. However, these compounds were successfully used for the polymerization of lactide and resulted in 3-arm star polymers with narrow molar mass distributions. Homopolymerization catalyzed by stannous octoate was impossible due to the high degree of steric hindrance.

7.6 Experimental Part

7.6.1 Materials

All chemicals were purchased from *Aldrich* or *Acros Organics*. Acetone p.a., tryptophan, phenylalanine, methanol p.a., Dowex[®] 50WX8, 200-400 mesh, ion exchange resin, and 1M potassium *tert*-butylate solution in THF were used as received. THF was distilled over sodium prior to use. Diglyme and glycidol were purified by distillation over calcium hydride. Chloroform-d and Methanol-d₄ were purchased from *Deutero GmbH*.

7.6.2 Synthesis of the Morpholinone Derivatives

7.6.2.1 Phenyl-alanine methyl ester

To a suspension of 33g (0.2mol) of phenylalanine in 600mL methanol 127mL (1.0mol) trimethylsilyl chloride was added dropwise at 0°C. After stirring for 12 hours a clear solution was formed. The solvent was removed in vacuo and the product was dried to give a colorless powder in quantitative yield.

¹H-NMR (300 MHz, MeOD): δ [ppm]: 3.15 – 3.32 (m, 2H, CH₂); 3.80 (s, 3H, -O-CH₃); 4.34 (t, 1H, -CH-NH₂), 7.41 – 7.76 (m, 5H, Ph).

7.6.2.2 Tryptophan methylester

To a suspension of 41g (0.2mol) of tryptophan in 600 mL methanol 127mL (1.0mol) trimethylsilyl chloride was added dropwise at 0°C. After stirring for 12 hours a clear solution was formed. The solvent was removed in vacuo and the product was dried to give a slightly purple powder in quantitative yield.

¹H-NMR (300 MHz, MeOD): δ [ppm]: 3.36 – 3.50 (m, 2H, CH₂); 3.79 (s, 3H, -O-CH₃); 4.33 (t, 1H, -CH-NH₂); 7.07 (t, 1H, indolyl-5); 7.15 (t, 1H, indolyl-6); 7.22 (s, 1H, indolyl-2); 7.40 (d, 1H, indolyl-4); 7.54 (d, 1H, indolyl-7).

7.6.2.3 3-Benzyl-4(2,3-dihydroxy-propyl)-6-hydroxymethyl-morpholin-2-one

25mL (0.4mol) glycidol were slowly added (2h) to a solution of 37.0g (0.2mol) phenylalanine methylester in 300mL THF under argon. The solution was allowed to warm to room temperature and the solvents were removed in vacuo. The product was heated to 100°C to remove all resulting methanol in vacuo to give an orange solid in quantitative yield. Further purification was carried out by column chromatography (methanol/chloroform 1:9) (R_f = 0.07).

MS (FD): m/z: 334.4 [M+1]⁺

7.6.2.4 4-(2,3-Dihydroxypropyl)-6-hydroxymethyl-3-indolylmethylmorpholin-2-one

25mL (0.38mol) glycidol were slowly added (2h) to a solution of 41.5g (0.19mol) tryptophan methylester in 350mL THF under argon. The solution was allowed to warm to room temperature and the solvents were removed in vacuo. The product was heated to 100°C to remove all resulting methanol in vacuo to give a brown solid material in quantitative yield. Further purification was carried out by column chromatography (methanol/chloroform 1:9) (R_f = 0.05).

MS (FD): m/z: 334.4 [M+1]⁺

7.6.3 Hyperbranched Polyglycerols with Amino Acids as Initiator Cores

All syntheses described in chapter 7.3 were carried out under argon atmosphere in the polymerization apparatus described in chapter 3.6.2. Freshly distilled THF (ca. 50 mL) was injected to the reservoir funnel under and the pump was run until no bubbles were observed upon THF addition to the reactor. The corresponding amino acid was dissolved/emulsified in 20ml freshly distilled diglyme and transferred into the reactor in Ar-counter flow. 1eq triethyl amine was added and the mixture was stirred for 1h at room-

temperature. Two eq of glycidol were dissolved in THF and added drop wise over a period of 2 hours. The desired amount of potassium *tert*-butanolate was added and the mixture was stirred for one more hour at room temperature. The oil bath was heated to 120°C and the stirrer was run at 600 revolutions per minute and the pump was started. The desired amount of glycidol was filled into the reservoir funnel to the remaining THF in Ar-counter flow. A pumping rate of 5 drops per minute was employed and the size of the drops was adjusted to 50%. When the addition of glycidol was completed, an additional 25 mL of freshly distilled THF were filled into the reservoir and the pump was restarted in order not to lose any glycidol remaining in the tube connected to the pump. After the reaction was finished, products were dissolved in methanol and stirred with a cation exchange resin. Subsequently, the solution was filtered over a sintered filter (pore size 1) and washed with methanol. The resulting polymer was precipitated twice into cold acetone as a methanol solution and dried for 12 h in vacuo at 100°C. The polymers are yellowish, transparent, viscous materials. Yields are between 80 and 95% depending on the polymer molecular weight.

7.6.4 Poly(L-Lactides) with Amino Acids as Initiator Cores

All polymerizations described in chapter 7.4 were carried out in reaction tubes of a carousel reaction station. The monomers were either melted at 120°C or dissolved in diglyme and subsequently heated to 120°C and degassed for 10 minutes. Under vigorous stirring a 10% solution of stannous octoate was added. The reactions were stirred for 12 hours and the mixtures were dissolved in little methanol and subsequently dried in vacuo.

7.7 References

1. Hawker, C. J.; Wooley, K. L.; Fréchet, J. M. J. *J. Am. Chem. Soc.* **1993**, 115, 4375.
2. Bhyrappa, P.; Young, J. K.; Moore, J. S.; Suslick, K. S. *J. Am. Chem. Soc.* **1996**, 118, 5708-5711.
3. Vestberg, R.; Nystrom, A.; Lindgren, M.; Malmström, E.; Hult, A. *Chem. Mater.* **2004**, 16, 2794-2804.
4. Bernal, D. P.; Bedrossian, L.; Collins, K.; Fossum, E. *Macromolecules* **2003**, 36, 333-338.

5. Pastor-Perez, L.; Barriau, E.; Berger-Nicoletti, E.; Kilbinger, A. F. M.; Perez-Prieto, J.; Frey, H.; Stiriba, S. E. *Macromolecules* **2008**, 41, 1189-1195.
6. Barriau, E.; Pastor-Perez, L.; Berger-Nicoletti, E.; Kilinger, A. F. M.; Frey, H.; Stiriba, S. E. *Journal of Polymer Science Part a-Polymer Chemistry* **2008**, 46, 2049-2061.
7. Leenslag, J. W.; Pennings, A. J. *Makromol. Chem.* **1987**, 188, 1809.
8. Schwach, G.; Coudane, J.; Engel, R.; Vert, M. *J. Polym. Sci., Part A: Polym. Chem.* **1997**, 35, 3431-3440.
9. Gottschalk, C.; Wolf, F.; Frey, H. *Macromolecular Chemistry and Physics* **2007**, 208, 1657-1665.
10. Lundberg, R. D.; Cox, E. F., In *Ring-Opening Polymerization*, Risch, K. C.; Reegen, S. L., Eds. Marcel Dekker: New York, London, 1969; Vol. 6, p 266.
11. Löfgren, A.; Albertsson, A.-C.; Dubois, P.; Jérôme, R., Recent Advances in Ring-Opening Polymerization of Lactones and Related Compounds. *J. Macromol. Sci. Rev. Macromol. Chem. Phys.* 1995, p 379.
12. Kricheldorf, H. R.; Sumbel, M. *Eur. Polym. J.* **1991**, 25, 585.
13. Kricheldorf, H. R.; Boettcher, C. *Makromol. Chem.* **1993**, 194, 1653.
14. Schindler, A.; Hibionada, Y. M.; Pitt, C. G. *J. Polym. Sci., Part a: Polym. Chem.* **1982**, 20, 319.
15. Kim, S. H.; Han, Y.; Kim, Y. H.; Hong, S. I. *Makromol. Chem.* **1992**, 193, 1623.

8 Amphiphilic Hyperbranched Block Copolymer Polyelectrolytes

8.1 Introduction

The term „polyelectrolytes“ refers to macromolecules with electrolyte units that can dissociate in aqueous solutions, making the polymers negatively or positively charged. One approach to polyelectrolytes is the incorporation of charges by transformation of the functional end groups of previously synthesized polymers. Polyelectrolytes combine the properties of electrolytes and the corresponding polymers. Their solutions are electrically conductive just like salt solutions, however they are commonly viscous like polymer solutions. Many biological molecules are polyelectrolytes, e.g., polypeptides (and thus all proteins) as well as DNA. Both natural and synthetic polyelectrolytes are used for a variety of industrial applications. These are mostly related to modification of flow and stability properties of aqueous solutions and gels. For instance, they can be used to either stabilize colloidal suspensions or to initiate flocculation. Additionally they are useful compounds to impart surface charges to neutral particles, enabling them to be dispersed in aqueous solution. Common practical applications thus include use as thickeners, emulsifiers, conditioners, flocculants, and even drag reducers, as well as for water treatment and oil recovery. Many soaps, shampoos, and cosmetics incorporate polyelectrolytes. Some polyelectrolytes can be used as food additives, for instance pectin, carrageenan, alginates, polyvinylpyrrolidone and carboxymethyl cellulose. Except for the latter two examples, all these compounds are of natural origin. Polyelectrolytes can also be found in some kinds of cement. Due to the water-solubility of some polyelectrolytes, they are also investigated for biochemical and medical applications. Intense research is being undertaken with respect to biocompatible polyelectrolytes for implant coatings and controlled drug release.

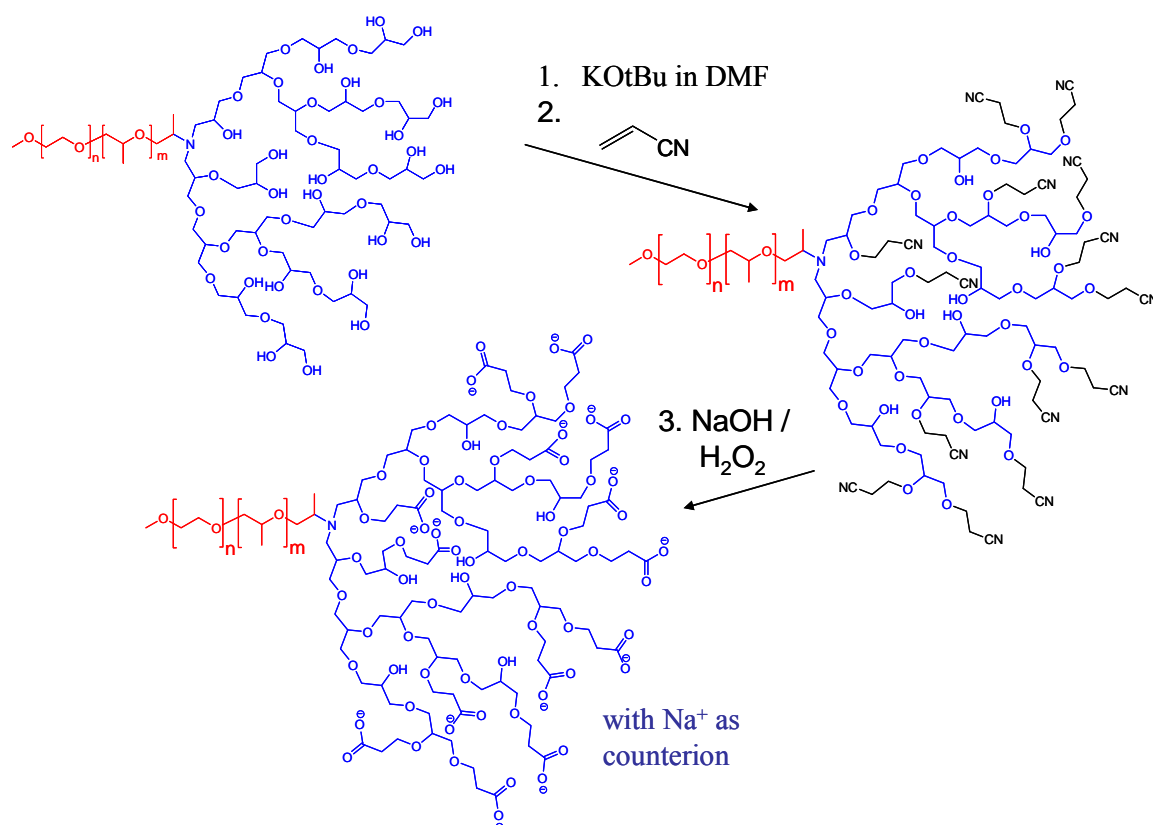
Several works have been focused on highly branched polyelectrolyte structures based on perfectly branched dendrimer scaffolds.¹⁻⁴ A versatile strategy for the preparation of hyperbranched polyelectrolytes via self condensing vinyl copolymerization (SCVCP) of protected acrylate monomers and subsequent hydrolysis has been presented by Müller et al.⁵ A further well-studied example of a highly branched polyelectrolyte is poly(ethylene imine), PEI, where the charge density of the amine groups is pH-dependent and consequently leads to a strong variation of the properties in aqueous solution.⁶ Furthermore a

number of theoretical works has treated branched polyelectrolytes bearing charges.⁷⁻⁹ Among hyperbranched structures, the preparation of carboxylated hyperbranched polyglycerols has been reported. As it is often the case for polymer modification reactions, higher degrees of functionalization were obtained for low molecular weight starting materials.^{10,11} The solution properties of the resulting materials were investigated by dynamic light scattering (DLS), showing the formation of large aggregates with pH-dependent size. After deposition on a negatively charged mica surface, the structures observed by atomic force microscopy show the coexistence of aggregates and single macromolecules. This chapter involves the investigation of the suitability of the respective synthetic strategy for the amphiphilic linear-hyperbranched block copolymers presented in chapter 4.

8.2 Synthesis of the Amphiphilic Hyperbranched Block Copolymer Polyelectrolytes

In Chapter 4, a synthetic strategy for amphiphilic linear-hyperbranched block copolymers (*l*-PPO-*b*-*hb*-PG) was presented. These polymers were modified in this approach. The first step involves the partial deprotonation of the polyglycerol hydroxyl groups subsequent conversion into nitrile groups via Michael addition reaction. After workup and characterization of these intermediates, the nitrile groups were transformed into carboxylic functionalities by hydrolysis with hydrogen peroxide in the presence of sodium hydroxide. Scheme 8.1 illustrates the synthetic pathway to the carboxyl-functionalized polymers.

The resulting polymers were characterized by NMR-spectroscopy and molar masses were calculated by comparing the respective peak integrals. The isolated signal of the propylene oxide side CH₃ groups was used as a reference, as this part of the block copolymer was not altered during the reaction. Table 8.1 summarizes the experimental data obtained by ¹H-NMR and CMC determination.



Scheme 8.1. 2 step-synthesis of novel amphiphilic block copolymer amphiphiles.

Table 8.1. $^1\text{H-NMR}$ data and CMC of the block copolymers.

Sample	X_{NMR}	Y_{NMR}	$M_{n,\text{NMR}}$ (g/mol)	Degree of functional- ization (x/y)	CMC (mol/l)
PPO ₃₅ -N-PG-OH _x	24.7	0	3,680	0 %	$3.92 \cdot 10^{-5}$
PPO ₃₅ -N-PG-OH _x -(RCN) _y	7.0	17.7	4,390	72 %	-
PPO ₃₅ -N-PG-OH _x -R'COONa _y	7.0	17.7	5,120	72 %	$7.27 \cdot 10^{-5}$
PPO ₃₅ -N-PG-OH _x	26.8	0	3,840	0 %	$4.24 \cdot 10^{-5}$
PPO ₃₅ -N-PG-OH _x -(RCN) _y	11.7	15.1	4,390	56 %	-
PPO ₃₅ -N-PG-OH _x -R'COONa _y	11.7	15.1	5,120	56 %	$6.87 \cdot 10^{-5}$

Both initial polymers exhibited similar molecular weights. The calculated degrees of functionalization of 56% and 72% are in agreement with previously reported data for hyperbranched polyglycerols.¹⁰ Transformation of the nitrile groups into carboxylic acid

groups was quantitative. Comparison of GPC data was problematic, since the chemical structure of the polymers is drastically changed within the course of the reaction. Additionally, the hydroxide terminated block copolymers were dissolved in DMF for GPC measurement and PEG or PS standards were applied, while the nitrile terminated polymers were dissolved in chloroform. The carboxylate functionalized molecules were insoluble in both of these solvents and had to be measured in water. As these measurements were carried out on a different GPC set-up that employs polyacrylic acid standards, a comparison of the molecular weight data is not useful. However, monomodal polymer distributions were retained throughout all reaction sequences. The GPC curve of the resulting polymer $\text{PPO}_{35}\text{-N-PG-OH}_7\text{-R}'\text{COONa}_{18}$ is shown in Figure 8.1.

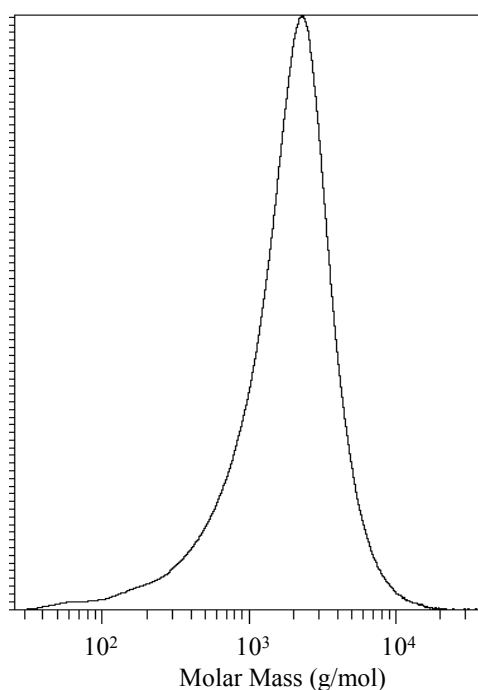


Figure 8.1. GPC curve of polymer $\text{PPO}_{35}\text{N-PG-OH}_5\text{-COONa}_{18}$ in H_2O using PAA standards.

Determination of the critical micelle concentration cmc was carried out by a fluorescence method using DPH (1,6-diphenyl-1,3,5-hexatriene). A decrease of the CMC was observed after modification of the hydroxyl into carboxylate groups. This confirmed the higher amphiphilicity of the resulting polymers.

8.3 Conclusion

It has been shown that the previously reported synthetic pathway to carboxylated hyperbranched polyglycerol polyelectrolytes can also be applied for the amphiphilic linear-hyperbranched block copolymers presented in chapter 4. These novel biocompatible and highly amphiphilic polyelectrolytes (Figure 8.2) offer great potential for further investigations.

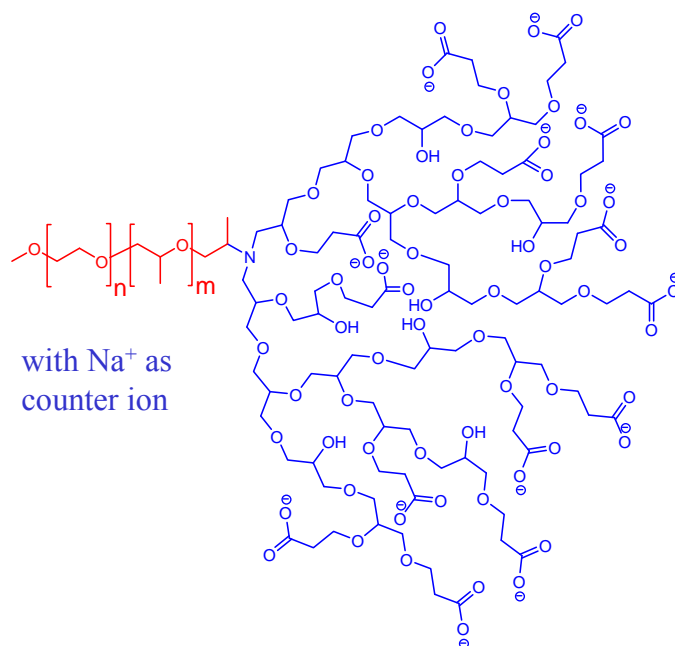


Figure 8.2. Structure of the novel amphiphilic linear-hyperbranched block copolymers.

8.4 Experimental Part

8.4.1 Materials

All chemicals were purchased from *Aldrich* or *Acros Organics* or *Fluka*. Acetone p.a., methanol p.a., isopropanol p.a., Dowex[®] 50WX8, 200-400 mesh, ion exchange resin, sodium hydroxide, 30 weight-% H₂O₂ and 1m potassium *tert*-butylate solution in THF were used as received. THF was distilled over sodium prior to use. Acrylonitrile and DMF were purified by distillation prior to use. Chloroform-*d* and Methanol-*d*₄ were purchased from *Deutero GmbH*.

8.4.2 Synthesis of the Nitrile Functionalized Block Copolymers

3.4 ml of a 1m KO^t-Bu-solution were added to a solution of 2.7mmol of the corresponding amphiphilic linear hyperbranched block copolymer (described in chapter 4.5.4) in 30ml DMF. The reaction mixture was stirred and heated to 90°C for 4 hours and then cooled to 0°C. 6.8mL distilled acrylonitrile were slowly added to the reactor using a sy-

ringe pump and the temperature was kept at 0°C. After 4 hours the mixture was warmed to 5°C and stirred for additional 20 hours at 5°C and finally for 24 hours at room temperature. Dowex[®] 50WX8, 200-400 mesh ion exchange resin was subsequently added to the reactor and stirred for one hour. The exchange resin was removed by filtration before DMF and residual acrylonitrile were removed in vacuo. The resulting polymer was obtained as brown viscous oil.

¹H-NMR (300 MHz, CDCl₃): δ [ppm]: 0.86-1.10 (-CH₃, PPO); 2.45-2.60 (-CH₂-CN); 3.26-3.83 (CH₂-CHCH₃-N, CH₂-CHCH₃-N, CH₂, PPO, CH₂, PEO, CH, PPO, CH₃-O-, CH, PG, CH₂, PG).

8.4.3 Synthesis of the Carboxylate Functionalized Block Copolymers

The water insoluble nitrile functionalized polymers were suspended in 80mL of a 3N aqueous NaOH solution. 6.75ml of a 30 weight-% H₂O₂ solution was carefully added and the mixture was stirred for 1 hour at 70°C, then for one day at 80°C and finally cooled down to room temperature for one more day. Isopropanol was added and the colorless upper layer was decanted. The yellow layer was concentrated by removing most of the solvent and purified by dialysis in water. Drying in vacuo gave the polymer as a highly viscous yellow oil.

¹H-NMR (300 MHz, D₂O): δ [ppm]: 1.05 (-CH₃, PPO); 1.66-2.52 (-CH₂-COONa); 3.32-3.91 (CH₂-CHCH₃-N, CH₂-CHCH₃-N, CH₂, PPO, CH₂, PEO, CH, PPO, CH₃-O-, CH, PG, CH₂, PG).

8.4.4 CMC Determination

Determination of the CMC was carried out according to Schubert.¹² A stock solution of 11.62 mg DPH (1,6-diphenyl-1,3,5-hexatriene) in 5 ml of THF (10 mmol/l) was prepared. From 0.25 ml of this solution, THF was evaporated at room temperature and atmospheric pressure for 30 min, before high vacuum was applied for 10 min. 5 ml of millipore water were added and the heterogeneous mixture was homogenized using an ultrasonic bath for 4 min. 20 µl of this DPH dispersion were added to the polymer solutions (2 ml), which were afterwards homogenized in the same manner. The samples were allowed to equilibrate for 48 hours in order to avoid relaxation processes.¹³ Fluorescence spectra were recorded employing an excitation wavelength of 366 nm and an emission wavelength of 400 - 500 nm (maximum 430 nm).¹⁴

8.5 References

1. Turner, S. R.; Walter, F.; Voit, B. I.; Mourey, T. H. *Macromolecules* **1994**, *27*, 1611-1616.
2. Gong, A. J.; Liu, C. Y.; Chen, Y. M.; Zhang, X.; Chen, C. F.; Xi, F. *Macromol. Rapid Commun.* **1999**, *20*, 492-496.
3. van Duijvenbode, R. C.; Rajanayagam, A.; Koper, G. J. M.; Baars, M. W. P. L.; de Waal, B. F. M.; Meijer, E. W.; Borkovec, M. *Macromolecules* **2000**, *33*, 46-52.
4. de Groot, D.; de Waal, B. F. M.; Reek, J. N. H.; Schenning, A. P. H. J.; Kramer, P. C. J.; Meijer, E. W.; van Leeuwen, P. W. N. M. *J. Am. Chem. Soc.* **2001**, *123*, 8453-8458.
5. Mori, H.; Seng, D. C.; Lechner, H.; Zhang, M. F.; Müller, A. H. E. *Macromolecules* **2002**, *35*, 9270-9281.
6. Dautzenberg, H. J., W.; Kötz, J.; Philipp, B.; Seidel, C.; Stscherbina, D.; , *Polyelectrolytes - formation, characterization and application*. Hanser: Munich, 1994.
7. Welch, P.; Muthukumar, M. *Macromolecules* **2000**, *33*, 6159-6167.
8. Ramzi, A.; Scherrenberg, R.; Joosten, J.; Lemstra, P.; Mortensen, K. *Macromolecules* **2002**, *35*, 827-833.
9. Borisov, O. V.; Daoud, M. *Macromolecules* **2001**, *34*, 8286-8293.
10. Barriau, E.; Frey, H.; Kiry, A.; Stamm, M.; Gröhn, F. *Colloid Polym. Sci.* **2006**, *284*, 1293-1301.
11. Kim, D. H.; Lee, O. J.; Barriau, E.; Li, X.; Caminade, A. M.; Majoral, J. P.; Frey, H.; Knoll, W. *J. Nanosci. Nanotech.* **2006**, *6*, 3871-3876.
12. Schubert, R. Habilitation Thesis, Pharmaceutical Institute, Faculty for Chemistry and Pharmacy of Eberhard-Karls-University, Tübingen. 1992.
13. Kabanov, A. V.; Nazarova, I. R.; Astafieva, I. V.; Batrakova, E. V.; Alakhov, V. Y.; Yaroslavov, A. A.; Kabanov, V. A. *Macromolecules* **1995**, *28*, 2303-2314.
14. Istratov, V.; Kautz, H.; Kim, Y. K.; Schubert, R.; Frey, H. *Tetrahedron* **2003**, *59*, 4017-4024.

9 Effect of Polyglycerol Block Copolymers on Insulin Fibril Formation

9.1 Introduction

Within the first two decades since their first appearance in the scientific literature, dendrimers were primarily considered to be useful for drug or gene delivery as well as for antibacterial and antitumor applications. Consequently, the less perfectly dendritic hyperbranched analogues were also studied in these areas. The amphiphilic block copolymers described in chapter 4 have been investigated regarding polymer mediated drug diffusion across biological membrane structures as well as copolymer-mediated increase of membrane ion or proton permeability. Studies with planar lipid bilayers that were carried out in order to understand the influence of the degree of polymerization of the polyglycerol block on (i) the doxorubicin transport rate, (ii) the ion permeability and (iii) the resistant factor of MDR cells (at non-toxic concentrations) can be found in the appendix of this thesis.

In 1999 Scott et al reported that cationic (both PAMAM and PPI) dendrimers as well as medium and high molecular weight branched PEI were effective in removing prion molecules in the infectious state.¹ The prion protein is a host protein, which is centrally involved in the so-called prion diseases, including the well-known Creutzfeldt-Jakob disease. The intriguing potential of dendrimers with respect to therapeutical applications is expanded to more prevalent types of protein misfolding diseases like Alzheimer's disease by their ability to perturb or solubilize other amyloid protein aggregates.^{2,3} Models illustrating the interaction of dendrimers with proteins are still speculative. Generally, both electrostatic and hydrophobic interactions are relevant, which can be modulated by the existence of clustered anionic or cationic patches on the protein surface. Not surprisingly the surface-exposed and flexible regions of the protein are particularly affected by the presence of dendrimers.⁴ Additionally, the effect of specific protein-ligand interactions have to be taken into consideration.^{5,6} Only a few studies directly address the effect of dendrimers on protein stability,⁷ which is of central importance to gain an understanding of the mechanisms regarding dendrimer-protein interactions. This is complicated by the difference of specific interactions depending on the specific nature of the protein. A very pronounced effect of PPI dendrimer and its guanidinium derivative concerning the stability and solubility of insulin was observed by Heegaard et al.⁸ Insulin is a small protein

hormone that is crucial for the control of glucose metabolism and in diabetes treatment. Upon exposure to elevated temperatures, low pH, organic solvents and agitation, insulin is susceptible to fibril formation.⁹ Nonionic surfactants like polysorbates (commercially known as Tween[®]) were found useful for an improvement of protein handling, permitting a higher degree of stability and safety upon processing, storage and drug use.¹⁰ Due to their similar structure, the influence of the polyglycerol-based amphiphiles (described in chapter 4) on the fibril formation was studied and is covered by this chapter.

9.2 Insulin Fibril Formation

Waugh was the first one to show that insulin fibrillation consists of three important steps: Formation of active centers (nucleation), growth of these centers to fibrils (elongation) and precipitation.^{11,12} It has also been found that fibril formation depends on several factors such as temperature, pH-value, ionic strength and acidic conditions. Insulin solutions with an air-water surface fibrillate much faster, when they are agitated. Exposed hydrophobic surfaces of the insulin molecule can interact with the hydrophobic environment of air, leading to insulin adsorption and subsequent conformational changes. In addition, a continuous new interface with a large surface area is created by shaking. The unfolded insulin monomers can then aggregate to higher structures (nucleation). As soon as this nucleus reaches a specific size, it can react to fibrils with unfolded or native insulin molecules.⁹ A proposed mechanism describing the decrease of the tendency for insulin fibrillation by surfactants assumes that surfactant molecules at the water-air interface reduce the contact of air to insulin and therefore lead to increased lag times. Several different methods have been used to study insulin fibrils. For the present work, the Thioflavin T assay (ThT) was applied, which is commonly used for investigations of amyloid fibril formation and the respective kinetics. The thiazole dye Thioflavin T (Figure 9.1) interacts with secondary or higher order structures of fibrils. It was determined that this compound selectively binds to fibrils with β -pleated sheet.

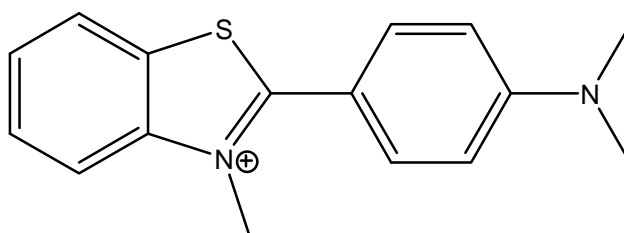


Figure 9.1. Structure of Thioflavin T.

In solution, ThT hardly fluoresces with the excitation and emission maxima of 350 and 438nm, respectively. When it is bound to fibrils, excitation and emission are enhanced and the corresponding maxima are shifted to 450nm and 482nm. It has also been shown, that the kinetics of fibril formation is not influenced by ThT. However, the specific binding of ThT to different fibrillar structures (and its possible dependence on fibril morphology) has not been further investigated to date,

In order to shorten the time until fibril formation, rather stringent reaction conditions were employed, (pH=1.6, elevated reaction temperatures (45°C) and vigorous shaking). Furthermore, bovine insulin, which is known for fast fibril formation, was chosen. It differs from human insulin in three positions (A8 Ala, B30 Ala and A10 Val). Table 9.1 summarizes the insulin fibril formation lag times in the presence of different block copolymers (chapter 4) at different concentrations. In order to obtain further insight, CMCs of all samples were determined.

Table 9.1. Insulin fibril formation lag times measured by ThT fluorescence intensity in absence and presence of block copolymers.

Sample	CMC (mg/mL)	Lag time 0.1 mg/ml	Lag time 2.0 mg/ml	Lag time 10.0 mg/ml	Lag time 20.0 mg/ml
pure insuline	-	3.8 h			
+ PPO ₁₀ -N-PG ₂	9.48	5.2 h	27.5 h	-	-
+ PPO ₁₀ -N-PG ₄₃	9.52	6.3 h	4.5 h	8.0 h	-
+ PPO ₃₅ -N-PG ₂	1.39	-	26.7 h	-	-
+ PPO ₃₅ -N-PG ₂₀	7.71	34.7 h	44.7 h	41.3 h	-
+ PPO ₃₅ -N-PG ₄₃	3.59	-	69.7 h	-	> 96.0 h
+ PPO ₃₃ -(N-PG ₂) ₂	2.58	-	48.0 h	46.3 h	55.2 h
+ PPO ₃₃ -(N-PG ₁₂₀) ₂	23.07	-	17.1 h	9.0 h	11.3 h
+ C ₁₈ -N-PG ₂₀	0.33	-	64.1 h	76.3 h	-

In nearly all cases, a significant influence on fibril formation was found. The measured lag times until fibrillation occurred were visibly higher in presence of the block copoly-

mers. If the influence of the polymers is based on the reduction of the water-air interface, higher polymer concentrations should result in higher lag times. Above the CMC, this increase is expected to be less pronounced. The CMCs of the polyglycerol block copolymers with short PPO chains are comparably high concerning the amount added in weight (ca. 10mg). Thus, their influence is not as pronounced as in the other cases and the extended lag times were below 30 hours in all measurements. The ratio of the short chain to the hyperbranched block does not appear to be the crucial factor, since linear alkyl chains, at a concentration of 2mg/ml, already show high lag times. The corresponding CMC were found to be only 0.33mg/mL which might be a great advantage. These assumptions are further affirmed by the results obtained from using ABA triblock copolymers. The macroinitiator PPO₃₃-(N-PG₂)₂ has a significantly lower CMC than the block copolymer PPO₃₃-(N-PG₁₂₀)₂ and exhibits a much stronger influence on the lag time at the same concentrations. However, having a closer look at the AB block copolymers with a PPO-chain of 35 units reveals that the CMC is not the only factor which has to be taken into account. The CMCs are in the same region as for the other block copolymers, but their ability to delay the fibril formation seems to be comparably stronger. Thus they are as promising as the results obtained from the hyperbranched polymers with linear alkyl chains. Consequently, the ratio of PPO to PG units might also be of great influence regarding the stabilization effects. The most promising results were found for PPO₃₅-N-PG₄₃ block copolymers. At concentrations of 20mg/ml no fibril formation was observed within 4 days.

9.3 Conclusion

The influence of different polyglycerol-based amphiphiles on the fibril formation was studied by Thioflavin T Fluorescence. It is remarkable that the lag times were generally increased, in some cases quite drastically. The CMC has been identified to be of major importance, although the polymer composition should not be neglected. Figure 9.3 illustrates the obtained results. Under the stringent reaction conditions applied, the used bovine insulin fibrillates after 4 hours (dark blue curve). The influence of the ABA block copolymer PPO₃₃-(N-PG₁₂₀)₂ was found to be comparably low (light blue curve). The most promising results were found for the AB block copolymer PPO₃₅-N-PG₄₃. At comparably low concentrations of only 2mg/mL fibril formation was already retarded to 70 hours, while at concentrations of 20mg/mL no fibril formation at all was observed within 96 hours.

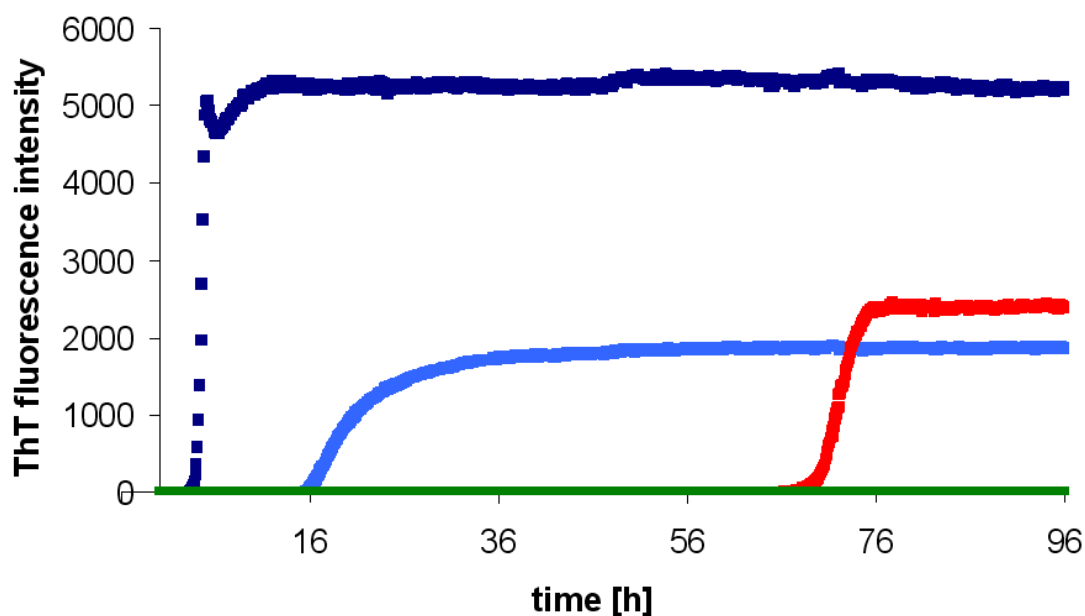


Figure 9.3. Insulin fibril lag time measured by ThT fluorescence intensity: pure insuline (dark blue); insuline + 2.0 mg/ml PG₁₆₀-N-PPO₃₃-N-PG₁₆₀ (light blue), insuline + 2.0 mg/ml PPO₃₅-N-PG₄₃ (red); insuline + 20.0 mg/ml PPO₃₅-N-P G₄₃ (green).

9.4 Experimental Part

9.4.1 Materials

1,6-diphenylhexa-1,3,5-triene was purchased from *Acros Organics*. Bovine insulin and Thioflavin T were obtained from *Sigma Aldrich*. The block copolymers were prepared as described in chapter 4. For the CMC measurements black 96-plates obtained from NUNC with closed bottom were used. All measurements were carried out during a stay in the research group of Prof. Marco van de Weert at the Danish University of Pharmaceutical Sciences in Copenhagen, Denmark.

9.4.2 CMC Measurements by DPH-Fluorescence Assay

12 mg DPH were dissolved in 5ml THF. 250 μ L were removed and dissolved in 5ml millipore water 4.75 ml THF. To each polymer sample (100 μ l) 4 μ L of DPH solution and 96 μ L millipore water were added. Afterwards the samples were excluded from light for 24 h. All measurements were carried out at 25 °C. Fluorescence was measured from the top after 3 min of shaking at FLUOstar BMG-Labtech, (extinction wavelength: 355 nm; emission wavelength: 410-450 nm).

9.4.3 Insulin Fibril Formation Measurements by Thioflavin T Assay

3.5 mg of Thioflavin T were dissolved in 10ml millipore water. 100 μ L were added to 9.9 ml of a solution of 80 mg bovine insulin in 0.025 M HCl. Then, different concentrations of each polymer in 0.025M HCl were prepared. In each well of the plate, 100 μ L of polymer were pipetted together with 100 μ L insulin/ThT solution. The fluorescence was measured at POLARstar BMG-Labtech running with excitation maximum at 450 nm and emission maximum at 482 nm. The experiment was carried out at 45 °C with agitation during 4 days. Settings for POLARstar: plates: Nunc C96 Microwell 96 black; measurement: from bottom; positioning delay: 0.2; no. of cycles: 216; measurement start time: 0.1s; no. of flashes per well and cycle: 10; cycle time: 400; excitation filter: 450-410; emission filter 480-410; gain: 700; shaking: double orbital, shaking width 1mm, additional shaking after each cycle, shaking time 300s; temperature: 45°C.

9.5 References

1. Supattapone, S.; Nguyen, H. O. B.; Cohen, F. E.; Prusiner, S. B.; Scott, M. R. *Proceedings of the National Academy of Sciences of the United States of America* **1999**, 96, 14529-14534.
2. Klajnert, B.; Cladera, J.; Bryszewska, M. *Biomacromolecules* **2006**, 7, 2186-2191.
3. Klajnert, B.; Cortijo-Arellano, M.; Cladera, J.; Bryszewska, M. *Biochem. Biophys. Research Commun.* **2006**, 345, 21-28.
4. Gabellieri, E.; Strambini, G. B.; Shcharbin, D.; Klajnert, B.; Bryszewska, M. *Biochim. Biophys. Acta-Proteins and Proteomics* **2006**, 1764, 1750-1756.
5. Patel, D.; Henry, J.; Good, T. *Biochim. Biophys. Acta -General Subjects* **2006**, 1760, 1802-1809.
6. Shi, X. Y.; Bi, X. D.; Ganser, T. R.; Hong, S. P.; Myc, L. A.; Desai, A.; Holl, M. M. B.; Baker, J. R. *Analyst* **2006**, 131, 842-848.
7. Klajnert, B.; Stanislawska, L.; Bryszewska, M.; Palecz, B. *Biochim. Biophys. Acta -Proteins and Proteomics* **2003**, 1648, 115-126.
8. Heegaard, P. M. H.; Boas, U.; Otzen, D. E. *Macromol. Biosci.* **2007**, 7, 1047-1059.
9. Brange, J.; Andersen, L.; Laursen, E. D.; Meyn, G.; Rasmussen, E. *J. Pharm. Sci.* **1997**, 86, 517-525.

10. Bam, N. B.; Cleland, J. L.; Yang, J.; Manning, M. C.; Carpenter, J. F.; Kelley, R. F.; Randolph, J. W. *J. Pharm. Sci.* **1998**, 87, 1554-1559.
11. Waugh, D. F. *J. Am. Chem. Soc.* **1946**, 68, 247-250.
12. Waugh, D. F.; Wilhelmson, D. F.; Commerford, S. L.; Sackler, M. L. *J. Am. Chem. Soc.* **1953**, 75, 2592-2600.

10 Summary / Abstract

Among hyperbranched polymers, polyglycerol is one of the most promising and commonly used macromolecules due to its biocompatibility and versatility. However, the synthesis of high molecular weight polyglycerols still involves many intricacies and has only been understood to a limited extent. Furthermore, only few complex structures like star or block copolymers incorporating polyglycerol have been realized so far. Particularly biocompatible block copolymers are considered promising candidates for biomedical applications.

The scope of this thesis was the enhancement of the synthetic process leading to polyglycerol derivatives which implies improved molecular weight control for a broad molecular weight range as well as the assembly of more complex structures like amphiphilic block copolymers. Further insight into the relation between reaction solvent, degree of deprotonation during the ring-opening multibranching polymerization of glycidol and the characteristics of the obtained polymers were achieved within the scope of this work. Based on these results, a novel concept for the preparation of hyperbranched polyglycerols with molecular weights up to 20,000 g/mol was developed, applying a two step synthesis pathway. Starting from a partially deprotonated TMP core, low molecular weight *hb*-PGs were prepared using the known synthetic protocol that has been established since the late 1990ies. In a subsequent reaction sequence, these well defined polymers were used as hyperbranched macroinitiator cores in order to obtain high molecular weight *hb*-PGs with remarkably low polydispersity ($M_w/M_n < 1.8$). Molecular weight control was shown to be excellent and undesired low molecular weight side products were absent. Furthermore, the technique of continuous spin fractionation has been discovered as an efficient method for polyglycerol work-up to remove quantitatively residual monomer- and oligomer traces from *hb*-PG compositions to result in samples with significantly reduced polydispersities. Based on these results the synthesis of amphiphilic block copolymers containing hydrophilic hyperbranched polyglycerol blocks and linear, apolar poly(propylene oxide) blocks has been significantly improved and augmented to *hb*-PG-*b-l*-PPO-*b-hb*-PG ABA block copolymers. The influence of different polyglycerol-based amphiphiles on the fibril formation was studied by Thioflavin T Fluorescence showing remarkably increasing lag times which is promising in order to enhance the stability of this protein. In addition the first synthesis of poly(glyceryl glycerols) (PGG), introducing a new solketyl glycidyl ether monomer (IGG) was shown. It was furthermore demonstrated that core-functional carbosilane wedges allow application in block copolymer synthesis. Bisglycidolized amine functional polymers were successfully employed as macroinitiators for glycidol polymerization. This resulted in the first example of amphiphilic hyperbranched-hyperbranched polymer structures. Finally, it has been shown that the previously reported synthetic pathway to carboxylated hyperbranched polyglycerol polyelectrolytes can also be applied for the amphiphilic linear-hyperbranched block copolymers. These novel biocompatible and highly amphiphilic polyelectrolytes offer great potential for further investigations.

11 Experimental Methods and Instrumentation

11.1 Nuclear Magnetic Resonance Spectroscopy (NMR)

¹H-NMR spectra were recorded at 300 MHz on a Bruker AC or at 400 MHz on a Bruker AMX 400. ¹³C and ¹³C inverse gated NMR spectra were measured at 75 MHz on a Bruker AC or at 100 MHz on a Bruker AMX 400. All samples were referenced internally to the residual proton signal of the deuterated solvents.

11.2 Gel Permeation Chromatographie (GPC)

For measurements in dimethylformamide (DMF) (containing 1 g/L of lithium bromide as an additive) an Agilent 1100 Series was used as an integrated instrument including a PSS Gral column (10⁴/10⁴/10² Å porosity), a UV (275 nm) and a RI detector. Calibration was performed using poly(ethylene glycole) or poly(styrene) standards provided by Polymer Standards Service.

GPC in trichloromethane (TCM) or tetrahydrofuran (THF) was performed on an instrument consisting of a Waters 717 plus auto sampler, a TSP Spectra Series P 100 pump and a set of three PSS SDV columns (104/500/50Å). Elution of samples was followed by measuring the specific refractive index increment (dn/dc) at 30°C on a Wyatt Optilab DSP interferometric refractometer (RI detector) and by UV absorption detection on a TSP Spectra System UV 2000 (UV detector, = 254nm). Calibration was carried out using poly(styrene) standards provided by Polymer Standards Service. For these systems, MALLS-detection (Multi Angle Laser Light Scattering) was carried out on a Wyatt Dawn 18 angle online light scattering detector.

11.3 Infra Red-Spectroscopy (IR)

IR spectra were recorded on a Thermo Nicolet 5DXC FT-IR spectrometer equipped with an ATR Unit.

11.4 Differential Scanning Calorimetry (DSC)

DSC curves were recorded on a Perkin Elmer DSC 7 operated with Perkin Elmer Thermal Analysis Controller TAC 7/DX in sealed aluminium pans under nitrogen atmosphere. Measurements were performed in the temperature range between -90°C and 100°C at scan rates of 10 K/min or 20 K/min. Samples weights were $\approx 10\text{mg}$. The instrument was calibrated using milipore water ($T_m=0^{\circ}\text{C}$) and high-purity indium ($T_m=156^{\circ}\text{C}$).

11.5 Matrix Assisted Laser Desorption Ionization – Time of Flight (MALDI-ToF)

All spectra were recorded on a Kratos Axima-CFR mass spectrometer (Shimadzu) equipped with a nitrogen laser delivering 3ns laser pulses at 337nm. The samples were measured in positive ion and in linear or reflectron mode of the spectrometer. CHCA (α -cyano-4-hydroxy-cinnamic acid, Acros, 97%) was the matrix of choice. Sodium and lithium trifluoro acetate were utilized for ion formation as 0.1N solutions in methanol. Sample preparation was performed by mixing matrix (10mg/mL), polymer (10mg/mL) and salt (0.1N solution in methanol) in a ratio of 10:1:1. A total volume of $0.9\mu\text{L}$ was pipetted onto the MALDI sample slide and allowed to dry to a thin film at room temperature for 2h prior to measurement.

11.6 Field Desorption Mass Spectrometry (FD)

FD mass spectra were measured on a Finnigan MAT 95.

11.7 Transmission Electron Microscopy (TEM)

High-resolution TEM studies were conducted on a Philips Tecnai F30 analytical TEM at an operating voltage of 300 kV and on a TEM EM420 electron microscope at an operating voltage of 120 kV.

12 Appendix

In the course of the experimental work of this thesis a number of collaborative efforts were undertaken that eventually led to several publications, shown in the ensuing section of the thesis.

Since these papers are strongly based on the work of the collaboration partners or on measurements carried out in other laboratories, they are not of the central chapters of this thesis. However, in order to document the activities in these areas and to demonstrate further application possibilities for the materials prepared in the course of the thesis, reprints of the respective publications constitute this appendix.

12.1 Synthesis of Hyperbranched Polyglycerol in a Continuous Flow Microreactor

12.2 Double-Hydrophilic Linear-Hyperbranched Block Copolymers Based on Poly(ethylene oxide) and Poly(glycerol)

12.3 Synthesis and Characterization of Poly(glyceryl glycerol) Block Copolymers

12.4 Gold Nanoparticles Coated with a Thermosensitive Hyperbranched Polyelectrolyte: Towards Smart Temperature and pH Nanosensors

12.5 Liquid Crystalline Hyperbranched Polyglycerols Forming Liquid Crystalline Mesophases

12.6 Polyglycerol-Based Copolymers: A New Family of Amphiphiles Circumventing Multidrug Resistance of Tumor Cells

12.1 Synthesis of Hyperbranched Polyglycerol in a Continuous Flow Microreactor

The research article

“Synthesis of Hyperbranched Polyglycerol in a Continuous Flow Microreactor”

can be seen in the printed version of this thesis and was published at:

Chem. Eng. Technol. **2007**, 30, No.11, 1519-1524.

Authors: Daniel Wilms, Jörg Nieberle, Johannes Klos, Holger Löwe, Holger Frey

12.2 Double-Hydrophilic Linear-Hyperbranched Block Copolymers Based on Poly(ethylene oxide) and Poly(glycerol)

The research article

“Double-Hydrophilic Linear-Hyperbranched Block Copolymers Based on Poly(ethylene oxide) and Poly(glycerol)”

can be seen in the printed version of this thesis and was published at:

Macromolecules **2008**, *41*(4), 1184-1188.

Authors: Frederik Wurm, Jörg Nieberle, and Holger Frey

12.3 Synthesis and Characterization of Poly(glyceryl glycerol) Block Copolymers

The research article

“Synthesis and Characterization of Poly(glyceryl glycerol) Block Copolymers”

can be seen in the printed version of this thesis and was published at:

Macromolecules **2008**, *41*(6), 1909-1911.

Authors: Frederik Wurm, Jörg Nieberle, and Holger Frey

12.4 Gold Nanoparticles Coated with a Thermosensitive Hyperbranched Polyelectrolyte: Towards Smart Temperature and pH Nanosensors

The research article

“Thermosensitive Hyperbranched Polyelectrolyte-Coated Gold Nanoparticles: Towards Smart Temperature- and pH-Nanosensors”

can be seen in the printed version of this thesis and was published at:

Angew. Chem. Int. Ed. **2008**, 47, 2227-2230.

Authors: Yi Shen, Min Kuang, Zhong Shen, Jörg Nieberle, Hongwei Duan, and Holger Frey

12.5 Liquid Crystalline Hyperbranched Polyglycerols Forming Liquid Crystalline Mesophases

This article can be seen in the printed version of this thesis and is not visible here due to protection of data privacy.

12.6 Polyglycerol-Based Copolymers: A New Family of Amphiphiles Circumventing Multidrug Resistance of Tumor Cells

This article can be seen in the printed version of this thesis and is not visible here due to protection of data privacy.

